Altered calcium signalling in prostate cancer facilitates progression to castrate resistance

A thesis submitted for the award of Ph.D by

Debbie O'Reilly, B.Sc

School of Nursing, Psychotherapy & Community Health

Faculty of Science & Health

Dublin City University

The work of this thesis was carried out under the supervision of:

Dr Paul Buchanan & Dr Patricia Johnson

September 2021

Declaration

I hereby certify that this material, which I now submit for assessment on the programme of study leading to the award of PhD is entirely my own work, that I have exercised reasonable care to ensure that the work is original and does not to the best of my knowledge breach any law of copyright and has not been taken from the work of others save and to the extent that such work has been cited and acknowledged within the text of my work.

Signed: 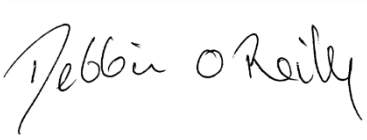 (Candidate) ID No.: 16212573

Date: 03/10/2021

Acknowledgements

People think that pursuing a PhD is a sign of remarkable character in a person. However, having just completed my PhD I have come to realise that it is an exercise in complete self-indulgence. To that end there are many people who deserve gratitude in facilitating this episode in my life.

First and foremost, I would like to extend my heartfelt gratitude to my supervisor Dr Paul Buchanan. I feel immensely privileged to be the first PhD student under your mentorship and to those who will follow, I can assure you that you are in the best of hands. Needless to say, this project would not have been possible without your extensive knowledge on the topic. Thank you for your guidance, encouragement, and consistent good humour and patience, even when things were not going to plan.

I would also like to thank Dr Patricia Johnson, who always had an open door and a friendly ear. Thank you for always making me feel welcome in the lab and for all your invaluable advice as I made my way through this project. Thank you to my lab mates Paula Maguire and John Redmond who were always available when I needed a chat. Your company over the years has made the lab a great place to come to work and I will always remember it fondly.

Thank you to my funders The Irish Research Council and the School of Nursing Psychotherapy and Community Health.

Thank you to my family and friends who have graciously excused me from many responsibilities and special occasions over the years and have endured my mood swings. Thank you, Mam and Dad, I know you have gone through every peak and trough with me.

Thank you Dáire, my source of pride and joy, my regular study buddy and fellow scientist. Thank you for always encouraging me and making me smile and for never growing tired of talking science with me.

Most importantly I would like to thank my husband Noel, you have endured the most. I may have done the PhD, but you have done everything else. You have been my council, my funder, my friend, and my rock. This piece of work belongs to both of us.

Finally, I would like to dedicate this thesis to the memory of my brother Martin O'Reilly, who left us suddenly just after I began this PhD. If I can do this in the wake of losing you, I can do anything. Ar dheis Dé go raibh a anam.

Contents

Abbreviations

$[Ca^{2+}]_i$	Intracellular Ca^{2+} concentration
18S	18S ribosomal RNA
ADT	Androgen deprivation therapy
AR	Androgen receptor
ARE	Androgen response element
β-Actin	Beta actin
BK_{Ca}	Big conductance Ca^{2+} activated K^+ channel
Br^-	Bromide
Ca^{2+}	Calcium
CAMKK	Calcium/Calmodulin-Dependent Kinase Kinase
CCB	Calcium channel blocker
cDNA	Complimentary deoxyribonucleic acid
CIM	Cell invasion and migration
Cl^-	Chloride
CRAC	Calcium release activated calcium
CRPC	Castrate resistant prostate cancer
CSC	Cancer stem cell
Ct	Cycle threshold
CtCV %	Coefficient of variance
dH_2O	Distilled water
DHEA	Dehydroepiandrosterone
DHP	Dihydropyridine
DHT	Dihydrotestosterone
DMSO	Dimethyl sulfoxide
EAG1	Ether-a-go-go
ECM	Extracellular matrix
EGF	Epidermal growth factor
EMT	Epithelial to mesenchymal transition

ENC	Epithelial sodium channels
ER	Endoplasmic reticulum
FBS	Fetal bovine serum
FSH	Follicle-stimulating hormone
GnRH	Gonadotropin-releasing hormone
HIF	Hypoxia inducible factor
HMBS	Hydroxymethylbilane synthase
HPRT1	Hypoxanthine phosphoribosyltransferase 1
I^-	Iodide
IGF	Insulin-like growth factor
IK_{Ca}	Intermediate Ca^{2+} activated K^+ channel
IMS	Industrial methylated spirits
IP_3	Inositol 1,4,5-triphosphate
IP_3R	Inositol triphosphate receptor
K^+	Potassium
K_{Ca}	Calcium activated potassium channels
KCl	Potassium chloride
K_v	Voltage gated potassium channels
LH	Luteinizing hormone
LHRH	Luteinizing hormone–releasing hormone
MAPK	Mitogen activated protein kinase
m-CRPC	Metastatic castrate resistant prostate cancer
MMCA	Mitochondrial membrane Ca^{2+}ATPase
MNCX	Mitochondrial NCX
Na^+	Sodium
NaCl	Sodium chloride
NCX	Sodium calcium exchanger
NFAT	Nuclear factor of activated T-cells
PBS	Phosphate buffered saline
PCa	Prostate cancer

PCR	Polymerase chain reaction
PCSC	Prostate cancer stem cells
PI3K	Phosphatidylinositol 3-kinase
PSA	Prostate specific antigen
PSS	Physiological saline solution
PVDF	Polyvinylidene fluoride
qPCR	Quantitative polymerase chain reaction
RACK1	Receptor for activated C-kinase 1
RIPA	Radioimmunoprecipitation assay buffer
RNA	Ribonucleic acid
ROC	Receptor operated channels
RT	Room temperature
RyR	Ryanodine receptor
SANDD	Sinoatrial node dysfunction and deafness
SD	Standard deviation
sem±	Standard error of the mean
SERCA	Sarco-endoplasmic reticulum Ca^{2+}ATPase
Shh	Sonic hedgehog
SK	Small conductance Ca^{2+} activated K^{+} channel
SOC	Store operated channels
SOCE	Store operated calcium entry
STIM	Stromal interaction molecule
TBP	TATA-Box binding protein
TBS	Tris buffered saline
Tg	Thapsigargin
TGF-β	Transforming growth factor- beta
T_M	Melting temperature
TME	Tumour microenvironment
TRP	Transient receptor potential
UV	Ultraviolet

VEGF	Vascular endothelial growth factor
VGCC	Voltage gated calcium channels
VGNC	Voltage gated sodium channels
VHL	Von Hippel-Lindau
WR	Working reagent

Publications:

Role of ion channels in natural killer cell function towards cancer

Redmond J, O'Reilly D, Buchanan P (2018) (Discov Med. 2017 23(129):353-360.)

Calcium channels and cancer stem cells

O'Reilly D, Buchanan P (2019) (Cell Calcium. 2019 Jul; 81:21-28)

Hypoxia induced cancer stem cell enrichment promotes resistance to androgen deprivation therapy in prostate cancer.

O'Reilly D, Johnson P, Buchanan P (2019) (Steroids. 2019 Dec: 152:108497.)

Articles:

Silicon Republic Science Uncovered Series: (02 Oct 2019) 'I would like to see research looking at cancer as a chronic illness'

https://www.siliconrepublic.com/innovation/debbie-oreilly-dcu-prostate-cancer-research

Credited Modules:

Research Ethics GS604 (5 Credits)

Communication module GS611NS (5 Credits)

Statistics Advanced Experimental Data Processing CS507A (5 Credits)

Biosafety & Lab Standard Operating Procedures BE550 (5 Credits)

Intellectual property and commercialisation GS601(5 Credits)

Uncredited Modules:

Digital storytelling

Academic writing

Writing for publication

Writing in the final year

CRDI Techniques & Strategies in molecular medicine

Presentation coaching with SNP

Grants

School of Nursing Psychotherapy & Community health

Irish Resrearch Council

Irish Research Council costed extension

Travel Grants

EU COST Action Project

HRB Ulysses Grant 2019

Oral Presentations & Abstract publications

SNHS Research seminar series	Dublin City University	**12/2016 & 03/2018**
IEPG 10th annual meeting	New Park hotel, Kilkenny	**27/10/2017**
Biological Research Society annual meeting	Dublin City University	**26/01/2018**
Researchfest at Inspirefest	Bord Gais energy Theatre	**16/05/2019**
Irish association for Cancer Research	Galway Bay Hotel, Galway	**28/02/2020**

Prizes

Best PhD presentation at IEPG 10th annual meeting 27/10/2017

Winning presentation at Researchfest 2019 16/05/2019

https://www.youtube.com/watch?v=aW3iA6mQjss

Poster Presentations:

RAMI Section of Biomedical Sciences Trinity College Dublin **22/06/2017**

Upregulation of CaV1.3 in Castrate Resistant Prostate Cancer drives Hypoxic Signaling and Stem Cell Maintenance

Debbie O'Reilly, Patricia Johnson, Paul Buchanan

Irish Association for Cancer Research Europa Hotel, Belfast **21/02/2019**

The Upregulation of CaV1.3 in Castrate Resistant Prostate Cancer (CRPC) could be driving Hypoxic Signaling & Stem Cell Characteristics

Debbie O'Reilly, Patricia Johnson, Tim Downing, Paul Buchanan

Irish Association for Cancer Research Galway Bay Hotel, Galway **28/02/2020**

Increased intracellular calcium through CaV1.3 promotes resistance to androgen deprivation therapy in TMPRSS2:ERG prostate cancer

Debbie O'Reilly, Patricia Johnson, Declan Mc Kenna, Tim Downing, Paul Buchanan

Abstract:

Altered calcium signalling in prostate cancer facilitates progression to castrate resistance.

Debbie O'Reilly

Prostate cancer (PCa) carries a significant clinical burden worldwide with ~1.3-million new cases annually. It is the most frequently diagnosed cancer in Irish men, excluding non-cutaneous skin cancer, and is the third most common cause of cancer related deaths among this cohort. The most utilised treatment for advanced or metastatic PCa is androgen deprivation therapy (ADT). Although this treatment initially shrinks the tumour, treatment resistance develops after ~2 years. At this stage, the disease is called castrate resistant prostate cancer (CRPC) and is associated with mortality. Calcium signalling has been implicated in the malignant progression of many cancers, particularly PCa. Research demonstrates that the L-type voltage gated calcium channel CaV1.3 is significantly increased in PCa tissues compared to normal prostate epithelia. The aim of this study was to explore the role CaV1.3 plays in ADT resistance and determine its underlying tumour biology.

This research investigates the mechanism associated with CaV1.3 upregulation and the progression to CRPC. Using clinical, *in vivo* and *in vitro* models we reveal that CaV1.3 is enhanced by ADT, which correlates with higher Gleason score and shorter time to biochemical recurrence. Herein we uncover a novel mechanism through which upregulated CaV1.3 functions to increase calcium mobilisation by enhancing store operated calcium entry (SOCE). Increased calcium results in altered cellular signalling and stable expression of Hif-1α under hypoxic conditions, it also increases the expression of PCa markers such as androgen receptor. This facilitates cell viability under conditions of ADT and maintaines the proliferative ability of CRPC. Confirming that CaV1.3 has a direct involvement in PCa progression and signifying that CaV1.3 could be utilised as both a biomarker for treatment resistance and as a drug target to prevent disease progression.

Chapter 1 - Introduction

1.1 Background

1.1.1 Overview of cancer

Cancer is a group of diseases which are initiated by genomic alterations resulting in uncontrolled growth. Uncontrolled cellular growth can occur anywhere in the body, forming a cellular mass called a tumour. Tumours can be benign non-cancerous or in the case of cancer, malignant with the potential to metastasise. There are over 200 types of cancer, highlighting the complexity and significant burden of the disease. In fact, cancer is the second most prevalent cause of death worldwide, next to cardiovascular disease. This was reported in the most recent World Health Organisation (WHO), International Agency for Research on Cancer (IACR) report (Bray et al., 2018). According to this report there were 18.1 million new cancer cases worldwide in 2018 and 9.6 million deaths attributed to the disease (Ferlay et al., 2019), with European countries accounting for 23.4% of the newly diagnosed cases. Worldwide breast, colorectal and prostate cancer have the highest incidence of individual cancers (Figure 1.1).

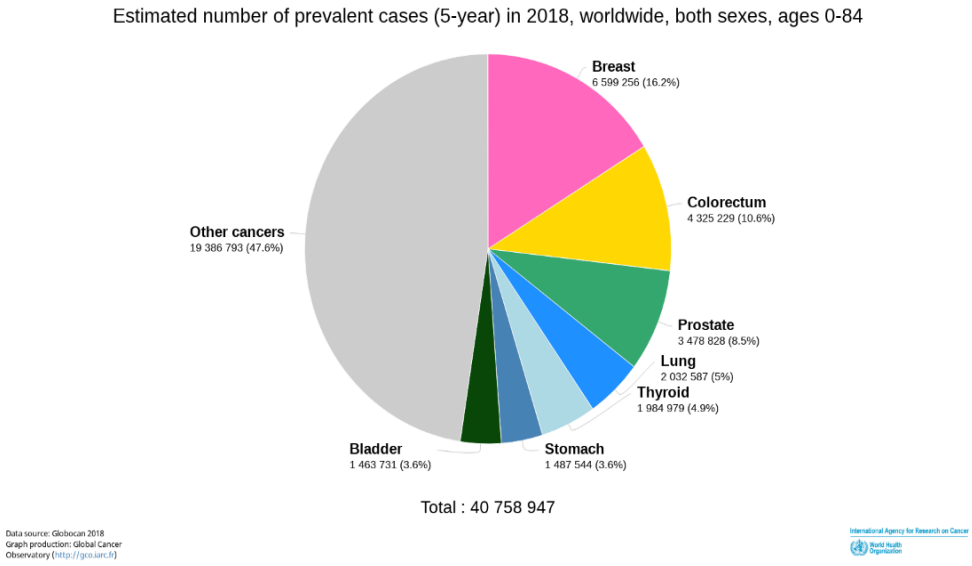

Figure 1.1: *Worldwide statistics for cancer prevalence occurring in both sexes over 5 years to 2018 (Bray et al., 2018)*

1.1.2 Hallmarks of Cancer

Hanahan and Weinberg delivered a substantial report initially defining six hallmarks of cancer (Hanahan and Weinberg, 2000)(Figure 1.2). They reported that cancer involved a multistep transformation of healthy cells to malignant cells, for which the cell must acquire a number of these six physiological changes as outlined briefly below. Genomic and proteomic changes acquired by cancer cells enable these various cancer hallmarks which ultimately promotes disease development and progression.

(1) Self-sufficiency in growth signals, enables the tumour cell to maintain proliferation without relying on the cell's normal growth factors, or proliferative signalling pathways. Usually growth factors bind to a transmembrane receptor which activates a downstream pathway such as the mitogen activated protein kinase (MAPK) or the phosphatidylinositol 3-kinase (PI3K) (Witsch et al., 2010). In tumour progression the cell undergoes genetic alterations or mutations which result in oncogenes, leading to persistent activation of these pathways which ultimately results in sustained proliferation.

(2) Evading growth suppressors allows the tumour cell to disable tumour suppressor genes (TSG) which normally negatively regulate the cell cycle. Like the growth factor pathways, most cells receive signals from growth suppressors which signal the cell to remain in a quiescent state. They also signal the cell to undergo repair or apoptosis following damage. TSG's such as retinoblastoma protein (pRb) force the cell into the G_0 phase of the cell cycle or into the post mitotic phase. pRb, when hypo-phosphorylated, binds to the transcription factor E2F, which prevent it from activating transcription of genes which signal proliferation (Amin et al., 2015). In cancer cells mutation of pRb prevents this inhibition of transcription, as a result, this leads to propagation of the cancer cells.

(3) Evading apoptosis, this infers immortality on tumour cells and prevents cells from undergoing normal apoptosis programmed cell death. Mutations in the cell which result in overexpression of the anti-apoptotic genes such as Bcl-2 allows the cell to evade apoptosis (Frenzel et al., 2009). Other mechanisms can contribute to evasion of apoptosis such as mutations or deletion of tumour suppressor genes such as p53, which is usually responsible for detecting DNA damage and recruiting pro apoptotic genes such as Bcl associated X protein (BAX) (Ozaki and Nakagawara, 2011).

(4) Enabling replicative immortality, allows the cell to continue cellular replication beyond the limits bestowed on normal cells. This is usually controlled through the gradual reduction of the chromosome end proteins called telomeres. Each replication results in a shorter telomere due to the inability of DNA polymerase to completely replicate the 3-prime end of the chromosome. Therefore, telomerase acts as a cell replication counter, limiting the number of times a cell can be replicated before it triggers senescence. In cancer cells this process is bypassed either through inhibition of senescence or through increased activity of telomerase, an enzyme which lengthens the telomeres.

(5) Induced angiogenesis is an essential process in tumour progression due to the rapid proliferation of the malignant cells (Nishida et al., 2006). Angiogenesis is the process by which a cell promotes growth of vasculature through the secretion of growth factors such as vascular endothelial growth factor (VEGF). It is an important process for cell oxygenation and waste removal, enabling tumours to grow large.

(6) Activating metastasis is the process by which the malignant cell loses the normal cell surface proteins, which anchor it to the basal membrane and are involved in cell-to-cell adhesion. Instead, they gain surface proteins which enable them to invade tissues and migrate to other body sites. The best documented of these cellular plasticity events is the epithelial to mesenchymal transition (EMT). During this process, the cell loses the cell surface adhesion molecules such as E cadherin and gain mesenchymal markers such as N cadherin and vimentin (Kalluri and Weinberg, 2009). This allows the tumour cells to migrate to distal sites where the space and nutrients are in less demand.

In an update to their original publication Hanahan and Weinberg included two additional hallmarks, deregulated metabolism and evading the immune system (Hanahan and Weinberg, 2011), which have since been widely accepted in the progression of cancer.

(7) Reprogramming metabolic pathways was first eluded to in studies by Otto Warburg (Warburg, 1956), wherein he described the increased switch to glycolytic pathway in cancer cells. This less efficient but faster means of energy production witnessed in cancer cells even under normal O_2 conditions would become known as the Warburg effect (Zhang and Yang, 2013). Allowing highly proliferative cells to obtain the energy required.

(8) Immune cell evasion is achieved by successful tumours despite an increased inflammatory response and angiogenesis. They achieve this through various mechanisms such as reducing antigen presentation and activation of immunosuppressive cytokines (Vinay et al., 2015).

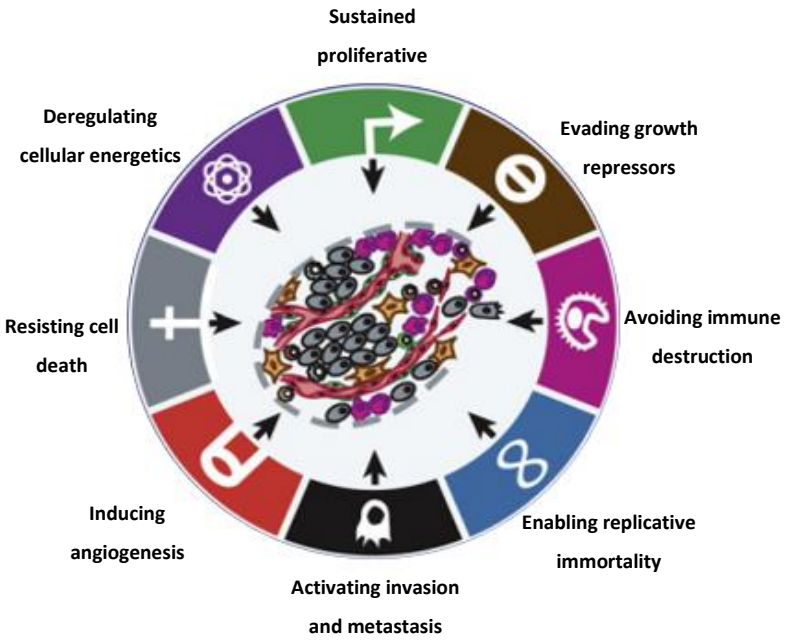

Figure 1.2: *The original six hallmarks of cancer as outlined by Hanahan and Weinberg 2000 and the additional two markers indicated in their updated paper in 2011 (Hanahan and Weinberg, 2011, 2000), indicating the physiological alterations required for the malignant transformation of healthy cells to cancerous cells.*

1.2 Prostate cancer

The focus of this thesis is prostate cancer (PCa), which as outlined, below is the second most frequently diagnosed cancer in men worldwide (Bray et al., 2018) (GLOBOCON 2018). Many parameters have been associated with the development of prostate cancer, with age, race and family history being the most definitive (Gann, 2002; Lesko et al., 1996; Yatani et al., 1982). Although the increased incidence observed in Asian immigrants after they relocate to a western society suggest that there are dietary and lifestyle influencers involved (Attard et al., 2016; Damber and Aus, 2008).

As recently outlined in a report published in Nature, PCa, like all cancer types, conforms with many of the cancer hallmarks outlined above (Datta et al., 2016), including the ability to become self sufficient in growth signals. In fact, the progression to androgen independent growth and the

development of treatment resistance is an area of much research although as of yet the mechanism driving this progression is unresolved.

1.2.1 The prostate gland

The prostate gland is a small walnut sized organ which is situated surrounding the urethra in males. The glands functions are not fully elucidated, although it produces some seminal secretions which make up ~30% of semen (D. Zhang et al., 2018) and may play a role in sperm motility (Oh et al., 2003). In the 1980's John Mc Neal was the first to designate zonal regions in describing the human prostate (McNeal, 1981). He identified the fibromuscular zone, situated to the anterior, and three glandular zones, the central zone (around the ejaculatory tubes), the transitional zone (surrounding the urethra) and the peripheral zone. The peripheral zone makes up ~70% of the prostate and is the most common site for PCa (Oh et al., 2003). Each of the glandular zones are made up of ducts and acini, which are lined with secretory luminal and basal epithelial cells and a small interspersed population of neuroendocrine cells (Figure 1.3) (Park et al., 2016), each briefly outlined below.

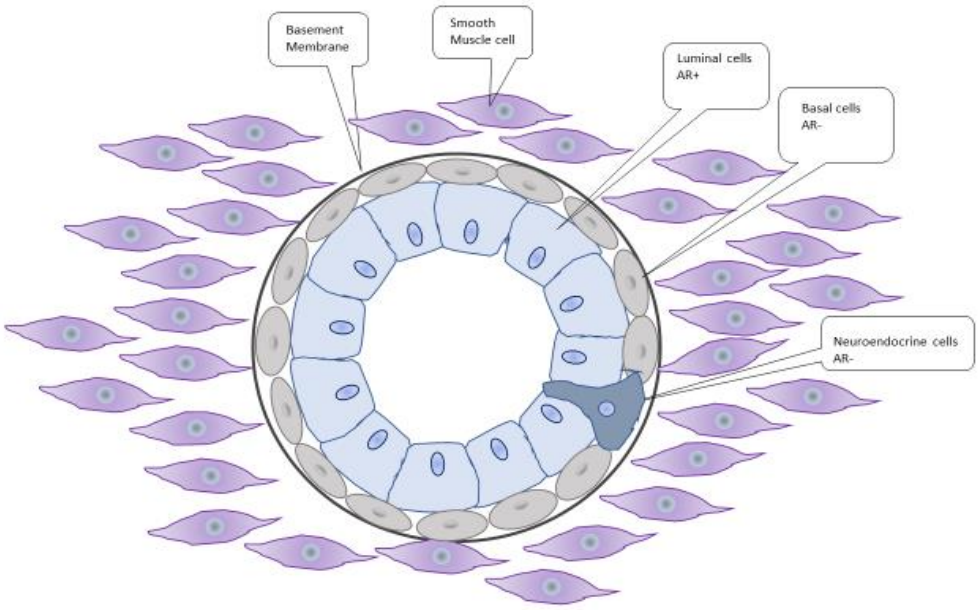

Figure 1.3: *The prostate gland is lined with secretory luminal epithelial cells which are reliant on androgens for growth. Below the luminal epithelial cells are a layer of basal epithelia which are not androgen sensitive and are thought to contain the population of stem cells. The gland is also interspersed with neuroendocrine cells.*

1.2.1.1 Luminal epithelial cells

Luminal cells line the lumen of the prostate and secrete luminal proteins such as prostate specific antigen (PSA). Luminal cells make up the predominant phenotype in the prostate, are androgen receptor (AR) positive and proliferate under the action of androgens. These cells express the luminal cytokeratins (CK) CK8 and CK18(Wang et al., 2001). PCa predominantly consists of a luminal phenotype, with strong AR expression and elevated PSA secretion.

1.2.1.2 Basal epithelial cells

Lining the basal membrane below the luminal cell population lies the basal cells, which contain the population of prostate stem cells. These cells express basal cell markers CK5 and CK14 and the stem cell transcription factor p63.(Wang et al., 2001). They are androgen insensitive expressing low levels of AR(Shen and Abate-Shen, 2010). However they are considered important in the development of PCa contributing to the development of the population of cancer stem cells.

1.2.1.3 Neuroendocrine cells

The prostate also contains a small population of neuroendocrine cells, which are scattered among the luminal cell population. These cells are AR and PSA negative and are identified by the surface markers neuron specific enolase (NSE). Neuroendocrine cells are quiescent, however they secrete cytokines which support the growth of the surrounding epithelial cells (Butler and Huang, 2021). These cells are unaffected by androgen deprivation therapy and are in fact enriched under treatment, implicating them in the progression to the castrate resistant disease.

1.2.2 Androgens and the Androgen receptor

The hypothalamic gonadal axis is responsible for the production of sex hormones produced in the body. Gonadotropin-releasing hormone (GnRH) is secreted from the hypothalamus in pulses

which stimulates the pituitary gland to release follicle-stimulating hormone (FSH) and luteinizing hormone (LH), which travel through the blood stream and act upon the gonadal organs, where it stimulates the production of sex hormones. In males, LH travels to the testes where it stimulates the Leydig cells to produce androgens (Debes and Tindall, 2002).

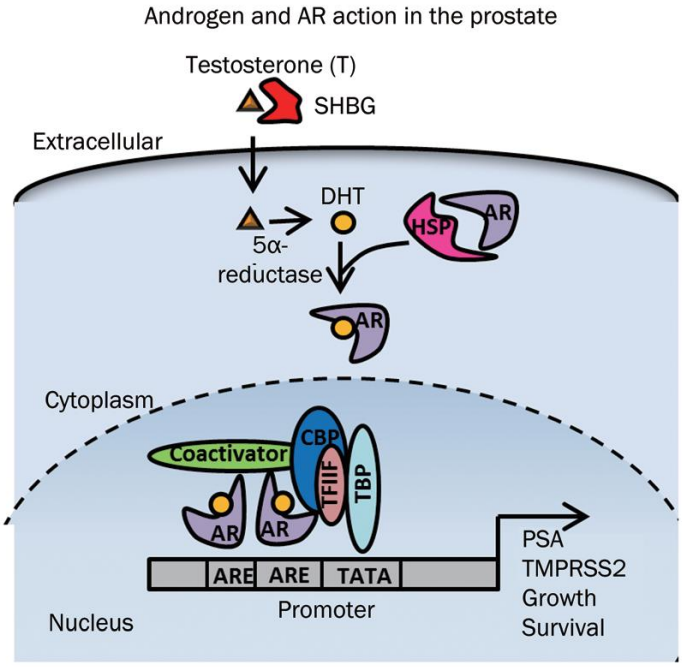

Figure 1.4: *Testosterone is secreted by the Leydig cells in the testes or by the adrenal gland. Once it reaches the prostate it is converted into the more active dihydrotestosterone by the enzyme 5-α-reductase. It binds to the androgen receptor and moves into the nucleus where it binds to the androgen response element and promotes transcription of various genes. (Tan et al., 2015)*

Androgens are produced predominantly by the Leydig cells but also to a lesser extent by the adrenal glands. Development and function of the male prostate relies on androgens, the most prevalent of which is testosterone (Debes and Tindall, 2002). Testosterone enters the cells of the prostate gland where it is converted to the more active dihydrotestosterone (DHT) by the enzyme 5-α-reductase. In the absence of androgens, the AR is located in the cytoplasm, where it is bound

by heat shock proteins and other inhibitory chaperones. Once actively bound by DHT the AR undergoes a conformational change and sheds the chaperones, enabling the complex to translocate to the nucleus (Figure 1.4). Once inside the nucleus the AR binds to the androgen response element (ARE) region and assisted by coactivators, it acts as a promoter of target genes such as those involved in survival and proliferation (Dehm and Tindall, 2006; Heinlein and Chang, 2004).

1.2.3 PCa Diagnostics

Since the discovery in the early 1980's of a test to analyse increased serum levels of prostate specific antigen (PSA) in the blood of PCa patients (Kuriyama et al., 1981, 1980), PCa screening has been increased in many western populations. PSA is a serine protease which is secreted by both normal and malignant prostate epithelia (Stenman et al., 1999) and is elevated in patients with PCa. The levels associated with potential PCa is 4 ng/ml, although PCa has been detected in patients with a lower PSA and higher levels have been associated with patients with benign prostatic hyperplasia, a condition of enlarged prostate. Despite the unclear diagnostic potential of PSA tests, they are routinely used to test for PCa (Carsin et al., 2010; Drummond et al., 2014). Patients who present an elevated PSA initially undergo a digital rectal examination, which evaluates the size of the prostate gland. Further investigation requires the patient to undergo a needle biopsy, in which multiple prostate tissue cores are removed via transperineal biopsy (Shariat and Roehrborn, 2008). These tissue samples are then graded according to the Gleason score (Humphrey, 2004). This is analysed via microscopic observation of the stained tissue sample, which is used to detect the histologic pattern. The score is assigned from 1-5 (Figure 1.5) with 1 being almost fully differentiated cells and 5 being the high-grade carcinoma with poorly differentiated cell masses. In PCa there are usually two scores given, the first score for the most prevalent cell type visible and second for the next most prevalent cell type, these scores are added together to obtain the overall Gleason score. The higher the Gleason score the more aggressive the cancer, with a score of 7-10 indicating high grade PCa. This invasive procedure currently used to diagnose PCa, coupled with the unreliable biomarker of PSA concentration, highlights the need for new reliable indicative biomarkers for PCa detection.

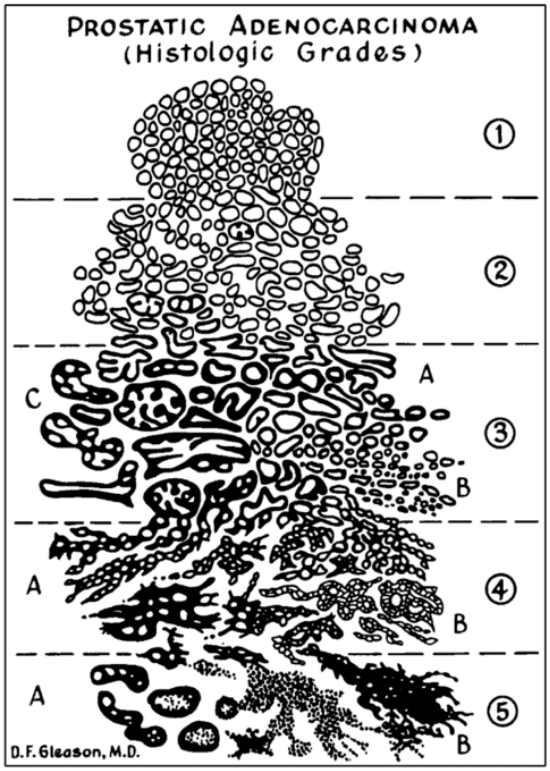

Figure 1.5: *Gleason grade standard drawing outlining the five distinct morphological patterns used to assign score to tissue biopsy of prostate cancer* (Humphrey, 2004)***.***

1.2.4 Epidemiology

PCa is the most prevalent cancer diagnosis in men in 12 regions of the world according to GLOBACON 2018 statistics, including America, Northern and Western Europe (including Ireland), Australia/ New Zealand and Sub-Saharan Africa (Bray et al., 2018). On a global scale it is the second most frequently diagnosed cancer in men (Rawla, 2019), next to lung cancer. Whilst most of the 1,276,106 cases recorded in GLOBACON's 2018 report were associated with an aging population, there is some variations due to testing regimes employed in different regions. African-American men had a higher incidence compared to white men (Kheirandish and Chinegwundoh, 2011), although the incidence in Africa and Asia was lower than that seen in western countries, indicating a lifestyle influence (Chu et al., 2011; Hassanipour-Azgomi et al., 2016). Although there is no overall understanding of the etiology of PCa, family history, age, obesity, and African American ethnicity indicate positive correlation with incidence.

According to the National Cancer Registry of Ireland (NCRI) latest statistics (*NCRI, Annual Statistical Report*, December 2020), PCa is the most prevalent cancer diagnosis given to Irish men, excluding non-melanoma skin cancer. There was an average annual increase of 3665 patients between 2017-2019 which accounts for almost 30% of all male cancer diagnosis. PCa is the third most common cause of cancer related mortality in Irish men, after lung and colorectal cancers with an average of 525 deaths each year. Although the 5-year survival rate of PCa patients in Ireland is quite high (~92%), there is a marked decrease worldwide in patients with CRPC (<5%) (Armstrong et al., 2020).

1.2.5 Current treatment

The current treatment strategy for PCa depends on disease stage at diagnosis (Wadosky et al., 2016). The least invasive option, which can be used in low grade slow growing PCa cases, is active surveillance. This is a strategy employed in consultation with the patient and the doctor, whereby no immediate action is taken, rather the patient is regularly monitored for any changes to the prostate which would imply a progression. This is a system used to prolong the time the patient has before being treated for the cancer, preventing unnecessary early interventions and associated side effects, delivering the best quality of life for the patient (Hayes et al., 2010). If active treatment is required and the disease is confined to the organ and in an early non-aggressive state, then a radical prostatectomy can be performed. This involves minor surgery to remove the prostate gland. This procedure can be preceded or followed by radiation therapy or brachytherapy. The benefits and risks associated with both these options are debated and well-reviewed elsewhere (Bill-Axelson et al., 2014; Drummond et al., 2015). In advanced or recurrent disease, the most common treatment is hormone therapy.

1.2.5.1 Androgen deprivation therapy

Once the disease has advanced past the margins of the prostate gland or is diagnosed as aggressive, as outlined in section 1.3, then the most common treatment is androgen deprivation therapy (ADT). This treatment has been used for advanced or metastatic PCa since the early 1940's (Huggins and Hodges, 1941). Originally ADT was achieved through an orchiectomy, which involved

the patient undergoing a physical castration operation, now many other methods of castration have been developed. Although considered the most effective method, the psychological stress associated with orchiectomy has led to oral or intravenous steroidal treatments or non-steroidal anti androgen drugs becoming the more commonly prescribed method (Schröder et al., 2012).

As discussed androgens are required for the growth of both normal and malignant prostate epithelium (Huggins and Clark, 1940). Therefore, treatment for advanced prostate cancer involves reduction of androgens to castrate levels. This is achieved either by reducing the levels of circulating androgens or by blocking the AR to prevent the androgens action on the cell (Figure 1.5). Pharmacologic castration consists of luteinizing hormone–releasing hormone (LHRH) agonists or antagonists. The LHRH signals the pituitary gland to release FSH or LH, which signal the testes to produce testosterone. Agonist drugs initially result in a spike in testosterone, but a negative feedback loop ultimately reduces the number of LHRH receptors which reduces the amount of circulating FSH and LH, curtailing the androgen secretion to levels observed under castrate conditions (Schally and Comaru-Schally, 2003). Whereas antagonists competitively bind to the LHRH receptors inhibiting LH and FSH release, which also prevents the initial testosterone spike. When LHRH agonists or antagonists are used they prevent the production of androgens by the testes, but as previously mentioned testosterone is also produced, in smaller quantities, by other cells such as the adrenal gland. Other pharmacologic interventions prevent the production of androgens by these cells through inhibition of the enzyme CYP17 (Alex et al., 2016). This enzyme is responsible for the catalytic conversion of pregnenolone and progesterone in progressive steps into weak androgen precursors dehydroepiandrosterone (DHEA) and androstenedione, which are further converted to testosterone or DHT.

Alternatively, there are pharmacologic interventions which prevent the action of androgens by competitively binding to the AR, these are called anti-androgens and are commonly used in conjunction with drugs which inhibit androgen production. There are two types of anti-androgens, steroidal and non-steroidal, although the non-steroidal anti-androgen were produced in the 1970's to alleviate the off-target effects associated with steroidal anti-androgens (Chen et al., 2009). These non-steroidal anti-androgens are specific for the AR, where they compete for binding sites and result in a conformational change which is not conducive to AR translocation, preventing downstream signaling (Rice et al., 2019). The first generation of anti-androgens consisted of flutamide, bicalutamide and nilutamide of which bicalutamide is the favored due to its 2-fold affinity to AR binding and reduced toxicity and reduced side effects (Chen et al., 2009). Initially these treatments prove effective and give some respite, however treatment ultimately fails after

initial remission with the development of castrate resistant prostate cancer (CRPC) (Karantanos et al., 2013), an androgen independent disease. Treatment resistance develops after 18-24 months, signified by androgen independent growth of the tumour. Second generation anti-androgens consist of abiraterone acetate, which targets CYP17 and is used in cases of metastatic CRPC (m-CRPC) or the AR targeting enzalutamide, apalutamide and darolutamide, which are used in cases of CRPC (Rice et al., 2019). There have been many clinical trials investigating treatment strategies with these drugs (Armstrong et al., 2020, 2010, 2007; Tannock et al., 2004). However, despite the huge advancement with these drugs ~20-40% of patients do not respond to treatment and although longer respite is observed eventually resistance inevitably occurs. Highlighting the need for better understanding of AR signaling and the ability to overcome blockade. Life extending treatments for mCRPC after hormone therapy fails are taxane chemotherapy, docetaxel and cabazitaxel or the immunotherapy sipuleucel-T (Nevedomskaya et al., 2018).

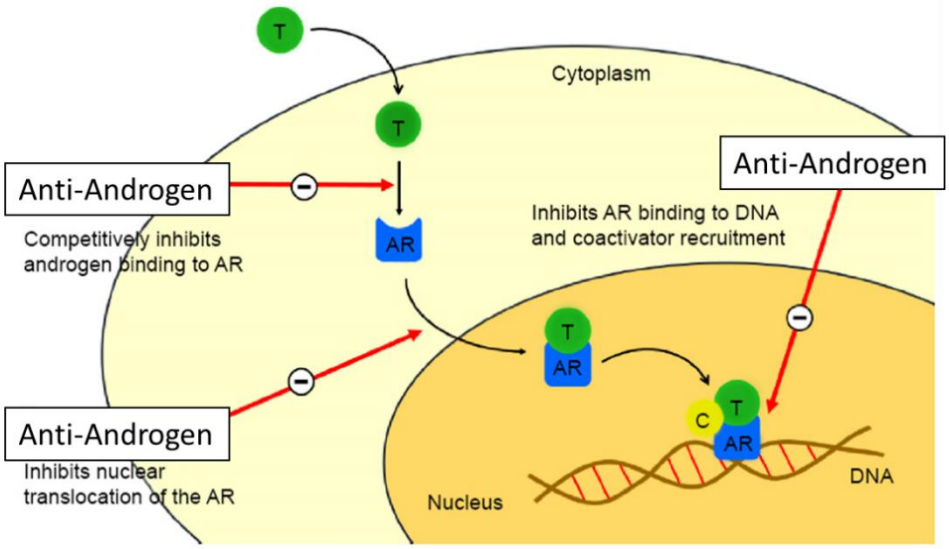

Figure 1.5: *Androgen deprivation therapy is mostly achieved through chemical androgen blockade. Anti-Androgens competitively bind to the androgen receptor, preventing the nuclear translocation of the testosterone activated unit, ultimately preventing the binding to the androgen response element and promotion of the genetic transcription.* (Rodriguez-Vida et al., 2015)

1.3 Castrate resistant prostate cancer

Once ADT fails, the tumour relapses and the disease is known as CRPC, due to the developed ability to grow in castrate levels of serum androgens. Approximately 20% of all PCa cases will progress to CRPC within five years of diagnosis (Kirby et al., 2011), with ~50% of patients receiving ADT progressing to CRPC within 12 months (F.-M. Huang et al., 2018) and almost all patients developing CRPC within 18-24 months (Dong et al., 2019). Due to its resistance to treatments CRPC is ultimately conferred a terminal diagnosis and is the main cause of death in PCa. There have been many developments in CRPC therapeutics with new AR targeting agents such as abiratarone and enzalutamide, however, CRPC eventually develop resistance to all treatments (Dong et al., 2019). Highlighting the need for new treatments and the identification of alternative targets.

Androgen free growth was demonstrated in nude mice xenografted with PCa cells, here it was found that whilst establishing the tumour xenografts was reliant on androgen levels, the growth rate of the established tumour was not (Horoszewicz et al., 1983). This suggests that androgens are not solely responsible for driving proliferation of PCa cells and long-term inhibition of the canonical androgen driven growth signals result in the development of alternative mechanisms. One study indicated progression under ADT was associated with the anti-apoptotic protein bcl-2, which is not expressed in normal epithelial prostate tissue, is overexpressed in some primary PCa cells, and consistently overexpressed in CRPC (Raffo et al., 1995). They went on to show that PCa cells which had been transfected with bcl-2 plasmid showed an increased proliferation in androgen deprived media when compared to control. The transfected cells could withstand the normal apoptotic signals associated with hormone deprivation. Highlighting the development of an anti-apoptotic mechanism with progression to CRPC. There is no clear research defining a definitive alternative growth mechanism in PCa progression under ADT, although there are many proposed, briefly outlined below.

1.3.1 Altered AR function

The AR in its classical genomic activity acts as a nuclear transcription factor, which as discussed translocate to the nucleus upon binding androgens. There are three distinct functional regions, the N-terminus, which is responsible for nuclear transcription, the DNA binding domain and the ligand binding domain (Davey and Grossmann, 2016). Other non-genomic AR activity includes activation of downstream signaling cascades which influence many cellular functions(Foradori et al., 2008). Interestingly androgen binding AR has also an influence the Ca^{2+} homeostasis of the cells (Sun et al., 2006). Both Ca^{2+} influx and intracellular store release have been attributed to this mechanism, resulting in the activation of the various Ca^{2+} regulated downstream signaling cascades some of which are outlined below in section 1.7.

Many reviews outline findings which suggest that alterations to the AR are responsible for the development of CRPC. Alterations such as AR amplification or mutations which result in alternative ligand binding or heightened sensitivity of the AR (Grossmann et al., 2001; Harris et al., 2009; Karantanos et al., 2013). It is widely reported that AR is upregulated in PCa after ADT (Edwards et al., 2003; Grossmann et al., 2001; Hamid et al., 2020) and this amplification, detected in a third of all CRPC (Visakorpi et al., 1995), allows the PCa cells to grow due to activation at low androgen serum levels. Mutations to the AR reportedly occur in ~20% of CRPC (Beltran et al., 2013), which result in loss of binding specificity and heightened sensitivity (Kahn et al., 2014). These mutations allow activation via alternative ligand binding of weak androgens or other hormones such as progesterone or estrogen (Culig et al., 1993; Tan et al., 1997; Taplin et al., 1995).

1.3.2 Epithelial to mesenchymal transition

EMT is a common phenomenon seen after ADT, which infers a metastatic benefit on PCa cells. Also thought to help development of resistance to treatment. The process of mesenchymal transition of epithelial cells is a conserved process which is essential for embryogenesis (Kalluri and Weinberg, 2009), wherein some cells must retain plasticity to allow for development of the embryo. Although it was once considered that upon completion of development these cells became terminally differentiated, it is now accepted that epithelial cells in the fully matured adult can undergo EMT for tissue regeneration or wound healing. Another process which has been shown to utilise this transition is cancer progression and metastasis (Santos Ramos et al., 2017).

The cellular plasticity allows the cell to shed its epithelial anchorage, losing attachment to the basal membrane and cell surface adherence, allowing the mesenchymal cell to migrate. There are many factors which influence EMT such as oncogene growth factors like transforming growth factor- beta (TGF-β), insulin-like growth factor (IGF) or epidermal growth factor (EGF) or signalling pathways like Wnt, sonic hedgehog (shh), PI3K and Notch (Figure 1.6) (Odero-Marah et al., 2018). These pathways activate many similar transcription factors such as Snail, Twist and Slug (Zhang et al., 2016), which inhibit E Cadherin transcription and promote transcription of mesenchymal genes such as Vimentin or N Cadherin. Studies have also indicated that stabilised hypoxia inducible factor (HIF)-1α can promote EMT through Snail activation in breast cancer (Lundgren et al., 2009) and hepatocellular cancer (Zhang et al., 2013).

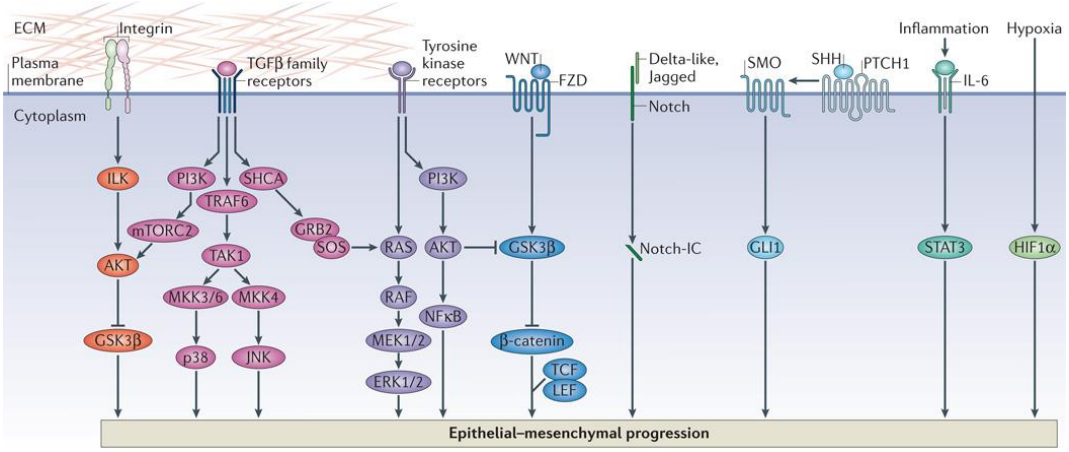

Figure 1.6: *The Epithelial to Mesenchymal transition occurs when an epithelial cell loses epithelial markers such as E-Cadherin and gains mesenchymal markers such as N-Cadherin. This enables the cell to lose the epithelial polarized state and gain the mesenchymal mobility which enables metastatic abilities in advanced cancer cells. There are many molecular pathways which can contribute to this transition.* (Lamouille et al., 2014)

1.3.3 Development of Cancer stem cells

The cancer stem cell (CSC) was first isolated in 1997 by Bonnet and Dick (Bonnet and Dick, 1997), when they demonstrated the ability of an acute myeloid leukemia cell to initiate human leukemia in non-obese diabetic/ severe combined immunodeficient (NOD/SCID) mice. These cells also had the potential to self-renew and proliferate like normal stem cells and had hematopoietic stem cell surface markers. CSC's have since become a highly researched area, it is considered by some as the cell of origin in cancer development, which causes tumorigenesis, can resist treatment and leads to cancer relapse (reviewed by Clevers, 2011; Jordan et al., 2009). Although there is some debate over the lineage, does it arise after a mutation of the normal stem cell, which transforms it to an oncogenic CSC, or does it originate from a progenitor cell which has undergone mutation to restore self-renewal capability (Al-Hajj and Clarke, 2004). CSC's, like normal stem cells can self-renew, show hierarchy, and can differentiate into the full lineage of cells. CSC's can form colonies from a single cell and can develop as spheres (Moltzahn and Thalmann, 2013), they can also resist treatment and drive metastasis (Islam et al., 2015). CSC's are involved in activating many downstream pathways involved in cancer progression, similar to those seen in EMT, such as Notch, Wnt/ß Catenin, TGF-ß, Hedgehog, PI3K/Akt/mTOR and Jak/Stat. This has led to suggestions that CSC's are differentiated cells which have undergone EMT (Hollier et al., 2009; Mani et al., 2008; Morel et al., 2008; Nieto, 2013). Since EMT is a commonly seen phenomenon in PCa after ADT (Byrne et al., 2016; Sun et al., 2012), this could have implications in PCa treatment, particularly for CRPC.

CSC are present in many solid tumours including PCa, which is clearly demonstrated by the repeated ability of the prostate epithelium to regenerate upon reintroduction of androgens after induced cell death through androgen withdrawal (Richardson et al., 2004). Research looking specifically at PCa stem cells (PCSC) have utilized this knowledge and suggested resistance to ADT develops due to stem cell survival under treatment and subsequent proliferation (Collins et al., 2005; Collins and Maitland, 2006; Harris et al., 2009). It is postulated that since PCSC's have no AR and are not reliant on androgens for growth and proliferation, they not only survive but are enriched through ADT and result in PCa recurrence after treatment (Tang et al., 2009). PCSC's can be isolated from PCa tissue or cell lines using cell surface markers CD44 and CD133 (Moltzahn and Thalmann, 2013).

Research specifically looking at PCa development from CSC is conflicted due to the heterogenous nature of the normal prostate. There is some debate as to the origin of the PCSC (Rybak et al.,

2015), with both basal and luminal cells demonstrating the ability to regress to CSC's (Goldstein et al., 2010; Wang et al., 2013). Some report that since PCa is phenotypically luminal, that the PCSC originates from the epithelial secretory luminal cells (Wang et al., 2009, 2014). However, with the basal cells ability to evade apoptosis under low androgen levels and then go on to repopulate the basal and luminal cell population on androgen normalisation, this is also regarded by many as the cell of origin for PCSC (Goldstein et al., 2010; Lawson et al., 2010; Smith et al., 2015).

1.3.4 Tumour Microenvironment

When considering the progression of any cancer it must be acknowledged that tumour cells do not exist alone, they are part of a complex biological system. This system influences the growth and invasiveness of the cancer, through interactions between the cancer cells, the extracellular matrix (ECM) and the circulating cellular components (Sounni and Noel, 2013). The tumour microenvironment (TME) consists of immune cells, ECM, inflammatory cytokines and cancer associated fibroblasts among others (Baghban et al., 2020). In order for cancer to progress and express the entire range of cancer hallmarks as outlined by Hanahan & Weinberg (Hanahan and Weinberg, 2011), the TME must play an integral role. PCa tumour progression is also assisted by the TME, incorporating such hallmarks as immune cell modulation, alteration in the ECM and enhanced angiogenesis.

The oxygen pressure experienced in the TME is an area of intensive research, due to the conflicting roles of hypoxia. On the one hand hypoxia drives cell arrest and death, whereas in cancer it has the potential to drive the emergence of an aggressive phenotype. Like many solid tumours, PCa tumours are associated with hypoxia, and HIF-1α expression is significantly correlated with Gleason score in PCa patients (M. Huang et al., 2018).

1.3.4.1 Hypoxia

Hypoxia is a condition of low oxygen levels which is associated with many cancers and is becoming the focus of many potential therapeutic interventions (Wigerup et al., 2016). The TME experiences lower oxygen pressure compared to normal tissue due to increased cellular proliferation and a

lack of developed vasculature (Kizaka-Kondoh and Konse-Nagasawa, 2009). Normal O_2 is often defined as 20% O_2, as this is the O_2 pressure (pO_2) experienced in air at atmospheric pressure. The pO_2 in tissues however generally ranges from 4%-7% depending on the tissue. The pO_2 found in tumour cells is generally much lower ranging from 0.2%-4%, with PCa generally exhibiting very low pO_2 ~0.4% (McKeown, 2014).

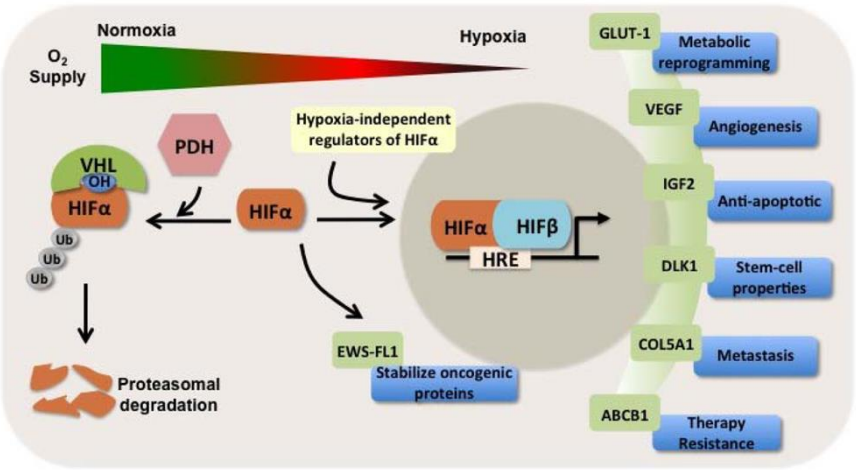

Figure 1.7: *Under normal oxygen conditions HIF-α become ubiquinated and undergoes proteasomal degradation, whereas under hypoxic conditions HIF-α translocate to the nucleus where they dimerise with HIF-ß and bind to the HIF response element (HRE) where they initiate transcription of a range of cancer promoting genes.*

HIF's are made up of two elements, the O_2 labile HIF-α's (HIF-1α, HIF-2α or HIF-3α) and the constitutively expressed HIF-1ß.(Harris, 2002; Vaupel, 2004; Ziello et al., 2007). Under normal pO_2 conditions HIF-1α becomes hydroxylated on two proline residues, which allows binding of Von Hippel-Lindau (VHL), a tumour suppressor protein. VHL then binds E3 Ubiquitin ligase which adds ubiquitin residues to the HIF-1α which is then tagged for proteasomal degradation (Cockman et al., 2000). Under hypoxic conditions HIF-1α does not undergo proteasomal degradation and therefore is available to translocate to the nucleus where it heterodimerizes with HIF-1ß and activates transcription (Figure 1.7).

Emerging research, has shown that HIF activation plays a role in promoting EMT and the emergence of stem cell populations (Masoud and Li, 2015; Vadde et al., 2017; Yeo et al., 2017). HIF-1α is directly responsible for the maintenance of stemness in hematopoietic stem cells

(Takubo et al., 2010) and the activation of pathways and genes which regulate stemness such as Oct3/4, Nanog and Notch (Keith and Simon, 2007; Kim et al., 2009) (Figure 1.8). Fully differentiated glioma cells have the ability to dedifferentiate under hypoxic conditions to stem like cells (Wang et al., 2017), which had increased proliferation and neurosphere formation which was inhibited by silencing HIF-1α. Interestingly increases in Oct3/4 expression levels could be directly correlated with increased HIF-2α expression over decreasing O_2 tensions, which was shown to regulate the hypoxic niche and mediate the stem cell phenotype (Seidel et al., 2010).

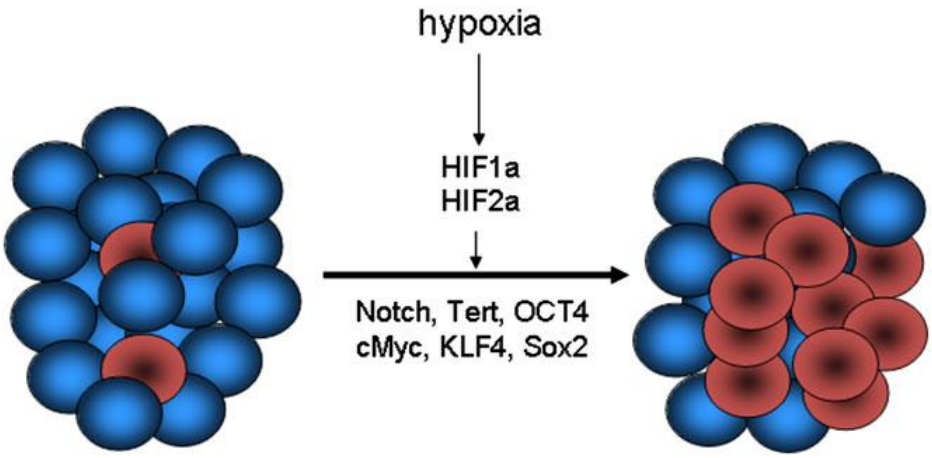

Figure:1.8*: Stem cell pathways are activated under Hypoxic conditions via HIF signalling.* (Carnero and Lleonart, 2016)

Studies have directly linked HIF to the emergence of PCa stem cell (PCSC) populations, with elevated levels of HIF-1α promoting stem cell survival in the hypoxic microenvironment (Marhold et al., 2015). PCa cell lines under hypoxic conditions with activation of HIF-1α have increased expression of stem cell transcription factors Oct3/4 and Nanog, as well as marker CD133, which correlated with an increase in stem cell populations (Sánchez et al., 2020) and with increased colony forming ability. Highlighting the fact that in PCa HIF selects for stemness and that the resultant stem cells have increased tumorigenic potential to promote tumour redevelopment. Since PCa is known to exist in a hypoxic environment, HIF signalling could be contributing to treatment resistance and progression to CRPC through enhanced PCSC.

Interestingly, castration, which results in cell death (Lekås et al., 1997; Shabsigh et al., 1998), also enhances the development of a hypoxic microenvironment (Shabsigh et al., 2001). This may seem

contradictory since a reduced cellular concentration should reduce the demand for available oxygen. However studies have shown that ADT treatment with the anti-androgen bicalutamide induces an immediate and dose dependent reduction in O_2 levels (Byrne et al., 2016). This low O_2 level allows the stabilized HIF-1α elicit transcription of genes which infer survival, such as migration, autocrine growth factors and metabolic reprogramming along with therapeutic resistance (Semenza, 2012; Vaupel, 2004). The mechanism which enhances the expression of HIF-1α under ADT is not fully understood, although calcium influx through cell membrane ion channels has been indicated in the regulation of HIF-1α, transcription, translation and nuclear translocation (Azimi, 2018).

1.4 Ion channels in cancer

The plasma membrane is a lipid bilayer which encapsulates the cell contents and acts as a barrier separating intracellular ions from extracellular ions. Ion channels are membrane spanning proteins which facilitate the passive passage of these inorganic compounds across the plasma membrane (Alberts et al., 2002). There are many types of ion channels, which are usually selective for a particular type of ion, although some are less selective, and are classified according to the type of ion they transport. These ion channels are tightly regulated and contain gating mechanisms which are usually voltage or ligand dependant (Figure 1.9). The primary ions, sodium (Na^+), potassium (K^+), calcium (Ca^{2+}) and chloride (Cl^-) each carry a charge, which creates the membrane potential. This is the difference in the electrical potential between the interior and the exterior of the cell, due to the unequal distribution of these ions. Through this tightly regulated ion channel transport mechanism the ions are maintained at a concentration gradient which is essential for the regulation of many cellular functions.

Cellular homeostasis requires a resting potential across the cell membrane, which is maintained in a polarised state, with a negative charge inside the cell relative to the extracellular space. This resting potential is the key to propagating action potentials in excitable cells, such as neurons and muscle cells. However, it also has a key biological function in non-excitable cells which do not propagate action potentials such as epithelial cells, where it has a role in regulating cellular functions such as apoptosis, proliferation, adhesion, migration, cell cycle regulation and volume control (Abdul Kadir et al., 2018; Leanza et al., 2016). This is achieved through changes in the resting membrane potential activating a range of voltage gated ion channels. The resting

membrane potential has been identified as a key regulator in cancer cells, which can have more depolarised membranes enabling heightened proliferation thus facilitating malignant progression (Yang and Brackenbury, 2013). Hence, alterations in the regulation of the resting membrane potential in cancer cells can be influenced through the altered expression of ion channels (Rao et al., 2015).

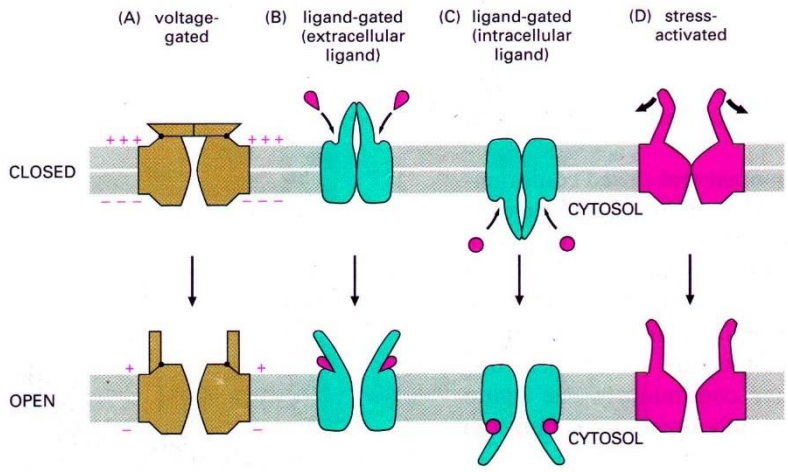

Figure:1.9*: Various mechanisms of ion channel gating including voltage gated which relies on a change in the transmembrane potential (cellular depolarisation or hyperpolarisation) to alter the permeability of the gate. Ligand gated relied on the binding of a particular substrate which alters the conformation of the channel or stress activated channels are opened under mechanical strain.*

The dysfunction of ion channels have long been associated with many diseases grouped as channelopathies, such as cystic fibrosis or atrial fibrillation (Kim, 2014), which can have serious or terminal prognosis. Given the historical identification of ion channels as therapeutic targets for such diseases, there have been many long-established pharmacological treatments developed. The exact mechanisms by which ion channels contribute to cancer progression is a relatively new area of research. Cancer occurs when there are alterations to the normal functioning of the cell. As stated, the balance of ion gradients across the plasma membrane controls many cellular functions such as proliferation and apoptosis. However, given that ion channels are linked to so many cellular process involved in cancer, it is no surprise that they have been identified as potential influencers on malignant progression (Bates, 2015; Kunzelmann, 2005). In fact, Ion channel alterations have been implicated in many studies as having an influence on the hallmarks

of cancer (Fraser and Pardo, 2008; Lastraioli et al., 2015; Litan and Langhans, 2015). This area of research holds great potential due to the fundamental knowledge obtained through the study of ion channels in relation to other diseases and the development of many ion channel targeting drugs. This indicates the potential for pharmacological intervention using currently available ion channel target drugs in conjunction with conventional cancer therapies.

1.4.1 Chloride channels

Cl^- channels are anion channels which facilitate the passage of Cl^- as well as to a lesser extent, bromide (Br^-) and iodide (I^-) (Fahlke, 2001). Chloride channels have a function in membrane potential and also in maintaining cellular volume (Peretti et al., 2015), which is essential to maintain cellular homeostasis and functions such as growth, migration and death. This chloride channel reliant cellular volume has also been demonstrated in PCa cells (Shuba et al., 2000). Dysfunction of these channels is associated with diseases such a cystic fibrosis (Gray et al., 1995) and they have also been identified in contributing to many types of cancers and the development of chemotherapeutic resistance (Hong et al., 2015). They have been particularly associated with CSC's (Peretti et al., 2015), with inhibition resulting in increased apoptosis and chemotherapy sensitivity of CSC's (Kang and Kang, 2008).

1.4.2 Sodium channels

Sodium channels are Na^+ specific and have two distinct types, epithelial Na^+ channels (ENC) and voltage gated Na^+ channels (VGNC). The ENC have specific functions in regulating reabsorption of salts and water in various epithelial cells, including the kidneys (Butterworth, 2010). Whereas the VGNC play an important role in the action potential propagation in excitable cells, although like all other ion channels have functions in non-excitable cells also. The upregulation of various VGNC has been associated with metastasis and invasive characteristic in breast cancer (Fraser et al., 2005), colon cancer (House et al., 2010) and cervical cancer (Hernandez-Plata et al., 2012). VGNC were associated with migration and aggressive potential in experiments carried out on LNCaP androgen sensitive and androgen insensitive cell types. The expression of VGNC was significantly

increased in the androgen independent cells compared to the parental LNCaP (Bennett et al., 2004).

1.4.3 Potassium channels

K^+ channels are responsible for the passage of potassium ions across the cellular membrane. These channels control the membrane potential of the cell, as they allow the passive diffusion of K^+ through the leak channels. K^+ concentration is higher inside the cell membrane than it is in the extracellular fluid, hence the K^+ ions diffuse down the concentration gradient, resulting in the loss of positive ions from inside the cell, leaving a negative resting potential (Chrysafides et al., 2020). They also have gating mechanisms which consist of voltage activation (K_v channels) or Ca^{2+} activation (K_{Ca} channels). K_{Ca} channels are classified according to the K^+ conductance they are responsible for on activation. BK_{Ca} (big) channels respond with a large conductance of K^+ when activated while IK_{Ca} (intermediate) and SK_{Ca} (small) channels have a smaller response (Vergara et al., 1998). Due to the functional influence inferred on many cellular mechanisms through K^+ channels, it is not surprising that they have been implicated in the progression of many cancers (Comes et al., 2015; Huang and Jan, 2014). Voltage gated potassium channels (VGKC) have been associated with proliferation of cancer cells. The VGKC KV10.1 ether-a-go-go (EAG1), is upregulated in many cancers including PCa (Hemmerlein et al., 2006). While an inverse association with KV1.3 has been associated with migratory potential of PCa cells (Abdul and Hoosein, 2002). BK_{Ca} channels have been identified as being upregulated in PCa cell lines compared to normal prostate cells, which resulted in increased proliferation, migration and invasive potential (Du et al., 2016). The expression of BK_{Ca} also correlated with Gleason score in prostate cancer patient tissue samples.

1.4.4 Transient receptor potential channels

Transient receptor potential (TRP) channels are non-selective ion channels which are present in most human cells. They function as ion regulators and have a sensory role in detecting among other things heat, cold and pain (Nilius and Owsianik, 2011; Venkatachalam and Montell, 2007). The TRP superfamily of proteins are subdivided into groups, five type 1 (TRPV, TRPM, TRPC, TRPN

and TRPA) and two type 2 (TRPP and TRPML) (Venkatachalam and Montell, 2007). All TRP channels with the exception of TRPM4 and TRPM5 are permeable to Ca^{2+} (Hasan and Zhang, 2018) and are an integral part of Ca^{2+} signalling. The altered expression of TRP channels have been implicated in tumorigenesis (Liu et al., 2014; Middelbeek et al., 2015; Natalia Prevarskaya et al., 2007; Sagredo et al., 2018), with expression level altering over progression of the disease. In breast cancer, TRPM7 expression has influence over the development of EMT (Davis et al., 2014). TRPM8 is overexpressed in androgen sensitive PCa (Tsavaler et al., 2001), while with progression to the androgen insensitive disease the expression is downregulated. It is also associated with HIF-1α transactivation and stabilisation in PCa (Yu et al., 2014). This suggests that TRP channels play a role in malignant progression.

1.5 Calcium channels

1.5.1 Calcium homeostasis

Calcium ions are common second messengers that are responsible for many processes required for normal cellular function (Clapham, 2007). Intracellular Ca^{2+} concentration ($[Ca^{2+}]_i$) is tightly regulated and maintained at ~10^4 fold lower than the extracellular concentration (Bagur and Hajnóczky, 2017). Intracellular free Ca^{2+} is maintained at ~100nM through the continual action of various pumps and channels of the plasma membrane as well as the ER and mitochondria. The ER acts as a Ca^{2+} store and can hold ~1 mM Ca^{2+}, whereas the mitochondria can hold ~200 nM (Varghese et al., 2019).Variation in $[Ca^{2+}]_i$ impacts many key cellular processes such as proliferation, cell signalling and apoptosis (Tajada and Villalobos, 2020), whereas variation in the oscillation frequency activates many second messenger Ca^{2+} signalling pathways (Berridge et al., 2003). Therefore oscillations in intracellular Ca^{2+} currents due to upregulation of Ca^{2+} channels in cancer cells drive the progression of tumorigenesis and the development of many cancer hallmarks as well as treatment resistance (Cui et al., 2017).

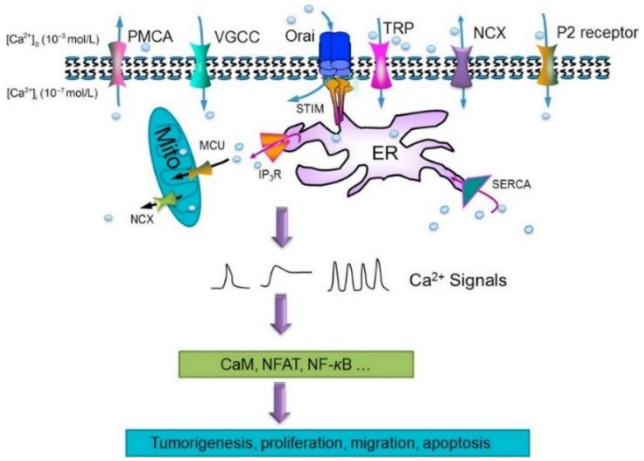

Figure 1.10: *Ion channels responsible for intracellular calcium homeostasis can be altered in cancer cells. This results in activation of downstream effectors due to disrupted calcium signals resulting from increased or prolonged intracellular calcium oscillations*. (Cui et al., 2017)

There are a variety of Ca^{2+} channels which allow the passage of Ca^{2+} and are named according to their mode of activation (Figure 1.10). There are receptor operated channels (ROC), which require binding of a peptide to open. There are store operated channels (SOC) which are controlled by the depletion of Ca^{2+} from intracellular stores (Parekh and Putney, 2005). Emptying of the Ca^{2+} stores from the endoplasmic reticulum (ER) triggers signals which facilitate store operated Ca^{2+} entry (SOCE), which is discussed in more detail below in section 1.5.2. There are also voltage gated calcium channels (VGCC), which are permeable under cellular depolarisation, as discussed in section 1.5.3. Efflux of Ca^{2+} is controlled mostly by the NCX, which can also add to the $[Ca^{2+}]_i$ when it works in reverse mode. The reverse mode is triggered in certain circumstances such as extreme depolarised states or in cases of high intracellular sodium concentrations. Increased intracellular Ca^{2+} is restored to normal concentrations with Ca^{2+} efflux through the plasma membrane calcium pump (PMCA) and NCX along with reabsorption into the ER.

1.5.2 Store operated channels

The main mechanism for Ca^{2+} mobilisation in non excitable cells, including cancer cells is through SOCE. This mechanism is facilitated through the Ca^{2+} release activated Ca^{2+} (CRAC) channels which are a family of channels that sit in the plasma membrane. These channels are activated upon ER store release and facilitate the refilling of the ER stores (Parekh and Putney, 2005). The recent discovery of the mechanism of SOCE has enlightened the research around CRAC channel function, Ca^{2+} signalling and cellular homeostasis. It has been known since the 1980's that cells have intracellular Ca^{2+} stores which release Ca^{2+} upon receiving certain signals. These signals activate ER bound proteins to release the Ca^{2+} stored in the ER (Figure 1.11). Ryanodine receptors (RyR) release Ca^{2+} from the ER upon sensing intracellular Ca^{2+} increase (Endo et al., 1970). The inositol triphosphate receptor (IP_3R) Ca^{2+} release from the ER is initiated when a G-protein coupled receptor (GPCR) on the plasma membrane receives a signal (Streb et al., 1983), which activates the enzyme phospholipase c (PLC), which in turn reduces phosphatidylinositol 4,5-bisphosphate (PIP2) to diacylglycerol (DAG) and IP_3 which transports to the ER and activates IP_3R. It was realised that this resulted in a Ca^{2+} influx from the extracellular space which refilled the internal stores (Takemura and Putney, 1989). However it is only recently discovered that stromal interaction molecule (STIM) 1 and 2 were Ca^{2+} sensors, which sensed the store depletion and signalled the opening of the membrane Ca^{2+} channels (J et al., 2005). This was shortly followed by the realisation that the plasma membrane channels Orai 1,2 and 3, which are highly selective for Ca^{2+} was responsible for CRAC currents (Feske et al., 2006). These discoveries have led to the understanding that SOCE is usually triggered when stimulus of a membrane receptor initiates inositol 1,4,5-triphosphate (IP_3) to signal Ca^{2+} release from the ER (Krizova et al., 2019). Upon depletion of the ER Ca^{2+} stores, STIM1 and STIM2 translocate to the plasma membrane where they physically interact with Orai1, resulting in Ca^{2+} influx. This is then reabsorbed into the ER through the action of the sarco-endoplasmic reticulum Ca^{2+}ATPase (SERCA). Prior to the discovery of the STIM1, Orai, SOCE mechanism TRP channels were thought to provide the entry point for CRAC Ca^{2+} (Huang et al., 2006; Montell et al., 2002), although still considered a small contributor (Salido et al., 2009; Worley et al., 2007).

SOCE channels have been implicated in many cancers with both STIM and Orai proteins being identified as cancer therapeutic targets (Fiorio Pla et al., 2016; Motiani et al., 2013; Parekh and Putney, 2005). STIM and Orai are critical components in Ca^{2+} homeostasis by controlling Ca^{2+} entry and store depletion and Ca^{2+} signalling is central to so many cellular processes. Therefore, it is not

surprising that these proteins have been linked to the emergence of many of the cancer hallmarks. STIM1 and Orai have an important role in migratory ability of breast cancer cells, inhibiting expression of either channel with siRNA reduced migration and increased focal adhesions (Yang et al., 2009, p. 1). They also have significant influence on PCa cells, where expression of Orai is dependent on the presence of androgens (Flourakis et al., 2010), which is consistent with the observation that Orai1 becomes downregulated with PCa progression. Inducing ADT by culturing LNCaP cells in androgen deprived media, reduced expression of Orai1, this coincided with a reduced apoptosis, suggesting that apoptotic resistance in androgen independent PCa could be due to this mechanism.

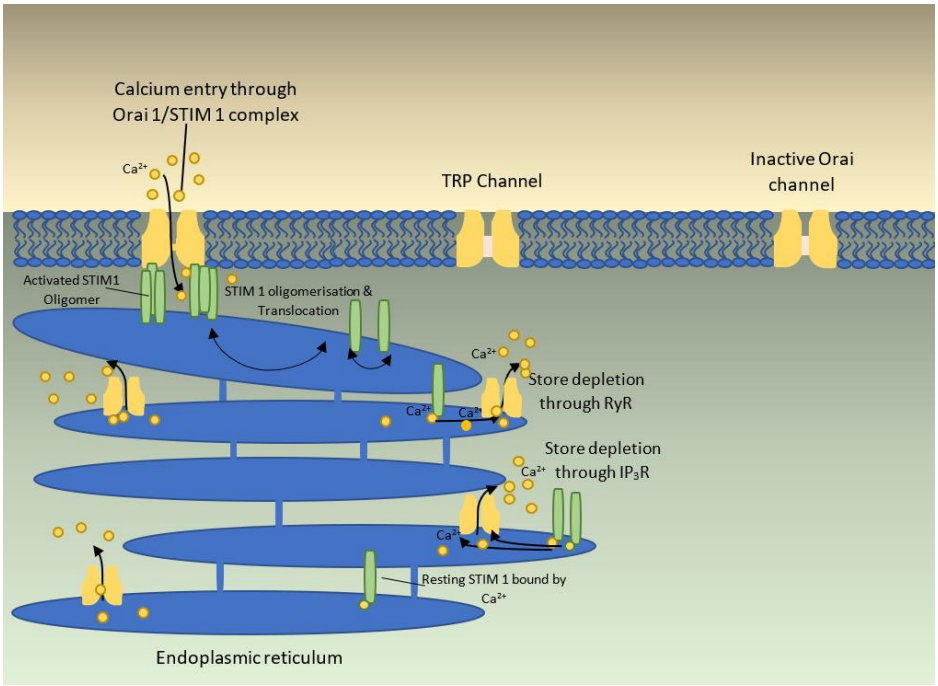

Figure 1.11 *SOCE is predominantly controlled upon store depletion via IP_3R or RyR facilitating the oligomerisation and translocation of STIM1 which binds to the surface channels ORAI or TRPC resulting in conformational change to open passage for calcium ions.*

1.5.3 Voltage gated calcium channels

As stated, Ca^{2+} entry is essential for most cellular functions. The best studied Ca^{2+} channels are the voltage dependant channels (Figure 1.12). VGCC are made up of five subunits, α1 (~190-250 kDa),α2 (~170 kDa),β (~55 kDa),γ (~56 kDa) and δ (~31 kDa), with α1 making up the pore forming unit (Buraei and Yang, 2010; Neely and Hidalgo, 2014; Takahashi et al., 1987). They are transmembrane, Ca^{2+} permeable channels which are activated via membrane depolarisation (Alexander et al., 2015). They are grouped into families, the low voltage activated T type Ca^{2+} channels and the high voltage activated L, N P/Q and R type Ca^{2+} channels (Catterall, 2011; Ertel et al., 2000), which have variations in their voltage activations and the length of activation (Table 1.1). VGCC are typically found in excitable cells, with a growing body of evidence implicating their altered expression in cancer (Buchanan and McCloskey, 2016; Phan et al., 2017; Wang et al., 2015) which has been shown to contribute to enhanced proliferation and metastasis (Kanwar et al., 2020; Warnier et al., 2015).

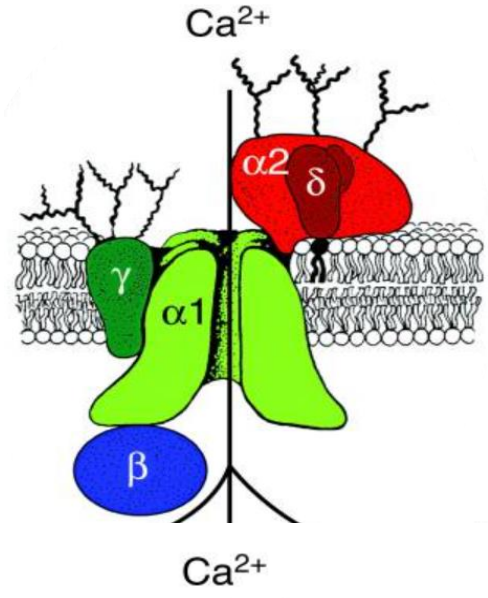

Figure 1.12: *The oligomeric structure of VGCC has five subunits the pore forming α1 subunit, the intracellular β subunit, the transmembrane glycoprotein γ subunit and the disulphide bound dimer subunits of α2 and δ glycoproteins in the extracellular domain (Catterall, 2011)*

1.5.3.1 P/Q-Type calcium channels

P/Q-Type Ca^{2+} channels are high voltage activated and are responsible for synaptic transmission in the central nervous system (Rajakulendran et al., 2012). These channels have also been shown to influence kidney function contributing to the excitation contraction coupling of the renal microvesicles(Hansen et al., 2011). CaV2.1 is the only channel in the P/Q-Type Ca^{2+} channels, but the P and Q-Type currents occur in different locations (Wang et al., 2015). The P-type was first discovered in the Purkinje neurons (Llinás et al., 1989), whereas the Q-Type are located in the cerebral granule neurons (Randall and Tsien, 1995) and are differentiated by splice variation. CaV2.1 is insensitive to dihydropyridine (DHP) but is blocked by a toxin derived from the venom of a funnel web spider, ω-agatoxin IVA (Catterall et al., 2005). Expression of CaV2.1 is downregulated in colorectal, oesophageal and gastric cancers and upregulated in leukaemia (Phan et al., 2017).

1.5.3.2 N-Type calcium channels

N-Type Ca^{2+} channels are activated at high voltages and contribute to neuropathic pain regulation (Phan et al., 2017). Along with P/Q-Type channels they contribute the bulk of synaptic transmission in the hippocampus (Mochida, 2019). CaV2.2 is also DHP insensitive but is again blocked by toxin, ω-conatoxin GIVA, derived from cone snail (Catterall et al., 2005). *CACNA1B* is upregulated in breast and prostate cancer (Wang et al., 2015), but has recently been shown to have a significant increased expression in non-small cell lung cancer and correlated with poor survival (Zhou et al., 2017).

1.5.3.3 R-Type calcium channels

The R-Type Ca^{2+} channels are predominantly located in the neurons and are particularly resistant to calcium channel blockers (CCB) and toxins which block other channels (Wray, 2010). They are recognised by the residual current detected when other currents are blocked. *CACNA1E* has low expression levels in prostate and breast cancer (Phan et al., 2017), but was overexpressed in oesophageal and uterine cancers, where it could be identified as a novel target (Wang et al., 2015).

1.5.3.4 T Type calcium channels

T-type Ca^{2+} channels are activated at more negative action potentials than other Ca^{2+} channels, approximately -55 mV, resulting in a large Ca^{2+} entry (Perez-Reyes, 2003), which make them essential in cardiac pace making and nervous synapse firing. They are part of the CaV3 family of Ca^{2+} channel α1 subunits and have three members CaV3.1, CaV3.2 and CaV3.3. (Santoni et al., 2012) and have highest expression in the heart, brain and nervous system (Ertel et al., 2000). T-type Ca^{2+} channels have been implicated in many cancers particularly brain cancers (Ruggieri et al., 2012; Santoni et al., 2012; Zhang et al., 2012). A recent research paper has implicated the overexpression of CaV3.1 in poor prognosis of lung cancer (Suo et al., 2018, p. 1). However, there are many reports which implicate the upregulation of CaV3.2 in the development of neuroendocrine differentiation in PCa (Gackière et al., 2013a; Hall et al., 2018; Mariot et al., 2002). These studies highlight the increased low voltage activated Ca^{2+} current in LNCaP cells treated with ADT, which drives NED, proliferation and migration in these cells.

1.5.3.5 L-Type calcium channels

L-type Ca^{2+} channels are high voltage activated Ca^{2+} channels which are slow to deactivate. They make up the CaV1 family of Ca^{2+} channel α1 subunits and have four members CaV1.1, CaV1.2, CaV1.3 and CaV1.4. CaV1 channels are DHP sensitive (Catterall, 2011, 2000). DHP's act as agonists (BayK8644) or antagonists (Nifedipine), by controlling the gating state of the channel (Alexander et al., 2015), although CaV1.3, which is coded for by the *CACNA1D* gene in humans, is not completely inhibited by DHP antagonists. In fact, L-type Ca^{2+} current play an integral role in PCa progression, it has been shown that blocking L-VGCC delays castration induced cell death (Connor et al., 1988). L-type Ca^{2+} channels are upregulated in many cancer types, including breast, pancreatic, oesophageal and prostate (Wang et al., 2015). Not only could they be contributing to cancer progression through altered Ca^{2+} entry but CaV1.2 and CaV1.3 have also been shown to have the ability to regulate the expression of other proteins. Both these channels have the ability to act as transcription factors through the nuclear translocation of the cleaved c-terminal fragment (Gomez-Ospina et al., 2006; Lu et al., 2015, p. 3). Therefore, L-type Ca^{2+} channels may also contribute to cancer progression through transcriptional regulation of other channels. Further to this, VGCC have many binding sites for proteins involved in the activation of other

transcription proteins such as NFAT and CREB (Kuzmenkina et al., 2019), which have been shown to drive cancer progression (Mancini and Toker, 2009; Xiao et al., 2010).

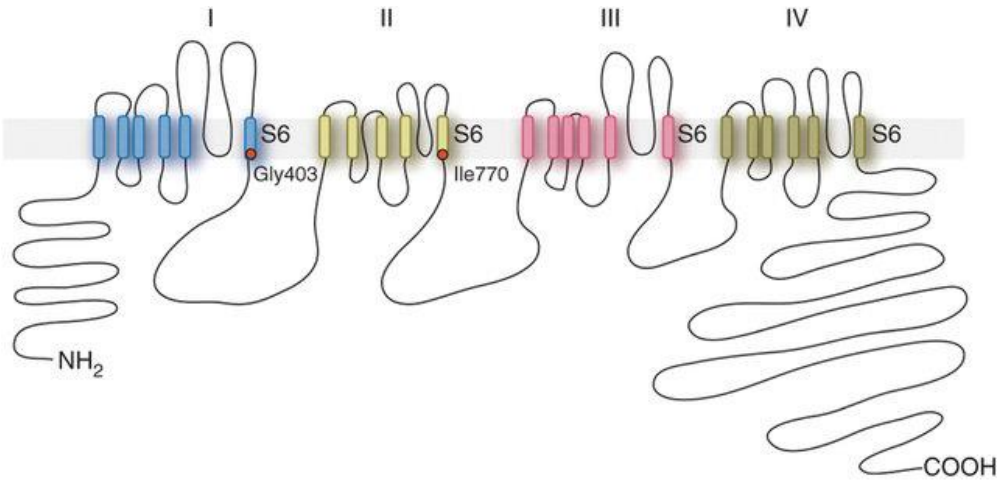

Figure 1.13 *Transmembrane structure of CaV1.3 encoded for by CACNA1D, the pore-forming unit has four homologous repeats (I-IV) consisting of six transmembrane sections with a membrane attached loop between section 5 and section six of each repeat* (Scholl et al., 2013).

1.6 CaV1.3

CaV1.3 is the focal point of this thesis and is the protein we will investigate in relation to progression to CRPC. As outlined CaV1.3 is the α1D member of the L-type VGCC family which is transcribed from the gene *CACNA1D*. This gene is located on chromosome 3 location 3p21.1 and has 16 transcript variants (The Human Protein Atlas, n.d.). CaV1.3, like other VGCC has five subunits, with the α1 subunit forming the pore. The pore is made up of four homologous repeats (I-IV), with each of those consisting of six transmembrane α-helices (S1-S6) and a membrane bound loop between S5 and S6 (Figure 1.13) (Catterall, 2011). S4 is the voltage sensing section of each repeat, which undergoes a conformational change moving outward under depolarised states and consequently opens the pore to Ca^{2+} ions.

Traditionally associated with excitable cells, CaV1.3 is expressed in the brain and central nervous system (although less abundant than CaV1.2) (Catterall, 2011). CaV1.3 plays an essential role in the cochlear hair cells with loss resulting in total hearing loss and CaV1.3 also has an essential role in the pace making activity of the atrial myocytes (Zhang Zhao et al., 2005), described in humans as sinoatrial node dysfunction and deafness (SANDD) (Baig et al., 2011). CaV1.3 has a less negative activation voltage than the other L-type VGCC (Table 1.1) and is less sensitive to inhibition by dihydropyridines (Catterall, 2011). The c-terminus has been shown to have a modulatory domain, which is responsible for both the activation voltage and the Ca^{2+} dependant inactivation of the channel (Lieb et al., 2012), with alternative splice variants resulting in different length c-terminus. The c-terminus has also been implicated in nuclear translocation in atrial myocytes where it acts as a transcriptional regulator (Lu et al., 2015).

1.6.1 CaV1.3 in cancer

Cav1.3 is highly expressed in many types of cancer including prostate cancer (Wang et al., 2015), with one report highlighting that it was downregulated in cancers such as lung, sarcoma and renal cancers (Phan et al., 2017). However, there is limited research available into the direct effects of CaV1.3 in cancer progression, or mechanisms associated with the upregulation. Since Ca^{2+} signalling is involved in many pathways associated with cancer progression (Bong and Monteith, 2018) altered expression of Ca^{2+} channels indicates a significant targetable protein for cancer treatment. Outlined below is the current research pertaining to CaV1.3 expression in cancer.

The expression of CaV1.3 was found to be upregulated in breast cancer, which was increased by estradiol in MCF-7 cells (Ji et al., 2016), resulting in increased Ca^{2+} induced proliferation. A similar estradiol influenced enhanced expression was witnessed in endometrial cancer, contributing to Ca^{2+} induced proliferation and migration (Hao et al., 2015). CaV1.3 has also been implicated in contributing to colorectal cancer migration and invasion through a non-canonical means (Fourbon et al., 2017). Upregulation of CaV1.3 was observed in colorectal cancer tissue samples and siRNA silencing of the α1 subunit of CaV1.3, in colorectal cancer cell line, reduced the cells migratory and invasion potential. Although no inward Ca^{2+} current was detected suggesting a non-canonical mechanism. Silencing α1D with siRNA reduced the $[Ca^{2+}]_i$, indicating that despite the lack of Ca^{2+} flow through the α1D pore, CaV1.3 was controlling $[Ca^{2+}]_i$. This study went on to show altered intracellular expression of α1D in the cytoplasm and nucleus of the cell line which controlled $[Ca^{2+}]_i$ by inhibiting NCX.

Table 1.1 Classification of voltage gated calcium channels indicating approximate voltage activation ranges.

Activation & Dihydropyridine sensitivity		Current	Channel	Gene name	Activation voltage
High Voltage activated	DHP sensitive	L-Type	CaV1.1	*CACNA1S*	8~14 mV
			CaV1.2	*CACNA1C*	-4~-18.8 mV
			CaV1.3	*CACNA1D*	-15~-37 mV
			CaV1.4	*CACNA1F*	-2.5~-12 mV
High Voltage activated	DHP insensitive	P/Q-Type	CaV2.1	*CACNA1A*	-5~10 mV
		N-Type	CaV2.2	*CACNA1B*	7.8~9.7 mV
		R-Type	CaV2.3	*CACNA1E*	-29.1~3.5mV
Low voltage activated	DHP sensitive (less potent)	T-Type	CaV3.1	*CACNA1G*	-46 mV
			CaV3.2	*CACNA1H*	-46 mV
			CaV3.3	*CACNA1I*	-44 mV

1.6.2 CaV1.3 in PCa

In relation to PCa, CaV1.3 has been noted to be increased in a number of studies at a gene (Wang et al., 2015) and protein level (Chen et al., 2014) particularly in CRPC. The upregulated genetic expression of *CACNA1D* has also been suggested as a potential biomarker for advanced PCa (Alinezhad et al., 2016). Interestingly the research by CHEN et al. demonstrated that CaV1.3 was involved in androgen stimulated Ca^{2+} entry and they exhibited how incubation with CCB prevented this and reduced proliferation. Epidemiologic studies carried out on PCa patients also indicate an inverse relationship between PCa progression and the use of CCB (Debes et al., 2004; Annette L. Fitzpatrick et al., 2001). However, research is lacking around CaV1.3 expression in relation to ADT and the functional efficacy of CaV1.3 in the absence of androgen stimulation. Since ADT is the main treatment strategy for advanced PCa and treatment evasion eventually results in the progression to CRPC, there is need for research into the expression and functionality of CaV1.3 in relation to treatment status.

1.7 Calcium dependent transcription factors and signalling

Another mechanism in $[Ca^{2+}]_i$ regulation are Ca^{2+} binding proteins, such as calmodulin (CaM) or calcineurin (CaN). These Ca^{2+} binding proteins readily bind to free Ca^{2+} and initiate signal transduction pathways and gene transcription. Ca^{2+} signalling has many roles in the propagation of cancer cells such as proliferation, apoptosis resistance, metastasis and immune response modulation (Tajada and Villalobos, 2020). However, there are transcription factors which are directly regulated by Ca^{2+}, such as nuclear factor of activated T cells (NFAT) and cyclic AMP response element binding protein (CREB) (Figure 1.14). Hence Ca^{2+} mobilisation through various Ca^{2+} channels can induce activation of these transcription factors. Both transcription factors rely on the activation of CaM, a Ca^{2+} binding messenger protein. CaM binds free Ca^{2+} and undergoes a conformational change allowing it to interact with a wide variety of proteins, affecting many Ca^{2+} signalling processes (Hoeflich and Ikura, 2002). Among the many binding partners of CaM are various protein kinases and phosphatases which can propagate cellular signals through phosphorylation or dephosphorylation of various proteins.

NFAT proteins are a family of transcription factors, of which four are regulated by Ca^{2+} (NFAT 1-4). NFAT is normally present in the cytosol as a phosphorylated protein. When CaM is activated

through increased $[Ca^{2+}]_i$ as a result of Ca^{2+} mobilisation via SOCE or VGCC, it binds to and activates the protein phosphatase CaN, which dephosphorylates NFAT and facilitates translocation to the nucleus. Once in the nucleus NFAT regulates the transcription of numerous genes including those associated with cell cycle regulation and differentiation (Viola et al., 2005). NFAT has been implicated in cancer progression (Quang et al., 2015; Viola et al., 2005) and inhibition of NFAT has been shown to reduce viability in PCa (Kawahara et al., 2015).

CREB is another protein responsible for gene regulation, situated in the nucleus it transcribes many genes including genes involved in cellular metabolism and proliferation (Mayr and Montminy, 2001). CREB when phosphorylated becomes activated and recruits the co-factor CREB binding protein (CRE) which initiates the gene transcription. CREB can be phosphorylated by many protein kinases, however the most common Ca^{2+} regulated phosphorylation occurs through the Ca^{2+}/CaM protein kinases (CAMK). As the name suggests activation of the CAMK is reliant on Ca^{2+} bound CaM, which binds to the CAMK and translocate to the nucleus where it phosphorylates CREB initiating activation and subsequent gene transcription. Activation of CREB has been implicated in cancer progression (Xiao et al., 2010) and in the NED of PCa (Sang et al., 2016).

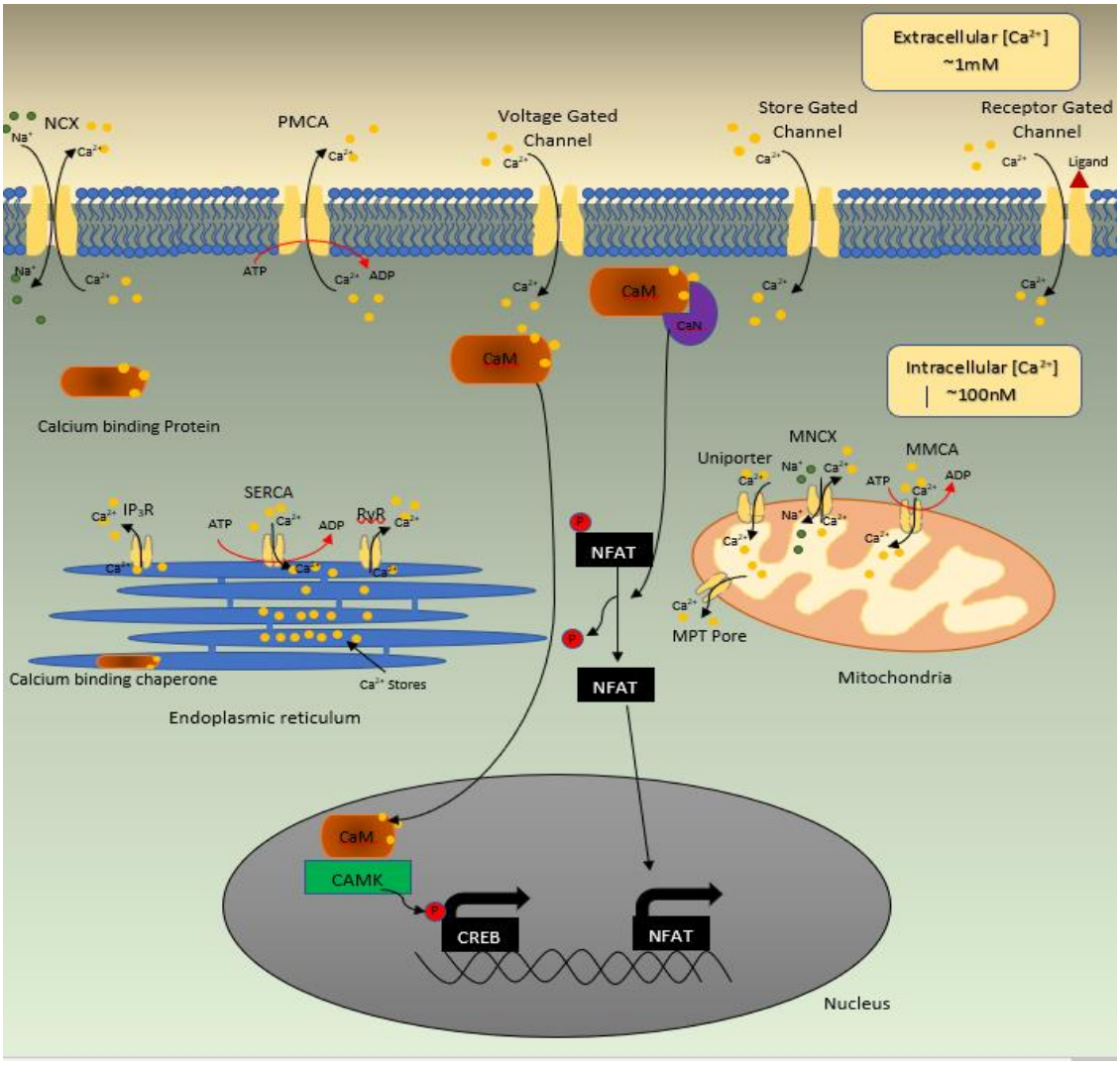

Figure 1.14: *Synopsis of intracellular Ca^{2+} homeostasis and Ca^{2+} sensitive transcription factors. Ca^{2+} homeostasis in the intracellular space is tightly controlled through various channels and stores. Increased intracellular Ca^{2+} occurs when Ca^{2+} is released from the ER through the IP_3R or the RyR or when Ca^{2+} enters the cell through the plasma membrane bound channels. Ca^{2+}efflux occurs through the NCX channel or the PMCA or it is taken up into the ER through the SERCA or into the mitochondria via the MMCA or the mitochondrial Ca^{2+} uniporter. Ca^{2+} effluxes from the mitochondria via the mitochondrial NCX channel or the mitochondria permeability transition pore. Intracellular Ca^{2+} is also bound by Ca^{2+} binding proteins including messenger proteins such as CaM. Ca^{2+} bound CaM initiates various Ca^{2+} signalling mechanisms including gene transcription. CaM binds to kinases such as CAMKII or CaMKIV which translocate to the nucleus and phosphorylate CREB initiating transcription. Alternatively, CaM can bind to CaN a phosphatase which dephosphorylates NFAT and facilitates translocation to the nucleus and transcriptional regulation.*

1.8 Aims and Objectives of the Project

It has become increasingly evident that Ca^{2+} signalling is an integral part of PCa development and progression (Boutin et al., 2015; Chen et al., 2014; Déliot and Constantin, 2015; Fiorio Pla et al., 2016; Flourakis et al., 2010; Lallet-Daher et al., 2009; N. Prevarskaya et al., 2007; Shapovalov et al., 2012). With influence over aspects of hypoxic signalling (Azimi, 2018; Guo et al., 2010; R. Li et al., 2015; Li et al., 2009; Salnikow et al., 2002; Seta et al., 2004) and the development of a stem cell population (Lu et al., 2017; Rosa et al., 2017). Indicating that controlling the Ca^{2+} oscillations at various time points in the development of the disease could be a key target for cancer development, progression and treatment resistance. With CaV1.3 having increased expression associated disease progression to CRPC (Chen et al., 2014; Wang et al., 2015) and reports indicating the potential for the c-terminus to act as a transcriptional regulator (Lu et al., 2015), there is scope to investigate this channel as a key modulator in PCa disease.

AIM: Develop a cell line model of PCa progression under ADT to investigate the impact of CaV1.3 on PCa disease. Determining the role of ADT on CaV1.3 and its associated effect on the modulation of intracellular calcium and associated signalling pathways. Establish the role role of CaV1.3 on PCa biology and in enabling resistance to ADT and progression to CRPC.

Hypothesis: ADT enhances the expression of CaV1.3 in PCa leading to increased intracellular Ca^{2+}, which facilitates treatment resistance and the emergence of CRPC.

Objective 1. Establish impact of ADT on CaV1.3 expression in PCa progression.

Objective 2. Investigate the effect upregulated CaV1.3 has on the Ca^{2+} homeostasis of PCa at various stages of ADT and the progression to CRPC.

Objective 3. Determine if CaV1.3 driven Ca^{2+} signalling has an influence on the stability of HIF-1α.

Objective4. Identify the mechanism of CaV1.3 and its impact on Ca^{2+} signalling in relation to progression of PCa under ADT.

Chapter 2 - Materials and Methods

2.1 Cell culture & Mouse models

Throughout the project we cultured a range of PCa cell lines which were used to represent PCa progression under ADT. We chose LNCaP cells treated with the ADT drug bicalutamide. These cells represented three distinct stages on the progression to CRPC under ADT as outlined in Figure 2.1.

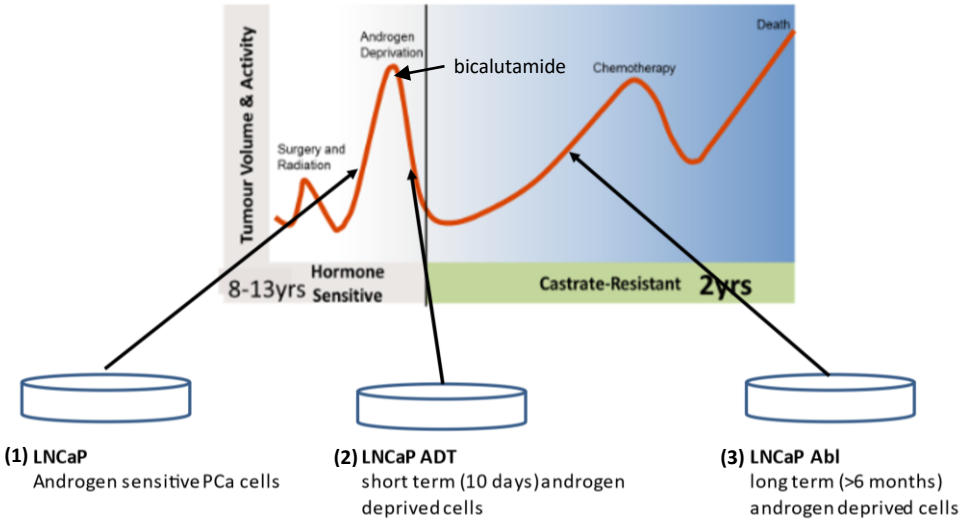

Figure 2.1: *Timeline of PCa progression with indications of various treatments over time. The black arrows indicate the stage of treatment represented by the cell lines used in the project.*

(1) LNCaP cells were first isolated by J.S Horoszewicz et al. in 1977 from the lymph node of a 50-year-old Caucasian male who had metastatic PCa (Horoszewicz et al., 1983). These epithelial cells are androgen receptor positive and respond to androgens with a doubling time of ~ 60 hours. LNCaP cells are loosely adherent and do not grow to confluency but rather have a non-uniform distribution *in vitro*. These cells were selected as they are androgen responsive and have been shown to be adaptive to growth in the presence or absence of hormonal stimulation (Langeler et al., 1993). This best facilitates the investigation of the effects of ADT on hormone responsive PCa through to androgen independence.

(2) The LNCaP-ADT cells were established in our lab by passaging LNCaP cells in media supplemented with 10 µM bicalutamide for 7-10 days. Bicalutamide was used to keep the experimental conditions both consistent and clinically representative to ADT. These cells were

used as an intermediary between androgen sensitive and androgen insensitive cell growth under ADT.

(3) The LNCaP-abl cells were previously established by Culig et al. through sustained passaging of LNCaP cells in androgen depleted media for >87 passages. The growth of these cells adapted to the continued androgen deprivation and eventually became inhibited by androgens and stimulated in the presence of the androgen receptor blocker bicalutamide (Culig et al., 1999). These cells were selected to represent the androgen independent cell line as they demonstrate castrate resistant like growth with continued ADT, whilst retaining the characteristics of prostatic epithelium directly derived from the LNCaP cell lineage. This eliminates any potential effects derived from molecular variances between cell lines (Dozmorov et al., 2009).

The *in vivo* experiments were performed on tumour tissues donated to our lab from Dr Declan McKenna's group in the University of Ulster. These tissues were selected due to the treatment strategies which reflected the cell model treatment (Byrne et al., 2016). Briefly BALB/C immune-compromised (SCID) mice ~8-10 weeks were housed in standard pathogen free conditions. Surgery was performed under aseptic conditions and body temperature was maintained using heat pads. Tumours were established on the back of the SCID mice by subcutaneous injection using a 21-gauge needle. Tumours were established using $2*10^6$ LNCaP cells suspended in 100 ml of Matrigel. After 7 days treatment was initiated, bicalutamide was prepared in 0.1% DMSO (vehicle) and orally administered once daily as 2-6 mg/kg with control mice receiving equivalent dose of vehicle. Mice were culled on day 0, 7, 14, 21 and 28 after treatment initiation and tumours were excised under aseptic conditions. Tumours were stored at -20^{o}C until required.

2.1.1 Sterile culture methods

All cell culture took place in a class II safety cabinet, which was regularly serviced and maintained. Prior to culture the cabinet was initially exposed to ultraviolet (UV) light for 30 mins and then sterilised with a 70% dilution of industrial methylated spirits (IMS) and wiped clean. All equipment used within the safety cabinet was sprayed with IMS prior to being placed inside. All pipette tips, microtubes and suitable solutions (such as PBS & water) were autoclaved before use and were opened within the safety cabinet. All other reagents used for cell culture were sterile on delivery and were aliquoted within the safety cabinet under sterile conditions.

2.1.2 Media preparation

Before culturing cells, the required culture media was prepared as outlined as below.

Supplemented RPMI

500mls RPMI 1640 (ATCC modified) (Gibco) was supplemented with 50mls (10%) fetal bovine serum (FBS) (Gibco) and 5mls (1%) Penicillin- Streptomycin (pen/strep) 5000 U/ml (Gibco). Once supplemented the media was aliquoted into sterile 50ml tubes and stored at 4^{o}C.

The stock FBS was aliquoted into sterile 50ml tubes and stored at -20^{o}C until required. The stock pen/strep was aliquoted in 5ml into sterile tubes and stored at -20^{o}C until required.

Charcoal stripped media

500 mls RPMI 1640 (ATCC modified) (Gibco) was supplemented with 50 mls (10%) charcoal stripped FBS (Gibco) and 5 mls (1%) pen/strep 5000 U/ml (Gibco). Once supplemented the media was aliquoted into sterile 50 ml tubes.

Androgen deprivation therapy media

Media used to induce ADT in LNCaP-ADT cells and to maintain LNCaP-ablcells was made up by adding 5 µl (10 µM) bicalutamide (Sigma Aldrich) to 50mls supplemented media as needed.

Bicalutamide stock concentration of 100 mM was made up by adding 43 mg bicalutamide (MW 430.390 g/mol) to 1 ml dimethyl sulfoxide (DMSO).

Cobalt chloride media

Cobalt Chloride media was made up to induce Hif-1α activation in the cells as a positive control for hypoxia. Media containing Cobalt Chloride was made up as needed by aliquoting out appropriate volume of supplemented RPMI and adding 1 µl/ml of 100 mM stock Cobalt Chloride to make final concentration of 100 µM Cobalt Chloride (Sigma Aldrich).

Cobalt Chloride stock concentration of 100 mM was made up by adding 23.79 mg cobalt (II) chloride hexahydrate (MW 237.9 g/mol) to 1 ml sterile distilled water.

Calcium channel blocker media

Media containing calcium channel blockers was made up as needed by aliquoting out appropriate volume of supplemented RPMI and adding 0.1 µl/ml of 100 mM stock nifedipine to make final concentration of 10 µM Nifedipine (Acros Organics).

Nifedipine stock concentration of 100 mM was made up by adding 34.63 mg Nifedipine (346.335 g/mol) to 1 ml DMSO.

2.1.3 Waking and feeding cells

Before waking the cells, the water bath was pre-heated to 37°C and the incubator was pre-set to 37°C at 5% CO_2. The prepared media (section 2.1.2) was pre-warmed in the water bath. Pipettes and T75 cell culture flask were sprayed with 70% IMS and placed in the cabinet. The cells were removed from the -80°C freezer and gently thawed in the water bath. The media and the cryogenic vial containing the cells were removed from the water bath, dried, and sprayed down with 70% IMS before being placed into the cabinet. 10 mls supplemented media was placed into a sterile 15 ml tube, 1 ml defrosted cell suspension in 10% DMSO was added to the 15 ml tube. The tube was centrifuged at 800 g for 5 mins. The supernatant was removed and discarded into Virkon™ antiviral disinfectant, the pellet was resuspended in 10mls fresh media, added to a sterile T75 and placed into the incubator at 37°C with 95% air and 5% CO_2. The cells were allowed 48 hours to adhere before the media was refreshed. Afterwards the media was changed every 48-72 hours by removing old media and discarding in Virkon™ antiviral disinfectant and pipetting fresh warmed media into the flask ensuring not to disturb the cells.

2.1.4 Splitting cells

Cells were split for counting or propagation into other flasks. Once the cells were approximately 80% confluent they were split 1:4. Water bath was pre-heated to 37°C, media, sterile phosphate buffered saline (PBS) and Trypsin EDTA (0.5%)(Gibco) was pre-warmed in the water bath. Flasks were placed in safety cabinet and the media was removed and discarded into Virkon™ antiviral

disinfectant. The cells were gently washed with 5 mls PBS ensuring that the cells did not detach from the flask. The PBS was removed and discarded into Virkon™ antiviral disinfectant and 3 mls of Trypsin 1X was added to the flask. The flask was returned to the incubator for 1-2 mins until the cells were no longer adhered. 3 mls of warm fresh media was added to the flask to inactivate the trypsin. The surface of the flask was washed down with the cell suspension to ensure that all the cells were removed from the surface of the flask. The cell suspension was placed into a sterile 15 ml tube. The cells were centrifuged at 800 g for 5 mins. The supernatant was removed, and the pellet was resuspended in 10 mls fresh media. For a 1:4 split 2.5 mls of the cell suspension was added to a new T75 flask and 7.5 mls fresh media was added to bring the total volume up to 10 mls. The flask was placed back into the incubator.

2.1.5 Counting cells

After resuspending the pellet in fresh media, the cells were counted. 10 µl cell suspension was added to 40 µl trypan blue (Gibco) and left for 1 min. 10 µl of the cell trypan blue mixture was added to a haemocytometer and counted under 10X magnification. The four outer quadrants were counted (Figure 2.2), and the cell number was calculated as outlined below:

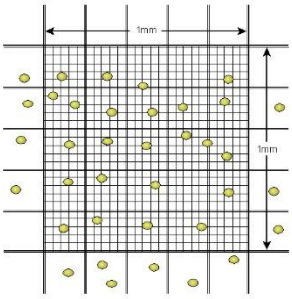

Total number counted/4 = average number per quadrant
Average number *dilution factor (5) = total number of cells 10^4 /ml

The number of cells per ml was used to calculate exact seeding densities for experiments.

Figure 2.2: *A quadrant of a haemocytometer showing 1 mm*1 mm*0.1 mm = 3 mm^3 or 10^4*

2.1.6 Cryopreservation of cells

Once a cryovial of cells were woken up two vials were frozen down to maintain cell stock. Cells were grown in T75 flask until they were at least 80-90% confluent. Cells were then removed from the flask as outlined (section 2.1.4). The pellet was resuspended in 1ml of supplemented media containing 10% DMSO. The cell suspension was placed in a cryogenic vial (Nunc) labelled with cell type, date, and passage number. The vial was placed into a Mr Frosty™ freezing container which contained isopropyl alcohol in the outer layer. This ensured that the cells decreased in temperature at a rate of 1^{o}C per minute to reduce shock. After 24 hours the cells were removed from the freezing container and stored at -80^{o}C until needed or placed into liquid nitrogen dewar for long term storage.

2.1.7 Androgen Deprivation Therapy

LNCaP cells were counted and seeded into a 6 well dish at $4*10^4$ cell/ml in supplemented RPMI (section 2.1.2). They were incubated for 24-48 hours, the media was then changed, and the cells were fed with androgen deprivation media, which contained anti androgen treatment bicalutamide as used to treat PCa patients. The cells were cultured under androgen deprived conditions for 7-10 days.

2.1.8 Hypoxic conditioning

Cell culture dishes containing cells were placed into hypoxic chamber (Figure 2.3), which contained a tray of sterile water for humidity, in the safety cabinet. The hypoxic chamber was clamped shut and moved to the fume hood. Once in the fume hood the chamber was flushed with 1% oxygen gas (1% O_2, 5% CO_2 and 94% N_2) at a rate of 20 litres per minute for 5 mins. The tubes were then clamped shut to retain the low oxygen level and the hypoxia chamber was placed into the incubator. This process was repeated after 1 hour to ensure removal of any oxygen which may have been contained within the media. Cells were incubated for 24 hours at 37^{o}C.

Figure 2.3: *Hypoxic chamber with inflow and outflow tube fitted with tube clamp clips and sealing chamber clamp.*

2.1.9 Calcium Channel Blockade

Cells were seeded into dishes at densities 5*10^5 cell/ml. All cells were allowed 48 hours to adhere and were then incubated with calcium channel blocker media (section 2.1.2) at the concentration indicated throughout the results chapters or media containing 1 µl/ml DMSO as control. Depending on the experiment the treated cells were either cultured under hypoxic conditions (section 2.1.8) or normal O_2 conditions (37^{o}C 5% CO_2.) for 24 hours.

2.1.10 Mycoplasma testing

All cell lines were routinely tested for mycoplasma using the MycoAlert™ mycoplasma testing kit (Lonza). These tests were carried out in the National Institute for Cellular Biotechnology (NICB) here in DCU. Briefly cells were cultured for at least three passages in media containing no antibiotic and no drugs. The media was collected from the cell culture 72 hours after media change and centrifuged at 800 g for 5 mins to remove any cell debris. 10 0µl of the conditioned media was added to a white 96 well plate (Sarstedt). 100 µl MycoAlert™ Plus reagent was added to each sample well and incubated at RT for 5 mins. Luminescence was recorded on a plate reader (Biotech). Then 100 µl of MycoAlert™ Plus substrate was added to each well and incubated at RT for 10 mins. The luminescence was recorded again and the ratio between the first and second reading was calculated. Luminescence ratio <1 was mycoplasma negative, 1-2 was considered borderline and >2 was mycoplasma positive.

2.2 RNA and Polymerase chain reaction (PCR)

2.2.1 RNA Extraction

Cell lines

Total ribonucleic acid (RNA) was extracted using High Pure RNA Isolation Kit (Roche). Briefly, media was removed from wells and the cells were gently washed with PBS. 200 µl PBS was then added to each well and the cells were scraped off using cell scraper and collected in sterile RNase free micro centrifuge tube (Sarstedt) and moved to the bench. The bench was sprayed with RNaze ZAP (Sigma) and Biosphere DNase, RNase free filter tips were used (Sarstedt). 400 µl lysis buffer was added to each tube and the tube was vortexed for 15-20 s and transferred to filtered collection tube and centrifuged at 8000 g for 15 s. The flow through was discarded and the contents of the filter was incubated for 15 mins with DNase incubation buffer containing DNase I. The RNA was then washed with wash buffer and eluted into a RNase free labelled tube and stored at -80^{o}C.

Mouse tissue

Frozen tissue samples were slowly thawed over ice and sectioned with a sterile blade. The sectioned tissue was placed into an RNAse free 1.5 ml tube (Sarstedt). The tissue was roughly homogenised with a sterile pipette tip (Sarstedt). TRIzol reagent (1 ml) (Invitrogen) was added to the tube containing the homogenised tissue sample and incubated at room temperature for 5 mins. Chloroform (0.2 ml) (Acros organics) was added to the tube and the tube was gently shaken for 15 s, followed by 3mins incubation at room temperature. The tubes were then placed into a centrifuge at 12000 g for 15 mins at 4^{o}C. When removed the homogenate had separated into three layers, with the upper aqueous phase containing the RNA. The upper layer was transferred to a fresh RNAse free 1.5 ml tube (Sarstedt), ensuring not to disturb the lower layers. Ice cold Isopropyl alcohol (0.5 ml) (Sigma) was added to the RNA mixture and incubated at room temperature for 10 mins to precipitate the RNA. The tubes were then centrifuged at 12000 g for 10 mins at 4^{o}C. The supernatant was discarded, and the RNA was adhered as a pellet attached to the side of the tube. The pellet was washed with 75% ethanol (Fisher chemical) and the tube was inverted gently ensuring not to dislodge the pellet. The ethanol was discarded, and the pellet was airdried for 2 mins. The pellet was not allowed to completely dry out as this would prevent resuspension. The

pellet was resuspended in 50 µl RNAse free water which was pipetted down the side of the tube and the tube was then incubated on ice for 10 mins.

2.2.2 RNA Quantification

Total RNA extracted was quantified using NanoDrop 1000™ (Thermo Scientific). 1 µl RNA extraction was used to give quantity in ng/µl. Purity of RNA was assessed using absorbance 260 nm and 280 nm (A_{260}/A_{280}) with a ratio of 1.8-2.2 accepted as pure RNA.

2.2.3 cDNA synthesis

Complimentary deoxyribonucleic acid (cDNA) was synthesised from RNA extractions using Transcriptor first strand cDNA synthesis kit (Roche). Briefly, between 500 ng-1 µg total RNA was added to a PCR tube on Ice containing 2.5 µM Anchored-oligo primer and 60 µM random hexamer primer and made up to 13 µl with PCR grade H_2O. The mixture was denatured at 65^oC in thermocycler with heated lid for 10 mins and immediately cooled on ice. Then added to the cooled tube was 4 µl transcriptor reverse transcriptase reaction buffer (5x), 0.5 µl Protector RNase inhibitor (40 U/µl), 2 µl deoxynucleotide mix and 0.5 µl Transcriptor reverse transcriptase (20 U/µl). The gently mixed tube was incubated in the thermocycler for 10 mins at 25^oC followed by 30 mins at 55^oC and finally the enzyme was deactivated by heating the tube to 85^oC for 5 mins. The tube was immediately placed on ice and stored at -20^oC until required.

2.2.4 Primer Design

All primers were designed using primer 3 (https://primer3.ut.ee/), using Exon spanning sequences where possible. Oligo Calc (http://biotools.nubic.northwestern.edu/OligoCalc.html) was used to detect any potential hairpin formations or self-annealing sites. All primers were acquired from Sigma Aldrich (Table 2.1). Lyophilised primers were reconstituted with PCR grade H_2O to stock concentration 100 µM. Stock was aliquoted into 50 µl aliquots, labelled appropriately and stored at -20^oC. Working stock primers (5 µM) made up by adding 5 µl of 100 µM stock and made up to

100 µl with PCR grade water. Stock was aliquoted into 10 µl aliquots, labelled appropriately and stored at -20°C. 5 µM working stock primer was added to reaction, 1 µl in 10 µl final PCR reaction total volume for a final concentration of 0.5 µM.

Table 2.1: **Primer sequences used for qPCR analysis of gene expression; all small scale desalt purification.**

Sequence (5'-3')		
Target gene	**FORWARD**	**REVERSE**
ACTB	CCAACCGCGAGAAGATGA	CCAGAGGCGTACAGGGATAG
HPRT1	TGGACAGGACTGAACGTCTT	GGGCTACAATGTGATGGCCT
HMBS	TGTGGTGGGAACCAGCTC	TGTTGAGGTTTCCCCGAAT
TBP	GAGCTGTGATGTGAAGTTTCC	TCTGGGTTTGATCATTCTGTAG
18s RNA	GGAGTATGGTTGCAAAGCTGA	ATCTGTCAATCCTGTCCGTGT
CACNA1D	ATGTAGGAGTGGCTGGGTTG	CCATGGTGATGCACTGAAAC
SRC	CCTCCTTCCCCGTACTTTGT	AGGCACTCTTTTCCCTCCTC
ENO2	CTGTGGTGGAGCAAGAGAAA	ACACCCAGGATGGCATTG
CDH1	GGTCTGTCATGGAAGGTGCT	GATGGCGGCATTGTAGGT
CDH2	ACGCTCTCCCTCCCTGTT	GGACTCGCACCAGGAGTAAT
AR	TTTTTCTAAGACCTTTGAACTGAATG	TCTGTGGAAGTCGCCAAGTT
SLC8A1	GAGACGTTGATATGTTGGATGTG	GGAGGGGTGTTGTGGAAAG
SLC8A2	AGTGGCTTAAGCGAGGGATT	TGTCCCCATCCCCTTGATTG
SLC8A3	GGAGGCTTGGAGATTGGCTT	CTTTGCCCATTAAGCTGCCG
CD44	TGGGATTGGTTTTCATGGTT	CGTACCAGCCATTTGTGTTG
CD133	GGTCAGGATATCAGGCTCCA	GCGAGTACTCAGGTTGCACA

Nanog	TTCCTTCCTCCATGGATCTG	AAGTGGGTTGTTTGCCTTTG
POU5F1	AGTGAGAGGCAACCTGGAGA	ACACTCGGACCACATCCTTC
S100A8	ATCAGGAAAAAGGGTGCAGA	ACGCCCATCTTTATCACCAG
S100A9	ATCATGGAGGACCTGGACAC	GTCACCCTCGTGCATCTTCT
NFATC1	AAATGACCTCTCCAGCACGA	TACCCCTGCTGAACTGAGTG
CALM1	TGGCACCATCACAACAAAGG	GACCCAGTGACCTCATGACA
CREB1	GCTGGCTAACAATGGTACCG	TGGTTAATGTTTGCAGGCCC
CAMK2B	TCTCACCTTGTCACCTCCAC	TGCTCTTTAGGGGTCATGCA
CAMK2G	CATCCTCACGACCATGCTTG	TTGTTGCTCTGTGGCTTGAC
CAMKK2	ACCCGTATGCTGGACAAGAA	GGATCTTGATTTCCGGCACC

2.2.5 qPCR experimental optimisation

Prior to initiating experimental analysis using quantitative polymerase chain reaction (qPCR), we wanted to determine the best conditions under which to obtain reliable consistent expression results for our housekeeping gene to ensure consistent comparable analysis between groups. For this we selected a range of housekeeping genes commonly used in cell culture analysis and tested the expression levels in our cell model under all treatment and environmental conditions.

Five genes were selected, Beta actin (B-Actin), Hypoxanthine Phosphoribosyltransferase 1 (HPRT1), Hydroxymethylbilane Synthase (HMBS), TATA-Box Binding Protein (TBP) and 18S ribosomal RNA (18S). These genes are all highly conserved with consistent expression across many cell and tissue types (Ohl et al., 2005). RNA was extracted from LNCaP, LNCaP-ADT and LNCaP-abl cells (section 2.3.1) which had been incubated in normal or hypoxic conditions (section 2.1.8). cDNA was synthesised (section 2.3.3) and qPCR was carried out (section 2.3.5). The Ct values were analysed across all cell types and conditions and the mean, standard deviation (SD), coefficient of variance (CtCV %) and the standard error of the mean (sem±) were calculated (Table 2.2) along with the minimum, maximum and range of the cycle threshold (Ct). The gene with the least variance calculated was HPRT1 which had CtCV% of 2.86 and a Ct range of 2.23 as can be seen in the Ct plots (Figure 2.4). HPRT1 was selected to analyse the gene expression going forward.

Table 2.2: HPRT1 has the most consistent expression across all experimental parameters as indicated by the lowest % coefficient of variance (CtCV) (N=3): *qPCR analysis of genetic expression of a range of housekeeping genes expressed in LNCaP cells, LNCaP-ADT cells treated with 10µM Nifedipine (7-10 days) and androgen insensitive long-term androgen deprived LNCaP-abl cells all tested under normal oxygen conditions and hypoxia incubated (1% O_2).*

Gene	Mean Ct	SD	CtCV(%)	sem±	Ct Min	Ct Max	Ct Range
B-Actin	15.2808547	1.165000646	7.623923322	0.254223983	13.36020091	18.20648672	4.846285808
HPRT 1	19.90023319	0.569581623	2.862185669	0.09493027	19.1083858	21.33941838	2.231032586
HMBS	20.88803367	0.979044167	4.687105462	0.163174028	19.65430573	23.61117676	3.956871031
TBP	22.6617803	1.092001935	4.818694387	0.182000323	20.93557367	26.18532533	5.249751656
18s RNA	7.355267716	0.567392862	7.714102107	0.094565477	6.508868892	8.513875321	2.005006429

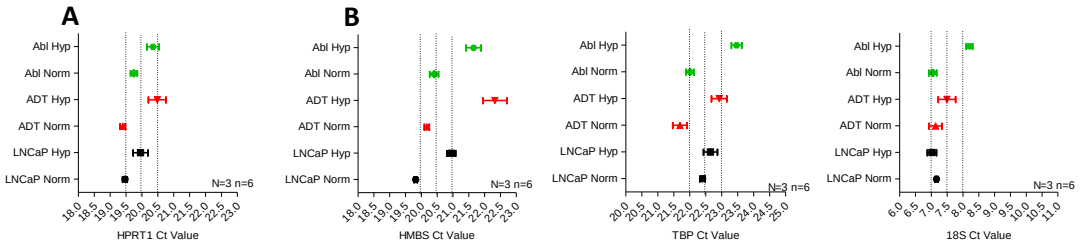

Figure 2.4: HPRT1 has the least variation in Ct values across all experimental parameters: *Ct values obtained for HPRT1 (A), HMBS (B), TBP (C) and 18s (D) assessed using qPCR analysis of cDNA from LNCaP cells (black), LNCaP-ADT cells (red) treated with 10µM Nifedipine (7-10 days) and androgen insensitive long-term androgen deprived LNCaP-abl cells (green) all tested under normal oxygen conditions and hypoxia incubated (1% O_2). Dashed lines represent variance across one ct value to demonstrate variation across results.*

2.2.6 Real Time Polymerase Chain Reaction (qPCR)

Master mix was prepared for multiple reactions in a 1.5 ml tube by adding 5 µl FastStart Essential DNA Green Master (Roche), 1 µl forward primer (0.5 µM) and 1 µl reverse primer (0.5 µM) per reaction. The master mix was stored on ice while the cDNA was loaded into each well of an 8 well PCR strip. 1-2 µl cDNA (25-50 ng) was added to each reaction, followed by 7 µl of the master mix and the volume was made up to 10 µl with PCR grade H_2O. The 8 tube PCR strip was placed in the LightCycler Nano™ (Roche) which was programmed to run as outlined in the FastStart Essential DNA Green Master protocol, with the annealing temperature adjusted according to the primer melting temperature (T_M). The housekeeping gene HPRT1 was used to determine the relative expression of each gene. The relative gene expression data was analysed using the $2^{-\Delta\Delta CT}$ method (Livak and Schmittgen, 2001). Statistical analysis was performed using Grahpad Prism 5 (Graphpad Software, CA, USA). Statistical significance was assigned to values $p<=0.05$.

2.2.7 siRNA transfection

All siRNA products were acquired from Dharmacon (Table 2.3) and received as lyophilised powder. The tubes were centrifuges and then reconstituted with 250 µl of PCR grade H_2O to stock concentration of 20 µM. The tube was incubated on constant roll for 30 mins at room temperature (RT). Working stocks (5 µM) were made up by adding 375 µl PCR grade H_2O to 125 µl stock. This was then aliquoted into 20 µl aliquots and stored at -20^oC.

Cells were seeded into the relevant plates and allowed to grow to 80% confluency in relevant media, without antibiotic, which assists with effective transfection. Once confluent, the media was removed and replaced with Opti-MEM™ (Gibco), reduced serum media. The transfection mix was made up using the relevant volumes for the plate outlined in Table 2.4. Tube 1 was made up with the diluted siRNA mix, containing either siCaV1.3 or non-targeting pool siRNA and tube 2 was made up with the transfection mix. Each tube was gently mixed by pipetting the mixture and incubated for 5 mins at RT. The tubes were then mixed by adding the contents of tube 2 to tube 1 and again gently mixed by pipetting. The transfection mix was incubated at RT for 20 mins and then the remaining volume of OptiMeM™ (Gibco) was added to make up the total volume required. Media was removed from the cells and replaced with the relevant transfection mix. The cells were place in the incubator at 37^oC with 5% CO_2 for 48 hours prior to RNA extraction (section

2.3.1) or 72 hours prior to protein extraction (section 2.4.1). Knockdown efficiency was regularly assessed by qPCR and western blotting with a minimum of 67% reduced genetic expression observed and a minimum of 87% reduced protein expression observed (Appendix B; Figure B1 and B2).

Table 2.3: Transfection products used for transient transfection of CaV1.3 and controls:

Catalog Number	**Transfection product**	**Quantity**
D-001830-10-05	ON-TARGETplus GAPD Control Pool (Human)	5 nmol
D-001810-10-05	ON-TARGETplus Non-targeting Pool	5 nmol
L-006124-00-0005	ON-TARGETplus Human *CACNA1D* (776) siRNA - SMARTpool	5 nmol
T-2003-02	DharmaFECT 3 Transfection Reagent,	0.75 mL

Table 2.4: Volumes of siRNA and transfection reagent used for final concentration of 25nM siRNA:

	Tube 1 diluted siRNA (µl/well)		*Tube 2 diluted Dharmafect™ transfection reagent (µl/well)*		
Plates used	Vol 5µM siRNA	Vol OptiMeM™	Vol Transfection reagent	Vol OptiMeM™	Vol OptiMeM™ added to make up to complete vol/well (µl)
6-well	10	190	5	195	1600
96-well	0.5	9.5	0.2	9.8	80

2.3 Protein extraction and Western Immunoblotting

2.3.1 Protein Extraction

Cell lines

Media was aspirated off cells in class II safety cabinet and discarded in Virkon™ antiviral disinfectant. Cells were gently washed with ice cold PBS twice. Cell culture plates were then moved to the bench where they were placed on ice to prevent protein degradation. The required volume of radioimmunoprecipitation assay buffer (RIPA) (Thermo Scientific) was aliquoted into a sterile 15 ml tube, Halt protease phosphatase inhibitor (PPI) cocktail (Thermo Scientific) was added to final concentration of 1X and placed on ice. PBS was aspirated off and 50µl of RIPA buffer mix was added to each 35 mm well. The cells were scraped off using a cell scraper and transferred to a 1.5 ml tube. Each tube was vortexed for 15 s and placed on ice to lyse for 30 mins with additional vortex after 15 mins. Each tube was centrifuged at 13000 rpm at 4^{o}C for 20 mins. The supernatant was transferred into fresh labelled tubes and stored at -80^{o}C.

Mouse tissue

Frozen tissue samples were slowly thawed over ice and sectioned with a sterile blade. The sectioned tissue was placed into an RNAse free 1.5 ml tube (Sarstedt) over ice. 100 µl RIPA buffer with 1X PPI was added to the tissue and the tubes were vortexed for 15-20 s. The tubes were then incubated at RT for 30 mins. The tubes were then vortexed again for 15-20 s and centrifuged at 13000 g at 4^{o}C for 10 mins. The supernatant was removed and placed in a fresh sterile labelled tube and stored at -80^{o}C until required.

2.3.2 Cell Fractionation Protein Extraction

To study the cellular location of expressed proteins a cell fractionation kit was used. The kit extracted three fractions, the cytosolic fraction, the membrane fraction, and the nuclear fraction. Cells were grown on 100 mm cell culture dishes to approximately 6*10^{6} cells. Cells were removed as per splitting protocol (section 2.1.3). Using cell fractionation kit (Abcam), cells were resuspended in buffer A (5 mls) to wash. Cell mix was centrifuged at 300 g for 5 mins and the supernatant was discarded. Pellet was resuspended in 500 µl buffer A and moved to the bench. Buffer B was prepared by adding 1000x Detergent I to 500 µl buffer A (0.5 µl Detergent I added to

500 µl Buffer A). The cell suspension was mixed with buffer B and allowed to incubate at room temperature for 7mins on constant rotator. This step permeabilised the plasma membrane releasing the cellular contents. The cell mixture was centrifuged at 5000 g for 1 min, to pellet the cell contents and separate it from the cytosol. The supernatant was transferred to a fresh tube and the pellet was retained on ice. The supernatant was centrifuged at 10000 g for 1 min, to ensure all the mitochondria and nuclei, which are still intact, are separated from the cytosol. The supernatant was transferred to a fresh tube and labelled as the cytoplasmic protein fraction. Both pellets from the first and second centrifugation steps were resuspended in 500 µl of Buffer A. Buffer C was made up by adding 25x Detergent II to 500 µl of Buffer A (20 µl Detergent II added to 500 µl Buffer A). The cell suspension was mixed with Buffer C and allowed to incubate at room temperature for 10mins on constant rotator. This step permeabilised the membranes and the mitochondria. The cell mixture was centrifuged at 5000 g for 1 min and the supernatant was transferred to a fresh tube and the pellet was retained on ice. The supernatant was centrifuged at 10000 g for 1 min, to ensure the nuclei, which are still intact, were separated from the membranous proteins. The supernatant was transferred to a fresh tube and labelled as the membrane protein fraction. Both pellets containing the nuclei were combined and resuspended in 200 µl of Buffer A and labelled as the nuclear protein fraction.

2.3.3 Protein quantification

Protein was quantified using the Pierce BCA Protein Assay Kit (Thermo Scientific). The kit contained a standard BSA which was diluted as per Table 2.5 with PBS to create a standard curve range of 20-2000 µg/ml. The standard was plated in triplicate on 96 well plate 25 µl/well. Protein samples were diluted 1:10 or 1:5 in PBS and 25 µl were plated in triplicate. Working reagent (WR) was made up by mixing 50 parts of BCA Reagent A with 1 part BCA Reagent B. The volume of WR required was calculated as follows:

(# standards + # unknowns) × (# replicates) × (volume of WR per sample) = volume WR required

200 µl of WR was added to each well and the plate was incubated for 30 mins at 37^{o}C. The absorbance was detected at 562 nm. The standards were used to create a standard curve from which the concentration of each protein sample was calculated using Graphpad Prism 5 (Graphpad Software, Ca, USA).

Table 2.5: Dilution of BSA standard (1ml of 2mg/ml) for working range 20-2000µg/ml

Vial	Volume of diluent (µl)	Volume of BSA (µl)	Final BSA concentration (µg/ml)
A	0	300 of stock	2000
B	125	375 of stock	1500
C	325	325 of stock	1000
D	175	175 of vial B solution	750
E	325	325 of vial C solution	500
F	325	325 of vial E solution	250
G	325	325 of vial F solution	125
H	400	100 of vial G solution	25
I	400	0	0 (Blank)

2.3.4 Western immunoblot.

2.3.4.1 Western blot buffers

Prior to initiating the western blot experiments the buffers required were prepared as follows:

Running Buffer

400 ml of 1X Running buffer prepared by adding 20x Bolt MOPS SDS running buffer (Invitrogen) to 380 ml dH_2O.

Transfer Buffer

1000 ml of transfer buffer was made by adding 50 ml 20X Bolt Transfer buffer (Invitrogen), 1 ml Bolt Antioxidant (Invitrogen) and 100 ml methanol (Fisher) to 849 ml dH_2O.

TBS

Prepared 10X tris buffered saline (TBS). 24.2 g Tris Base and 80 g NaCl dissolved in 500 ml distilled water (dH_2O). Adjusted pH to 7.6 and made volume up to 1000 ml with dH_2O. Used at 1X concentration.

TBS/T

Prepared wash buffer using TBS with tween 20 (0.1%) (TBS/T). 50 ml of 10X TBS added to 450 ml dH_2O with 0.5 ml Tween-20 (Fisher).

Blocking buffer

Blocking buffer was used to prevent any non-specific binding sites by blocking available binding sites with protein. This was made up by adding 5% non-fat milk powder or BSA (Fisher) to TBS/T. 50 mls blocking buffer was made by adding 2.5 g protein to 50mls TBST.

2.3.4.2 Electrophoresis

The proteins were initially separated on a precast gel using electrophoresis, which was performed using the Mini Gel Tank (Invitrogen). The gels used throughout the project were Bolt Bis-Tris Plus pre-cast Gels (Invitrogen), which were made of polyacrylamide at a concentration gradient of 4-12% or 10%.

The protein lysates, which had been quantified as per section 2.4.3, were prepared for electrophoresis as follows. In a microcentrifuge tube 50 µg total protein was added to 5 µl Bolt LDS sample buffer (Invitrogen) and 2 µl Bolt reducing agent (Invitrogen). The total volume was made up to 20 µl with sterile dH_2O. The sample was then mixed by pipetting and then loaded into a thermocycler. The protein sample was heated at 70^{o}C for 10 mins to denature and then transferred to ice once the cycle was complete.

Note: Total volume was occasionally made up to 40 ul if required. Amount of protein varied from 50 to 100 µg depending on antibody.

While the protein was undergoing the denaturation step the running gel cassette was removed from the gel cassette pouch. The comb was gently removed to prevent the wells being damaged and the wells were rinsed three times with 1X running buffer (section 2.4.4.1). The tape was then

removed from the lower end of the cassette. The chamber of the mini blot tank had been pre-filled with 1X running buffer up to the cathode. The cassette was then placed into the chamber with the wells facing toward the front. The wells were filled with 1X running buffer and at this stage the mini blot tank was moved to the fume hood and the samples were loaded into the relevant wells. The tank was topped up to the indicated level with 1X running buffer and the lid was placed on top. The tank was connected to the electrical supply and run at 200 V for 25-30 mins depending on protein size, ensuring that the blue indicator dye had run off the bottom of the gel before stopping run.

2.3.4.3 Protein Transfer

While the electrophoresis was underway the sponge pads required for the protein transfer step were soaked in 200 ml transfer buffer (section 2.4.4.1) until saturated ensuring all bubbles were removed. The protein transfer was performed using the Mini Blot module (Invitrogen) and polyvinylidene fluoride (PVDF) (Invitrogen). The PVDF membrane was activated by soaking it in methanol (Fisher) for 30 s using tweezers to prevent any protein contamination. The membrane was rinsed in dH_2O and submerged in transfer buffer until required. Filter paper was wet with transfer buffer immediately prior to use.

When the electrophoresis was complete the cassette was removed and rinsed with dH_2O. The plastic cover of the cassette was opened gently with the gel knife, exposing the precast gel. Once open the wells were trimmed off and a piece of pre-soaked filter paper was placed on top of the gel. The PVDF paper was placed on the other exposed side of the gel and covered with another piece of pre-soaked filter paper. The blot sandwich was assembled as outlined in Figure 2.5, ensuring that the process was completed quickly to prevent drying.

Once the blot sandwich was assembled it was placed into the mini blot gel tank with the cathode core (-) facing forward ensuring the module core was completely submerged with buffer. The protein was transferred at 20 V for 60 mins.

2.3.4.4 Wash and Develop Membrane

When the transfer was complete the module was opened, and the membrane was carefully removed using the tweezers. Following this it was washed twice in TBS (section 2.3.4.1) for 5 mins. The membrane was incubated in blocking buffer (section 2.3.4.1) for 1 hour at room temperature. Following this it was washed in TBST (section 2.3.4.1) for 5 mins, 3 times. The membrane was now ready to be incubated with the primary antibodies. These were made up in TBST containing 5% milk to the specified concentration (Table 2.4) and incubated over night at 4^{o}C with gentle agitation.

After the overnight incubation, the membrane was washed in TBST for 5 mins, 3 times. Then it was incubated in the secondary antibody for 1 hour at room temperature with gentle agitation. Once the incubation was complete the membrane was again washed for 3 mins with TBST followed by 5 mins with TBS 3 times. Once this stage was complete the membrane was ready to be developed. This was achieved by incubating the membrane in a 1:4 dilution of Supersignal West Dura Chemiluminescent Substrate (Thermo Scientific) with gentle agitation for 1min at room temperature. The drained membrane was then placed into the cassette and covered with cling film and taken to the dark room for detection. A piece of X-ray film was cut to size and placed over the membrane. The time of exposure depended on protein and antibody. The cassette was opened in dark room and the x-ray film was placed into developer solution (1:5 dilution in dH_2O) (Tetenal) until an image appeared. The membrane was then quickly submerged in water to wash off excess developer. Next it was transferred into fixer solution (1:4 dilution in dH_2O) (Tetenal) until image was fixed and again submerged into water to wash off excess fixer. The x-ray image was left to air dry.

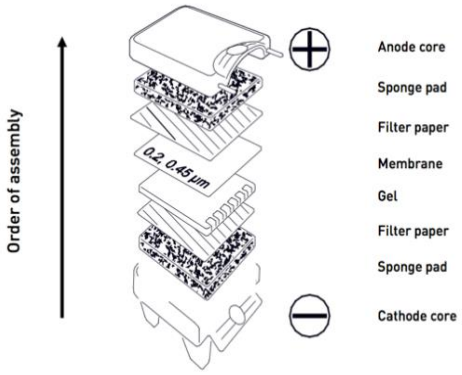

Figure 2.5: *Image of blot sandwich layout and how to assemble for protein transfer to PVDF membrane.*

2.3.4.5 Densitometry and relative expression

Digital images of the developed immunoblots were obtained by scanning the x-ray film and loading as a Jpeg file. The densitometry of the images was quantified using Image J software (https://imagej.net/), each band was gated using the rectangular shape and the profile plots were produced representing the relative density of each lane of the immunoblot. The area of each profile plot was analysed and compared to the housekeeping gene to obtain the relative density. Protein expression was calculated using GraphPad Prism 5. Statistical significance was assigned to values $p<0.05$.

2.3.5 Antibodies

The antibodies were aliquoted (10 µl) and stored at -20°C until required. All the antibodies used throughout the project are outlined below in Table 2.6.

Table 2.6: Antibodies used in western immunoblotting:

Antibody	Company	Catalog number	Concentration	Dilution	Host & Clonality
Primary Antibodies					
Actin	BD Transduction Laboratories	612656	50µg (0.25mg/ml)	1-10000	Mouse IgG Monoclonal
CaV1.3	Abcam	Ab-84811	100µg (1mg/ml)	1-500	Mouse IgG Monoclonal
Hif-1α	BD Transduction Laboratories	610958	50µg (0.25mg/ml)	1-500	Mouse IgG Monoclonal
RyR2	Almone Labs	ARR-002	25µg (0.8mg/ml)	1-100	Rabbit IgG polyclonal
Secondary Antibodies					
HRP-Anti Mouse	BD Pharmigen	554002	1ml	1-1000	Goat antiserum Polyclonal

2.4 Functional Assays

2.4.1 Proliferation

Proliferation was assayed using a Wst-1 assay kit (Roche), which measures proliferation by the formation of formazan through the enzymatic cleavage of tetrazolium salt by the mitochondrial dehydrogenases present in viable cells. Cells were seeded into 96 well plates 100 µl per well at a density of $5*10^5$ cells per ml and placed into the incubator at 37°C with 5 % CO_2 for 48 hours, afterwards cells were treated with test conditions and controls as required. At the treatment end point 10 µl of Wst-1 reagent was added to each well and replaced back into the incubator for 4 hours. The plate is then placed onto a plate shaker and gently shook for 1 min. The plate was then placed on the VICTOR multilabel plate reader and the absorbance was recorded at 440 nm, for treated and untreated cells (triplicate). The background control (duplicate) was also recorded at 440 nm containing Wst-1 in media. The averaged blank measurement was subtracted from each measurement and the triplicate average was used for analysis. The experiments were compared to the LNCaP parental control cells, with the results presented as percentage change.

2.4.2 Colony forming assay

Cell survival was assessed using the colony forming assay (CFA), by measuring the ability of an individual cell to undergo unlimited cell divisions. It measures the ability of each cell to form a colony, which is considered any growth of a cluster of 50 or more cells. The cells were seeded at a density of 2500 cells per well (6 well dish) and allowed to attach for 48 hours. The cells were then treated with test conditions or control and placed into incubator and allowed to grow for 14 days. After 14 days the media was aspirated off in the safety cabinet. The cells were gently washed with PBS and moved to the bench. The PBS was aspirated off and the cells were fixed by adding 1 ml/well methanol (100%) (Fisher). The methanol was left to fix the cells for 30 mins. This was followed by staining with 1 ml/well 1:10 dilution of crystal violet solution (Sigma). The stain was left on the cells for 60 mins before removal with a pipette. Excess was washed off by submerging the dish into fresh H_2O until the dishes were clean. The individual colonies were counted, clusters of approximately 50 cells were considered colonies. The experiments were compared to the LNCaP parental control cells, with the results presented as percentage change.

2.4.3 Migration

Migration is a key characteristic of tumorigenicity in cancer cells as this is ultimately what drives metastasis. We used the Xcelligence™ system, a Boyden chamber-based assay, to assess the migratory potential of the cell model. Cells were seeded at a density of $8*10^4$ cells/well in duplicate in the top chamber of the cell invasion and migration (CIM) plate (Figure 2.6) in 100 µl media containing 2% FBS. The bottom chamber had media containing 10% FBS as a chemoattractant or 2% FBS in the negative control wells. The cells were pre-treated with test conditions or control as outlined in the appropriate sections above and seeded into the top well in the cell culture hood. The plates were clamped closed and the cells were allowed settle in the hood for 20-30 mins to prevent interference from thermal currents within the incubator. CIM plates were set into the Xcelligence™ which was contained within the incubator at 37°C with 5% CO_2. The cell electrical impedance was recorded every 15 mins for a total of 60 hours. The extended time of recorded migration was chosen due to the slow migration of the LNCaP cells.

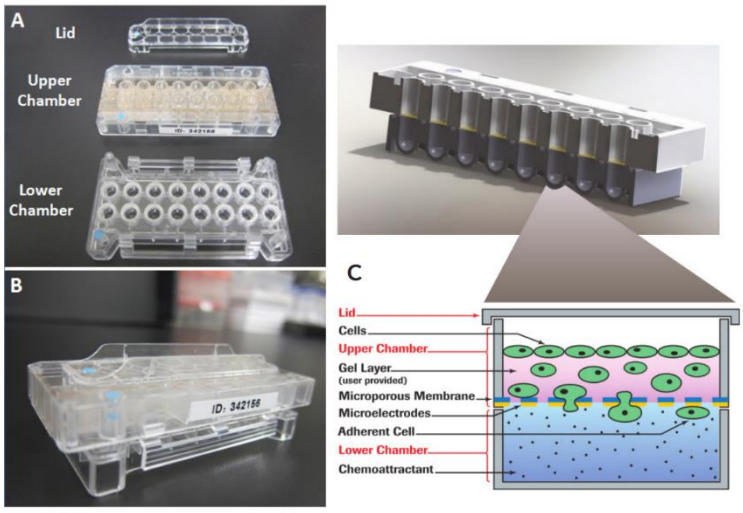

Figure 2.6: *CIM plates (A) components of plates, (B) assembled plate, (C) detailed outline of the plate mechanism indicating the lower chamber containing chemoattractant and the upper chamber containing the seeded cells, with cells migrating through the microporous membrane containing the gold-plated electrodes on the underside which record the electrical impedance resulting from migrated cells.*

2.5 Calcium Measurements

Using a membrane permeable Ca^{2+} binding fluorophore, Fura 2- acetoxymethyl ester (Fura 2-AM) (Invitrogen), we were able to measure fluctuations in intracellular Ca^{2+} by determining changes in fluorescence. Once inside the cell Fura 2-AM is cleaved by cellular esterase to form fura-2, which is trapped within the cell membrane (Yates et al., 1992). Fura-2 is UV light excitable and delivers a ratio metric analysis of intracellular Ca^{2+} concentration. The emission wavelength is 505nm and the excitation wavelength changes from 340 nm to 380 nm on binding Ca^{2+}, in this way the ratio metric calculation allows accurate Ca^{2+} measurement, which is not affected by the concentration of dye load or the cell thickness (Barreto-Chang and Dolmetsch, 2009).

2.5.1 Buffers and Calcium calculations

For the Ca^{2+} imaging experiments cells were suspended in physiological saline solution (PSS) which was made up with and without Ca^{2+}. Outlined below are the buffers used for the Ca^{2+} imaging experiments. Along with the calculated concentrations required for loading the Victor plate reader with SERCA inhibitor Thapsigargin (Tg) (Invitrogen), calcium chloride (CaCl), potassium chloride (KCl) and sodium chloride NaCl) to result in addition of the correct final concentration to the individual well.

Buffers

PSS solution was made up with NaCl 140 mM, $MgCl_2$ 1 mM, KCl 4 mM, $CaCl_2$ 2 mM, D-glucose 11.1 mM and HEPES 10 mM pH balanced to 7.4 with NaOH.

For the 0% Ca^{2+} PSS the $CaCl_2$ was omitted and 1mM EGTA was added.

For high external KCl both 56 mM and 76 mM KCl was injected and for high external NaCl injection of NaCl 56 nM and 76 nM.

Calculations for loading concentrations:

Tg was stored at stock concentration of 10 mM at -20°C. Preparation for preloading the plate reader with 2 ml solution. 4.9 µl Tg (10mM) was added to 1995.1 µl 0% Ca^{2+} PSS for a concentration of 24 µM Tg solution. 20 µl of the Tg solution was added to each well containing 100 µl cell solution resulting in 4 µM final Tg solution in each well (Figure 2.7 (B)).

$CaCl_2$ was stored as 1 M solution at room temperature. Preparation for preloading the plate reader with 2 ml solution. 28 µl $CaCl_2$ (1 M) was added to 1972 µl dH_2O for concentration of 14 mM $CaCl_2$ solution. 20 µl of $CaCl_2$ solution was added to each well containing 100 µl cell solution and 20 µl Tg (120 µl total in well), resulting in 2 mM final $CaCl_2$solution in each well (Figure 2.7 (B)).

KCl and NaCl were both made up as needed as 1 M solution. Preparation for preloading the plate reader with 2ml solution. 672 µl KCl or NaCl (1 M) was added to 1328 µl dH_2O for a concentration of 336 mM solution. 20 µl of solution added to each well containing 100 µl cell solution resulting in 56 µM final solution per each well. 912 µl Kcl or NaCl (1 M) was added to 1088 µl dH_2O for a concentration of 456 mM solution. 20 µl of solution was added to each well containing 100 µl cell solution resulting in 76 µM final solution per well.

2.5.2 Store operated Ca^{2+} entry

Cells were grown in 6 well dishes with relevant test conditions for experimental parameters. Cells were then removed, counted (section 2.1.5), and resuspended in a tube in OptiMEM™ low serum media at a concentration of $5*10^5$ cells/ml. Fura 2-AM was added to the tube to a final concentration of 2 µM and incubated at RT in the dark for 45 mins. The cells were centrifuged at 8000 g for 5 mins and the supernatant was discarded. The pellet was then resuspended in 1 ml OptiMEM™ and incubated in the dark for 30 mins. This process was repeated, and the cells were incubated in the dark for 45 mins to allow complete de-esterification of the dye. Tubes were then centrifuged, and the supernatant was discarded, the pellet was resuspended in 500 µl physiological saline solution (PSS) 0% Ca^{2+}. 100 µl was added to each well of a black walled 96 well plate, which was $1*10^5$ cells/well.

The plate was then placed into the VICTOR multilabel plate reader with excitation wavelengths set at 340 and 380 nm and the emission wavelength set at 510 nm with measurements recorded every 5 s. The plate reader was preloaded with the Tg and Ca^{2+} solutions (section 2.6.1) which

were injected at a volume of 20 µl/well. Baseline Ca^{2+} levels were determined for 100 s then Tg was injected at final concentration of 4 µM and recorded for 400 s after which $CaCl_2$ was injected at a final concentration of 2 mM with measurements recorded for a further 200 s. Tg results in the depletion of the ER Ca^{2+} stores by inhibiting the action of SERCA, which is responsible for pumping Ca^{2+} back into the ER. As outlined in the introduction (section 1.5.1), ER Ca^{2+} depletion activates SOCE. Introducing Ca^{2+} to the extracellular fluid allows us to see the level of extracellular Ca^{2+} that is taken into the cell as a result of ER store depletion (Figure 2.7 (A)).

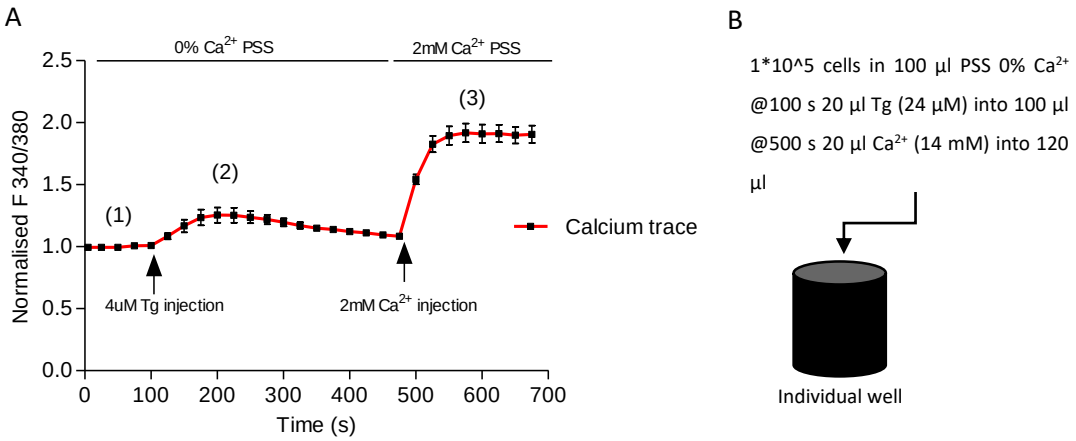

Figure 2.7: *(A) Calcium trace indicating (1) the normalised base, (2) the Thapsigargin induced peak which represents the calcium release from the ER and (3) the calcium peak which represents the calcium influx from the extracellular fluid after calcium is introduced. (B) Image representation of an individual well with an indication of the cell volume and the Thapsigargin and calcium injection with the relevant times at concentrations.*

2.5.3 Voltage dependent Ca^{2+} entry

External Potassium (K^+) was used to induce cell depolarisation in order to investigate the voltage gating mechanism of CaV1.3. The cells were loaded with Fura 2-AM as stated above with the pellet resuspended in the final stage in PSS with 2 mM Ca^{2+}, containing 50 µM of the potassium channel

activator, NS1619 (1,3-dihydro-1-[2-hydroxy-5-(trifluoromethyl)phenyl]-5-(trifluoromethyl)-2H-benzimidazole-2-one). This was used to allow potassium ions to freely pass through the cell membrane and ensure the induction of cell depolarisation. 100 µl cell suspension was added to each well and baseline recorded for 600 s then injection of high external KCl (section 2.6.1) was achieved by injecting either 56 mM or 76 mM KCl to achieve KCl concentrations of 60 mM and 80 mM. High external potassium was used to alter the equilibrium potential across the cell membrane, hence the cell membrane becomes depolarised. To ensure any effect observed was due to KCl and not due to osmotic pressure a control experiment was performed using injection of 56 mM and 76 mM NaCl (section 2.5.1).

2.6 Statistical analysis

Statistical analyses were performed using GraphPad Prism version 5.0 (GraphPad Software). Results were expressed as mean +/- standard error of the mean (sem). Independent experiments were conducted to a minimum of 3 biological replicates (N), with technical replicates of 2 (n). Treated groups were compared to control and fitted with Kruskal-Wallis significance test and Dunn's multiple comparison post hoc test, Mann-Whitney test was utilised for paired comparisons. Larger sample sizes were tested using a one-way analysis of variance (ANOVA) and a Tukey's post hoc test, with a student t-test used for paired comparisons. A 5% significance interval was used; p-values less than 0.05 were considered significant and are indicated as follows: *$p<0.05$, **$p<0.01$, ***$p<0.001$.

2.7 Prostate cancer patient bioinformatics

The bioinformatics analysis was carried out under request by Dr. Tim Downing, below is a brief outline of the data, statistical packages and statistical tests used in the analysis.

Examining the DNA Affymetrix Human Exon 1.0 ST microarray data from (Taylor et al., 2010) (n=185 samples, accession GSE21032) with 6,553,600 potential probes was downloaded with R packages Biobase v2.30.0 and GEOquery v2.40.0. After quality control, this had information for n=130 primary cancers, n=18 metastases and n=24 control normal adjacent epithelial samples. 29 of the primary and adjacent samples were paired, allowing comparison of relative expression. The

signal intensity data was screened using Bioconductor v3.9 to perform quality control and to visualise the variation in expression across samples using principal components analysis (PCA). Evidence for outliers was examined based on PCA and the distribution of values across samples and probes. These samples were background-adjusted, quantile-normalised, and log-transformed using the RMA (Robust Multi-chip Average) algorithm from the affy v3.0 R package (Irizarry et al., 2003) to obtain the normalised expression of each sample across 22,011 informative probes.

The expression of each gene was tested for differential expression using linear models in limma v3.34.4 based on the $\log_2$ fold-change (LogFC) and adjusted p value. Statistical analyses, comparisons with patient phenotypes, and visualisations were completed with additional R packages dplyr v0.7.6, ggplot2 v3.0.0, grid v3.4.1, magrittr v1.5, plyr v1.8.4, readr v1.1.1, survival v2.42.6, tidyr v0.8.1, tidyverse v1.2.1, tidyselect v0.2.4, and xtable v1.8.2. All reported and unreported raw p values (n=124) were corrected for multiple tests using the Benjamini-Hochberg approach in R.

Chapter 3 – Investigating the effect of ADT on the expression of CaV1.3 in prostate cancer.

3.1 Introduction

3.1.1 Background

PCa is the most prevalent male cancer affecting one in seven Irish males in their lifetime. It is generally considered a disease of the elderly, with 67 being the mean age of diagnosis in Ireland. However, it is still associated with significant mortality worldwide with ~360,000 male cancer deaths in 2018 as a result of PCa (Rawla, 2019). Due to PCa's reliance on androgens for growth, ADT is the most utilised treatment for advanced or metastatic disease. Initially effective, this method of treatment inhibits androgen action on the prostate, shrinking the tumour. However, it ultimately fails, and the disease progresses to the terminal castrate resistant PCa (CRPC). CRPC is an aggressive phenotype, which develops the ability to grow in the absence of androgens or with continued AR inhibition. Treatment options for CRPC have evolved over the years, with the development of new drugs that prolong the life of patients. However, there is an unmet need for a curative or preventative treatment for this stage of disease. Further research is required to establish the mechanisms driving the progression to CRPC under ADT and identify targets which could prevent or prolong the progression to this incurable stage of disease.

It is generally accepted that there are some phenotypic changes that occur under ADT which indicate and aid the progression to CRPC, such as over expression of AR (Grossmann et al., 2001) which facilitates AR activity in a low androgen environment. There is also progression to a neuroendocrine phenotype (Hirano et al., 2004) with increased expression of NSE and epithelial to mesenchymal transition (Byrne et al., 2016; Shiota et al., 2015), with upregulated N cadherin and downregulated E cadherin. It has also been stated that ADT drives the progression of a stem cell phenotype (Tang et al., 2009), particularly in the short term showing heightened expression of stem cell surface markers such as CD133 and CD44. All these changes are associated with disease progression and treatment resistance, identification of common targets that could be initiating these changes could assist in the treatment of PCa in conjunction with ADT.

Ca^{2+} is a ubiquitous second messenger which controls many aspects of cellular function such as proliferation, transcription, apoptosis and migration (Prakriya, 2020). Altered Ca^{2+} signalling has

been defined as being a contributory factor in each of the hallmarks for cancer (Stewart et al., 2015). Altered expression of channels which control Ca^{2+} signalling have been indicated in the progression of many malignancies (Tajada and Villalobos, 2020), including PCa (Chen et al., 2017; N. Prevarskaya et al., 2007; Wang et al., 2015).

CaV1.3 is a VGCC associated with excitable cells; but has also been identified as having important cellular functions in many non-excitable cells such as cancer (Davenport et al., 2015; Pitt et al., 2021). CaV1.3 has recently been highlighted as a potential target for PCa, with upregulated expression identified. Recently an extensive meta-analysis was conducted, looking at the expression of VGCC in a wide variety of cancers (Wang et al., 2015). This research identified that CaV1.3 was upregulated in many cancers, with significantly increased expression in PCa tissues compared to normal prostate tissue controls. This coupled with the research highlighting that the increased expression of CaV1.3 in primary PCa was significantly enhanced in patient tissue samples after they have progressed to CRPC (Chen et al., 2014) lead to the hypothesis that CaV1.3 could be assisting in the progression to CRPC and treatment resistance.

While the function of CaV1.3 upregulation in driving CRPC is unknown, we do know that this channel facilitates the passage of Ca^{2+} and thus potentially drives various hallmarks of cancer. In addition, emerging research has also suggested the channel can act in a non-canonical role, mobilising Ca^{2+} through direct interaction with other ion channels or through gene regulation (Fourbon et al., 2017; Lu et al., 2015). Therefore, identifying the mechanisms associated with the upregulation of CaV1.3 may indicate how PCa develops treatment evasion and cancer progression under ADT. To investigate this, we sought to develop a cell model using androgen sensitive LNCaP cells which reflected progression to CRPC under ADT. Research indicates that CaV1.3 expression increases with disease progression, but it is not clear if ADT is involved in enhancing CaV1.3. Here we wanted to determine if PCa cells under ADT expressed CaV1.3 and to what degree this expression was affected by ADT.

3.1.2 Aims of chapter 3

To gain a better understanding of the role of CaV1.3 in PCa disease progression from the androgen sensitive to castrate resistant stages we sought to develop a disease model of these transition stages and validate it against clinical phenotypes. With this model we aimed to explore the underlying mechanisms that drive progression under ADT and how this is associated with the upregulation of CaV1.3. For this we utilised three prostate cancer cell lines which represented the disease at various stages under androgen deprivation. The androgen sensitive Lymph Node Carcinoma of the Prostate (LNCaP), the short term androgen deprived (LNCaP-ADT) and the long term androgen deprived (LNCaP-abl) (Culig et al., 1999). We further sought to verify the association between ADT and CaV1.3 expression in an *in vivo* mouse model and in clinical patient samples.

Aim: Investigate the effect ADT has on the expression of CaV1.3 in the cell line, in vivo and in clinical samples.

Hypothesis: Expression of CaV1.3 increases with disease progression under treatment with ADT.

Objectives:

1. Establish and characterise a cell model which represents PCa progression under ADT.
2. Examine the expression of CaV1.3 in relation to ADT and disease progression in patient tissue analysis.
3. Establish the expression of CaV1.3 in the *in vitro and in vivo* models to further investigate mechanisms driving progression.

3.2 Results

3.2.1 Cell model characterisation

3.2.1.1 Morphology and phenotypic alterations

Initially we aimed to establish a clinically representative cell model of PCa progression under ADT with which to investigate the expression and effect of CaV1.3. As outlined (section 2.1) the cell model consists of LNCaP cells treated for various periods of time with bicalutamide. The morphology of LNCaP cells under ADT is proposed to transform in the short term to a sparsely populated cell pattern with a neuroendocrine morphology (Bennett et al., 2013), while the LNCaP-abl cells have been reported to have a clustered growth pattern (Culig et al., 1999).

Morphology of the parental LNCaP (Figure 3.1 (A)) is altered in the LNCaP-ADT cells after ~7 days treatment with bicalutamide (Figure 3.1 (B)), indicated by the neurite extension (black arrow) and sparse growth. The morphology is altered again in the androgen independent LNCaP-abl cells (Figure 3.1 (C)), indicated by the condensation of the cell body and the aggregated growth pattern.

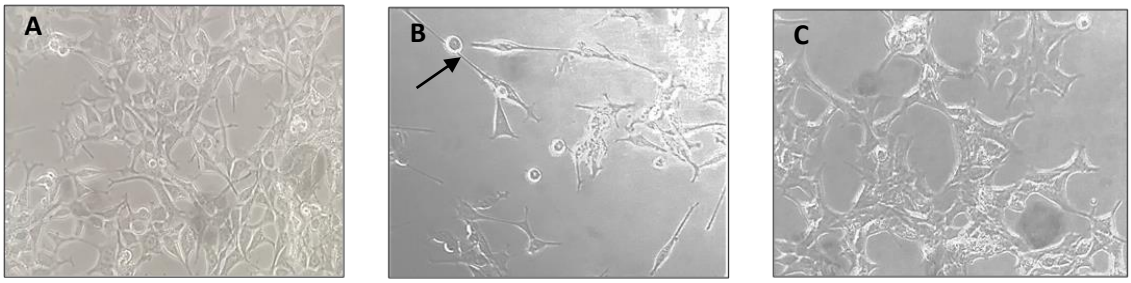

Figure 3.1: Typical morphology of LNCaP cells, LNCaP-ADT cells & LNCaP-abl cells in culture: *(A) LNCaP cells, (B) LNCaP-ADT cells cultured for 10 days with 10 µM bicalutamide and (C) LNCaP-abl cells cultured for 90 passages in androgen deprived media and 10 µM bicalutamide.*

Once we had established the morphological changes associated with PCa progression under ADT, we next wanted to determine the phenotypic alterations commonly associated with PCa progression to CRPC. We examined the genetic expression of the key characteristic markers highlighted in the introduction to indicate PCa progression.

Enhanced expression of AR is a common phenomenon seen under ADT (Visakorpi et al., 1995), here we see a significant 2.14-fold (+/- 0.146 sem) increase of expression in ADT cells and a 1.8-fold (+/- 0.087 sem) increase in LNCaP-abl cells compared to LNCaP control (Figure 3.2 (A)).

The expression of the neuroendocrine marker NSE indicates progression to androgen independence. A significant increase is observed in the short-term androgen deprived cells LNCaP-ADT 2.2-fold (+/- 0.29 sem) (Figure 3.2 (B)). This expression is less pronounced in the long-term androgen deprived LNCaP-abl cells although there is still a 1.825-fold (+/- 0.16 sem) increase.

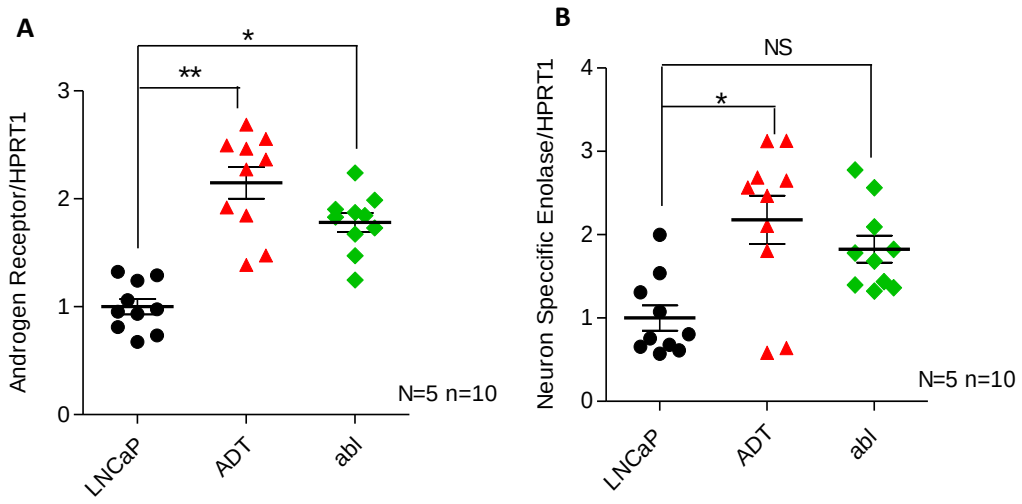

Figure 3.2 Bicalutamide treatment significantly increases expression of androgen receptor and marker of neuroendocrine differentiation, neuron specific enolase: Genetic expression of (A) *Androgen receptor and (B) neuron specific enolase, assessed using qPCR normalised to control LNCaP. Analysis of androgen sensitive LNCaP cells (black), LNCaP-ADT cells treated with 10μM bicalutamide (7-10 days) (red) and androgen insensitive long-term androgen deprived LNCaP-abl cells (green). Analysed using Kruskal-Wallis significance test and Dunn's multiple comparison post hoc test between cell types and treatments. * P<0.05, ** P<0.01, ***P<0.001, NS not significant.*

3.2.1.2 EMT under ADT

EMT is associated with cancer progression and resistance to treatment in PCa (Marín-Aguilera et al., 2014), with research demonstrating an association between EMT and ADT (Jennbacken et al., 2010).

E Cadherin had a 1.5-fold (+/- 0.108 sem) increase of expression in the LNCaP-abl cells compared to LNCaP suggesting that LNCaP-abl cells had an increased epithelial phenotype (Figure 3.3 (A)(i)). N-cadherin, which is indicative of a mesenchymal phenotype, has a 4.9-fold (+/- 2.79 sem) increased expression in the ADT cells and 1.37-fold (+/- 0.588 sem) increase in the LNCaP-abl (Figure 3.3 (A)(ii)). However, the Ct values of these experiments were below the threshold of reliability for N-cadherin (Appendix A, Figure A1), indicating that N-cadherin has a very low expression in these cells. Owing to this we were unable to detect EMT in the cell model.

However, there is some indication that the xenografted LNCaP cells undergo EMT under treatment with bicalutamide. Using our LNCaP xenograft mouse model we measured E-cadherin expression in bicalutamide treated compared to vehicle control and found no significant difference across all time points for 28 days (Figure 3.3(B)(i)). N-cadherin expression was significantly enhanced in bicalutamide treated mice compared to associated vehicle control with a 2-fold (2.17 +/- 0.82 sem) increased expression on day 14 and a 3-fold (3.027 +/- 1.082 sem) increased expression on day 21 (Figure 3.3 (B)(ii)).

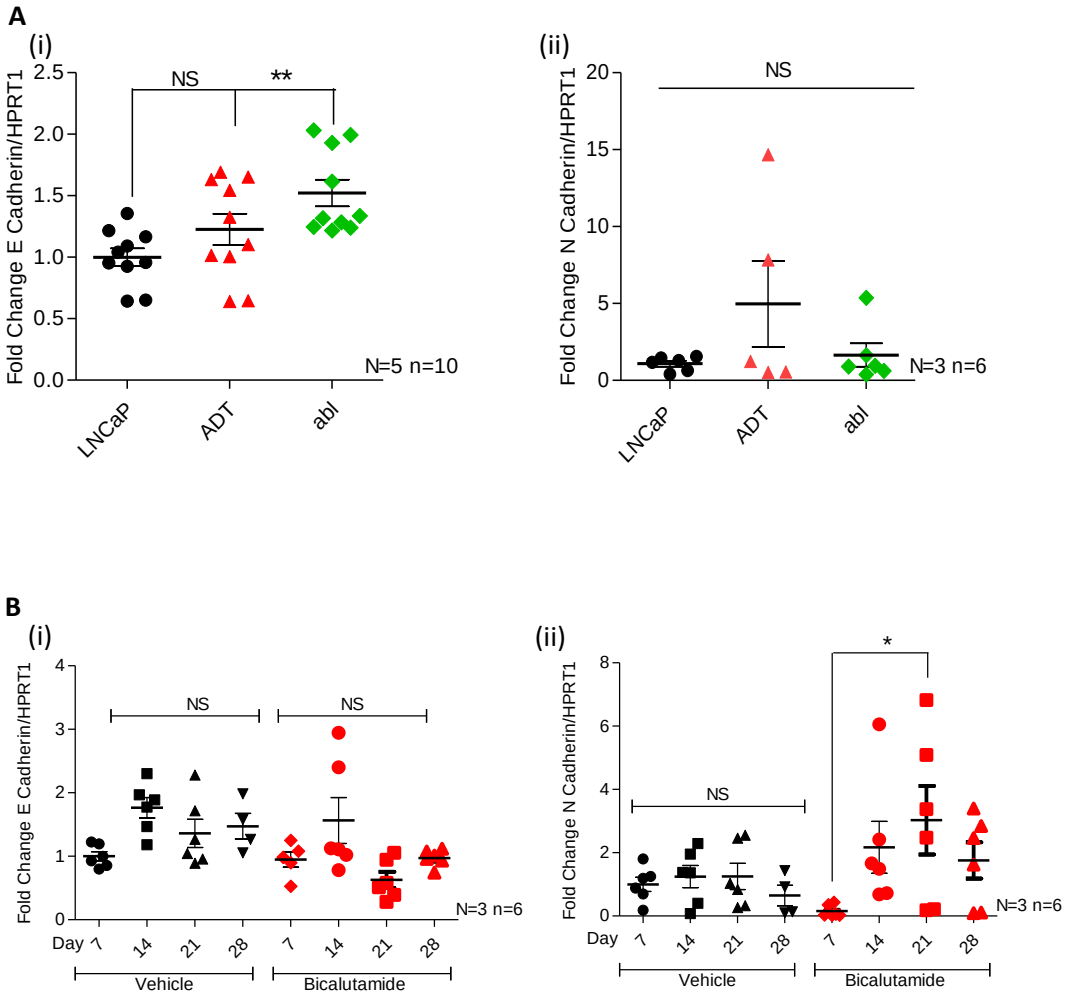

Figure 3.3 Epithelial to mesenchymal transition occurs with bicalutamide treatment in vivo, but not in vitro. *(A) Genetic expression of (i) E cadherin and (ii) N cadherin in PCa cell lines assessed using qPCR and normalised to control LNCaP. Analysis of androgen sensitive LNCaP cells (black), LNCaP-ADT cells treated with 10μM bicalutamide (7-10 days) (red) and androgen insensitive long-term androgen deprived LNCaP-abl cells (green). (B) Genetic expression of (i) E cadherin and (ii) N cadherin in LNCaP xenograft mouse model was assessed using qPCR and normalised to vehicle Day 7. BALB/c immunocompromised mice xenografted with 2x10^6 LNCaP cells in Matrigel treated daily with 10μM/2kg Bicalutamide or with equivalent vehicle control. Analysed using Kruskal-Wallis test*

*followed by Dunne's multiple comparison test. * P<0.05, ** P<0.01, ***P<0.001, NS not significant.*

3.2.1.3 CSC enrichment under ADT

There are many reports highlighting the influence that EMT and CSC's have on the progression of PCa to CRPC under continued ADT (Li et al., 2014). Indicating an inferred advantage on treatment resistance and subsequent reestablishment of a treatment resistant tumour. We examined the genetic expression of the surface markers associated with EMT and CSC in PCa. The expression was assessed in the LNCaP cell model under ADT and in the LNCaP xenografted *in vivo* mouse model, treated with bicalutamide or vehicle control.

The emergence of a stem cell phenotype can be indicated by the expression of the stem cell surface markers CD44 and CD133, among others. Here we find CD44 has an almost 2-fold (1.997 +/- 0.7 sem) increased expression in LNCaP-ADT cells (Figure 3.4 (A)(i)) with CD133 (0.967 +/- 0.25 sem) unaffected by treatment in the same cells (Figure 3.4 (A)(ii)). Interestingly LNCaP-abl cells had reduced expression of both CD44 (0.69 +/-0.139 sem) and CD133 (0.12 +/-0.17 sem). There was no altered expression detected for the stem cell transcription factors Oct4 or Nanog in any of the cells (Appendix A, Figure A.2). Treatment with bicalutamide *in vivo* significantly increased the expression of stem cell surface markers in LNCaP xenografted mice. CD44 (Figure 3.4 (B)(i)) and CD133 (Figure 3.4 (B)(ii)) have an 8-fold (8.871 +/- 2.9 sem) and 10-fold (10.67 +/- 3.3 sem) increased expression respectively by day 14 in bicalutamide treated mice compared to vehicle control. This increased expression is also seen by day 21 in treated mice with CD44 and CD133 both having a 6-fold increased expression (CD44 6.455 +/- 1.7 sem, CD133 6.254 +/- 1.8 sem) but did not reach significance.

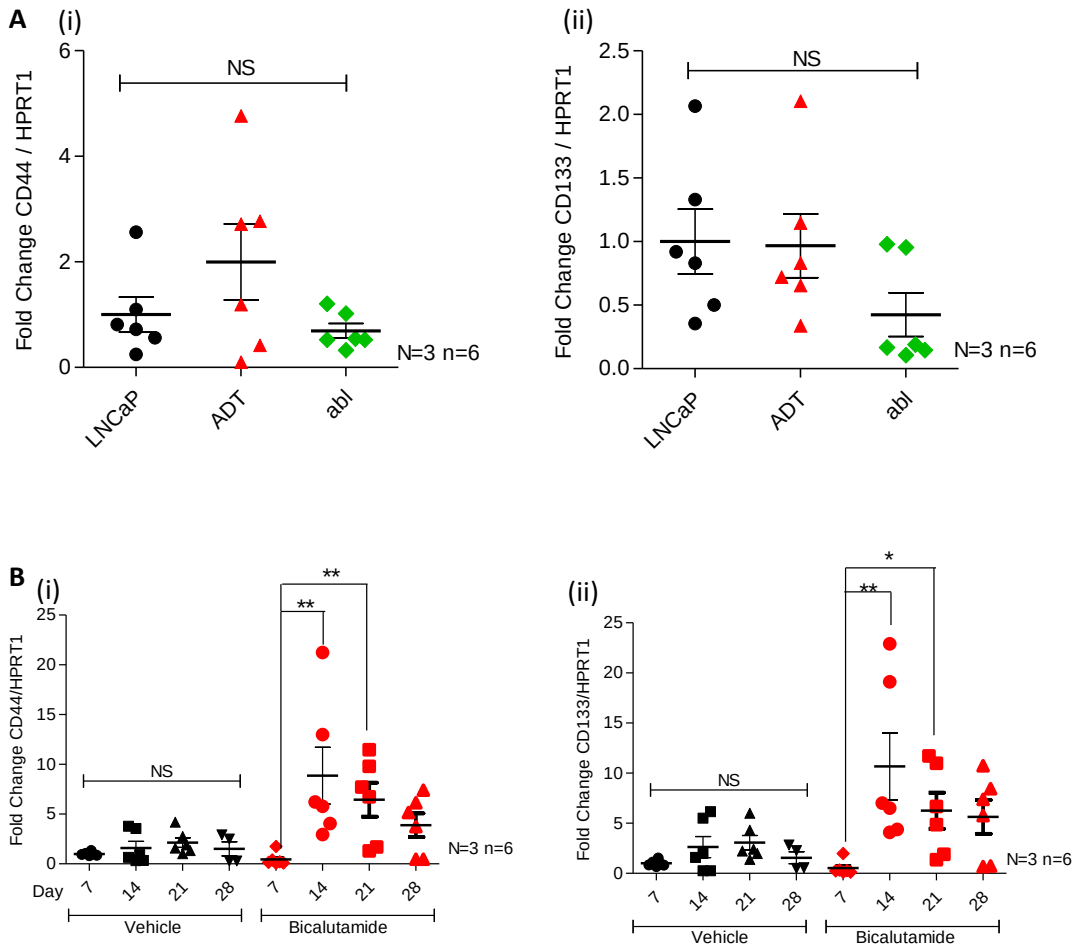

Figure 3.4 Bicalutamide treatment enriches the population of stem cells in vivo: *(A) Genetic expression of (i) CD44 and (ii) CD133 in PCa cell lines assessed using qPCR and normalised to control LNCaP. Analysis of androgen sensitive LNCaP cells (black), LNCaP-ADT cells treated with 10 µM bicalutamide (7-10 days) (red) and androgen insensitive long-term androgen deprived LNCaP-abl cells (green). (B) Genetic expression of (i) CD44 and (ii) CD133 in LNCaP xenograft mouse model was assessed using qPCR and normalised to vehicle Day 7. Analysis of BALB/c immunocompromised mice xenografted with 2x106 LNCaP cells in Matrigel treated daily with 10 µM/2kg bicalutamide or with equivalent vehicle control. Analysed using Kruskal-Wallis test followed by Dunne's multiple comparison test. * P<0.05, ** P<0.01, ***P<0.001, NS not significant.*

3.2.1.4 Functional effects of ADT

The progression of PCa to CRPC is indicated by the ability to proliferate under continued ADT hence we examined the proliferative ability of the cells to determine if continued ADT impacted cell growth. Proliferation is significantly reduced in LNCaP-ADT cells to more than half that seen in LNCaP's (0.305-fold +/- 0.02 sem), whereas in the androgen insensitive LNCaP-abl cells the proliferation rate has significantly increased 1.7-fold (+/- 0.25 sem) (Figure 3.5 (A).

We also investigated the cells survival ability with a CFA that will highlight a cells ability to grow and resist apoptosis. The increased proliferative ability seen in the LNCaP-abl cells also translated to the colony forming assay (Figure 3.5 (B)), with the LNCaP-abl cells forming significantly more colonies over 2 weeks averaging 167 colonies (+/- 6.9 sem) compared to the LNCaP cells which averaged 48 colonies (+/- 8.8), a 3.5-fold increase. Despite having a reduced proliferative ability, the LNCaP-ADT cells maintained tumorigenicity, forming an average of 37 colonies (+/- 2.9 sem). Overall indicating that the prohibitory effect of bicalutamide on cellular function is lost in the androgen independent LNCaP-abl cells.

Metastasis is another key marker of PCa progression and the emergence of CRPC, here we recorded the migration status of LNCaP cells under ADT using the CIM plates (section 2.5.3) with an increase in electrical impedance indicating the level of migration. Electrical impedance indicated by the cell index score is reduced after treatment with bicalutamide (Figure 3.5 (C)(i)) with the LNCaP having a maximum peak at 0.2548, whereas LNCaP-ADT and LNCaP-abl cells peaked at 0.008 and 0.001 respectivly. At 40 hours impedance is reduced by 153% in the LNCaP-ADT cells and 222% in the LNCaP-abl (Figure 3.5 (C)(ii)), by 60 hours impedance has increased slightly but it is still much less than that seen in the LNCaP cell with LNCaP-ADT cells reduced 106% and LNCaP-abl cell reduced 145% (Figure 3.5 (C)(iii)). These results indicate that there is very little migration occurring in these cells. We also recorded the cell index for PC3 cells which were used as a positive control (Appendix A, Figure A.4) and LNCaP cells incubated with 2% FBS chemoattractant as a negative control. These results indicated a significant increased migration in the PC3 cells, which had a maximum peak of 1.214. Whereas the LNCaP cells incubated with low 2% FBS chemoattractant had a maximum peak of 0.2386, which is similar to the migration observed with the LNCaP cells incubated with 10% FBS as a chemoattractant.

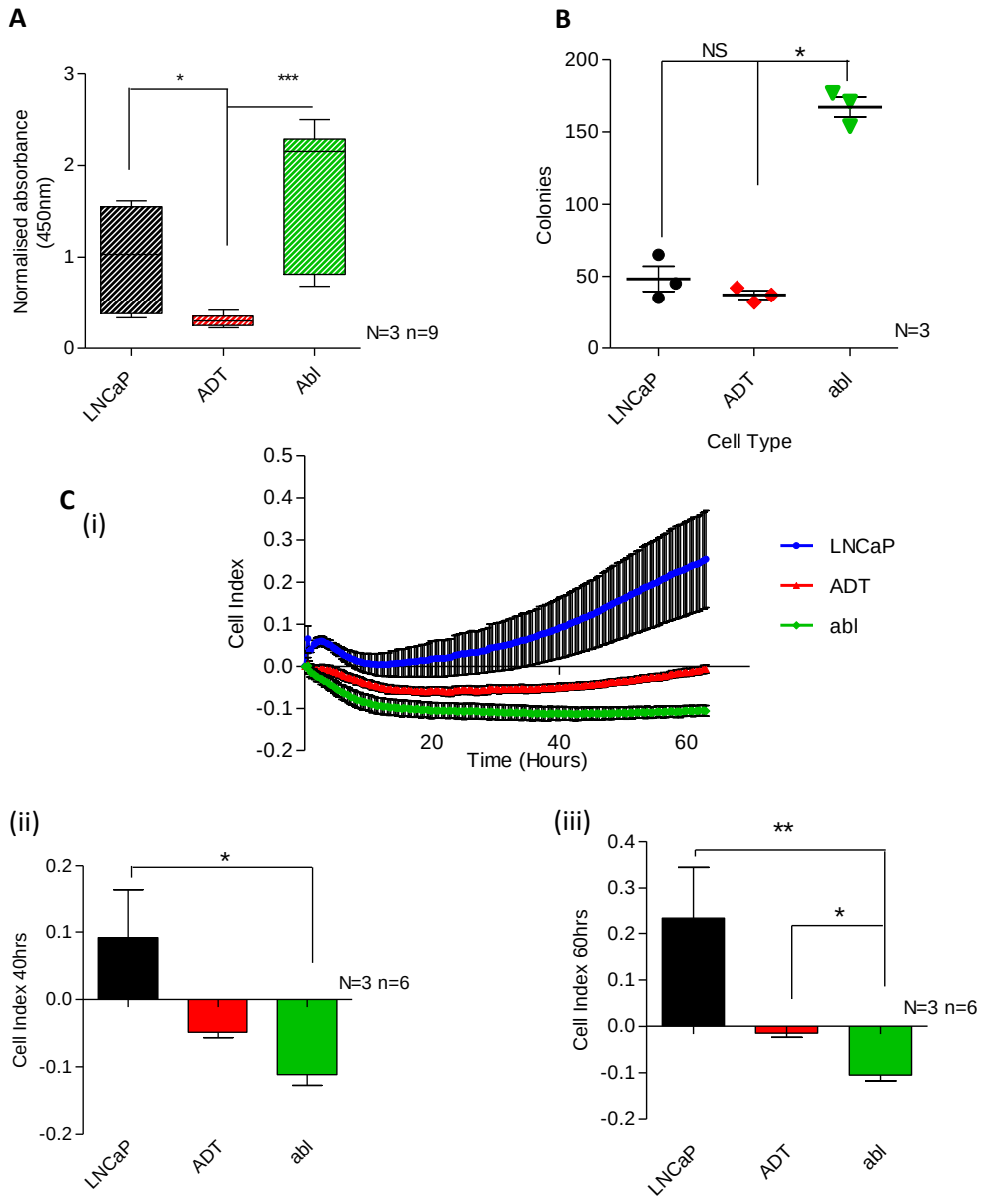

Figure 3.5: Proliferation and colony forming ability are significantly decreased after initiation of ADT but significantly increases in cells which are androgen independent but migratory capacity is reduced in both: *(A) Proliferation assessed using WST-1 assay absorbance at 450nm normalised to control LNCaP. (B) Colony forming assay performed over 14 days. (C(i)) Migration assessed using the Xcelligence™ system cell invasion and migration plates with chemoattractant 10% FBS. Assesses as cell index at (ii) 40 hours and (iii) 60 hours. Analysis of androgen sensitive LNCaP cells (blue), LNCaP-ADT cells treated with 10μM bicalutamide (7-10 days) (red) and androgen insensitive long-term androgen deprived LNCaP-abl cells (green). Analysed using Kruskal-Wallis significance test and Dunn's multiple comparison post hoc test between cell types and treatments. * P<0.05, ** P<0.01, ***P<0.001, NS not significant.*

3.2.2 CaV1.3 expression

3.2.2.1 CaV1.3 gene expression is associated with ADT in patient samples.

To confirm the increased expression of CaV1.3 with PCa stage and also investigate the impact of ADT we utilised the Taylor et al microarray database (Taylor et al., 2010). In this cohort it was observed that *CACNA1D* expression in the 28 paired primary samples had 10.3% higher CaV1.3 than their adjacent normal pairs (paired t-test t=3.15 with p=0.018, paired Wilcoxon signed rank p=0.034). While expression was 11.3% higher on average in the n=18 metastatic compared to the n=130 primary tumours (t-test t=2.7 with p=0.035, Wilcoxon signed rank p=0.032) (Figure 3.6(A)). Furthermore, the n=18 metastatic tumours had 23.5% higher CaV1.3 expression than the adjacent normal samples (t-test t=5.0 with p=0.000000114, Wilcoxon signed rank p=0.0000021). While this matches the observations of previous studies demonstrating that *CACNA1D* expression is higher in metastatic CRPC (Chen et al., 2014), we wanted to investigate if ADT was a direct driver for this increase. We compared *CACNA1D* expression across patients post-ADT (n=10, median=3.27) and ongoing ADT (n=24, median=3.21) to those who had no recorded hormone therapy status (n=114, median=3.11). Higher expression was observed for ADT versus the untreated (t=2.643 with p=0.0407, Wilcoxon p=0.0315) and for the pooled ADT and post-ADT (n=34) relative to the untreated group (t=2.637 with p=0.0448, Wilcoxon signed rank p=0.0315) (Figure 3.6 (B)). Despite displaying higher expression no significant difference was found for post-ADT compared to the untreated, nor for post-ADT relative to ADT.

Using the associated clinical data matched to the dataset we sought to identify correlations between CaV1.3 expression and various clinical parameters. Here expression was associated with higher combined Gleason scores in combined primary and metastatic tumour samples (Figure 3.6 (C)), whose scores were determined originally from radical prostatectomy specimens. This was supported by one-way ANOVA across Gleason scores 6 to 8 for all samples ($F_{2,24}$=8.1, p=0.012) and the primary ones alone ($F_{2,19}$=7.4, p=0.018). Similarly, t-tests of Gleason scores 6 versus 7 for primary samples (n=41 vs n=73, t=3.6, p=0.0007) showed the same association of CaV1.3 expression with a higher score. This increased expression of CaV1.3 was also correlated to an increased risk of biochemical recurrence (Figure 3.6 (D)). The highest quintile of CaV1.3 expression had worse risk of biochemical recurrence over time (n=27, median=5.8 months) compared to low CaV1.3 (n=27, median=84.3 months, 95% CI 77.4-100.2). It was also observed that CaV1.3 expression did not have any correlation with lymph node status or positive margin status.

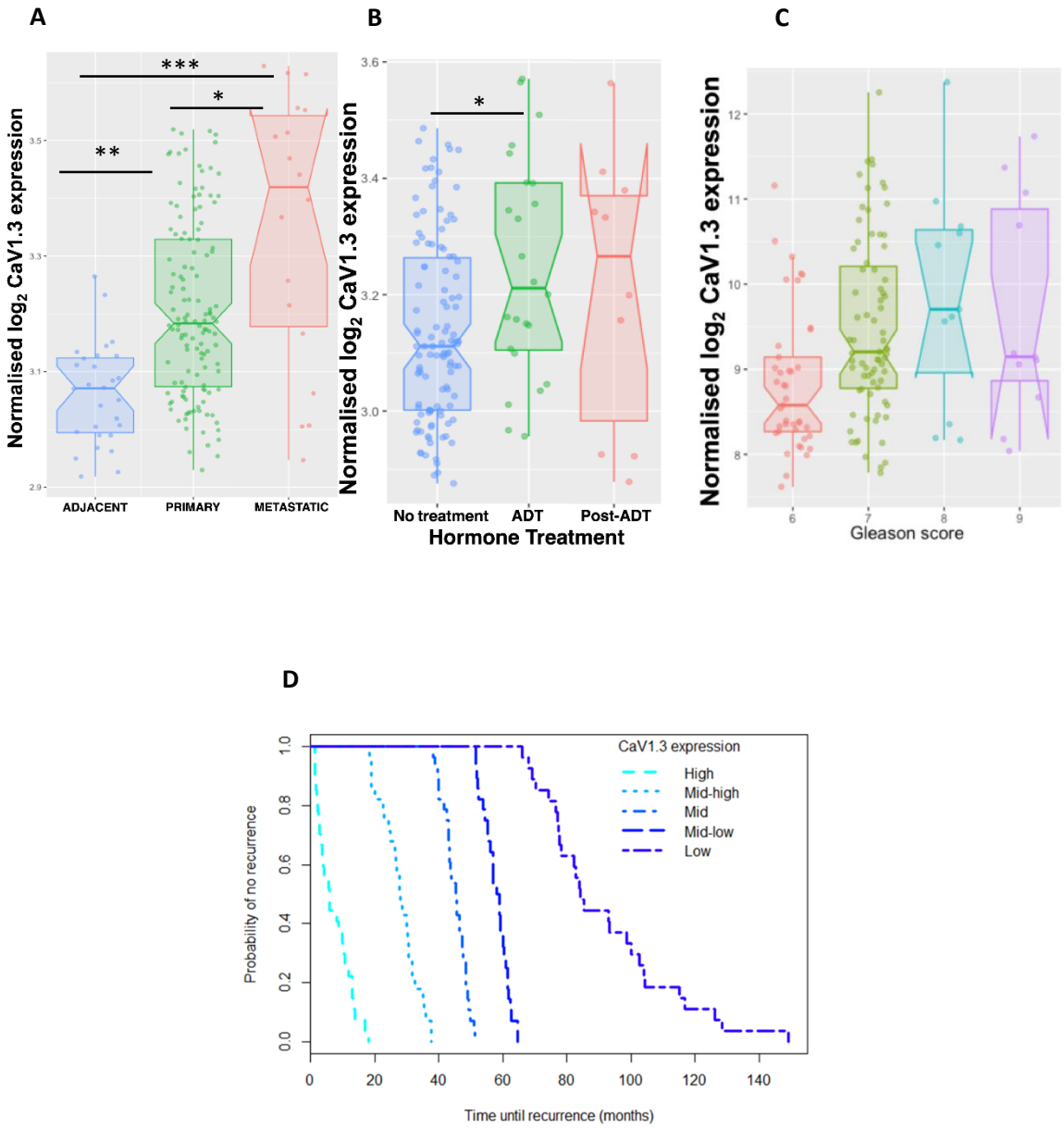

Figure 3.6: Increases in CACNA1D (CaV1.3) expression in prostate cancer patients is associated with sample type, androgen deprivation treatment and Gleason score. *(A) Normalised Log2-scaled CaV1.3 expression according to sample type, metastatic tumours (red), primary tumours (green) and adjacent normal samples (blue). (B) Normalised Log2-scaled CaV1.3 expression according to hormone therapy status post-ADT samples (red, median=3.27), ADT samples (green, median=3.21) and untreated samples (blue, median=3.11). (C) CaV1.3 was positively correlated with combined Gleason score for the combined primary and metastatic sample sets. (D) High expression of CaV1.3 is associated with shorter time (months) to biochemical relapse (n=27). Generated from bioinformatical analysis of publicly available meta-analysis (Taylor et al., 2010), (Bioinformatic analysis completed upon request by Dr Tim Downing).*

3.2.2.2 CaV1.3 expression is significantly increased after treatment with bicalutamide.

Given that the clinical data has highlighted an association between ADT and the expression of CaV1.3, we wanted to establish the expression of CaV1.3 in LNCaP cells under treatment with bicalutamide in both the cell culture model and the *in vivo* mouse model.

In our cell culture model, we observed gene expression in LNCaP-ADT cells to be significantly higher than that of the control LNCaP cells (1.633-fold +/- 0.189 sem), with LNCaP-abl cells having a less pronounced increased expression (1.28-fold +/- 0.2 sem) (Figure 3.7(A)). There was no significant increased genetic expression of *CACNA1D* in our LNCaP xenograft mouse model treated with bicalutamide compared to control at any time point (Figure 3.7(B)). However, there is an increased trend seen in bicalutamide treated mice on day 14 with a 1.7-fold (+/- 0.6 sem) increased expression compared to vehicle control mice.

In terms of protein expression, western blot analysis carried out on the cell model indicates reduced CaV1.3 expression in the LNCaP-ADT cells (0.57 +/- 0.196 sem) but a significant increase in the LNCaP-abl cells (2.77 +/- 0.2 sem) compared to the LNCaP (Figure 3.7 (C)). Analysis of CaV1.3 detected in LNCaP xenografted mice treated with bicalutamide (Figure 3.7 (D)) showed significantly enhanced expression by day 21 in the bicalutamide treated mice compared to corresponding control treated mice. The bicalutamide treated mice had a 12-fold increase expression (12.09 +/- 1.2 sem), whereas the vehicle treated mice had a 7-fold (7.27 +/- 0.1 sem) increased expression by day 21 compared to day 7. When we directly compare the bicalutamide treated samples at day 21 to the vehicle treated samples at day 21 a 66.25% increased expression is observed.

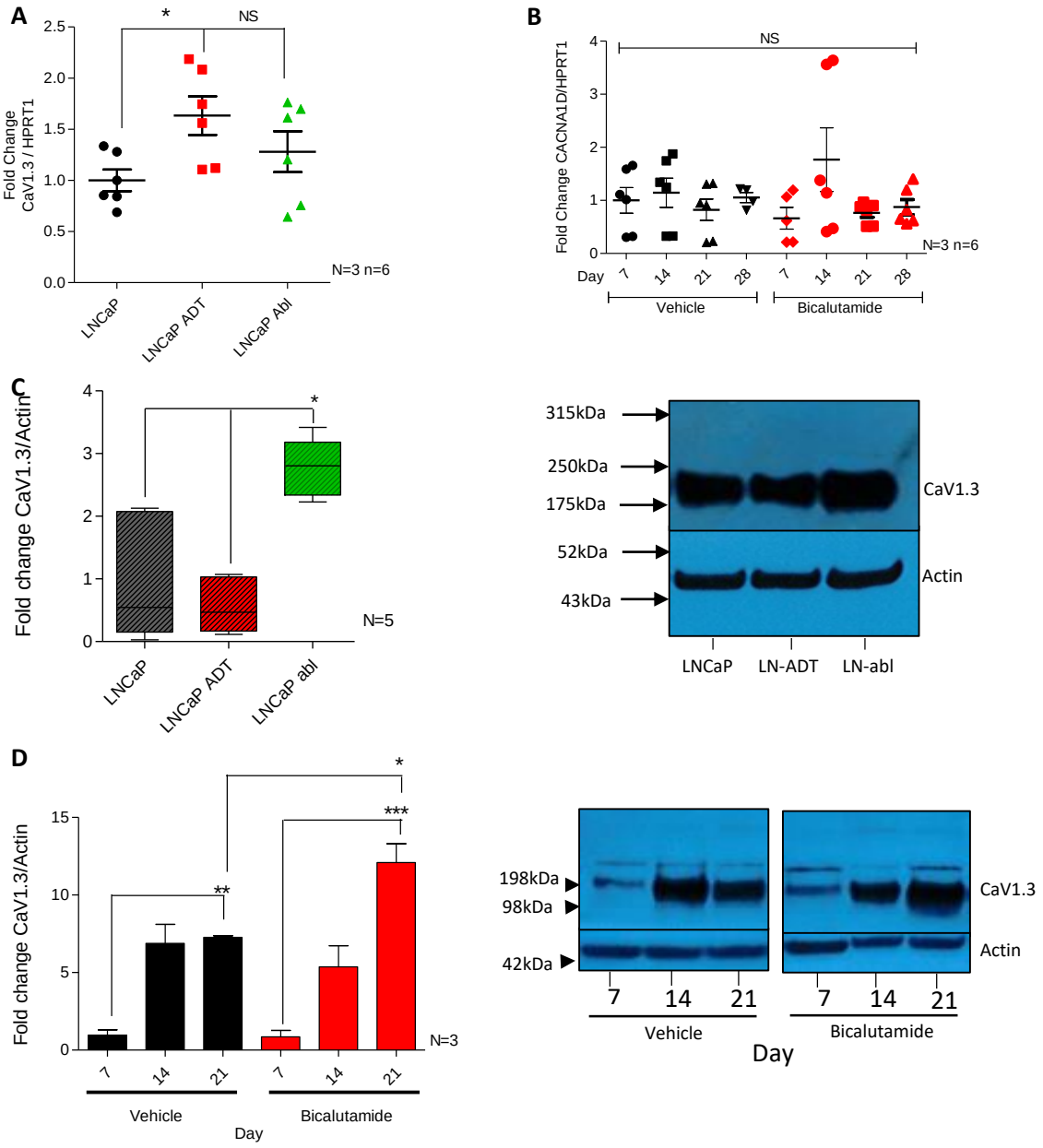

Figure 3.7: Expression of CaV1.3 is significantly increased after ADT with bicalutamide*: PCR analysis of CaV1.3 in (A) Cell lines normalised to LNCaP and (B) LNCaP Mouse xenograft compared to control day 7. Western blot analysis of CaV1.3 normalised by expression of the housekeeping gene Actin of cell. (C & D) Western blot analysis of protein expression of CaV1.3 normalised by expression of the housekeeping gene Actin. Analysis of (A, C) androgen sensitive LNCaP cells (black), LNCaP-ADT cells treated with 10 µM bicalutamide (7-10 days) (Red) and androgen insensitive long-term androgen deprived LNCaP-abl cells (Green) or (B,D) BALB/c immunocompromised mice xenografted with 2x10^6 LNCaP cells in Matrigel treated daily with 1 0µM/2 kg bicalutamide (Red) or with equivalent vehicle control (Black). Analysed using one-way analysis of variance followed by Tukey's multiple comparison test. * P<0.05, ** P<0.01, ***P<0.001, NS not significant.*

3.2.2.3 CaV1.3 expression is detected on the cell membrane of all cells, as well as in the nucleus of LNCaP and LNCaP-ADT but absent in LNCaP-abl

CaV1.3 is usually located in the plasma membrane of cells where it facilitates the passage of Ca^{2+} ions across the plasma membrane under depolarised states. However previous research has also identified expression of CaV1.3 in the cytosol and the nucleus of the cell (Fourbon et al., 2017). We investigated the cellular location of CaV1.3 in LNCaP cells under ADT by protein fractionation (section 2.4.2). These results also demonstrated the expression of CaV1.3 in the cytosol, the membranes, and the nucleus (Figure 3.8 (A)).

Expression of CaV1.3 in different cellular fractions identified three different band widths. The 250kDa band width had expression in the cytosol and the membranes of the cells. The 175 kDa band width was present in all fractions and the 70 kDa band width was mainly detected in the nucleus of the LNCaP and the LNCaP-ADT cells but was absent in the LNCaP-abl cells. The expression of the 250 kDa band was predominantly expressed in the cytosol. When expression was compared to the LNCaP cytosol fraction we found the expression levels in the LNCaP-ADT cytosolic fraction was 0.9-fold (+/- 0.39 sem), the LNCaP-abl cytosolic fraction was 3.86-fold (+/- 2.0 sem) increased expression. The 170kDa band was predominantly expressed in the membrane fraction with some expression seen in all fractions. Expression levels in the membrane is 0.57-fold (+/- 0.2 sem) in the LNPaP-ADT cells and 0.96-fold (+/- 0.56 sem) in the LNCaP-abl cells compared to the LNCaP cells. The 70 kDa fraction was only expressed in the nuclear fraction, with LNCaP-ADT cells having 3.164-fold (+/- 1.8 sem) increased expression compared to LNCaP nuclear fraction, with no expression detected in the LNCaP-abl cells.

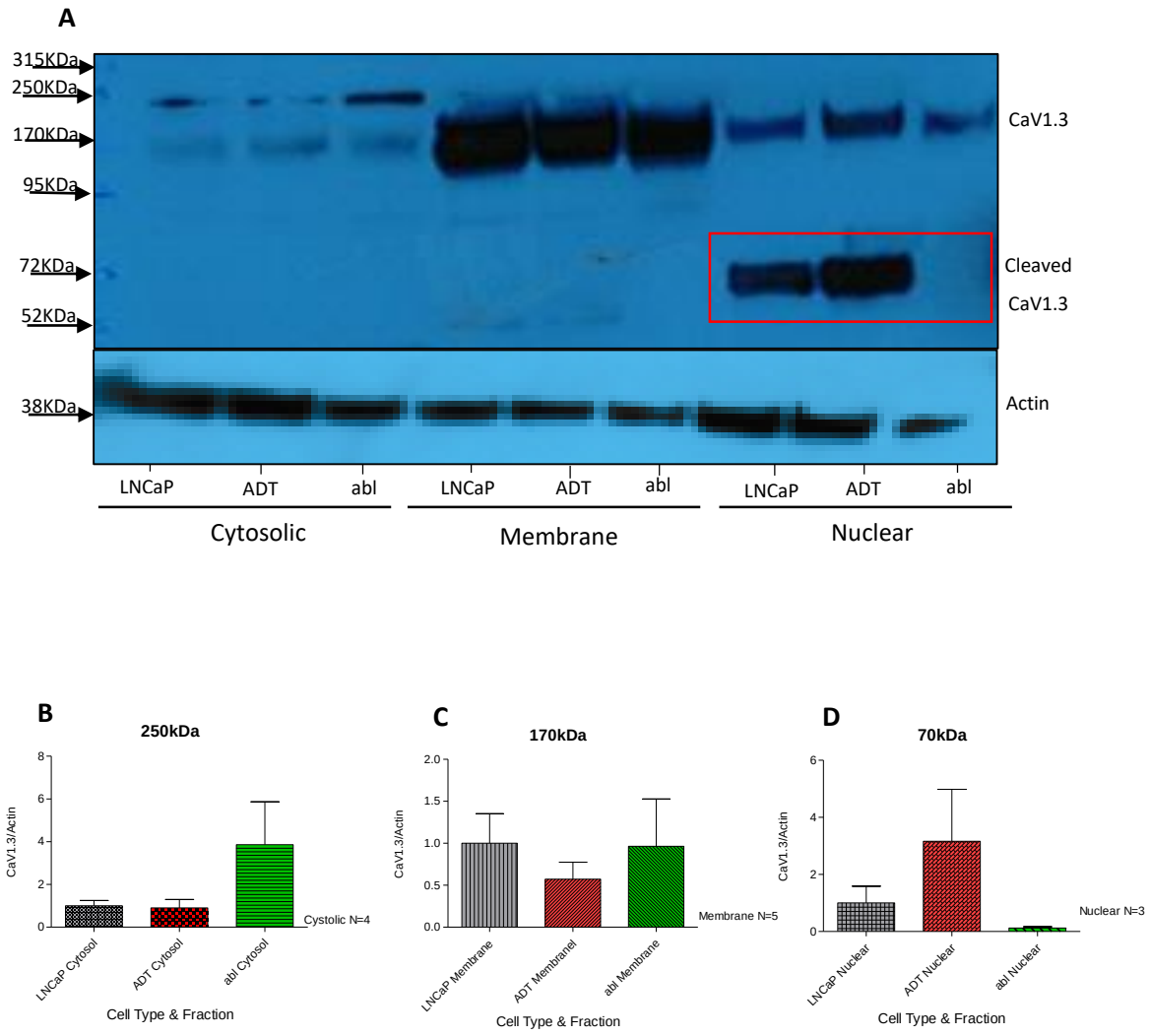

Figure 3.8: Protein expression of CaV1.3 is present in a cleaved form in the nuclear fraction of androgen sensitive prostate cancer cells and absent in androgen insensitive cells*: (A) Western blot analysis of protein expression of CaV1.3 detected in cytosolic, membrane and nuclear fractions. Expression of bands detected at (B) Cytosol – 250 kDa, (C) Membrane – 170 kDa and (D) Nuclear – 70 kDa. Analysis of androgen sensitive LNCaP cells, LNCaP-ADT cells treated with 10 µM bicalutamide (7-10 days) and androgen insensitive long-term androgen deprived LNCaP-abl cells.*

3.3 Chapter discussion

ADT is the main treatment employed for advanced PCa, however the progression to the incurable CRPC occurs in most patients after a couple of years. The mechanism through which the disease acquires the ability to grow in the absence of androgen stimulation, or with continued AR inhibition has been the topic of much research. There is no clear conclusion, although it is thought that the cells develop alternative signalling mechanism through the AR (Karantanos et al., 2013), enhanced anti-apoptosis signals (Raffo et al., 1995) and altered Ca^{2+} signalling (Ardura et al., 2020). The VGCC CaV1.3 has been identified as having an upregulated expression in PCa patients compared to normal prostate tissues, which is significantly increased in those who develop CRPC (Chen et al., 2014). This was confirmed in a meta-analysis study undertaken to investigate the expression of VGCC in various cancer subtypes (Wang et al., 2015), which highlighted the significant expression of CaV1.3 in PCa.

As mentioned, resistance to ADT promotes progression to CRPC therefore we wanted to establish if this was driving changes in CaV1.3 expression. To do this we established a cell model to mimic PCa disease progression under ADT which allowed us to investigate changes in CaV1.3 expression, function, and its biological impact on progression to CRPC. Initially we looked at verifying the suitability of the cell model before using it to confirm the role of CaV1.3.

3.3.1 Cell model characterisation

Our research aims to investigate the potential mechanism through which CaV1.3 could be driving the progression to CRPC under ADT. Using LNCaP cells as the parental cell line we developed an early ADT transition stage cell line, LNCaP-ADT, and for long term androgen independent cell line we used LNCaP-abl (Culig et al., 1999). Initially we needed to characterise the cell model and look for certain markers which represent progression to castrate resistance. Many studies have outlined altered expression of certain proteins under ADT which indicate progression to CRPC. Particularly an increased expression of AR (Karantanos et al., 2013), EMT (Jennbacken et al., 2010) and an increased population of neuroendocrine cells (Yuan et al., 2006). We also wanted to explore the emerging evidence surrounding CSC's which have been linked to treatment evasion and PCa progression (Sánchez et al., 2020; Tang et al., 2009).

The first thing that we observed was a morphologic change in the cells treated with bicalutamide (Figure 3.1). The LNCaP-ADT cells developed neurite outgrowth (indicated with the arrow) after approximately 4 days treatment, which is consistent with reports suggesting the morphology represents NED (Bennett et al., 2013). The LNCaP-abl cells had a condensed cell body and a aggregated clustered growth pattern consistent with previous observations (Culig et al., 1999).

Previous research has shown that the AR is overexpressed in patients who have developed CRPC (Bubendorf et al., 1999; Edwards et al., 2003), so here we look at the molecular expression of AR in our cell model to measure if upregulation occurred after ADT. The genetic expression of AR was significantly increased in our LNCaP-ADT cells representing change at an early stage of ADT before progression to CRPC (Figure 3.2 (A)). This is consistent with recent findings, which highlight that AR amplification occurs in patients treated with ADT, as soon as three months after treatment initiation. This research also observed that later stage treatment samples indicated an increased but less pronounced expression, which our model mimicked in the LNCaP-abl cells (Hamid et al., 2020). This increased AR expression is thought to lead to resistance from continued ADT through various mechanisms, including increased sensitivity to low levels of circulating androgens (Chandrasekar et al., 2015; Gregory et al., 2001). Hence, despite continued ADT there is evidence of AR activation. Various reports show that the activation of AR can increase $[Ca^{2+}]_i$ in many cell types (Foradori et al., 2007; Gorczynska and Handelsman, 1995; Zarif and Miranti, 2016), this process has been shown to be L-type VGCC dependent in LNCaP cells (Steinsapir et al., 1991). Suggesting that activation of the AR could assist in cell survival and differentiation through increased Ca^{2+} signalling via L-type VGCC. As outlined by Culig et al. when defining the characteristics of the LNCaP-abl cell line, this upregulated AR has an increased transactivation activity in the presence of bicalutamide (Culig et al., 1999). Interestingly this AR transactivation activity has been shown to be reduced when the L-type VGCC CaV1.3 is inhibited (Chen et al., 2014).

ADT has also been shown to increase the population of neuroendocrine cells present in the tumour cell population, which coincides with the progression to castrate resistance (Hirano et al., 2004) and is indicative of androgen independence (Ito et al., 2001). This was also observed in our cell model, with significantly increased expression of NSE seen in the LNCaP-ADT cells (Figure 3.2 (B)) and continued upregulation in the LNCaP-abl cells, indicating an increase in the population of neuroendocrine phenotype. While neuroendocrine cells are part of the normal and malignant prostate cell population, differentiation of the epithelial cell to the neuroendocrine cell type is associated with malignant progression (Yuan et al., 2006). This is a commonly observed form of

differentiation under ADT (Patel et al., 2019; Yuan et al., 2006), although the driving mechanism behind it is not fully understood. Neuroendocrine cells do not express the AR, so they are not susceptible to ADT and are also thought to assist in treatment evasion through anti-apoptotic cell survival mechanisms (DaSilva et al., 2013; Xing et al., 2001). In LNCaP cells it has been demonstrated that ADT leads to increased expression of the T-type Ca^{2+} channel, CaV3.2, which induces a Ca^{2+} current responsible for the neurite extension of cells undergoing NED (Hall et al., 2018; Mariot et al., 2002). It appears that the emergence of NED under ADT could be reliant on altered Ca^{2+} signalling in PCa cells.

3.3.1.1 EMT

EMT is a common phenomenon seen in many cancers, which has been identified and associated with disease progression in PCa (Li et al., 2014; Odero-Marah et al., 2018). It is characterised by reduced expression of the cell surface adhesion molecule E-cadherin and increased expression of N-cadherin (Gravdal et al., 2007). Since ADT has been shown to induce EMT (Sun et al., 2012) we looked at the expression in our cell line and mouse models. The LNCaP cells had no expression of N-cadherin in our 2D cell model (Figure 3.3 (A)(ii)) (Ct exceeds 40). ADT did not induce expression of N-cadherin in the LNCaP-ADT or the LNCaP-abl cells, so we were unable to detect EMT. This is not an unprecedented phenomenon, previous studies looking at EMT have also reported a lack of N-cadherin in parental LNCaP cells (Jennbacken et al., 2010; K et al., 2016; Tran et al., 1999), with Jennbacken et al. reporting no induction in subcutaneous xenografts under castration conditions, similar to that reported in the 2D culture LNCaP-ADT cells. However, they did report expression of N-cadherin in an androgen independent cell line (LNCaP-19) which was increased with castration. We found no expression in the LNCaP-abl cell line, which would represent an androgen independent cell type. Interestingly, when we look at our subcutaneous LNCaP xenografted mouse model (Figure 3.3(B)), indications are that EMT is present in the tumour samples treated with bicalutamide (Figure 3.3 (B)(ii)) compared to vehicle control (Figure 3.3 (B)(i)), suggesting that bicalutamide treatment can induce EMT in xenografted LNCaP cells. This is clearly seen in day 21 samples where E-cadherin has a 37% reduced expression compared to vehicle control at day 7, while the expression of N-cadherin is significantly upregulated in the bicalutamide treated tumours by day 21. This reflects the findings of Dr McKenna's group, who investigated these mouse models in relation to induced vascularisation. They reported detection of other markers of EMT in the bicalutamide treated mice by day 21 (Byrne et al., 2016), so there is consensus on the

emergence of EMT in this mouse model. Although EMT is associated with PCa progression under ADT, we need to discuss the potential reasons we do not detect this change in the 2D model. There are many influencing factors present in an *in vivo* model which could be influencing the TME such as the presence of immune cells and growth factors. As reported by Dr McKenna's group there is an immediate induction of hypoxic TME in these mice when treated with bicalutamide and it is regularly reported that EMT is induced under hypoxic conditions in many cell types due to their inter-related pathways (Tam et al., 2020). These inter-related pathways have recently been indicated in PCa studies (Bery et al., 2020; Iwasaki et al., 2018). Interestingly Bery et al. describe a positive feedback loop between Zeb 1, a common transcription factor for EMT and a Ca^{2+} activated potassium channel SK3, which increases the SOCE in PCa cells under hypoxia. The increased expression of Zeb 1 and SK3 could be reduced by blocking this SOCE with Ohmline, an SK3 inhibitor. This informed us that going forward experiments for the project needed to be designed with hypoxic conditions in mind as HIF signalling appears to play an important role in many of the reported mechanisms associated with PCa progression.

3.3.1.2 Stem cell markers

Stem cell surface markers CD44 and CD133 are commonly associated with cancer stem cells, which can become enriched in PCa after ADT (Ojo et al., 2015). This may assist with treatment evasion and tumour regrowth (Tang et al., 2009). Stem cell surface markers were not significantly altered with treatment in our cell model (Figure 3.4 (A)), although CD44 (Figure 3.4 (A)(i)) does have an almost 2-fold averaged increased expression, suggesting some upregulation. There was also no altered expression of transcription factors Oct4 and Nanog detected (Appendix A, Figure A2), which are associated with pluripotency maintenance and indicative of cancer stem cells (Amini et al., 2014; Rodda et al., 2005). There is some difficulty in detecting stem cells among a population as they are generally present in low numbers and are difficult to enrich in 2D cell cultures due to their anchorage independent growth (Gao et al., 2018; Skvortsov et al., 2018). Stem cells usually make up less than 1% of the population within tissue samples (Klonisch et al., 2008), and rely on TME factors to expand including hypoxia (Carnero and Lleonart, 2016). Therefore, it is not surprising that stem cell enrichment was not significantly detected here using our 2D cell culture model. Of particular interest to our cell model is the research by Sánchez et al., who describe the propagation of a neuroendocrine phenotype and stem cell enrichment in LNCaP cells incubated for 3 months in androgen depleted medium (LNCaP-NE). They also found a similar response in

cells which had been incubated with the non-steroidal anti-androgen 2-hydroxyflutamide for 2 months (LNCaP-FLU). For comparison they also tested the expression of NED and stem cells in LNCaP-abl cells. However, while they did detect NSE in the LNCaP-abl cells they noted no detection of stem cells surface markers in these cells. This is consistent with our findings in this cell line. The distinct difference between the LNCaP-abl and the LNCaP-NE was the expression of AR, which is absent in the LNCaP-NE but upregulated in the LNCaP-abl (Figure 3.2 (A)). This suggests that the emergence of a stem cell population could be a transient condition seen in the early stages of ADT, which allows the cells survive the harsh environment and subsequently differentiate into a more robust phenotype. When we examined the xenografted mouse model (Figure 3.4 (B)), where anchorage independent growth could be better modelled, there was an increased population of stem cells detected in the tissue samples which had been treated with bicalutamide compared to the vehicle control. This increased expression of both CD44 and CD133 (Figure 3.4 (B)(i)(ii)) was significant from day 14, which indicated an early stem cell enrichment. This is in agreement with other research of stem cell enrichment under ADT (Sánchez et al., 2020; Tang et al., 2009). Tang et al. investigated LNCaP xenografted mice who were castrated and evaluate the expression of stem cell markers at days post castration. They show that they had increased expression of CD44 and c-kit which peaked at day 15 before declining back to base levels by day 30. This reflects our findings where CD44 and CD133 peak at day 14 with bicalutamide treatment before reducing. Supporting the proposed transient stem cell state under initial ADT. However, it is evident, due to lack of expression detected in the 2D cell model that there is a reliance on TME factors for stem cell propagation. There are many factors in the TME such as growth factors and extracellular matrices which could be contributing to the stem cell enrichment detected in the xenografted mouse model. There have been many studies linking the expression and propagation of stem like cells in cancers with a dependence on HIF signalling (Heddleston et al., 2010; Keith and Simon, 2007; Yun and Lin, 2014). Added to this, as we will discuss later, hypoxia and HIF signalling have been closely associated with Ca^{2+} signalling and the ion channels involved in Ca^{2+} signalling (Azimi, 2018),. Therefore, we will look at enhancing the cell model stem cell enrichment under ADT through low O_2 conditioning.

3.3.1.3 Functional efficacy

Given that prostate cells require androgen binding to AR to initiate growth signals it was expected that ADT should inhibit the proliferation of LNCaP cells. This was observed with LNCaP-ADT cells

which had a significant reduction in proliferation (Figure 3.5 (A)). However, both proliferation and colony forming ability (Figure 3.5 (B)) were significantly increased in the LNCaP-abl cells, which was indicative of progression to androgen independence and castrate resistance (Williams et al., 2011). It is widely reported that Ca^{2+} fluctuations are known to drive PCa proliferation and differentiation through various proposed mechanisms (Ardura et al., 2020; Flourakis and Prevarskaya, 2009). Ardura et al. present a comprehensive review in which they propose many Ca^{2+} dependent mechanisms for androgen independent proliferation in PCa, including activation of Nuclear factor of activated T-cells (NFAT), AR reactivation through activation of Calcium/Calmodulin-Dependent Kinase Kinase (CAMKK) and over activation of Akt and extracellular-regulated kinases (ERK) by S100 Ca^{2+} binding proteins, some of which will be explored throughout this thesis.

Migration was not significantly altered in any LNCaP cells either prior to or after treatment with ADT (Figure 3.5 (C)). This however could be due to the low metabolic rate of LNCaP cells, since they have a slow growth pattern, they have little requirement to migrate for nutrients. These results were reflective of previous migration rates observed in LNCaP cells using the Xcelligence™ (Debelec-Butuner et al., 2014; Dondoo et al., 2017). Where the addition of external stimulants in the form of growth factors or conditioned media was required to elicit migration in the CIM plates.

Overall, these findings suggest that the cell model is a robust reflection on many aspects associated with PCa progression to CRPC. There is a phenotypic change observed when the LNCaP cells are treated with ADT. The model has increased expression of AR and undergoes NED. There is EMT and stem cell enrichment in the mouse model but not the 2D model indicating a reliance on TME factors. We also reported enhanced proliferation and CFA in the LNCaP-abl indicating androgen insensitive progression and emergence of CRPC.

3.3.2 Expression of CaV1.3

CaV1.3 is a voltage gated Ca^{2+} channel which is associated with excitable cells; however, it has also been identified in many non-excitatory cells (Davenport et al., 2015; Pitt et al., 2021). There have been two studies carried out which have both identified significant CaV1.3 upregulation in PCa tissues compared to normal prostate epithelium (Chen et al., 2014; Wang et al., 2015), with Chen et al. demonstrating that the expression was further enhanced as the cancer progressed to CRPC. This led to the hypothesis that bicalutamide treatment could promote enhanced CaV1.3

expression which in turn leads to treatment resistance and progression to CRPC through enhance Ca^{2+} mobilisation.

3.3.2.1 CaV1.3 expression in clinical data

The meta-analysis study carried out by Wang et al. presented the evidence of upregulation of VGCC's across many cancers (Wang et al., 2015). Of interest they highlighted that CaV1.3 was significantly increased in PCa, along with CaV1.2 and the T-type VGCC CaV3.1. The limitations of Wang et al.'s meta-analysis, for the purposes of this project, were the lack of associated data with disease or treatment status. Since the progression to CRPC is associated with ADT, we wanted to determine if it had any impact on CaV1.3 expression, which in turn could be promoting treatment resistance. We sought to examine the expression of CaV1.3 specifically in relation to disease stage as well as expression changes related to ADT. We also wanted to determine if expression was related to aggressive disease type and resurgence of CRPC after ADT. For this we examined data previously collected and outlined by Taylor *et al*. where they examined 176 samples of which 130 were primary cancers and 18 were metastatic. A subset of primary cancers also had 28 paired adjacent normal samples (Taylor et al., 2010). From this analysis we showed that CaV1.3 expression holds significant clinical relevance in PCa patients, with an increased expression detected in primary PCa compared to normal tissue, which was further enhanced in CRPC (Figure 3.6 (A)), in agreement with previous studies (Chen et al., 2014).

There are studies identifying an increased expression of the T-type VGCC CaV3.2 (Hall et al., 2018) in PCa cells treated with bicalutamide, which they equate to the development of NED. Here we reveal that ADT also increases the expression of CaV1.3. When we looked at the expression of CaV1.3 in relation to ADT status (Figure 3.6 (B)) in the patient samples it was significantly increased in samples on or post treatment. This has not been previously identified to our knowledge, highlighting a distinct gap in the research of PCa progression under ADT. We also found that CaV1.3 was associated with increasing Gleason score (Figure 3.6 (C)), and shorter time to biochemical recurrence (Figure 3.6 (D)). This highlights that not only is CaV1.3 upregulated under ADT, but it is also associated with clinical parameters which indicate poor prognosis. Highlighting that the upregulation of this channel under ADT is playing a role in disease progression. This reflects the findings of a study which looked at the association of six biomarkers, which included *CACNA1D*, with an aggressive PCa phenotype (Zhu et al., 2015). They found that *CACNA1D* was a marker for Gleason score and biochemical relapse. To our knowledge this is the first time these distinct parameters have been looked at in conjunction with CaV1.3 expression in relation to ADT.

These findings reflect our hypothesis that there is a mechanism driving the progression to treatment resistance and development of CRPC which involves CaV1.3 expression post ADT.

3.3.2.2 CaV1.3 expression in cell line models

Once we had established the association between CaV1.3 expression and PCa progression after initiation of ADT in the clinical data analysis, we needed to confirm that our LNCaP cell model under ADT mimicked the in vivo. This would verify the use of the cell model to further investigate associated mechanisms going forward. The expression of CaV1.3 mRNA was significantly upregulated in the LNCaP-ADT cells. This indicates that mRNA upregulation occurs at an early timepoint after initiating bicalutamide treatment (Figure 3.7 (A)). The expression in the LNCaP-abl cells also indicated upregulated genetic expression of CaV1.3, although this did not have statistical significance. This suggests that our cell line model follow similar trends to that observed in patient samples as outlined above. The genetic expression in the mouse model indicates that there is no significant increase in mRNA detected for CaV1.3 in mice treated with bicalutamide compared to those treated with vehicle (Figure 3.7 (B)), although there is an increased trend observed at day 14.

On a protein level there is a significant increased expression of CaV1.3 in the LNCaP-abl cells (Figure 3.7(C)), which reflects our finding in the clinical data which had enhanced expression in the CRPC samples (Figure 3.6 (A)). This correlates with the increased proliferation and colony forming ability (Figure 3.5 (A)(B)), suggesting that CaV1.3 could be influencing the survival and tumorigenic potential of CRPC. This is also reflected in the mouse model where there is a significant increased expression in the bicalutamide treated mice by day 21 (Figure 3.7(D)), with some increased expression seen in the untreated over time, which will be discussed below.

As stated, the protein levels of CaV1.3 detected in our mouse model showed an upregulation of CaV1.3 over time in both the vehicle treated and those treated with bicalutamide. This is consistent with the study by Chen et al, where they demonstrated expression of CaV1.3 is upregulated in primary PCa samples compared to benign tissue which increases with disease progression to CRPC (Chen et al., 2014) and also what we found in our clinical data analysis (Figure 3.6 (A)). However, the bicalutamide treated samples displayed a 60% increase in expression by day 21 compared to linked time point vehicle control. This suggests that even in the absence of bicalutamide treatment, CaV1.3 expression increases with tumour progression, although treatment with bicalutamide significantly enhances expression over time. Interestingly, this

correlates with increased levels of hypoxia seen after initiation of ADT in this mouse model (Byrne et al., 2016; Wang et al., 2008). This initial hypoxic response seen after bicalutamide treatment could in part be related to the increased expression of CaV1.3 in our mouse model. This ties in with research in this area that has highlighted a coregulatory relationship between L-type VGCC and the hypoxic response element HIF-1α (Guo et al., 2010; R. Li et al., 2015). Guo et al demonstrated exposure of progenitor cells to hypoxic conditions led to increased $[Ca^{2+}]_i$ by influx through L-type VGCC, resulting in proliferation. Li et al. show that hypoxic conditions enhanced the expression of CaV1.2 and CaV1.3 in PC12 cells, which was reduced by echinomycin, a HIF-1α inhibitor. Whereas Hui et al. demonstrated that expression of HIF-1α was reliant on influx of extracellular Ca^{2+} in PC12 and HEK cells, which could be reduced by chelating Ca^{2+} or through inhibition of VGCC with nifedipine (Hui et al., 2006). This suggests a co-dependency between HIF-1α and Ca^{2+} influx through VGCC in PC12 cells. Drawing from this association in chapter 4 we will discuss the correlation between CaV1.3 and hypoxia in our cell model and the potential for these factors to regulate PCa progression.

As reported by Chen et al. silencing CaV1.3 expression or blocking the channel with CCB inhibited androgen induced Ca^{2+} influx and AR transactivation to the nucleus in PCa (Chen et al., 2014). This androgen mediated Ca^{2+} influx was confirmed in LNCaP cells (Sun et al., 2006) to be facilitated by L-type VGCC. Although they show that inhibiting the intracellular AR did not reduce $[Ca^{2+}]_i$ nor did preventing the transmembrane passage of testosterone by binding it to large chaperones. Instead they present evidence that inhibiting G protein coupled receptors (GPCR) could reduce the fast activating Ca^{2+} signal, suggesting that the androgen stimulated increase $[Ca^{2+}]_i$ was due to stimulated surface GPCR. However, it is not stated in any of these studies which L-type VDCC is responsible for this androgen regulated Ca^{2+} influx. Reports have identified an upregulation of both CaV1.3 and CaV1.2 in PCa (Wang et al., 2015), which are both sensitive to inhibition by dihydropyridines. Therefore, it was necessary to investigate the functional ability of the upregulated CaV1.3 in our cell model to determine if it is actively contributing to Ca^{2+} mobilisation, which we explore in the next chapter.

3.3.2.3 Cellular location of CaV1.3

The cellular localization of the channel is also of importance when considering the functional aspects of Ca^{2+} mobilisation. CaV1.3 is an ion channel which is normally situated in the plasma

membrane which senses voltage changes. Under depolarised states CaV1.3 conformationally changes, allowing the entry of Ca^{2+}. However, this channel has also been identified in the cytosol (Fourbon et al., 2017) and in the nucleus (Lu et al., 2015) where it has alternative effects through binding Ca^{2+} associated proteins or working as a transcriptional regulator. To determine the cellular localization of CaV1.3 in PCa under ADT we used protein fractionation experiments. We separated the cytosol, the membrane bound and the nuclear associated proteins into separate fractions. The molecular weight of the α-1 subunit of CaV1.3 is 245kDa this subunit consists of the pore forming section containing the dihydropyridine binding site. In the fractionation blots (Figure 3.8(A)), we detected complete protein, indicated by the 250kDa band which had predominant expression in the cytosolic fraction, with some expression in the membrane fraction. This suggests that most of the complete CaV1.3 protein may be in the cytosol, which may impact the functional efficacy of the channel. There have been previous studies outlining the subcellular location of this channel in colon cancer cells (Fourbon et al., 2017), with expression detected in the cytosol and also the nucleus. It was shown to contribute to $[Ca^{2+}]_i$ through the functional interaction with the NCX channel. Demonstrating that the increased expression of CaV1.3 may contribute to increased Ca^{2+} mobilisation through interaction with other Ca^{2+} regulating proteins.

We also detected cleaved fragment, indicated by the 70 kDa band, which was present in all fractions. However, since this size protein would be too large to diffuse into the intact nucleus (Wang and Brattain, 2007), we must assume that the 170 kDa protein detected in the nuclear fraction is instead due to the incomplete separation of the fractions. We also detected a 170 kDa subunit, located predominantly in the nuclear fraction. This corresponds to research looking at CaV1.2 in neurons, where a 70 kDa protein was reported in the nucleus (Gomez-Ospina et al., 2006). This protein was identified as the proteolytically cleaved c-terminus of the CaV1.2 channel. The c-terminus was responsible for activating transcription of genes involved in neurite growth, among others. Interestingly we found the nuclear expression of the 70 kDa fragment expressed in the LNCaP cells and the LNCaP-ADT cells, but it was absent in the LNCaP-abl cells, which do not have neurite extension as demonstrated in the morphology observation (Figure 3.1). This suggest that perhaps there is a similar regulation of neurite growth involved in the nuclear translocation of the c-terminus of CaV1.3 in PCa cells. The c-terminal subsection of CaV1.3 has also been found in the nucleus, which one study demonstrated was differentially localised at different developmental stages of the heart development (Qu et al., 2011). The c-terminal expression in the nucleus of this study also highlighted a role in transcription regulation, where it was shown to regulate expression of the Ca^{2+} activated K^+ channel SK2 (Lu et al., 2015).

3.4 Concluding remarks

This chapter has established a robust cell model which mimicks PCa progression under ADT which will be used to investigate the role of CaV1.3. The cell model demonstrates genetic changes associated with ADT such as enhanced AR expression and NSE markers validating its suitability and similarity to in vivo. Through this we have for the first time demonstrated that CaV1.3 expression is enhanced after ADT and that this correlated with enhanced prolfiereation and tumourgenic capacity on CRPC cell line, LNCaP-abl. Importantly we confirmed that CaV1.3 expression was on the cell membrane where it is required to transport Ca^{2+}. Interstingly we also found a CaV1.3 c-terminus fragment within the nucleus suggesting a potential role also as a transcription regulator. Lastly we confirmed in PCa samples an association of CaV1.3 upregulatuon with ADT treatment, as well as highlight correlations with Gleason score and biochemical relapse.

Taken together this work indicates a potential role of upregulated CaV1.3 in driving PCa disease progression. However further work is required to not only directly confirm this association but also to uncover how CaV1.3 is functionally impacting intracellular Ca^{2+}.

Chapter 4 - Investigating the effects of upregulated CaV1.3 on calcium mobilisation under ADT and associated neoplastic phenotypes.

4.1 Introduction

4.1.1 Background of Intracellular Calcium and CaV1.3 in cancer

Ca^{2+} mobilisation is an essential part of normal cell function and is required to support cellular homeostasis. Ca^{2+} is tightly regulated and circulated between the extracellular space, the cytosol, the ER and the mitochondria. Fluctuations in the form of sparks, spikes and sustained intracellular increases trigger different cellular processes such as proliferation, migration and apoptosis, lending to the maintenance of a normal cell cycle (Berridge et al., 2003; Bootman et al., 2001). These are also important processes in the emergence of cancer, altered control of which have been identified as significant requirements for malignant transformation in the hallmarks of cancer (Hanahan and Weinberg, 2000). Hence, altered expression and regulation of intracellular Ca^{2+} is widely reported in contributing to cancer progression (Monteith et al., 2007; Parkash and Asotra, 2010).

CaV1.3 is typically associated with excitatory cells and has a significant role in sinoatrial node activation (Mangoni et al., 2003) and synaptic plasticity (Clark et al., 2003). While this channel is significantly less studied in the context of non-excitatory cells, it has been identified in epithelial cells (Radhakrishnan et al., 2016) including many types of cancer (Fourbon et al., 2017; Ji et al., 2016), where it has been shown to contribute to tumour development (Chen et al., 2014; Hao et al., 2015). These studies highlighted that CaV1.3 expression contributed to cancer progression through increased $[Ca^{2+}]_i$. As outlined in chapter 1, CaV1.3 is a VGCC, which is closed to Ca^{2+} permeation at resting potential but upon membrane depolarisation a conformational change induces an open state, facilitating the passage of Ca^{2+} into the cell.

However, CaV1.3 has also been shown to contribute to $[Ca^{2+}]_i$ in cancer cells in a non-canonical manner, through interactions with other channels such as regulating the activation and function of the NCX channel in colon cancer (Fourbon et al., 2017), which contributed to an increased basal Ca^{2+} level and increased invasion and migration potential. The predominant Ca^{2+} entry mechanism in most non excitable cells, including cancer cells is the SOCE (Parekh and Putney, 2005), which is now known to involve activation of the ER bound STIM and plasma membrane bound ion channel

Orai and some members of the TRPC channels (Perrouin Verbe et al., 2016). These channels are activated when Ca^{2+} is released from the ER via IP_3R or RyR, as described in chapter 1 (section 1.5.1). STIM1 senses the reduced Ca^{2+} levels in the ER and functionally couples with and opens the Orai or TRPC channel to allow Ca^{2+} entry (Derler et al., 2016). This increases the $[Ca^{2+}]_i$, which allows ER Ca^{2+} replenishing via the SERCA pump. A functional role for CaV1.3 in this process has not been conclusively defined although one report identified an L-type low threshold activated Ca^{2+} current in pyramidal neurons, which they demonstrated assisted with maintaining ER Ca^{2+} stores (Power and Sah, 2005). There is also evidence that a functional coupling can occur between RyR and CaV1.3 which induces ER Ca^{2+} depletion through RyR when CaV1.3 is activated through membrane depolarisation (Kim et al., 2007). Therefore, the upregulated expression of CaV1.3 detected in PCa under ADT may be capable of influencing the SOCE current as well as through more traditional voltage gated mechanisms at the plasma membrane.

Ca^{2+} influx through VGCC including CaV1.3 have been shown to be inhibited by calcium channel blockers (CCB). Specifically, studies have shown a small positive inflection on the association between long term CCB use and the development of PCa. However, there are many studies which refute this, finding no connection (Perron et al., 2004; Rodriguez et al., 2009; Ronquist et al., 2004) or an inverse association (Debes et al., 2004; Annette L. Fitzpatrick et al., 2001). There is also research which indicates reduced aggression and longer progression free survival for PCa patients with CCB use (Poch et al., 2013).

Taken together this strong link between disrupted intracellular Ca^{2+} and cancer progression, we wanted to establish the functional efficacy of CaV1.3 on Ca^{2+} mobilisation under conditions of ADT and determine if it contributes to PCa progression. We examined both the canonical mechanism of VGCC activation under membrane depolarisation and the non-canonical role CaV1.3 could have on the non-excitatory Ca^{2+} mobilisation mechanism of SOCE.

4.1.2 Aims of chapter 4.

As highlighted previously in a range of models, CaV1.3 expression is signficantly increased following ADT, therefore our main objective was to determine if the channel is functionally active in regulating intracellular Ca^{2+}. Furthermore, if it influences Ca^{2+} what role does it play on the malignant progression of PCa.

Aim: Investigate if and how CaV1.3 contributes to altered Ca^{2+} mobilisation during ADT and its resultant impact on PCa progression using the previously identified cell models (Figure 3.1).

Hypothesis: Upregulation of CaV1.3 contributes to aberrant Ca^{2+} mobilisation after ADT assisting and/or promoting neoplastic transformation enabling treatment resistance and progression to CRPC

Objectives:

1. Establish the impact of ADT on intracellular calcium in PCa and how this correlates with CaV1.3 expression.
2. Determine using siRNA Knockdown and CCB's if CaV1.3 is directly and functionally involved in the mobilisation of Ca^{2+}.
3. Examine the neoplastic impact conferred by any altered intracellular Ca^{2+} as result of increased CaV1.3 expression under ADT.

4.2 Results

4.2.1 Investigating the voltage gated activity of CaV1.3 Ca^{2+} mobilisation.

CaV1.3 is upregulated in PCa (Chen et al., 2014; Wang et al., 2015), and while it has been clearly implicated in the androgen induced Ca^{2+} influx in PCa (Chen et al., 2014; Sun et al., 2006), there are no studies investigating its voltage gated properties, especially under ADT conditions, where androgen action is inhibited. We have demonstrated increased expression of CaV1.3 in PCa cells which have been treated with ADT (Figure 3.6 and 3.7), thus we wanted to investigate if this channel is functionally active and through its expected voltage gating mechanism.

4.2.1.1 Voltage gated Ca^{2+} current was not detected in any PCa LNCaP cells

The plasma membrane was depolarised by increasing the extracellular K^+ in a PSS solution with 2 mM Ca^{2+} and the BK_{Ca} activator NS1619 (section 2.6.2). Osmotic control was carried out by increasing the extracellular NaCl (Appendix B; Figure B8). There was no indication of a voltage gated Ca^{2+} current in LNCaP cells nor was there any response in ADT treated cells (LNCaP-ADT and LNCaP-abl) which had the increased expression of CaV1.3 (Figure 4.1 (A)(B)(i)). Furthermore, there was no difference detected in the basal cytosolic Ca^{2+} levels between LNCaP, LNCaP-ADT or LNCaP-abl cells, which was recorded prior to KCl injection (Figure 4.1 (B)(i)) at 500 s. The Ca^{2+} peak levels recorded after the cells were depolarised with 60 mM KCl (Figure 4.1 (A)(ii)) or 80 mM KCl (Figure 4.1 (B)(ii)) had no significant change when compared to the LNCaP basal Ca^{2+} levels, as outlined in Appendix B Table B.1. We also performed osmotic control tests to ensure that any effect we may have seen was not due to osmotic stress (Appendix B; Figure B.5). Overall, indicating that CaV1.3 does not function in its traditionally expected canonical manner under depolarisation in these cells, nor does it influence the basal Ca^{2+} level.

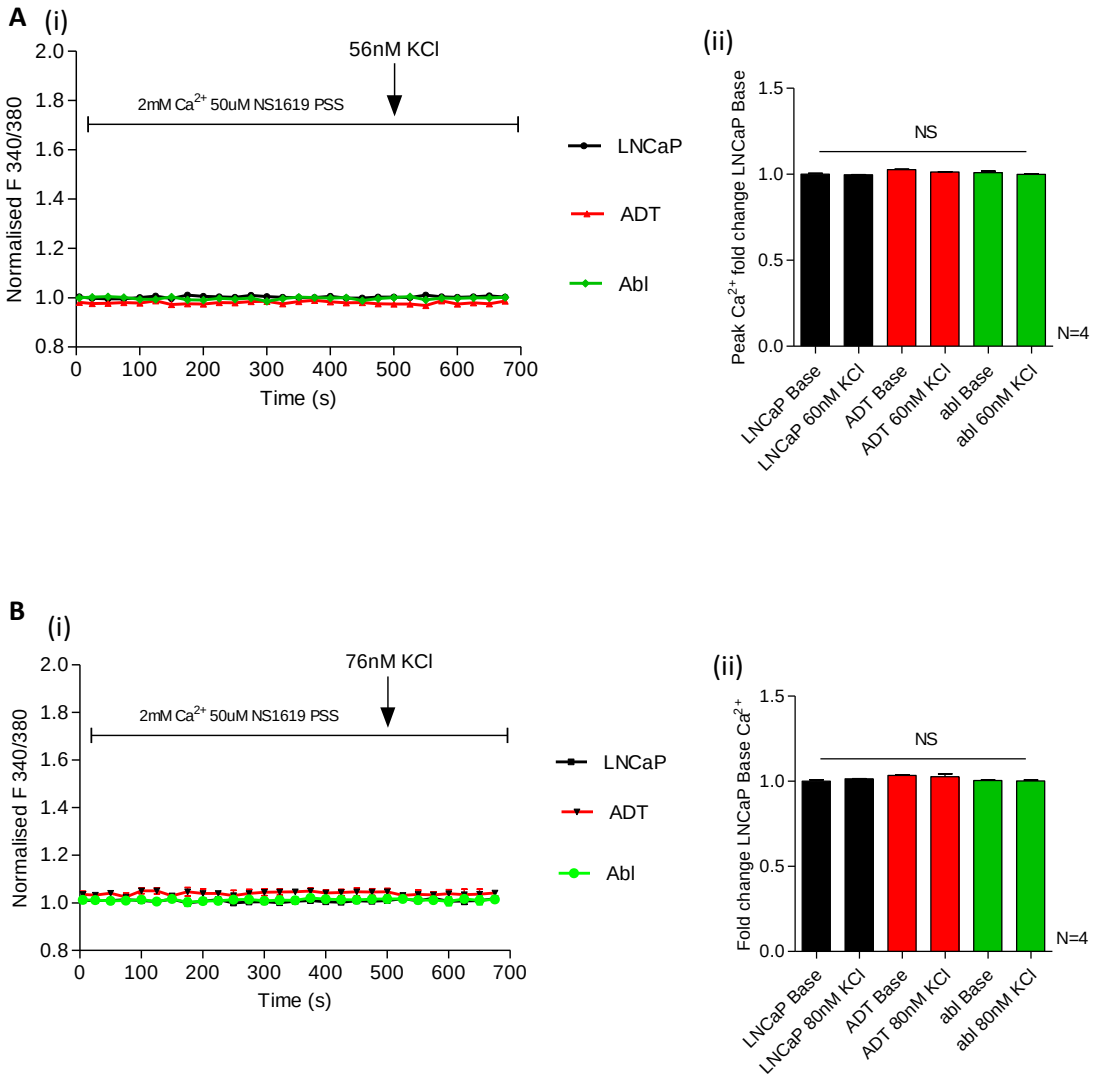

Figure 4.1: CaV1.3 does not function through voltage gating following membrane depolarisation in PCa*: Cells incubated with NS1619 followed by Fura 2-AM underwent ratiometric analysis of calcium concentration over time. Androgen sensitive LNCaP cells (black), LNCaP-ADT cells treated with 10 µM bicalutamide (7-10 days) (Red) and androgen insensitive long-term androgen deprived LNCaP-abl cells (Green) where depolarised with high external potassium concentrations of* ***(A)*** *60 nM KCl or* ***(B)*** *80 nM KCl. (i) Analysed using 2-way ANOVA significance of fluorescence ratio 340:380 at time (s) between cell types (ii) Normalised peak of Base level Ca^{2+} and Ca^{2+} after KCl analysed using Kruskal-Wallis significance test between cell types and treatments. * P<0.05, ** P<0.01, ***P<0.001, NS not significant.*

4.2.2 Investigating the effect increased expression of CaV1.3 has on SOCE in PCa

As previously stated SOCE is the predominant Ca^{2+} mobilisation mechanism in non-excitable cells such as those found in cancer (Mo and Yang, 2018), which promotes the emergence of many cancer hallmarks (Chen et al., 2019). The mechanism involves depletion of the intracellular stores which increases the influx of extracellular Ca^{2+} into the cell as described in section 1.5.1. SOCE has been implicated in promoting cancer associated mechanisms in PCa, such as enhanced proliferation, migration and inhibited apoptosis (Kappel et al., 2017). Although SOCE is primarily considered to be facilitated by the STIM1-Orai1 functional interaction mechanism, there is research that highlights a role for other calcium channels in this mechanism including VGCC such as CaV1.3.

4.2.2.1 SOCE is increased in cells which have the increased expression of CaV1.3

Ca^{2+} imaging experiments were performed on our PCa cell model (LNCaP, LNCaP-ADT, LNCaP-abl) to establish if the increased expression of CaV1.3 detected in the cells after treatment with ADT influenced the SOCE. The intracellular basal Ca^{2+} levels were established for the cells, which were suspended in PSS solution containing no Ca^{2+}. Then Tg was introduced to inhibit the SERCA pump, which results in ER store depletion, hence initiating the SOCE mechanism. The first peak indicates the Ca^{2+} released from the ER (Figure 4.2 (A)) and the second peak indicates the SOCE in response. The second peak is only initiated when Ca^{2+} is introduced to the extracellular fluid, which demonstrates the increase is due to the activity of the plasma membrane bound channels.

The Tg induced ER Ca^{2+}store release (Figure 4.2 (A) first peak) compared to the normalised base Ca^{2+} level of 1, has a maximum peak level of Ca^{2+} of 1.148 in LNCaP cells, 1.150 in LNCaP-ADT cells and 1.341 in the LNCaP-abl cells. This translates to a significant increased peak in the LNCaP-abl cells of 1.9-fold (+/- 0.09 sem) (Figure 4.2 (C)). There is also a significantly increased 2.029-fold (+/- 0.2 sem) slope in the LNCaP-abl cells compared to the LNCaP cells (Figure 4.2 (D)). There was no significant difference observed in the Tg peak or slope between the LNCaP-ADT cells and the LNCaP-cells.

After ER Ca^{2+} release extracellular Ca^{2+} is introduced to induce the SOCE response (Figure 4.2 (A) second peak). Compared to the normalised base Ca^{2+} level of 1 a maximum peak of 1.575 in LNCaP cells, 1.734 in LNCaP-ADT cells and 1.943 in LNCaP-abl cells was observed. Indicating a significant increase in the amount of Ca^{2+} entering the LNCaP-ADT 1.378-fold (+/- 0.09 sem) (Figure 4.2 (E)) and the LNCaP-abl cells 1.616-fold (+/- 0.13 sem) compared to the LNCaP. The slope statistics indicate no significant increase in the LNCaP-ADT cells (0.974-fold +/- 0.14 sem), whereas the slope of the LNCaP-abl is significantly increased 1.74-fold (+/- 0.186 sem) (Figure 4.2 (F)).

Finally we looked at the area under the curve (AUC), which indicates the overall increased $[Ca^{2+}]_i$ in the cells, both ER store release and the SOCE. The LNCaP-ADT cells have no significant overall increased Ca^{2+} compared to LNCaP cells 1.04-fold (+/- 0.01 sem), whereas the LNCaP-abl cells had a significant increased overall Ca^{2+} increase which was 1.132-fold (+/- 0.01 sem) compared to LNCaP cells.

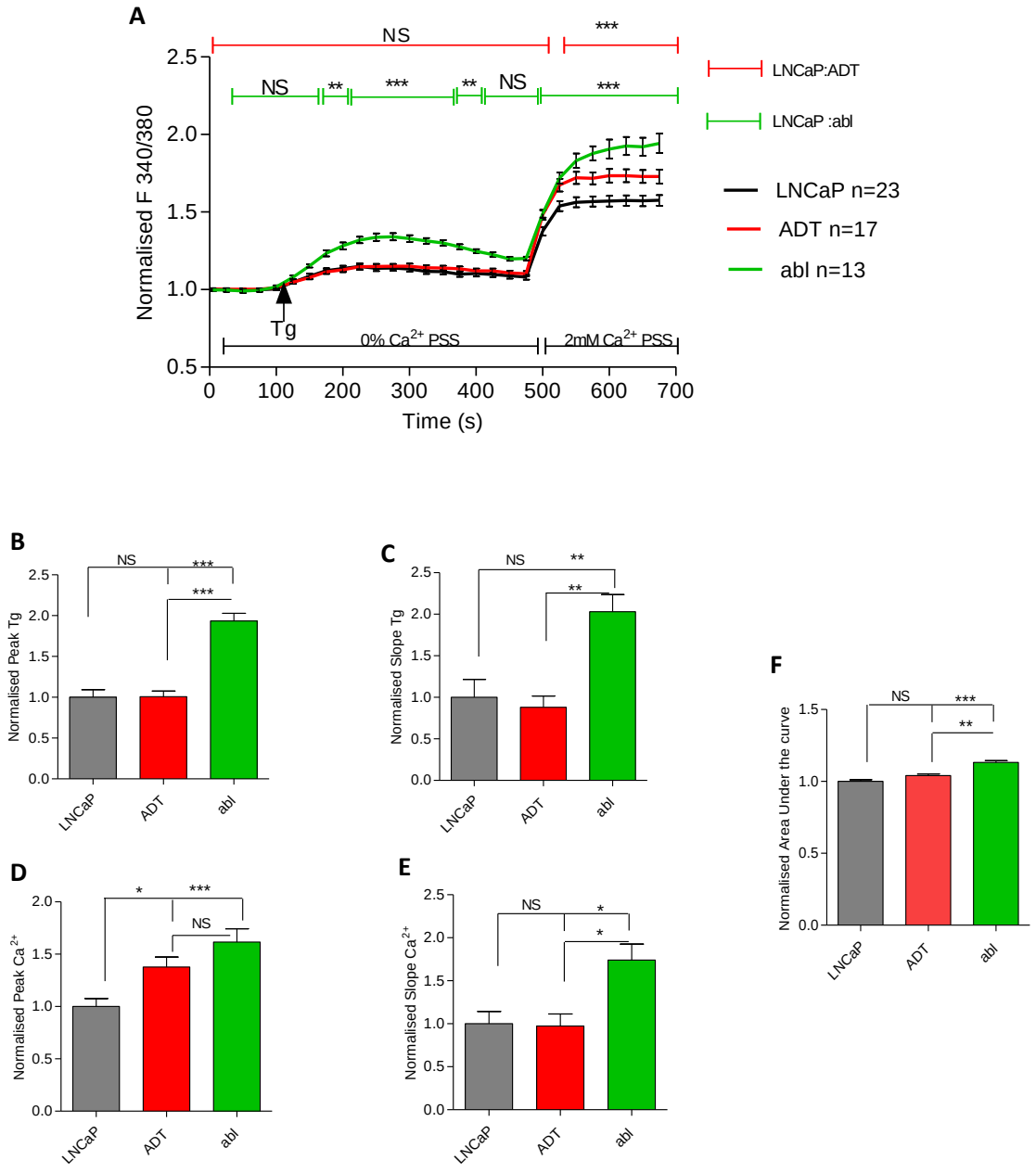

***Figure 4.2: SOCE is increased in LNCaP-ADT cells and further increased in LNCaP-abl cells**: Thapsigargin (Tg) induced store operated calcium entry (SOCE) indicated by Fura 2-AM ratio metric analysis of calcium concentration over time (s). Analysis of androgen sensitive LNCaP cells (black), LNCaP-ADT cells treated with 10 µM bicalutamide (7-10 days) (Red) and androgen insensitive long-term androgen deprived LNCaP-abl cells (Green). **(A)** Analysed using 2-way ANOVA significance of fluorescence ratio 340:380 at time (s) between cell types. Normalised **(B)** Tg peak, **(C)** Tg slope, **(D)** calcium peak, **(E)** calcium slope and **(F)** AUC indicated for each cell type and treatment. Analysed using Kruskal-Wallis significance test between cell types and treatments. * P<0.05, ** P<0.01, ***P<0.001, NS not significant.*

4.2.3 Investigating the impact of CaV1.3 on increased SOCE in LNCaP cells under ADT.

4.2.3.1 Validation of siRNA knockdown at a genetic level

To assess genetic expression of *CACNA1D* cells were transfected with siRNA targeted against CaV1.3 or non-targeting control as outlined (section 2.3.7), which was performed 48 hours prior to RNA extraction. cDNA was synthesised and qPCR was performed to assess the level of *CACNA1D* present in the cells. The expression levels of the cells transfected with siRNA targeting *CACNA1D* (siCaV1.3) were compared to untransfected (UT) cells and to non-targeting control siRNA (siCtr) transfected cells (Figure 4.3). The LNCaP cells (Figure 4.3 (A)) had a 3.4% increased expression in the siCtr cells compared to the UT cells, with 79.17% reduced expression of *CACNA1D* seen in the siCaV1.3 cells compared to UT. The difference between siCtr LNCaP cells and siCaV1.3 cells was 82.2% reduced expression. The LNCaP-ADT cells (Figure 4.3 (B)) had a 28.14% reduced expression in the siCtr compared to the UT cells. The siCaV1.3 cells had 77.45% and 49.31% reduced expression compared to UT and siCtr respectively. The LNCaP-abl cells (Figure 4.3 (C)) had a 34.1% reduced expression between the siCtr and the UT. This still gave an effective reduction in the siCaV1.3 which had 61.34% reduced expression compared to Ut and 30.24% reduced expression compared to siCtr.

4.2.3.2 Validation of siRNA knockdown at a protein level

For protein analysis of CaV1.3 knockdown, cells were transfected 72-80 hours prior to protein extraction. Western blot was carried out (section 2.4) using 50µg total protein. There were some variations between repeats due to exposure of the blots, hence the statistical analysis did not produce significance (Figure 4.4). However, the column statistics reveal an effective knockdown. LNCaP cells (A) have 86.11% reduced expression in the siCaV1.3 transfected compared to untransfected and 86.21% reduction compared to siCtr. LNCaP-ADT cells (B) have 87.09% decreased expression in the siCaV1.3 cells compared to the untransfected control, and 87.82% decreased expression compared to siCtr. The LNCaP-abl cells (C) have 99.61% decreased expression between the siCaV1.3 and the untransfected control but LNCaP-abl did show some decreased expression between the untransfected control and the siCtr with a 65.25% decrease. Despite this there is still 88.96% decreased expression between the siCtr and the siCaV1.3 in these cells.

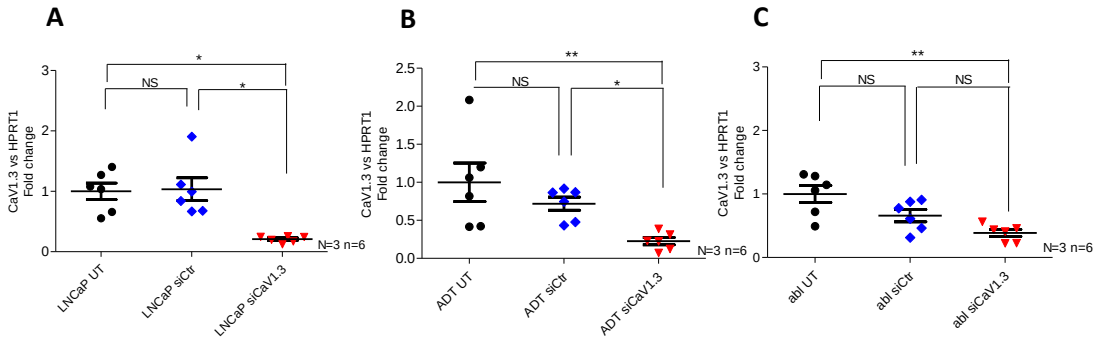

Figure 4.3: Gene expression of CaV1.3 is significantly decreased in cells treated with siRNA targeting CaV1.3 compared to control*: PCR analysis of expression of CaV1.3 in cells transfected with control siRNA (blue) or siRNA targeting CaV1.3 (red), normalised to untransfected cell of type (black). Analysis of androgen sensitive LNCaP cells* ***(A)****, LNCaP-ADT cells treated with 10µM bicalutamide (7-10 days)* ***(B)*** *and androgen insensitive long-term androgen deprived LNCaP-abl cells* ***(C)****. Analysed using Kruskal-Wallis significance test and Dunn's multiple comparison post hoc test between treatments. * P<0.05, ** P<0.01, ***P<0.001, NS not significant.*

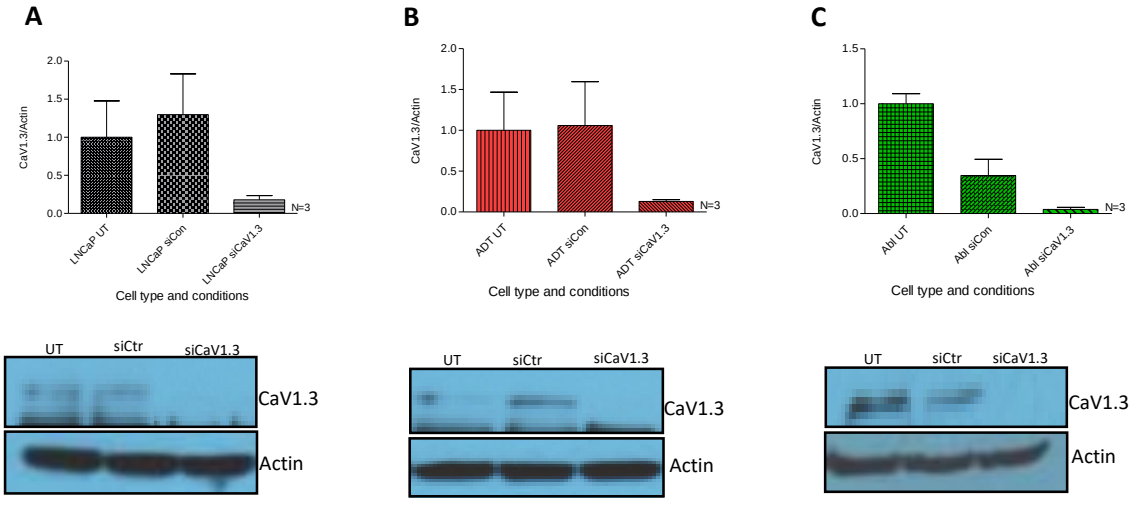

Figure 4.4: Protein expression of CaV1.3 is decreased in cells treated with siRNA targeting CaV1.3 compared to control*: Western blot analysis of expression of CaV1.3 in cells transfected with non-targeting control siRNA (siCtr) or siRNA targeting CaV1.3 (siCaV1.3), normalised to untransfected cell of type (UT). Analysis of androgen sensitive LNCaP cells* ***(A)****, LNCaP-ADT cells treated with 10µM bicalutamide (7-10 days)* ***(B)*** *and androgen insensitive long-term androgen deprived LNCaP-abl cells* ***(C)****. Analysed using Kruskal-Wallis significance test and Dunn's multiple comparison post hoc test between treatments. * P<0.05, ** P<0.01, ***P<0.001, NS not significant.*

4.2.3.1 CaV1.3 has an impact on SOCE in PCa progression

To establish if CaV1.3 plays a role in the increased SOCE witnessed in the LNCaP-ADT and LNCaP-abl cells (Figure 4.2) we measured SOCE with and without CaV1.3 knockdown under the same conditions (section 2.6.1).

Initially we directly compared the SOCE traces recorded for the knockdown samples with the samples transfected with control siRNA in each cell type (LNCaP, LNCaP-ADT and LNCaP-abl). This allowed us directly to establish if silencing CaV1.3 influenced the SOCE at each stage under ADT in the transition to CRPC.

When the expression of CaV1.3 was silenced in LNCaP cells there was no significant overall effect, as can be seen by the Ca^{2+} trace (Figure 4.5 (A)(i)). The Tg induced ER Ca^{2+} store release (Figure 4.5 (A) first peak) has a maximum Ca^{2+} peak of 1.148 in the LNCaP siCtr cells and 1.181 in the LNCaP siCaV1.3 cells compared to the normalised basal Ca^{2+} level of 1. This is reflected in the fold change analysis of the Tg peak (Figure 4.5 (A)(iii)) and slope (Figure 4.5 (A)(iv)), with no significant change. The SOCE response (Figure 4.5 (A) second peak) compared to normalised base Ca^{2+} level of 1, has a maximum peak of Ca^{2+} of 1.542 in the LNCaP siCtr cells and 1.482 in the LNCaP siCaV1.3 cells. This again failed to reach significance in the SOCE peak (Figure 4.5 (A)(v)) and slope (Figure 4.5 (A)(vi)). The overall AUC (Figure 4.5 (A)(ii)) confirms unaltered $[Ca^{2+}]_i$ when CaV1.3 is silenced with the LNCaP siCaV1.3 having 1.001-fold (+/- 0.01 sem) compared to the LNCaP siCtr cells.

Silencing the expression of CaV1.3 in the LNCaP-ADT cells highlighted a significant effect on the SOCE, depicted in the Ca^{2+} trace (Figure 4.5 (B)(i)). There is no significant effect on the Tg induced ER Ca^{2+} store release (Figure 4.5 (B) first peak), where the maximum peak of Ca^{2+} is 1.150 in the LNCaP-ADT siCtr cells and 1.132 in the LNCaP-ADT siCaV1.3 cells. Evident from the Tg peak (Figure 4.5 (B)(iii)) and slope (Figure 4.5 (B)(iv)). However, interestingly the SOCE response (Figure 4.5 (B) second peak) has a maximum Ca^{2+} peak of 1.734 in the LNCaP-ADT siCtr cells which is significantly reduced when CaV1.3 is silenced to 1.592 in the LNCaP-ADT siCaV1.3 cells. This is reflected in the fold change analysis of the Ca^{2+} peak (Figure 4.5 (B)(v)) where there is a 0.765-fold (+/- 0.077 sem) reduced Ca^{2+} peak after CaV1.3 is silenced. There is no significant change to the slope (Figure 4.5 (B)(vi)) or the overall AUC.

Interestingly the effect of silencing CaV1.3 in the LNCaP-abl cells has the opposite effect, increasing the SOCE (Figure 4.5 (C)(i)), again without having a significant influence on the ER store release. When we look at the Tg induced ER Ca^{2+} store release (Figure 4.5 (C) first peak) there is

little change in the maximum peak of Ca^{2+}, which is 1.341 in the LNCaP-abl siCtr cells and 1.384 in the LNCaP-abl siCaV1.3 cells. Confirmed with an insignificant altered Tg peak (Figure 4.5 (C)(iii)) and slope (Figure 4.5 (C)(iv)). This indicates that the upregulation of CaV1.3 does not influence the increased ER store release, as silencing CaV1.3 had no impact on the Tg peak observed.

The SOCE response (Figure 4.5 (C) second peak) had a maximum Ca^{2+} peak of 1.943 in the LNCaP-abl siCtr cells and 2.167 in the LNCaP-abl siCaV1.3 cells. This translates to a significant increase 1.351-fold (+/- 0.106 sem) in the SOCE peak (Figure 4.5 (C)(v)) in LNCaP-abl siCaV1.3 compared to LNCaP-abl siCtr. There is also an increase in the Ca^{2+} slope (Figure 4.5 (C)(vi)) of 1.406-fold (+/- 0.23 sem), although not significant. The overall AUC (Figure 4.5 (C)(ii)) confirms the significant increased $[Ca^{2+}]_i$ when CaV1.3 is silenced with LNCaP-abl siCaV1.3 having 1.054-fold (+/- 0.02 sem) compared to the LNCaP-abl siCtr cells.

This informed us that the upregulation of CaV1.3 observed in the cells which had been treated with ADT was having a significant influence on the SOCE in these cells. We next wanted to determine the level of this effect compared to the parental LNCaP cells. We looked at the fold change between the combined siCtr and siCaV1.3 cells for LNCaP and LNCaP-ADT and between LNCaP and LNCaP-abl cells which is outlined in Table 4.2.

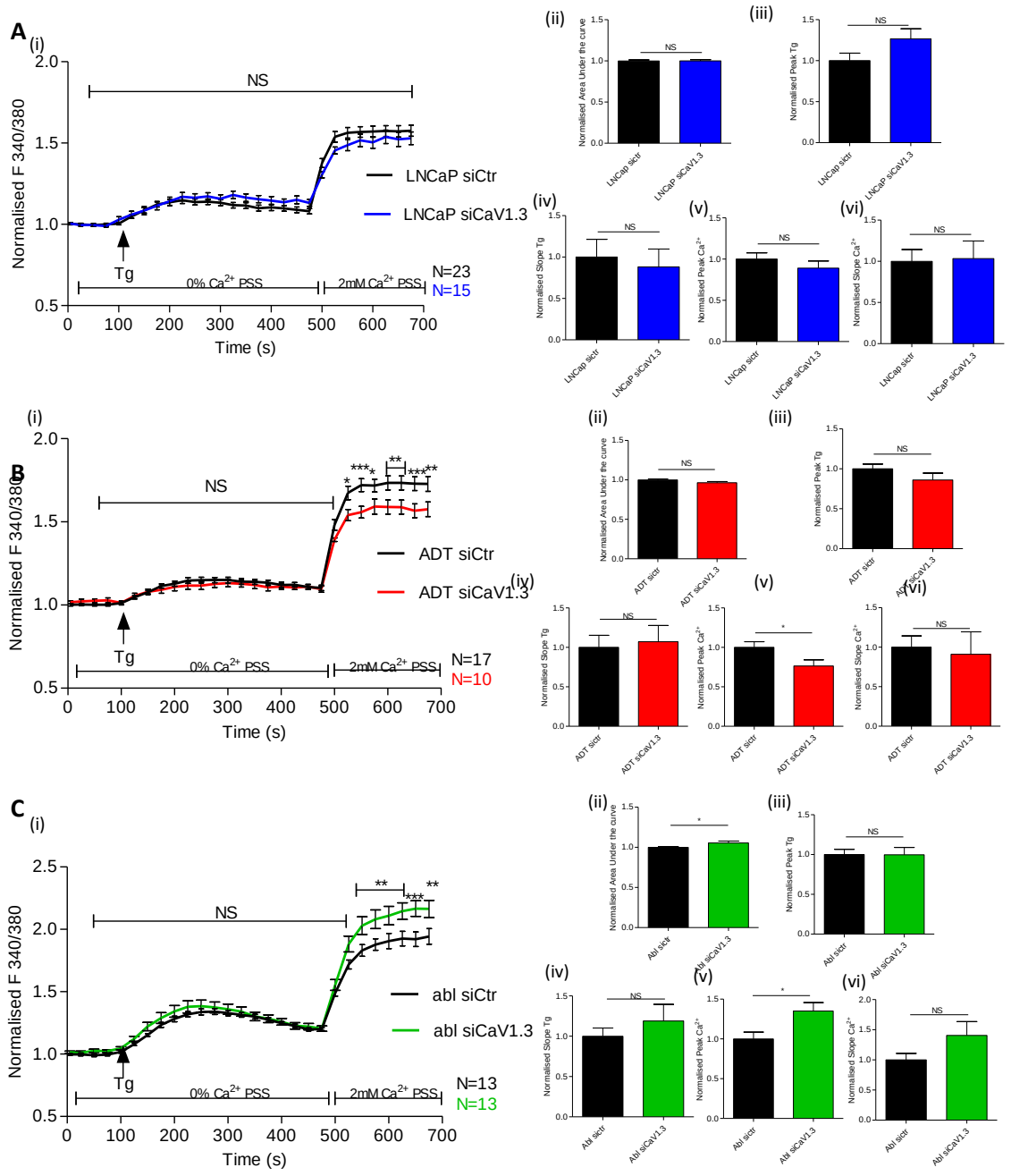

Figure 4.3: CaV1.3 knockdown highlights a key role in regulating SOCE. *Thapsigargin (Tg) induced store operated calcium entry (SOCE) indicated by Fura 2-AM ratiometric analysis of calcium concentration over time (s). Analysis of* ***(A)*** *androgen sensitive LNCaP cells,* ***(B)*** *LNCaP-ADT cells treated with 10μM bicalutamide (7-10 days) and* ***(C)*** *androgen insensitive long-term androgen deprived LNCaP-abl cells. Analysed using* ***(i)*** *2-way ANOVA significance of fluorescence ratio 340:380 at time (s) between cell treatments. Normalised* ***(ii)*** *AUC,* ***(iii)*** *Tg peak,* ***(iv)*** *Tg slope,* ***(v)*** *normalised calcium peak and* ***(vi)*** *calcium slope indicated for each cell treatment. Analysed using Mann-Whitney significance test between cell treatments. * P<0.05, ** P<0.01, ***P<0.001, NS not significant.*

4.2.3.2 Silencing the expression of CaV1.3 removes the significant SOCE effect observed in the LNCaP-ADT siCtr cells.

Analysis of the LNCaP-ADT cells when compared directly to the LNCaP cells indicates that the increased SOCE observed in the LNCaP-ADT siCtr cells (Figure 4.2) is reduced when CaV1.3 is silenced, with no overall effect observed in the ER Ca^{2+} store release as evident from the combined Ca^{2+} trace (Figure 4.6 (A)).

The combined analysis had no significance in the Tg peak (Figure 4.6 (B)) or Tg slope (Figure 4.6 (C)) when compared to the LNCaP siCtr cells. As indicated, there is a significant increased SOCE in the LNCaP-ADT siCtr cells which is reduced when CaV1.3 is silenced. This is evident when we compare the SOCE Ca^{+} peak (Figure 4.6 (A) second peak) to the normalised base Ca^{2+} level of 1. The maximum peak of Ca^{2+} is 1.575 in the LNCaP siCtr cells and 1.538 in the LNCaP siCaV1.3 cells. This is significantly increased to 1.734 in the LNCaP-ADT siCtr cells, which is reduced when CaV1.3 was silenced back to 1.592 in the LNCaP-ADT siCaV1.3. This was reflected in the analysis of the SOCE peak (Figure 4.6 (D)) where the LNCaP-ADT siCtr cells had an increased SOCE 1.378-fold (+/- 0.09 sem) compared to LNCaP siCtr which is reduced to 1.079-fold (+/- 0.076 sem) in the LNCaP-ADT siCaV1.3 cells.

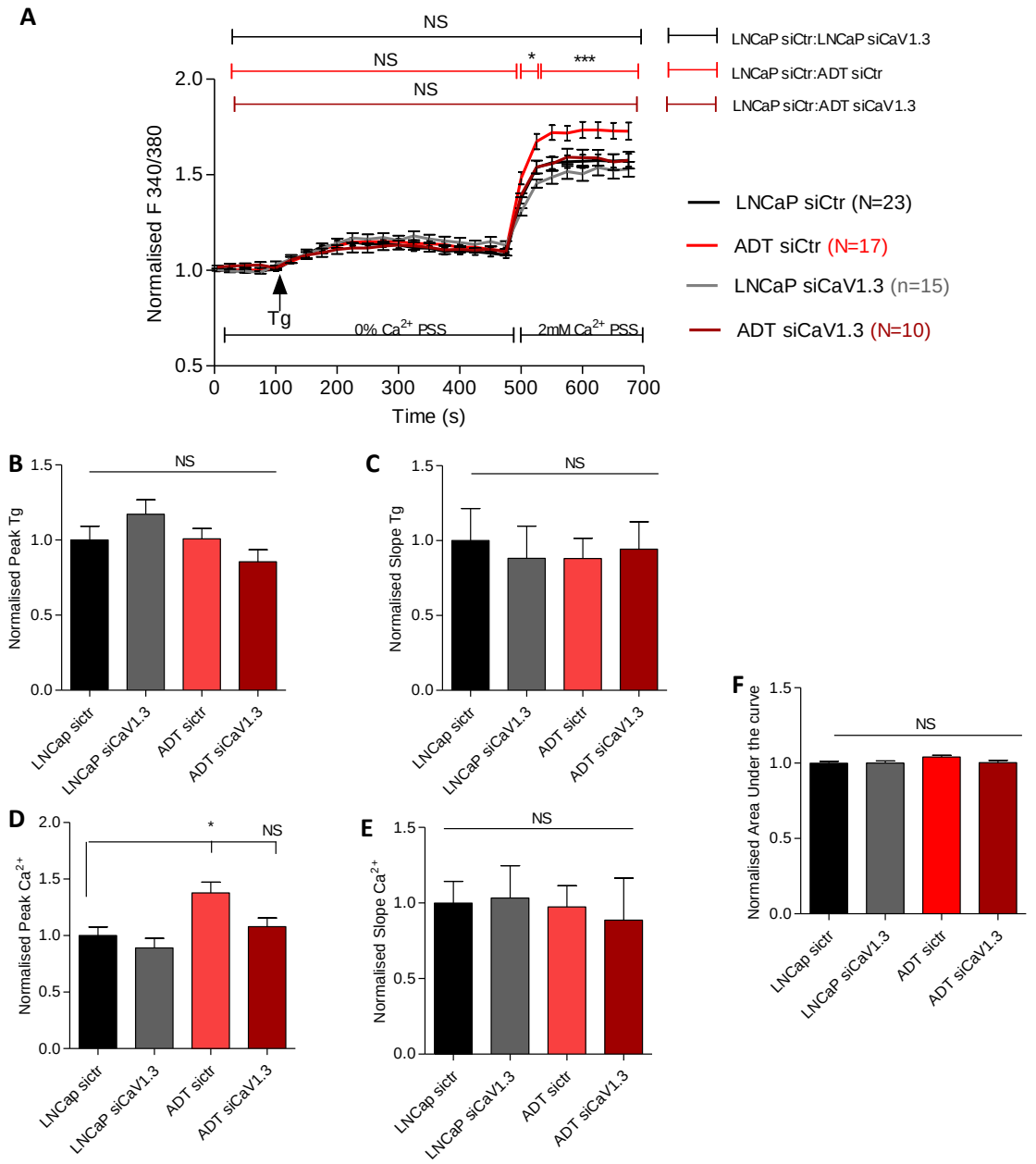

Figure 4.6: SOCE is significantly increased in LNCaP-ADT cells transfected with control siRNA compared to LNCaP cells transfected with control siRNA, which is reduced in cells transfected with siCaV1.3*: Thapsigargin (Tg) induced store operated calcium entry (SOCE) indicated by Fura 2-AM ratiometric analysis of calcium concentration over time (s). Analysis of androgen sensitive LNCaP cells (Black) and LNCaP-ADT cells treated with 10 µM bicalutamide (7-10 days) (Red), transfected with non-targeting control siRNA* ***(siCtr)*** *or transfected with siRNA targeting CaV1.3* ***(siCaV1.3)****.* ***(A)*** *Analysed using 2-way ANOVA significance of fluorescence ratio 340:380 at time (s) between transfections. Normalised* ***(B)*** *Tg peak,* ***(C)*** *Tg slope, (****D****) calcium peak,* ***(E)*** *calcium slope and* ***(F)*** *AUC, indicated for each cell type and treatment. Analysed using Kruskal-wallis significance test with Dunns post hoc test. * P<0.05, ** P<0.01, ***P<0.001, NS not significant.*

4.2.3.3 Silencing the expression of CaV1.3 enhances the significant SOCE effect observed in the LNCaP-abl siCtr cells and has no impact on the enhanced ER Ca^{2+} store release.

As highlighted earlier the LNCaP-abl cells have an increased SOCE compared to LNCaP cells (Figure 4.2), which is increased further when CaV1.3 is silenced (Figure 4.5 (C)(i)). When we look at the Tg induced ER Ca^{2+} store release (Figure 4.7 (A) first peak) we see that the maximum peak of Ca^{2+} compared to the LNCaP cells (1.148 siCtr and 1.181 siCav1.3) is significantly increased in the in the LNCaP-abl siCtr cells to 1.341 and 1.384 in the LNCaP-abl siCaV1.3 cells. This is reflected with the Tg peak fold change (Figure 4.7 (B)) with LNCaP-abl siCtr having 1.935-fold (+/- 0.09 sem) and LNCaP-abl siCaV1.3 having 1.941-fold (+/- 0.197 sem) when compared to LNCaP siCtr cells. Overall highlighting that the increased Tg peak observed in the LNCaP-abl cells is not influenced by the increased expression of CaV1.3, as silencing this expression does not reduce the Tg peak. There is also a significant fold change in the Tg slope (Figure 4.7 (C)) when compared to the LNCaP siCtr cells with LNCaP-abl siCtr cells having 2.029-fold (+/- 0.2 sem) and LNCaP-abl siCaV1.3 having 2.413-fold (+/- 0.42 sem).

The SOCE response (Figure 4.7 (A) second peak) compared to normalised base Ca^{2+} level of 1, is significantly increased compared to the LNCaP cells (1.575 in the LNCaP siCtr cells and 1.538 in the LNCaP siCaV1.3 cells) with a maximum Ca^{2+} peak of 1.943 in the LNCaP-abl siCtr. This is further increased after CaV1.3 is silenced to 2.167 in the LNCaP-abl siCaV1.3 cells. The SOCE peak (Figure 4.7 (D)) compared to LNCaP siCtr has a significant increased fold change with LNCaP-abl siCtr cells is having 1.616-fold (+/- 0.1 sem) and the LNCaP-abl siCaV1.3 cells again indicating further enhanced SOCE of 1.996-fold (+/- 0.162 sem). There is also a significant fold change in the Ca^{2+} slope (Figure 4.7 (E)) compared to LNCaP siCtr with LNCaP-abl siCtr having 1.74-fold (+/- 0.186 sem) and LNCaP-abl siCaV1.3 having 2.447-fold (+/- 0.4 sem). The AUC reflects the significant altered level of $[Ca]_i$ when compared to LNCaP siCtr (Figure 4.7 (F)), LNCaP-abl siCtr cells have 1.132-fold (+/- 0.01 sem) and LNCaP-abl siCaV1.3 cells have 1.193-fold (+/- 0.03 sem).

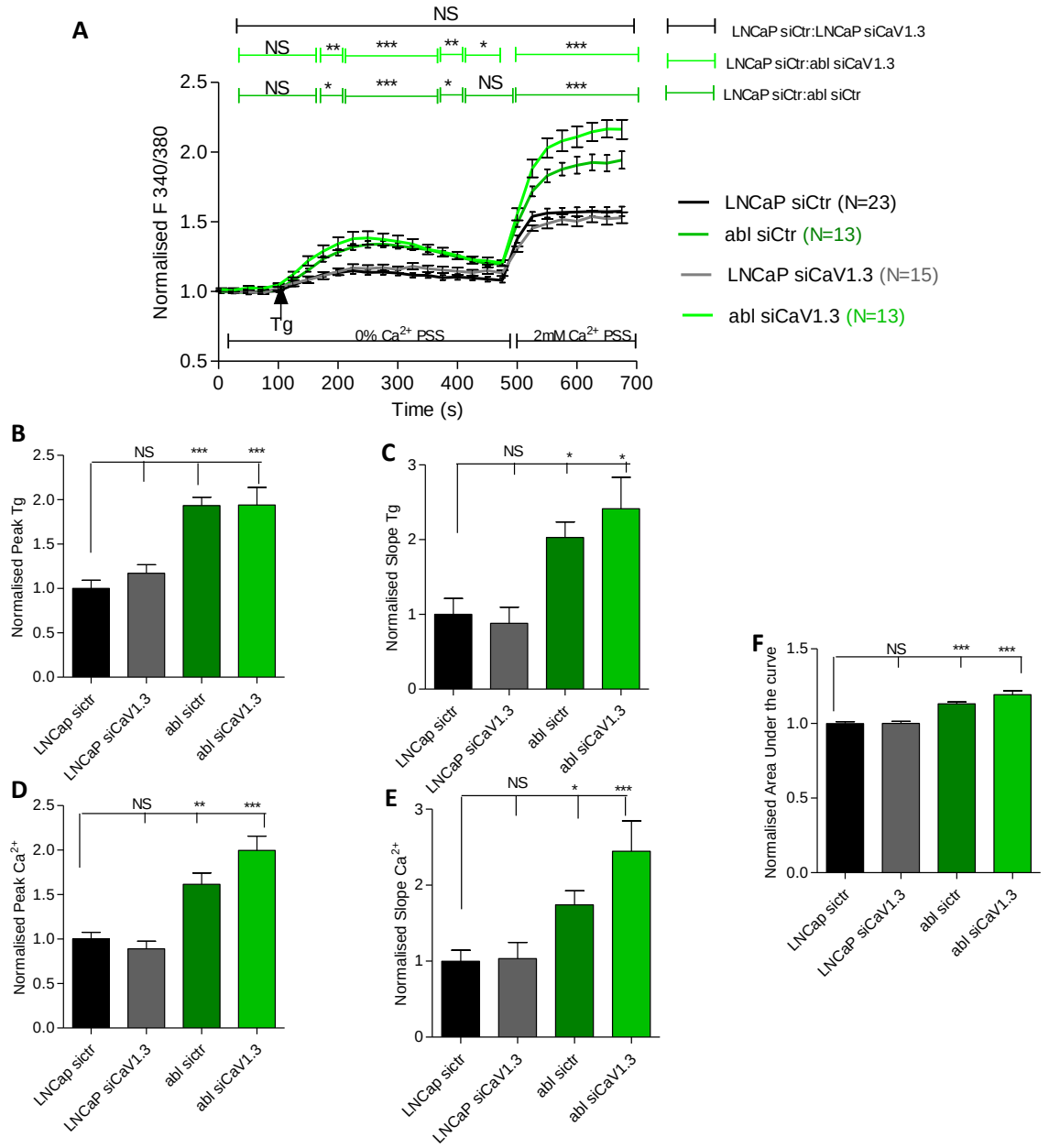

Figure 4.7: SOCE is significantly increased in LNCaP-abl cells transfected with control siRNA compared to LNCaP cells transfected with control siRNA, which is further increased in cells transfected with siCaV1.3*: Thapsigargin (Tg) induced store operated calcium entry (SOCE) indicated by Fura 2-AM ratiometric analysis of calcium concentration over time (s). Analysis of androgen sensitive LNCaP cells (Black) and androgen insensitive long-term androgen deprived LNCaP-abl cells (Green), transfected with non-targeting control siRNA* ***(siCtr)*** *or transfected with siRNA targeting CaV1.3* ***(siCaV1.3)****.* ***(A)*** *Analysed using 2-way ANOVA significance of fluorescence ratio 340:380 at time (s) between transfections. Normalised* ***(B)*** *Tg peak,* ***(C)*** *Tg slope,* ***(D)*** *calcium peak,* ***(E)*** *calcium slope and* ***(F)*** *AUC indicated for each cell type and treatment. Analysed using Kruskal-wallis significance test with Dunns post hoc test. * P<0.05, ** P<0.01, ***P<0.001, NS not significant.*

Table 4.2: Fold change of Ca^{2+} measurements in LNCaP cells transfected with siCaV1.3 compared to control: *summarised changes detected in Ca^{2+} measurements between cell types in cells transfected with non-targeting siRNA (siCtr) or siRNA targeting CaV1.3 (siCaV1.3). Measured AUC, Thapsigrargin (Tg) peak and slope and Calcium (Ca^{2+}) peak and slope as fold change from LNCaP control (+/- standard error of the mean) * P<0.05, ** P<0.01, ***P<0.001.*

	LNCaP siCtr	**LNCaP siCaV**	**LNCaP-ADT siCtr**	**LNCaP-ADT siCaV1.3**	**LNCaP-abl siCtr**	**LNCaP-abl siCaV 1.3**
AUC	1.000 (+/- 0.01)	1.001 (+/- 0.01)	1.040 (+/- 0.01)	1.004 (+/- 0.01)	1.132 *** (+/- 0.01)	1.193 *** (+/- 0.02)
Tg peak	1.000 (+/- 0.09)	1.267 (+/- 0.01)	1.008 (+/- 0.07)	0.855 (+/- 0.08)	1.935 *** (+/- 0.09)	1.941 *** (+/- 0.2)
Tg slope	1.000 (+/- 0.22)	0.882 (+/- 0.22)	0.8801 (+/- 0.14)	0.944 (+/- 0.18)	2.029 * (+/- 0.21)	2.413 * (+/- 0.42)
Ca^{2+} peak	1.000 (+/- 0.08)	0.890 (+/- 0.09)	1.378 * (+/- 0.09)	1.079 (+/- 0.08)	1.616 ** (+/- 0.13)	1.996 *** (+/- 0.16)
Ca^{2+} slope	1.000 (+/- 0.14)	1.033 (+/- 0.21)	0.9744 (+/- 0.14)	0.8869 (+/- 0.28)	1.740 * (+/- 0.19)	2.447 ** (+/- 0.40)

4.2.4 Investigating the impact of silencing CaV1.3 and resultant altered Ca^{2+} mobilisation on the neoplastic function of PCa cells under ADT.

As previously stated Ca^{2+} levels bear influence on many molecular mechanisms within the cell, such as proliferation, apoptosis, cell cycle and migration. Altered Ca^{2+} has been shown to drive these mechanisms in a range of cancers including PCa (Ardura et al., 2020; Maly and Hofmann, 2018). Alterations in Ca^{2+} homeostasis are linked to PCa progression (Flourakis and Prevarskaya, 2009), apoptosis resistance, differentiation and cell survival under ADT. While Ca^{2+} fluctuations may be indicated in the enhanced survival of PCa cells, it can also lead to apoptosis in PCa cells, which occurs under sustained increased $[Ca^{2+}]_i$ (Ardura et al., 2020; N. Prevarskaya et al., 2007). Our research indicates that there is an increased $[Ca^{2+}]_i$ mediated by increased expression of CaV1.3 in LNCaP cells which have been treated with ADT, in the short term androgen deprived (LNCaP-ADT) and the CRPC (LNCaP-abl). To determine if this could potentially contribute to the malignant progression to CRPC we examined the cellular functions of the model with CaV1.3 knockdown.

4.2.4.1 Proliferation & colony forming ability.

When we examined the proliferation of the cells, we see that the trend follows our previous observations with a reduced proliferation in the LNCaP-ADT siCtr (73.43% +/- 2.7) and an increased proliferation in the LNCaP-abl siCtr (65.3% +/- 12.57) compared to the LNCaP siCtr (Figure 4.8 (A)(i)). However when CaV1.3 was silenced the proliferation was reduced in all cell lines, although this only reached significance in the LNCaP-abl cells which had a 35.49% (+/- 9.7 sem) when CaV1.3 was silenced compared to LNCaP-abl siCtr (Figure 4.8 (A)(iv)).

The CFA of the cells when normalised to the LNCaP siCtr cells, has no significant change (Figure 4.8 (B)(i)), although it appears to have a significant reduced ability in the LNCaP-abl cells when CaV1.3 is silenced. When we compare the CFA directly between cells transfected with siCtr and siCaV1.3 there is no significance detected in the LNCaP and the LNCaP-ADT cells, however, when we compare the LNCaP-abl siCaV1.3 cells to the LNCaP-abl siCtr cells (Figure 4.8 (B)(iv)) they have a significantly 50.77% (+/- 13.63 sem) reduced CFA.

4.2.4.2 Migration

The migration of the cells was not substantially altered through silencing CaV1.3 (Figure 4.9). There was, as previously stated (Figure 3.8), very little migration detected in any of the cell types after 60 hours assessment in the Xcelligence™ CIM plates. The maximum peak cell index indicated for LNCaP siCtr was 0.255, LNCaP-siCaV1.3 was 0.297, the LNCaP-ADT siCtr was 0.008, LNCaP-ADT siCaV1.3 was 0.039, for the LNCaP-abl siCtr it was 0.001 and the LNCaP-abl siCav1.3 was 0.00 (Figure 4.9 (A)(i)). When compared to the LNCaP siCtr this translated to a significant reduced migration in the LNCaP-abl cells at 40 hours and 60 hours ($P<0.005$) (Figure 4.9 (A)(ii)(iii)). When we look at the changes between cells transfected with control siRNA compared to those transfected with siRNA targeting CaV1.3, the LNCaP cells (Figure 4.9 (B)) have no significant change in the cell index at 40 hours or at 60 hours. The LNCaP-ADT cells (Figure 4.9 (C)) had no significant change in cell index at 40 hours, however we see at 60 hours that there is a significant increase in migration when CaV1.3 is silenced (LNCaP-ADT siCtr -0.015 +/- 0.009 sem and LNCaP-ADT siCaV1.3 0.029 +/- 0.01 sem). The LNCaP-abl cells (Figure 4.9 (D)) have no significant change in cell index observed when CaV1.3 is silenced at 40 hours or at 60 hours.

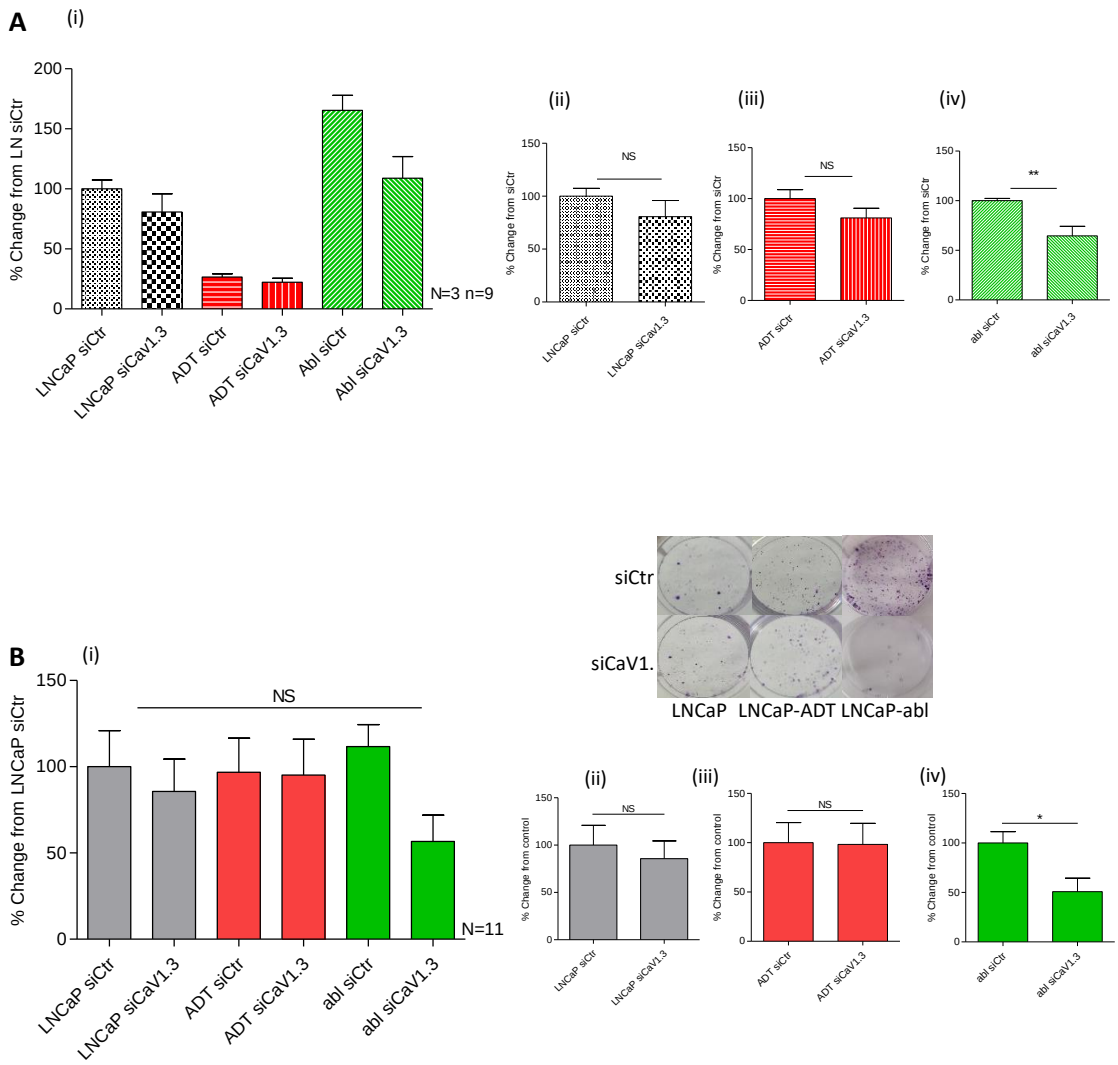

Figure 4.8: CaV1.3 knockdown alters proliferation and colony forming ability in androgen insensitive LNCAP-ABL cells. *: **(A)** Proliferation was assessed using the WST-1 assay and **(B)** colony forming formation determined over a 14 day assay both with cells transfected with non-targeting control siRNA **(siCtr)** or siRNA targeting CaV1.3 **(siCaV1.3)**. Analysis of androgen sensitive LNCaP cells (black), LNCaP-ADT cells treated with 10 µM bicalutamide (7-10 days) (Red) and androgen insensitive long-term androgen deprived LNCaP-abl cells (Green). Analysed using Kruskal-Wallis significance test and Dunn's multiple comparison post hoc test between cell types and treatments **(A& B(i))** or Mann-Whitney significance test between cell types and treatments **(A&B (ii) (iii) (iv))**. * P<0.05, ** P<0.01, ***P<0.001, NS not significant.*

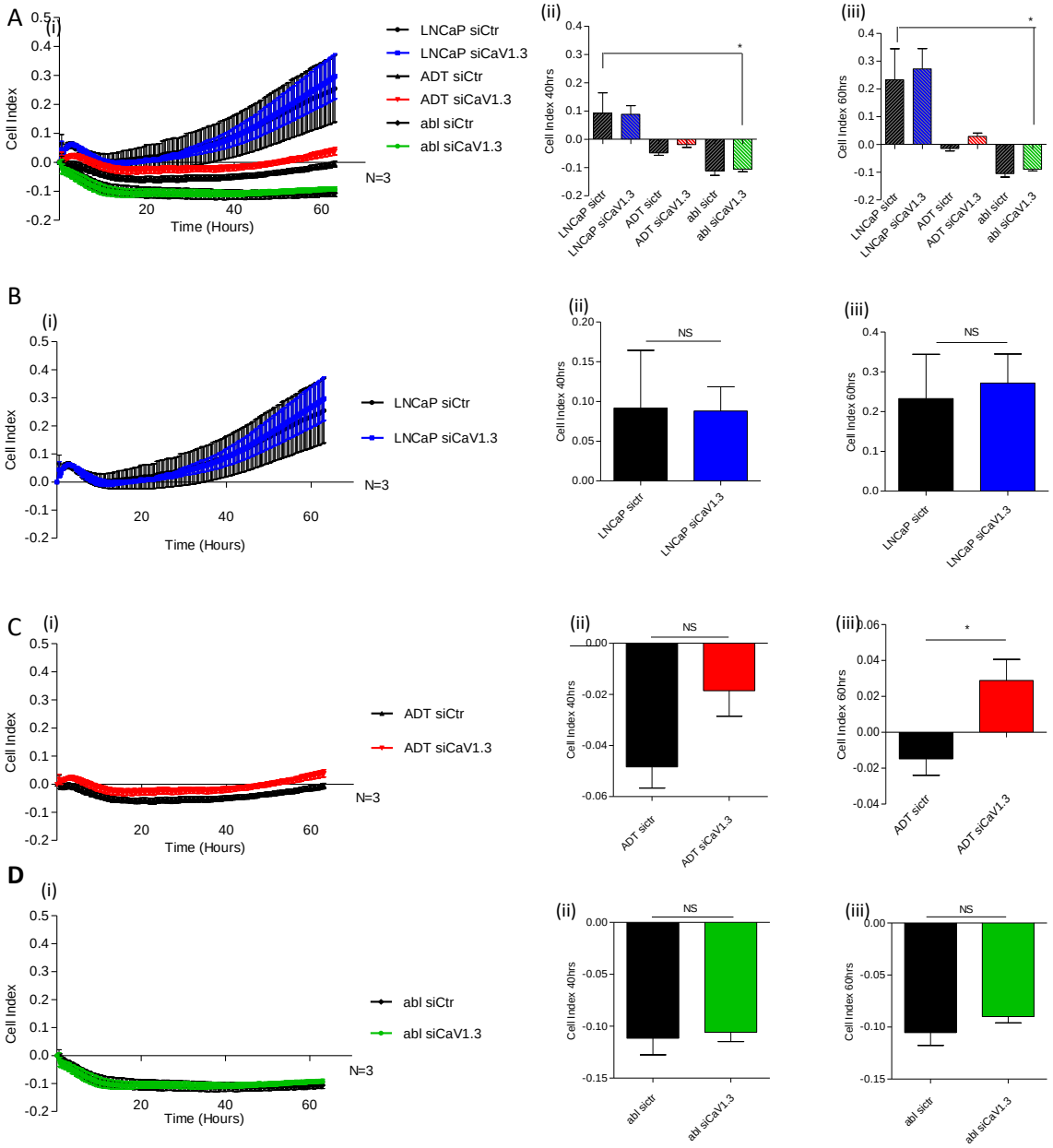

Figure 4.9: Migration is significantly reduced in androgen insensitive cells with little effect after siRNA knockdown of CaV1.3*: **(A)** Migration assessed using the Xcelligence™ system with cell invasion and migration plates with chemoattractant. Analysis of **(B)** androgen sensitive LNCaP cells (blue/black), **(C)** LNCaP-ADT cells treated with 10 µM bicalutamide (7-10 days) (red/black) and **(D)** androgen insensitive long-term androgen deprived LNCaP-abl cells (green/black). Transfected with non-targeting control siRNA **(siCtr)** or siRNA targeting CaV1.3 **(siCaV1.3)**. Assessed as cell index at **(ii)** 40 hours and **(iii)** 60 hours**.** Analysed using **(A (ii) (iii))** Kruskal-Wallis significance test and Dunn's multiple comparison post hoc test between cell types and treatments or **(B (ii) (iii), C (ii) (iii)** & **D (ii) (iii))** Mann-Whitney significance test between cell types and treatments. * P<0.05, ** P<0.01, ***P<0.001, NS not significant.*

4.2.5 Investigating the impact of CaV1.3 pharmacological inhibition on PCa cells during ADT.

In light of our recent finding demonstrating that upregulation of CaV1.3 in LNCaP cells under ADT is involved in the SOCE mechanism, we decided to investigate if inhibiting VGCC's with CCB would influence the SOCE. For this purpose, we chose the CCB nifedipine, which is a 1,4 dihydropyridine antagonist, shown to inhibit a range of VGCC including the L-type Ca^{2+} channel, CaV1.3 (Bell et al., 2001).

4.2.5.1 Effects of Nifedipine of SOCE

Inhibiting VGCC using nifedipine had no significant effect to the SOCE in any of the cells, as clearly demonstrated when we compare the combined results of the LNCaP, LNCaP-ADT and the LNCaP-abl cells (Appendix B; Figure B.3). There is no obvious separation between treatments contrary to the separation observed in the combined results for the cells transfected with siRNA to silence CaV1.3 (Appendix B; Figure B.1).

To further analyse the results obtained from the SOCE in cells treated with nifedipine we analysed the LNCaP-ADT and the LNCaP-abl compared to the parental LNCaP cells separately (Figure 4.10 and 4.11 respectively). This enabled us to determine if nifedipine inhibited Ca^{2+} mobilisation at any stage in the SOCE and how this compared to the effect we observed when CaV1.3 was silenced. However, this indicates that the increased SOCE in the LNCaP-ADT and LNCaP-abl cells is not significantly altered when cells are treated with nifedipine as outlined in Table 4.3.

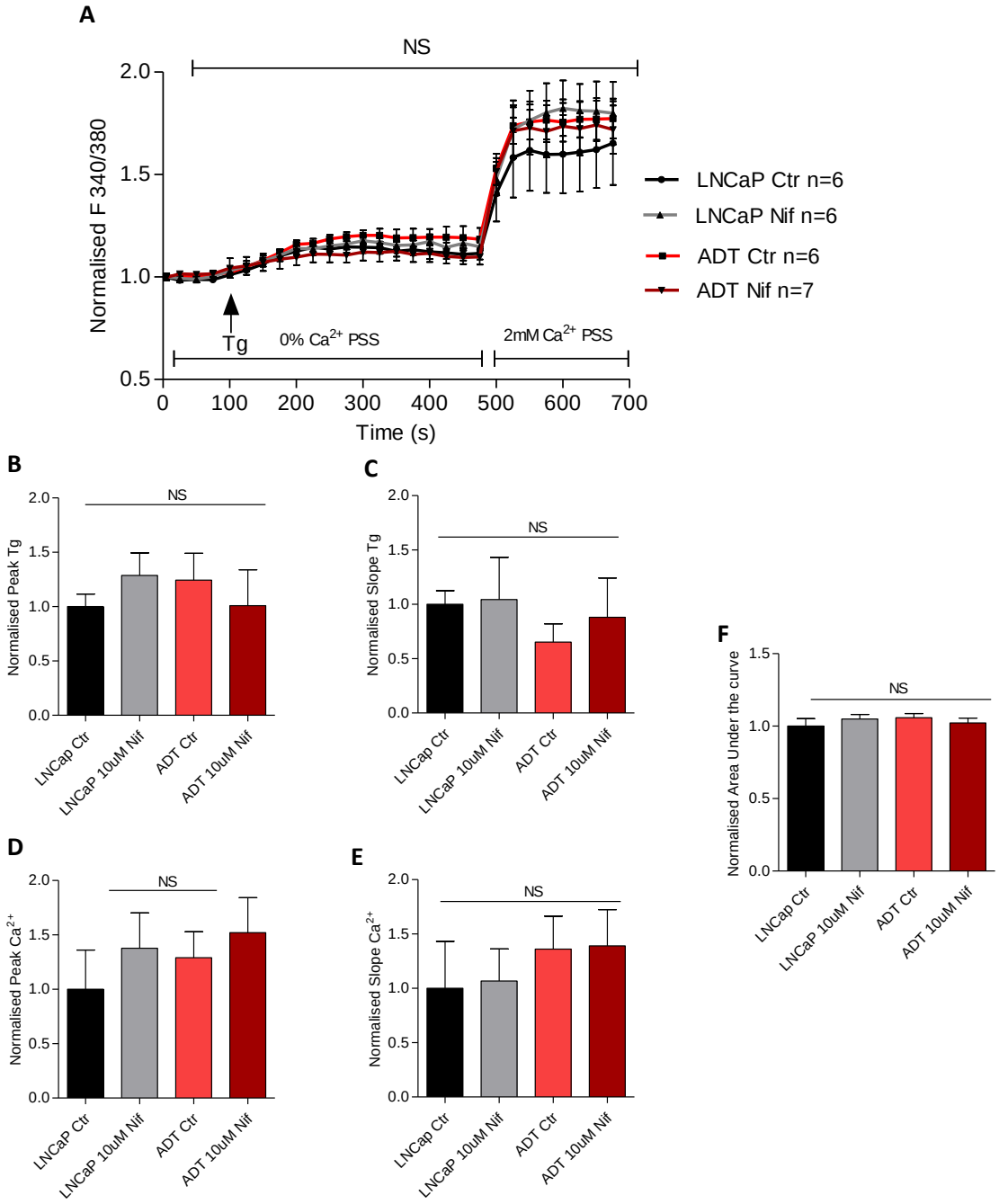

Figure 4.10: Treatment with Nifedipine has no significant effect on LNCaP or LNCaP-ADT cells*: Thapsigargin (Tg) induced store operated calcium entry (SOCE) measured by Fura 2-AM ratiometric analysis of calcium concentration over time (s). Analysis of androgen sensitive LNCaP cells (Black) and LNCaP-ADT cells treated with 10 µM bicalutamide (7-10 days) (Red), treated with DMSO control* ***(Ctr)*** *or 10 µM Nifedipine* ***(Nif)****.* ***(A)*** *Analysed using 2-way ANOVA significance of fluorescence ratio 340:380 at time (s) between transfections. Normalised* ***(B)*** *Tg peak,* ***(C)*** *Tg slope,* ***(D)*** *calcium peak,* ***(E)*** *calcium slope, and* ***(F)*** *AUC indicated for each cell type and treatment. Analysed using Kruskal-wallis significance test with Dunns post hoc test. * P<0.05, ** P<0.01, ***P<0.001, NS not significant.*

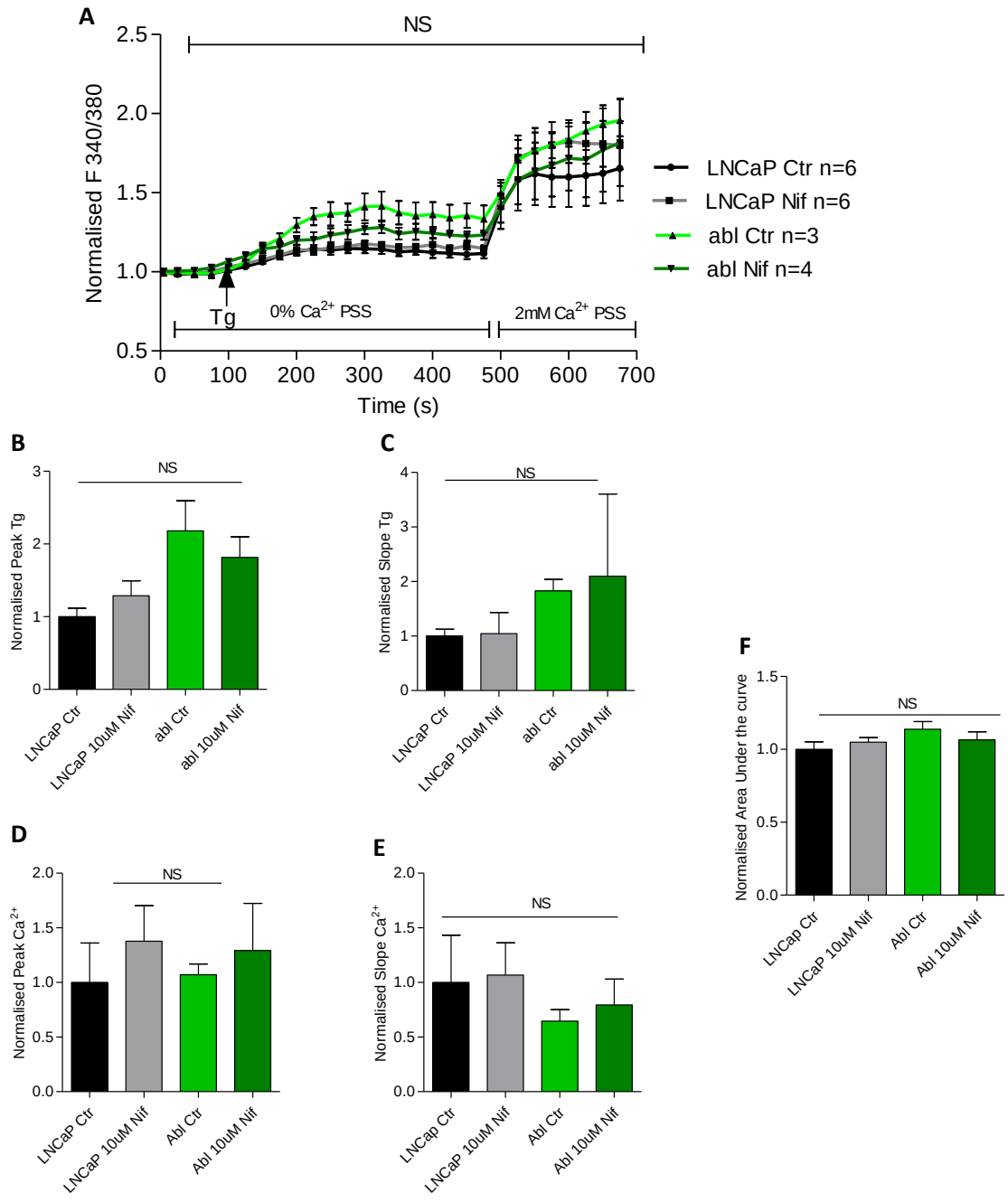

Figure 4.11: Treatment with nifedipine has no significant effect on LNCaP or LNCaP-abl cells*: Thapsigargin (Tg) induced store operated calcium entry (SOCE) indicated by Fura 2-AM ratiometric analysis of calcium concentration over time (s). Analysis of androgen sensitive LNCaP cells (Black) and androgen insensitive long-term androgen deprived LNCaP-abl cells (Green), treated with DMSO control* ***(Ctr)*** *or treated with 10 µM Nifedipine* ***(Nif)****.* ***(A)*** *Analysed using 2-way ANOVA significance of fluorescence ratio 340:380 at time (s) between transfections. Normalised* ***(B)*** *Tg peak,* ***(C)*** *Tg slope,* ***(D)*** *calcium peak,* ***(E)*** *calcium slope and* ***(F)*** *AUC, indicated for each cell type and treatment. Analysed using Kruskal-wallis significance test with Dunns post hoc test. * P<0.05, ** P<0.01, ***P<0.001, NS not significant.*

Table 4.3: Fold change of Ca^{2+} measurements in LNCaP cells when treated with Nifedipine compared to control: *summarised changes detected in Ca^{2+} measurements between cell types in cells treated with DMSO control (Ctr) or 10 µM nifedipine (Nif). Measured AUC, Thapsigrargin (Tg) peak and slope and Calcium (Ca^{2+}) peak and slope as fold change from LNCaP control (+/- standard error of the mean) * P<0.05, ** P<0.01, ***P<0.001.*

	LNCaP Ctr	**LNCaP Nif**	**LNCaP-ADT Ctr**	**LNCaP-ADT Nif**	**LNCaP-abl Ctr**	**LNCaP-abl Nif**
AUC	1.000 (+/- 0.05)	1.050 (+/- 0.03)	1.058 (+/- 0.02)	1.022 (+/- 0.03)	1.138 (+/- 0.05)	1.066 (+/- 0.06)
Tg peak	1.000 (+/- 0.1)	1.288 (+/- 0.01)	1.244 (+/- 0.2)	1.009 (+/- 0.3)	2.181 (+/- 0.4)	1.816 (+/- 0.2)
Tg slope	1.000 (+/- 0.13)	1.045 (+/- 0.4)	0.653 (+/- 0.17)	0.881 (+/- 0.36)	1.827 (+/- 0.2)	2.099 (+/- 1.5)
Ca^{2+} peak	1.000 (+/- 0.36)	1.377 (+/- 0.3)	1.291 (+/- 0.2)	1.521 (+/- 0.3)	1.070 (+/- 0.1)	1.292 (+/- 0.4)
Ca^{2+} slope	1.000 (+/- 0. 4)	1.067 (+/- 0.3)	1.361 (+/- 0.3)	1.390 (+/- 0.3)	0.646 (+/- 0.1)	0.784 (+/- 0.2)

4.2.5.2 Functional effects of Nifedipine

The proliferation experiments followed the same trend as previous findings (Figure 3.5 (A)) with a reduced proliferation in the LNCaP-ADT and an increased proliferation in the LNCaP-abl cells compared to the LNCaP (Figure 4.12 (A)(i)). When the cells were treated with nifedipine there was no significant change in the proliferation of the LNCaP-ADT cells. The LNCaP incubated with nifedipine have a significant 14.3% (+/0 3.2 sem) reduced proliferation while the LNCaP-abl cells incubated with nifedipine also have a significantly reduced proliferative ability which is 33.68% (+/- 6.64 sem) less than LNCaP-abl Ctr.

The CFA also follows our previous findings (Figure 3.5 (B)) with the LNCaP-abl cells having a significant increased number of colonies compared to the LNCaP cells (Figure 4.12 (B)). The CFA is visibly reduced in all the cell types after incubation with nifedipine. The LNCaP cells treated with nifedipine produced 3% of the colonies compared to the LNCaP Ctr (Figure 4.12 (B)(ii)) and the LNCaP-ADT cells treated with nifedipine produced 13% of the colonies observed in the LNCaP-ADT Ctr (Figure 4.12 (B)(iii)). There was also a reduced CFA observed in the LNCaP-abl cells treated with nifedipine which produced half (51%) the colonies observed in the LNCaP-abl Ctr cells (Figure 4.12 (B)(iv)). Indicating that inhibiting Ca^{2+} mobilisation through VGCC with nifedipine reduces the tumorigenic potential of PCa cells.

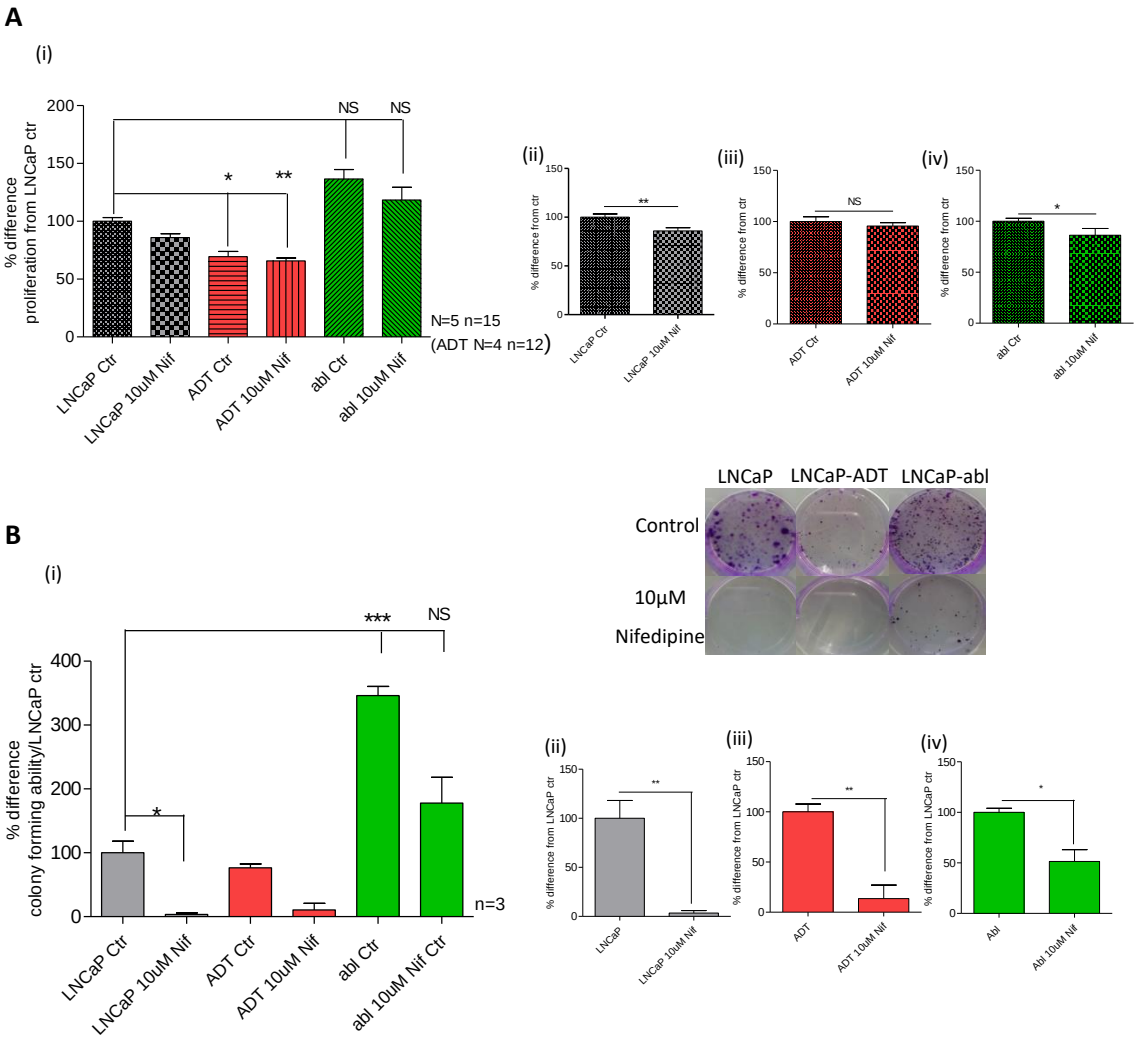

Figure 4.12: Colony forming ability & proliferation is inhibited by Nifedipine: (A) *Proliferation assessed using WST-1 assay and* ***(B)*** *colony forming assay performed over 14 days assessed in cells treated with 10µM nifedipine or DMSO control. Analysis of androgen sensitive LNCaP cells (black), LNCaP-ADT cells treated with 10 µM bicalutamide (7-10 days) (Red) and androgen insensitive long-term androgen deprived LNCaP-abl cells (Green). Analysed using* ***(i)*** *Kruskal-Wallis significance test and Dunn's multiple comparison post hoc test between cell types and treatments or* ***((ii) (iii) (iv))*** *Mann-Whitney significance test between cell types and treatments * P<0.05, ** P<0.01, ***P<0.001, NS not significant.*

4.3 Chapter discussion

As outlined in chapter 3 CaV1.3 is upregulated in PCa cells which is enhanced under ADT. Here we wanted to establish if CaV1.3 was functionally active and if the upregulation of this channel had any impact on the Ca^{2+} mobilisation, which may be contributing to disease progression and treatment resistance.

4.3.1 Effects under depolarisation

$[Ca^{2+}]_i$ does not change at any stage under cellular depolarisation indicating that CaV1.3 does not function in a canonical way. Since CaV1.3 is a VGCC, we initially suspected that the upregulation detected in the cells after ADT (Figure 3.7) would result in an increased Ca^{2+} influx upon depolarisation in these cell types. LNCaP cells have a resting membrane potential of approximately -30 mV to -40 mV (Gackière et al., 2013b; Mariot et al., 2002). L-type VGCC's have a window of activation -40 mV to 10 mV, with a peak at 0mV (Buchanan and McCloskey, 2016). However, CaV1.3 is activated at lower voltages than other L-type VGCC, with some studies suggesting that CaV1.3 channels can be activated at -55 mV and can achieve 60% peak activation by -40mV (Lipscombe et al., 2004; Xu and Lipscombe, 2001). This means that under the normal resting potential of LNCaP cells CaV1.3 could be activated which could result in the absence of detected current under depolarisation. To mitigate this, we initially hyperpolarised the cells, which occurs when incubated with NS1619 (Kuhlmann et al., 2004; Yamamura et al., 2001). NS1619 is a BK_{Ca} channel activator, which results in the open state of the large conductance potassium channel. Since under normal conditions the intracellular potassium level is much higher than the extracellular concentration, opening BK_{Ca} channels result in K^+ diffusion down the concentration gradient to the extracellular fluid. This release of positive ions from the intracellular space results in a hyperpolarised membrane potential. Introducing increased concentration of KCl to the extracellular fluid then reverses the gradient and the cell membrane becomes depolarised. Under the canonical function of CaV1.3, this depolarisation would trigger the voltage activation of the channel, resulting in Ca^{2+} influx across the plasma membrane. However, our results demonstrated the absence of Ca^{2+} current with introduction of K^+ up to 80 mM to the extracellular fluid, which indicates a distinct lack of voltage activation in these cells.

This coupled with our previous findings on the predominant cellular location of complete CaV1.3 in the cytosol (Figure 3.8), led to our consideration of potential non-canonical functions associated with upregulated expression. Which we hypothesised may influence Ca^{2+} mobilisation through interaction with other proteins. As previously discussed increased CaV1.3 has been shown to have such non-canonical functions in other cancer types (Fourbon et al., 2017). For example, the study by Fourbon et al. indicated that CaV1.3 was functioning as a regulator of the NCX channel. They showed that CaV1.3, present in the cytosol, was inhibiting the function of NCX. This reduced Ca^{2+} extrusion from the intracellular space, resulting in an increased basal Ca^{2+} level in colon cancer. However, as we can see from the basal Ca^{2+} levels recorded prior to KCl injection (Table 4.1), increased expression of CaV1.3 detected in the LNCaP-ADT and the LNCaP-abl cells, did not increase the basal Ca^{2+}level compared to the LNCaP cells. Indicating that CaV1.3 was not involved in the increased $[Ca^{2+}]_i$ through interaction with the NCX channels in PCa.

Due to the lack of voltage gated activation and the unaltered basal Ca^{2+} levels, we decided to investigate the effect that upregulated CaV1.3 after ADT had on the fundamental epithelial Ca^{2+} mobilisation mechanism of SOCE. As outlined earlier previous studies have highlighted that CaV1.3 can influence SOCE via interaction with RyR (Kim et al., 2007; Torrente et al., 2016) or in refilling ER after store depletion (Power and Sah, 2005).

4.3.2 Increased SOCE in cells with increased CaV1.3

Previous studies have demonstrated the presence of a SOCE current in LNCaP cells upon Tg induced store depletion. This was indicated by a second sustained plateau peak of Ca^{2+} (Skryma et al., 2000), reflecting the Ca^{2+} trace observed in Figure 4.2. They confirmed the second peak was due to extracellular Ca^{2+} influx as a response to store depletion, as it was absent when Ca^{2+} was omitted from the extracellular fluid. Therefore, we can confidently assume that the peaks observed are due to the mechanism associated with SOCE. Interestingly this study was performed prior to the discovery of the STIM/Orai mechanism which is outlined in Figure 1.11. The study therefore assumed the uptake of Ca^{2+} from the extracellular fluid was due to the action of other cell membrane bound Ca^{2+} permeable channels. They demonstrated that inhibiting T-type Ca^{2+} channels with Nickel (Ni^{2+}), a specific inhibitor of CaV3.2 (Kang et al., 2006), also reduced the SOCE response, implicating the activity of VGCC's in SOCE of LNCaP.

It is evident that there are some differences in the SOCE in LNCaP cells which have undergone ADT and have an upregulated expression of CaV1.3 (LNCaP-ADT and LNCaP-abl). The SOCE response is significantly upregulated in the LNCaP-ADT cells (~30%) and the LNCaP-abl cells (~60%) compared to the LNCaP cells (Figure 4.2 (D)). The increased SOCE may be influenced by the increased expression of CaV1.3 (Figure 3.7), which we will investigate further below. However, the LNCaP-abl cells also have a significant increased Tg induced Ca^{2+} released from the ER (Figure 4.2 (B)), which in turn could contribute to an increased SOCE response. This may explain the further increased SOCE in these cells evident in the second peak (Figure 4.2 (A)). This led us to think that perhaps CaV1.3 upregulation in the LNCaP-abl cells may also contribute to the increased Ca^{2+} released from the ER, since CaV1.3 has been shown to have a functional coupling with the ER Ca^{2+} channel RyR in the central nervous system (Kim et al., 2007; Ouardouz et al., 2003; Vierra et al., 2019). This functional coupling resulted in a mechanism where activation of CaV1.3 controlled Ca^{2+} release from the ER through the RyR channel. Increased expression of CaV1.3 may be influencing an increased Ca^{2+} release from the ER in the LNCaP-abl cells through an interaction with RyR.

However, we have demonstrated that there is a correlation between increased expression of CaV1.3 in LNCaP cells under ADT and an increased SOCE. We needed to definitively identify CaV1.3 as having an influence on the SOCE in these cells. To further elucidate the involvement of CaV1.3 in increased SOCE we investigated the effect of silencing CaV1.3 expression. To achieve this, we transfected the cells with siRNA which directly inhibited the gene coding for CaV1.3 (*CACNA1D*) (section 2.3.7). This allowed us to successfully silence the expression of CaV1.3, which we confirmed at both a genetic and protein level (Figure 4.3, 4.4).

4.3.3 Impact of CaV1.3 on SOCE in LNCaP cells under ADT.

CaV1.3 is usually associated with voltage dependent activation, here we have shown that depolarisation does not induce channel activation or Ca^{2+} mobilisation through the channel. Furthermore, it does not appear to have a role in regulating the basal Ca^{2+} level under ADT conditions. Therefore, we investigated the potential role for CaV1.3 in influencing Ca^{2+} mobilisation in a non-canonical manner. Here, we have demonstrated for the first time that the increased expression of CaV1.3 in LNCaP cells which have been treated with ADT, contributes to the regulation of SOCE. We have confirmed the involvement of CaV1.3 in this mechanism as

silencing expression elicited an impact specifically on the SOCE. Interestingly there was a contrasting response detected whereby inhibiting CaV1.3 prevented the increased SOCE in the androgen sensitive LNCaP-ADT cells, however, it further increased the SOCE in the androgen insensitive LNCaP-abl cells. Indicating that the upregulation of CaV1.3 may have alternative functions at various stages under ADT. Combined analysis can be seen in Appendix B (Figure B.1), highlighting the SOCE changes between the parental LNCaP cells and the LNCaP-ADT and LNCaP-abl, and alterations driven by silencing CaV1.3.

This indicates a novel mechanism for CaV1.3 in regulating SOCE in the progression to CRPC under ADT. Although this direct correlation has not been demonstrated in relation to PCa before, studies have shown in excitable cells that CaV1.3 can have an interactional role in relation to ER store release. CaV1.3 has been shown to form a functional interaction with the ER plasma membrane channel RyR in the hippocampus (Kim et al., 2007) and the sinoatrial node (Torrente et al., 2016), where it contributes to RyR mediated Ca^{2+} release. Recently published data even suggests a triple protein interaction between CaV1.3, RyR and the potassium channel $K_{Ca}3.1$ (Sahu et al., 2019), which regulates hyperpolarisation in excitable cells by activating the potassium channel. While these associations are in neuronal cells, which have shown excitation contraction coupling is involved in synaptic plasticity (Kim et al., 2007; Vierra et al., 2019), there could be a potential role for a protein association of this kind in the process of NED or EMT.

An association between ADT and ER Ca^{2+} pool [ER_{Ca}] has been previously demonstrated, by culturing LNCaP cells in androgen depleted media (charcoal stripped FBS) (Boutin et al., 2015). However, the results reported are in direct contrast to the findings of our study. Boutin et al. reported a decrease in the Tg peak was observed in the cells grown in the absence of androgens, with a higher Tg release and Ca^{2+} influx in the cells which were grown in the presence of synthetic androgens. Suggesting that ADT results in decreased Ca^{2+} influx due to a decreased [ER_{Ca}]. Our investigation showed no real difference in Tg peak in the LNCaP-ADT cells with an increased Ca^{2+} influx. Whereas the LNCaP-abl cells had a significantly enhanced [ER_{Ca}], which upon depletion resulted in a significant increased Ca^{2+} entry. There are some distinct differences between experimental parameters to note, they induced ADT by growing the cells in media supplemented with charcoal stripped FBS for 48 hours before carrying out measurements. At 48 hours we have observed no difference in the morphology of the cells, which is why we induce ADT for 7-10 days prior to experiments in the LNCaP-ADT cells. They also report achieving similar results in bicalutamide treated cells, although they failed to report if this was bicalutamide added to media supplemented with FBS or charcoal stripped FBS, or if these experiments were carried out after 2 days treatment or longer. The standout difference is that they used the addition of synthetic

androgen R1881 to the charcoal stripped media for 48 hours to compare as their control. This media would be void of all other growth factors contained in normal FBS supplemented media, which could influence the cellular responses. Therefore, we suggest that our cell model of PCa under ADT depicts a more clinically relevant reflection on Ca^{2+} responses and PCa progression under ADT. Since bicalutamide specifically targets the AR, our research is directly examining the effect of AR inhibition. We use the parental LNCaP cell type as our control model, which is grown in media supplemented with 10% FBS and we induce ADT by directly targeting the AR with bicalutamide. Therefore, our results reflect the effects of androgen receptor targeting only rather than a global effect of hormone and growth factor removal.

Overall our research thus far highlights that upregulated CaV1.3 is having an influence on the $[Ca^{2+}]_i$ in LNCaP after ADT through the SOCE mechanism. These findings suggest that the increased Ca^{2+} influx in the short-term androgen deprived LNCaP-ADT cells is controlled by CaV1.3 as it is reduced when CaV1.3 is silenced. These cells have an increased CaV1.3 mRNA (Figure 3.7), reduced proliferation and colony forming ability (Figure 3.5) but increased expression of the AR and NSE (Figure 3.2). Whereas the androgen independent LNCaP-abl cells indicated an increased SOCE and an increased $[ER_{Ca}]$. The Ca^{2+} mobilisation in these cells is also influenced by CaV1.3, as silencing CaV1.3 increased the Ca^{2+} influx from the extracellular space. These cells had increased expression of CaV1.3 and AR, with a significantly enhanced proliferation and colony forming ability. Further to these findings we wanted to establish if the effects observed upon silencing CaV1.3 were reflected in the functional aspects of the cell model.

4.3.4 Functional effects with CaV1.3 gene silencing

Silencing CaV1.3 had no significant effect on either proliferation or CFA in the LNCaP-ADT cells, despite the increased SOCE induced by CaV1.3 detected in these cells. However, there are many other mechanisms influenced by Ca^{2+} fluctuations which may be facilitating cell survival under the stress of ADT. One such mechanism is the emergence of NED which we observed in these cells, demonstrated by the significant increased expression of NSE (Figure 3.2 (B)). Many studies highlight the requirement for Ca^{2+} signalling in the process of NED, implicating the expression of T-type VGCC's (Chemin et al., 2002; Silver and Bolsover, 1991; Warnier et al., 2017). The upregulation of the T-Type VGCC CaV3.2 has also been identified as having a direct influence on NED in PCa (Mariot et al., 2002), although this research suggested that the low voltage activated Ca^{2+} current detected had to be as a result of CaV3.2 as there was no other VGCC expressed on

LNCaP cells. This could be due to the treatment used to induce NED, treatment with cAMP, whereas as we have shown increased expression of CaV1.3 occurs after treatment with ADT. While we were unable to detect a voltage activated current in this channel, there is a potential role for CaV1.3 in regulating NED in LNCaP cells under ADT through increased SOCE. Other studies have implicated the activation of CREB in the development of NED and treatment evasion in PCa (Deng et al., 2008). As highlighted in section 1.5.3.1, CREB is a transcription factor which is associated with some Ca^{2+} signalling pathways, where activation of a protein kinase by the increased cytosolic Ca^{2+} results in the phosphorylation of CREB. This in turn initiates the transcription of genes, amongst which are genes that regulate NED. The activation of CREB has recently been associated with ADT (Y. Zhang et al., 2018), hence increased expression of CaV1.3 observed in cells under ADT and the subsequent increased SOCE, may be influencing the neurite outgrowth and NED in the LNCaP-ADT cells.

Proliferation is significantly increased in the LNCaP-abl cells, which is consistent with previous results (Figure 3.5). This enhanced proliferative ability could be due to the increased SOCE, which we have demonstrated here after store depletion. Alternatively, increased proliferation could be due to the increased $[ER_{Ca}]$, which is larger in the LNCaP-abl cells than the control LNCaP cells or the LNCaP-ADT cells. Studies have shown that the amount of Ca^{2+} stored in the ER is related to the proliferative ability and growth rate of LNCaP cells (Legrand et al., 2001). Legrand et al. increased proliferation of LNCaP cells by incubating them with epidermal growth factor (EGF), which in turn resulted in an increased $[ER_{Ca}]$. This was demonstrated by the increased Ca^{2+} release observed in the EGF treated cells upon Tg induced store release. Another study shows that the Ca^{2+} content of the ER alters according to the growth stimulation or inhibition in LNCaP cells (Humez et al., 2004). Here they treated the cells with insulin growth factor (IGF), which increased the growth of the cells and consequently increased the $[ER_{Ca}]$, while treatment with tissue necrosis factor (TNF-α) reduced proliferation and in turn the $[ER_{Ca}]$. Both studies implicate the expression of the SERCA pump which is reportedly upregulated and thought to result in an increased Ca^{2+} uptake into the ER.

This led us to hypothesise that the increased proliferation observed in the LNCaP-abl cells may be due to the increased $[ER_{Ca}]$ in these cells. However, our research shows that the proliferative ability of LNCaP-abl cells is significantly reduced when CaV1.3 is knocked down without having any observable effect on the $[ER_{Ca}]$ (Figure 4.7 (B)). This phenomenon may be explained by the dual role Ca^{2+} signalling has in the cell. Ca^{2+} fluctuations have the potential to promote proliferation and survival in cells, however a sustained Ca^{2+} increase via SOCE induces apoptosis (Skryma et al.,

2000; Vanoverberghe et al., 2004). The LNCaP-abl cells had an increased SOCE in the cells which had silenced CaV1.3 (Figure 4.7 (D)), which coincides with the reduced proliferation (Figure 4.8 (A)). Therefore, the reduced proliferation may be due to sustained Ca^{2+} entry upon silencing CaV1.3 resulting in apoptosis. Sustained Ca^{2+} results in ER stress or mitochondrial Ca^{2+} overload, leading to the production of reactive oxygen species (ROS). ROS when coupled with Ca^{2+} leads to activation of the permeable transition pore in the mitochondrial membrane. This facilitates transmembrane ion transfer, resulting in loss of mitochondrial membrane potential, ATP depletion, and ultimately necrosis (Bruce and James, 2020). This is also evident in the CFA where there is an increased number of colonies in the LNCaP-abl cells, with a significant loss of ability when CaV1.3 in silenced. This could also be explained due to loss of viability through increased apoptosis. Indicating the potential for CaV1.3 to work as a Ca^{2+} regulator, preventing ER stress and mitochondrial Ca^{2+} overload and subsequent apoptosis.

Overall migration is not a feature of LNCaP cells and increased expression of CaV1.3 in cells treated with ADT does not induce migration. Since many papers have implicated EMT with metastasis after ADT in PCa (Shang et al., 2014; Sun et al., 2012), it is not surprising that migration was not present due to the lack of EMT in 2D culture of this model. Although there was a significant increase in migration observed in the LNCaP-ADT cells at 60 hours, this was initiated from a low base, therefore it is difficult to indicate a direct correlation. Perhaps due to the reduced proliferative ability of the LNCaP-ADT cells there could be some benefit in allowing the migration experiment to run for longer with these cells. Papers which had used the Xcelligence™ system with LNCaP cells have used 10% FBS as a chemoattractant with lower FBS % in the upper chamber (Debelec-Butuner et al., 2014; Dondoo et al., 2017). Led by this we also used 10% FBS as a chemoattractant however, both studies had altered the LNCaP cells to induce migration. Dondoo et al. transfected LNCaP cells with Galactin-3 which resulted in migration, while very little, or negative migration was recorded for the control LNCaP at 60 hours. Whereas Debelec-Butner et al. used conditioned medium containing monocyte secreted cytokines to represent inflammation which induced migration in the LNCaP cells, again with very little migration recorded in control cells up to 132 hours. The findings of our research indicates that in LNCaP cells the increased expression of CaV1.3 in cells treated with ADT is not driving migration.

4.3.5 Effects of Nifedipine on SOCE

These experiments were carried out to determine if CCB's could inhibit Ca^{2+} influx through CaV1.3 and reduce its associated SOCE which we previously discovered (Figure 4.6 and 4.7). Furthermore, there is previous research which indicates an inverse association with the development and progression of PCa in patients prescribed CCB for hypertension (Debes et al., 2004; Annette L Fitzpatrick et al., 2001; Poch et al., 2013). As outlined in our analysis of the patient dataset (Figure 3.6) CaV1.3 expression is increased following ADT and is associated with progression to CRPC as well as a shorter time to biochemical recurrence. Therefore, we hypothesised that inhibiting CaV1.3 with CCB may reduce the SOCE and prevent disease progression under ADT.

The LNCaP-ADT Ctr cells had an increased Ca^{2+} influx, which is consistent with our earlier studies (Figure 4.2). This was not reduced when CaV1.3 was inhibited with nifedipine (Figure 4.10 (D)), unlike our findings when CaV1.3 was silenced. This suggests that the increased SOCE in these cells may not be due to Ca^{2+} entry through CaV1.3, but rather CaV1.3 has an indirect effect on the SOCE mechanism. The LNCaP-abl Ctr cells have an increased Tg peak, which conforms with our previous findings (Figure 4.2), which is reduced when cells were incubated with CCB. However, the Ca^{2+} influx in these cells again was elevated compared to LNCaP which reflects our previous findings but increases after incubation with nifedipine. Although the AUC indicates that the overall $[Ca^{2+}]_i$ is elevated in the LNCaP-abl Ctr cells and is reduced when the LNCaP-abl is treated with nifedipine (Figure 4.11 (F)), which may infer that nifedipine is reducing the overall $[Ca^{2+}]_i$.

Overall, the impact of nifedipine on the SOCE in the PCa cells is inconclusive and requires further investigation to confirm the findings of these experiments. These repeats indicate a lack of consistency between runs as indicated by the error bars. This can be explained by potential Tg induced stress which can sometimes reduce the viability in these cells and inhibit good consistent Ca^{2+} measurements. When performing previous Ca^{2+} imaging experiments approximately 15-30 runs were performed for each condition. A confidence interval (CI) was calculated for the range of the complete set of results obtained. Any runs which gave readings outside of the CI were eliminated from the analysis, this allowed us to eliminate any repeats which suffered significant cell loss, which would have skewed the results. But this could not be applied to this set of results due to the small N numbers. We combined the nifedipine experiments with those obtained for the siRNA experiments (Appendix B; Figure B.4), to analyse if the traces were significantly different. There was no significant difference detected in the overall trace, which informed us that the nifedipine experiments were not significantly outside the expected traces, therefore we continued with the analysis.

Treating cells with nifedipine had an impact on malignant progression reducing the proliferative ability and the CFA at all stages in the progression to CRPC. This is similar to the effect we observed when CaV1.3 was silenced. Although there was a more significant inhibition observed when cells were treated with nifedipine, it is difficult to draw a comparison directly to CaV1.3 inhibition in these experiments. Since there are a number of available binding sites for dihydropyridines in PCa cells (Rosenthal et al., 1990), there could be off target effects associated with nifedipine use other than direct inhibition of CaV1.3. Nifedipine has inhibiting effects on CaV1.1, CaV1.2, CaV1.3 as well as the beta subunit associated with these channels. This drug also has inhibitory effects on T-type VGCC's CaV3.1, CaV3.2 and CaV3.3 (Shcheglovitov et al., 2005) and the Ca^{2+} binding protein calmodulin (Minocherhomjee and Roufogalis, 1984). There is also inhibition of the potassium channel Kv4.3 (Hatano et al., 2003), which is associated with cellular repolarisation, although not reported in association with PCa. Therefore, any effects detected in the functional ability could be attributed to overall inhibition of Ca^{2+} mobilisation, or interruption of the cellular membrane potential.

In addition, it has been reported that the alternative splicing of the c-terminus of CaV1.3 can both alter the activity of the channel and significantly affect the sensitivity to inhibition of dihydropyridines (Huang et al., 2013). The c-terminus of CaV1.3 has been detected in the nucleus of both the LNCaP and the LNCaP-ADT cells (Figure 3.8). Therefore, it is possible that nifedipine may not be as effective at specifically targeting CaV1.3 in these cells. Further work is needed to confirm the impact of nifedipine on Ca^{2+} mobilisation in PCa, although there does appear to be some effect. This coupled with the significant effect on the CFA and the proliferation, overall supports our hypothesis that Ca^{2+} plays a key role in PCa progression. However, the nonspecific aspect of the drug means that we cannot confirm that the effects detected are as a direct result of CaV1.3 inhibition as there may be some off target effects.

4.4 Concluding remarks.

In this chapter we wanted to determine if the enhanced expression of CaV1.3 was involved in PCa progression through altered Ca^{2+} mobilisation. Here we have shown that CaV1.3 does not function through the normal mechanism as a voltage gated channel, as indicated by the lack of Ca^{2+} influx detected following cell depolarisation with high external K^+. However, we have identified a novel mechanism in which upregulated CaV1.3 increases SOCE after ADT in the short term and into the CRPC stage. What was interesting was that this mechanism appeared to alter with disease progression. Inhibiting the expression of CaV1.3 with siRNA reduced the SOCE in the LNCaP-ADT cells, back to the levels detected in the LNCaP cells. However, silencing CaV1.3 in the LNCaP-abl cells increased the SOCE. Indicating an alternative mechanism whereby CaV1.3 regulates SOCE in the CRPC stage. This association has not been identified in PCa before to our knowledge and may indicate a substantial target for treatment to prevent progression under ADT.

The exact mechanism through which CaV1.3 is influencing SOCE is not yet clear, however due to the lack of effect observed with nifedipine we can assume that it is not as a direct result of Ca^{2+} entry through plasma membrane bound CaV1.3. This would agree with our previous findings of a predominant subcellular localisation of the CaV1.3 channel. This indicates that CaV1.3 may be influencing the SOCE through interaction with other Ca^{2+} channels such as RyR, STIM, Orai or TRP channels.

While further investigation into the the role of CaV1.3 on SOCE is required it is clear however that the enhanced SOCE in CRPC phenotype LNCaP-abl is promoting cell proliferation and survival. Knockdown of CaV1.3 was able to reduce both indicating a direct role of CaV1.3 in PCa disease. This highlights CaV1.3 as a potential target in particular for ADT resistant CRPC.

Chapter 5 - Investigating the effect of upregulated CaV1.3 on hypoxia signalling in PCa progression under ADT

5.1 Introduction

5.1.1 Background of HIF-1α under ADT

As alluded to earlier, hypoxia is a key characteristic associated with cancer progression and treatment resistance (Semenza, 2012). It is characterised as a condition of low oxygen pressure in the TME, which is a common feature of solid tumours due to the rapidly proliferating mass of cells and the lack of adequate vascularisation (Sørensen and Horsman, 2020). Under hypoxic conditions the expression of HIF-1α protein is upregulated due to loss of O_2 dependant proteasomal degradation which occurs under normal conditions. Hence, hypoxia initiates HIF signalling which in turn drives cancer progression through activation of genes required for cell growth, proliferation, angiogenesis, and anti-apoptosis (Harris, 2002; Hubbi and Semenza, 2015; Park et al., 2010; Raffo et al., 1995). HIF proteins have been commonly associated with treatment resistance in many cancers (Li et al., 2009; Lukashev et al., 2007) and are known to promote pathways that result in cancer progression as reviewed previously (Wigerup et al., 2016). Hypoxia is particularly prevalent in PCa tumours, which have a distinctly low O_2 level which is associated with clinical stage (Movsas et al., 2001, 2000).

In PCa, ADT has been shown to enhance hypoxic conditions within the TME (Byrne et al., 2016; Ming et al., 2013), in doing so driving a number of malignant influences. Hypoxia levels have been shown to elevate over time using the anti-androgen treatment, bicalutamide (Ming et al., 2013), with a fall in O_2 levels detected within LNCaP tumours in mouse models treated with bicalutamide (Byrne et al., 2016). The levels fell to approximately 0.1% O_2 within 3-7 days and remained at this level for up to 10-14 days. HIF-1α signalling in PCa has been shown to influence disease progression and treatment resistance, such as the inference of persistent AR transcription after ADT, consistent with that seen in CRPC (Mitani et al., 2011).

Interestingly research has demonstrated that ion channels play key roles in promoting the activation of hypoxic signalling (Arcangeli, 2011). Research has indicated an association between HIF activation and Ca^{2+} (Azimi, 2018; Riganti et al., 2009) in a range of tissues, including PCa. It has been reported that TRPM8, an ion channel permeable to Ca^{2+}, enhances HIF-1α expression by

interfering with the ubiquitination of HIF-1α protein, required for proteasomal degradation (Yu et al., 2014). In PC12 cells it has been demonstrated that, under hypoxic conditions, cells undergo membrane depolarization (Seta et al., 2004). This occurs due to the hypoxic deactivation of KV1.2, resulting in the voltage dependent activation of membrane bound VGCC which facilitate Ca^{2+} influx into the cell. This bears significance, since some reviews suggest that Ca^{2+} influx influences gene transcription and cellular proliferation (Kanatous et al., 2009; Pinto et al., 2015; Resende et al., 2013). In relation to this, we have demonstrated that under ADT VGCC Ca^{2+} influx is enhanced, leading to increased intracellular Ca^{2+} and that this has a beneficial effect on PCa cell survival under ADT, with increased proliferation seen in the LNCaP-abl cells (Figure 4.10). Taken together this suggests that CaV1.3 could potentially play a role in supporting hypoxic signalling.

Studies have shown that Ca^{2+} influx is required for hypoxic signalling through the activation of HIF-1α transcriptional activity (Mottet Denis et al., 2006). Demonstrated through increased luciferase activity in cells under hypoxic conditions which was reduced when Ca^{2+} was chelated. Further to this, Ca^{2+} influences the stabilisation of HIF-1α as chelation of Ca^{2+} in PC12 cells reduces the levels of HIF-1α (Hui et al., 2006). In fact, this research demonstrated that either internal or external Ca^{2+} chelators were capable of inhibiting HIF expression. Indicating that Ca^{2+} for this process is acquired through the activation of Ca^{2+} permeable channels on the plasma membrane. Research suggests that this Ca^{2+} influx in PC12 cells is facilitated via VGCC, as demonstrated by the reduced HIF-1α accumulation under treatment with the VGCC blocker nifedipine. Interestingly, upregulation of VGCC CaV1.2 and CaV1.3 has also been reported in PC12 cells under hypoxic conditions (R. Li et al., 2015). While a dose dependent reduction in both protein expression levels was detected when the cells were incubated with the HIF-1α inhibitor echinomycin, indicating a potential coregulatory relationship. However, since we have indicated a lack of inhibition in LNCaP cells with nifedipine treatment there may be another mechanism influencing HIF-1α stabilisation in these cells, potentially through enhanced SOCE.

Together this work highlights that ion channels, particularly Ca^{2+} channels, play a key role in promoting HIF-1α stabilization and activation. Collectively this suggests that an increase in $[Ca^{2+}]_i$ could lead to the development of many of the hallmarks of cancer (Hanahan and Weinberg, 2011), by driving hypoxic signalling.

5.1.2 Aims of chapter 5

We have observed enhanced intracellular Ca^{2+} facilitated through upregulated CaV1.3 during ADT. Here we wanted to investigate if this could play a role in enhancing HIF signalling under normoxic and or hypoxic conditions.

Aim: Determine if there is any association between enhanced CaV1.3 expression under ADT in driving hypoxia signalling in PCa cells.

Hypothesis: Enhanced intracellular Ca^{2+} facilitated through upregulated CaV1.3 drives HIF-1α stabilisation facilitating cell survival and treatment resistance.

1. Examine the association between enhanced Ca^{2+} via CaV1.3 in driving HIF-1α signalling.
2. Determine the impact of enhanced HIF signalling related to CaV1.3 expression on cellular functions.
3. Investigate if the CaV1.3 HIF-1α axis has influence on the malignant phenotype under hypoxia.

5.2 Results

5.2.1 CaV1.3 expression is not altered under hypoxic conditions.

Research in other cell types has suggested that hypoxia can influence the expression of VGCC including CaV1.3 (R. Li et al., 2015). Here we investigate the effect hypoxia has on the expression of CaV1.3 in PCa cells, or if the enhanced CaV1.3 expression detected in cells treated with bicalutamide was influenced by hypoxia.

Western blot analysis of CaV1.3 expression indicates the LNCaP-abl cell express the largest CaV1.3 protein expression compared to the LNCaP with a 1.6-fold (+/- 0.165 sem) increased expression (Figure 5.1 (A(i))), which reflects the protein expression observed previously (Figure 3.7 (C)). Following hypoxic treatment (low oxygen conditions (1%O_2) of PCa cells no significant alteration was detected in the protein expression of CaV1.3 compared to those cultured in normal oxygen levels (20% O_2) (Figure 5.1(A)(iii)(iv)(v)). qPCR analysis revealed that LNCaP-ADT cells had a 1.7-fold (+/- 0.3 sem) increased expression of CaV1.3 compared to LNCaP cells with no significant differences seen on genetic expression under hypoxic conditioning (1% O_2) (Figure 5.1 (B)(i)). LNCaP cells (Figure 5.1 (B)(ii)) and LNCaP-abl cells (Figure 5.1 (B)(iv)) indicate no altered genetic expression either under hypoxic conditions compared to control. Overall, these results indicate that hypoxia does not enhance the expression of CaV1.3 in PCa cells.

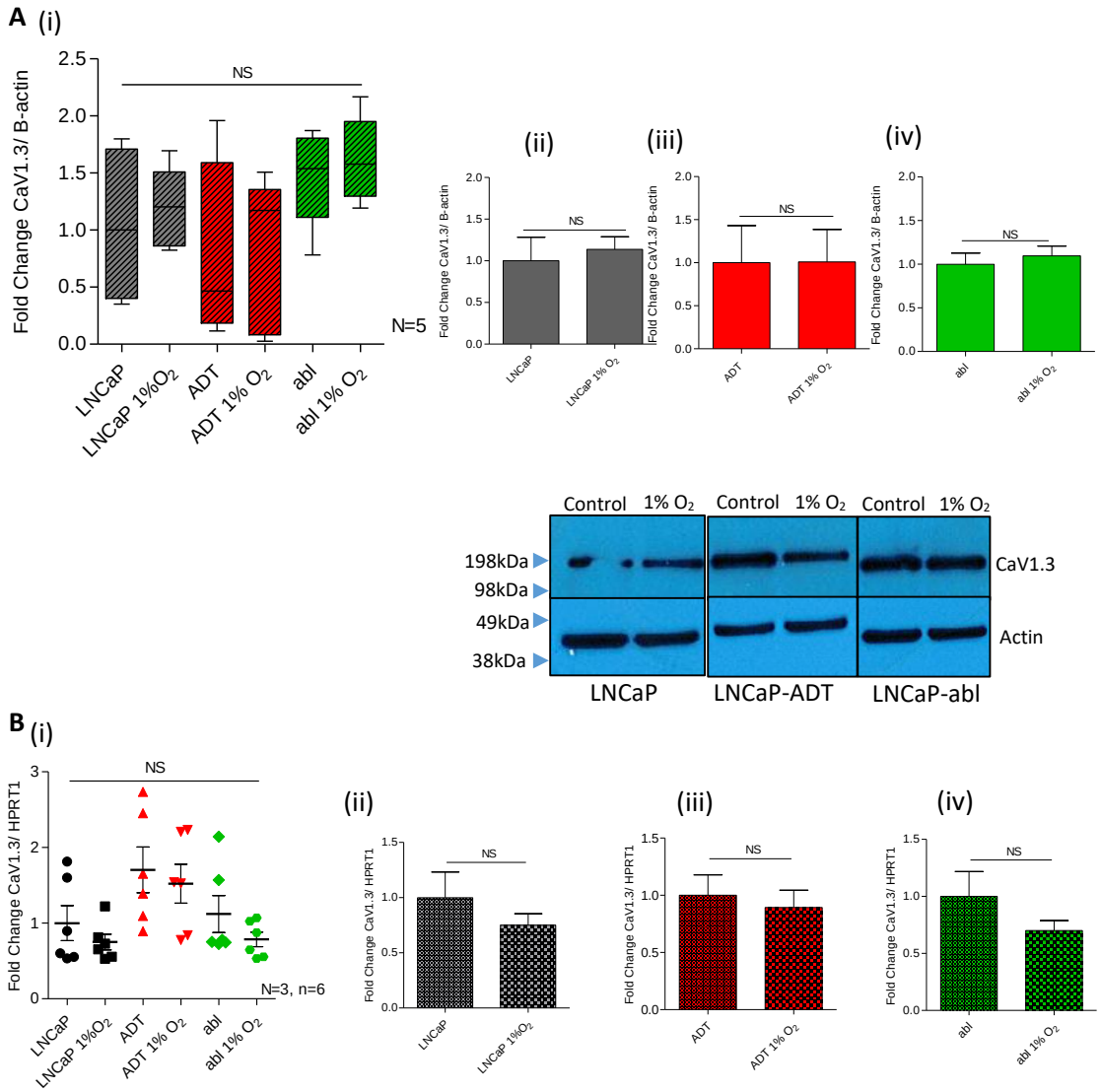

Figure 5.1: Expression of CaV1.3 is unaffected by hypoxic conditions: (A) *Western blot analysis of protein expression for CaV1.3 normalised by expression of the housekeeping gene Actin, compared to (i) LNCaP control or (ii,iii,iv) normal cell of type* ***(B)*** *Genetic expression of CaV1.3 assessed using qPCR of fold change normalised to (i) LNCaP control or (ii,iii,iv) normal cell of type. Analysis of androgen sensitive LNCaP cells (black), LNCaP-ADT cells treated with 10 µM bicalutamide (7-10 days) (Red) and androgen insensitive long-term androgen deprived LNCaP-abl cells (Green) incubated in normal oxygen conditions or in hypoxic conditions (1% O2). (A(i), B(i)) Analysed by Kruskal-Wallis significance test between cell types and conditions normalised to LNCaP Control. (A(iii)(iv)(v), B(ii)(iii)(iv)) Analysed using Mann-Whitney significance test between cell types and treatments. * P<0.05, ** P<0.01, ***P<0.001, NS not significant.*

5.2.2 Expression of HIF-1α is regulated by CaV1.3 under hypoxic conditions.

As previously outlined HIF-1α is proteolytically degraded under normal O_2 tension, a mechanism which is inhibited under low O_2 conditions resulting in stable expression of HIF-1α. However, research has also indicated a correlation between upregulated HIF expression and ADT (Byrne et al., 2016; Rothermund et al., 2005) with other research indicating a reliance on Ca^{2+} signalling (Hui et al., 2006). Therefore, we wanted to examine the expression of HIF-1α in our cell line model to determine if there was a correlation with CaV1.3 expression.

5.2.2.1 Hif-1α expression is increased following bicalutamide treatment.

Western blot analysis shows a significant upregualtion in the expression of HIF-1α in the LNCaP-ADT cells grown under normal O_2 conditions, with a 4.65-fold (+/- 1.8 sem) increase compared to LNCaP cells. LNCaP-abl cells have a decreased expression in normal oxygen (0.5-fold +/- 0.28 sem) (Figure 5.2(A). Suggesting that treatment with bicalutamide increases the HIF-1α expression in the androgen sensitive cells even under normal O_2 conditions.

When incubated under hypoxic conditions (1% O_2), there is an increased expression of HIF-1α in all cell types (Figure 5.2(B)(i)). When compared to their matching normoxic control LNCaP cells have a significant 2.798-fold (+/- 1.04 sem) increased HIF-1α (Figure 5.2(B)(ii)), LNCaP-ADT cells have 1.399-fold increase (+/- 0.575 sem) (Figure 5.2(B)(iii)) and the LNCaP-abl cells have a significant 6-fold increase (+/- 2.58 sem (Figure 5.2(B)(iv)).

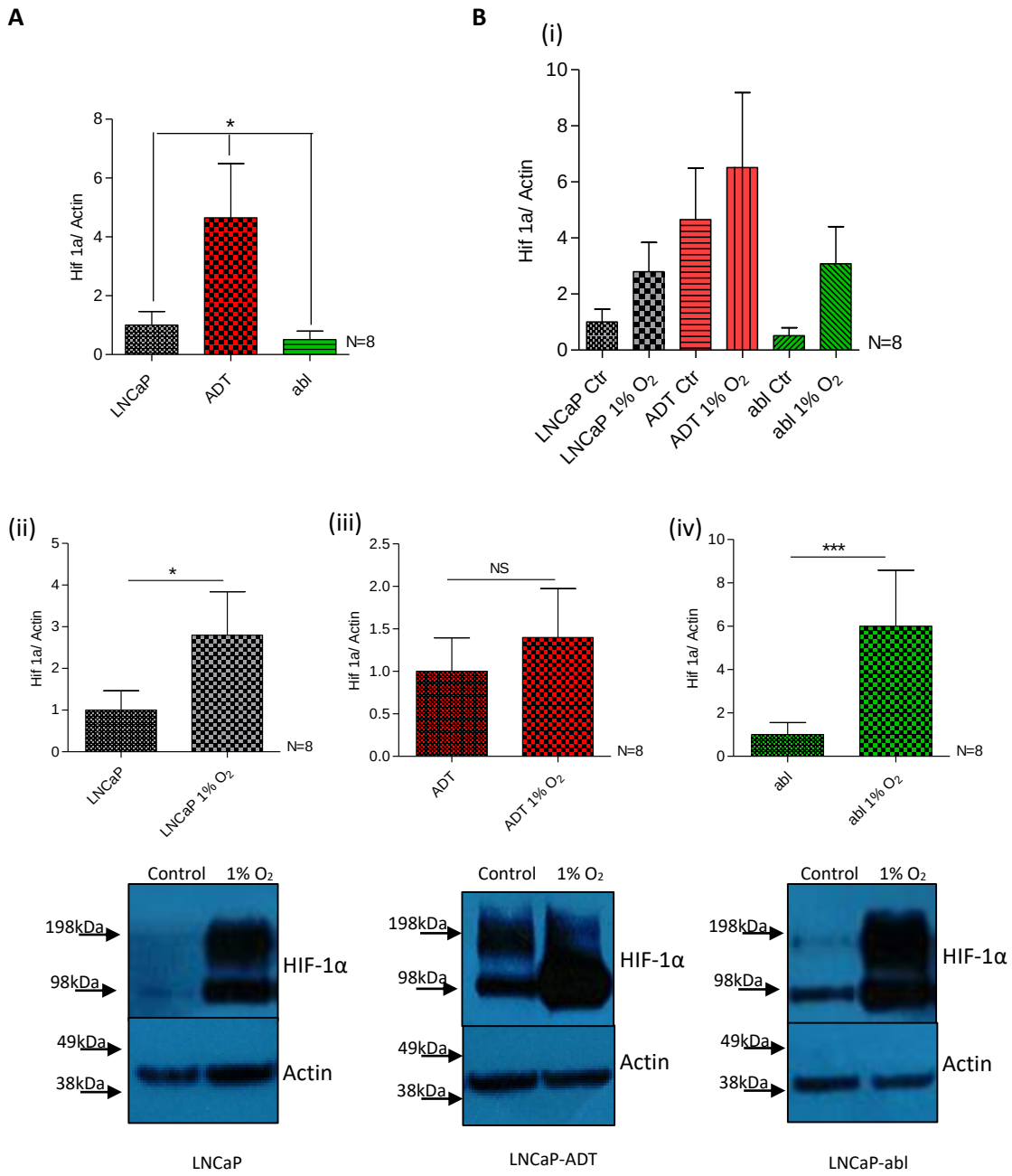

Figure 5.2: Protein expression of HIF-1α is upregulated in ADT under normal O_2 is significantly increased under hypoxic conditions*: Western blot analysis of HIF-1α expression normalised to the housekeeping gene Actin. Analysis of androgen sensitive LNCaP cells (black), LNCaP-ADT cells treated with 10 μM bicalutamide (7-10 days) (Red) and androgen insensitive long-term androgen deprived LNCaP-abl cells (Green) incubated under (A) normal oxygen conditions (B)(i) induced hypoxic conditions (1% O_2) normalised to LNCaP control. Analysed by Kruskal-Wallis significance test between cell types and conditions normalised to LNCaP Control. Protein expression of CaV1.3 in (B)(ii) LNCaP 1% O_2, (B)(iii) LNCaP-ADT 1% O_2, (B)(iv) LNCaP-abl 1% O_2 normalised to control. Analysed using Mann-Whitney significance test between cell types and treatments. * P<0.05, ** P<0.01, ***P<0.001, NS not significant.*

5.2.2.2 HIF-1α response is not signficantly reduced when Ca^{2+} entry is inhibited by the VGCC blocker Nifedipine.

When incubated with the CCB nifedipine there was reduction in HIF-1α expression under hypoxia across all cell types, although none were significant.

LNCaP cells had 5.6-fold (+/- 0.7 sem) increased expression of HIF-1α when incubated under hypoxic conditions, which was reduced to 4.646-fold (+/- 0.99 sem) when incubated under hypoxia with nifedipine (Figure 5.3(B)). LNCaP-ADT cells has a 12.57-fold (+/- 2.4 sem) increased HIF-1α expression under hypoxia which was again reduced to 10.62-fold (+/- 2.3 sem) when nifedipine was introduced (Figure 5.3(C)). LNCaP-abl cells had a 3.8-fold (+/- 1.879 sem) increase in hypoxic conditions which was unchanged when the cells were treated with nifedipine 3.32-fold (+/- 3.566 sem) (Figure 5.3(D)).

Overall, these results reflect our previous findings in this cell model with nifedipine incubation. We have demonstrated that the increased SOCE, observed in cells which had increased expression of CaV1.3, had no significant effect observed when incubated with nifedipine.

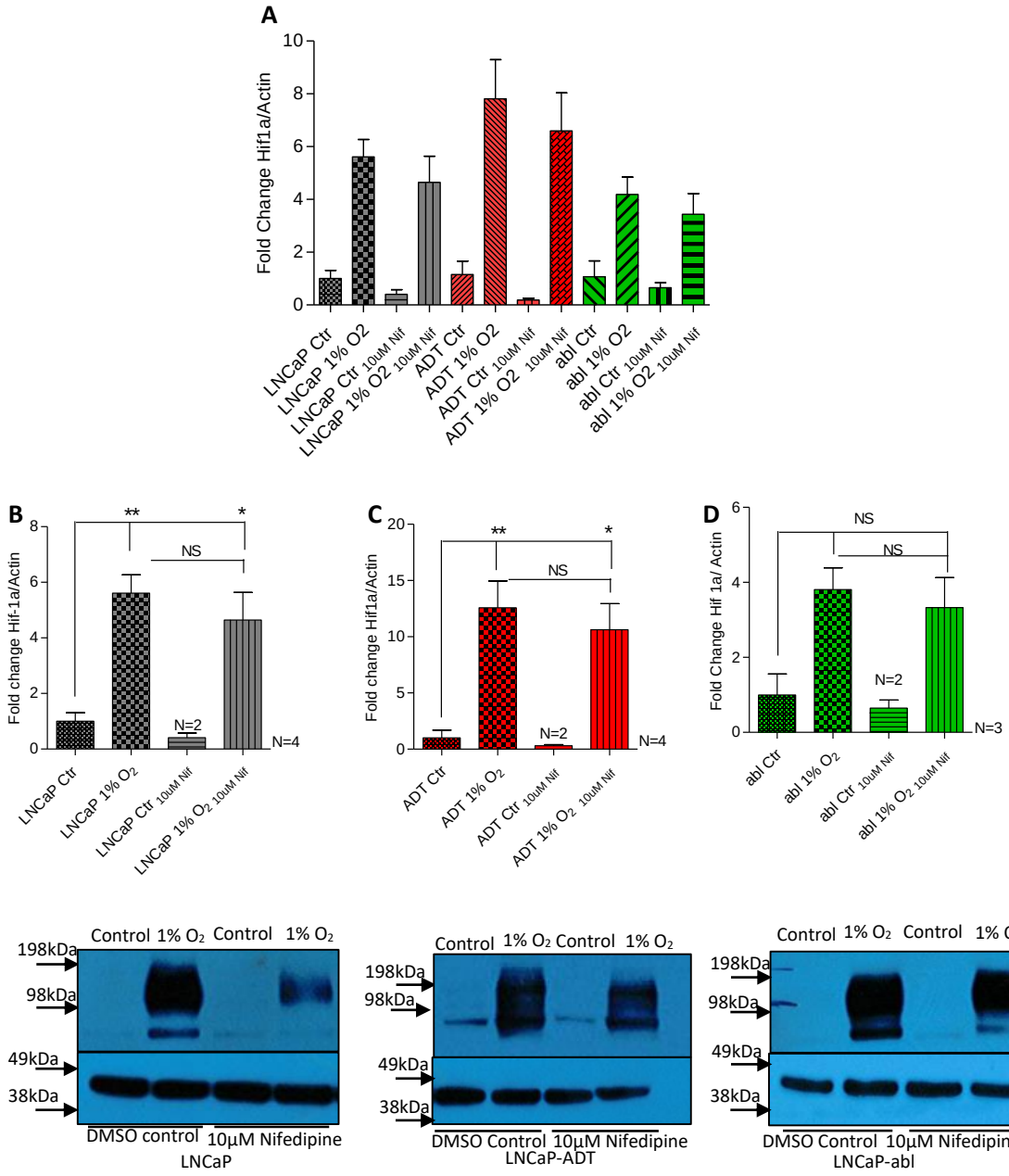

Figure 5.3: Protein expression of HIF-1α is not significantly reduced when incubated with Nifedipine*: Western blot analysis of protein expression of HIF-1α normalised by expression of the housekeeping gene Actin. Analysis of androgen sensitive LNCaP cells (black), LNCaP-ADT cells treated with 10 µM bicalutamide (7-10 days) (Red) and androgen insensitive long-term androgen deprived LNCaP-abl cells (Green) incubated in normal oxygen conditions or in hypoxic conditions (1% O_2) incubated with 10µM Nifedipine or DMSO control. Protein expression of HIF-1α in (A) LNCaP, (B) LNCaP-ADT, (C) LNCaP-abl normalised to normoxic control. Analysed using One-way analysis of variance and Tukey's multiple comparison post hoc test between cell types and treatments. * P<0.05, ** P<0.01, ***P<0.001, NS not significant.*

5.2.2.3 Silencing CaV1.3 inhibits HIF-1α expression in androgen sensitive PCa cells under hypoxia.

Knocking down CaV1.3 reduces the HIF-1α expression in LNCaP and LNCaP-ADT cells under hypoxic conditions but does not reduce HIF-1α in the LNCaP-abl cells (Figure 5.4(A)).

Under hypoxic conditions the LNCaP siCtr cells have a 2.3-fold (+/- 0.478 sem) increased expression which is significantly reduced to 0.1157-fold (+/- 0.06 sem) when transfected with siCaV1.3 (Figure 5.4(B)). The LNCaP-ADT siCtr cells have 1.445-fold (+/- 0.359 sem) increased expression of HIF-1α under hypoxia which is again significantly reduced to 0.09-fold (+/- 0.05 sem) when CaV1.3 is silenced (Figure 5.4(C)). Expression of HIF-1α is significantly increased in the LNCaP-abl siCtr cells under hypoxia 5.739-fold (+/- 1.68 sem) which is increased to 7.295-fold (+/- 1.7 sem) expression in the cells transfected with siCaV1.3 (Figure 5.4(D)).

These results indicate that the SOCE detected in chapter 4 has some influence on the HIF-1α expression in the cell model. Silencing CaV1.3 reduced the SOCE in the LNCaP-ADT cells, which also reduced the expression of HIF-1α. Interestingly silencing CaV1.3 in the LNCaP-abl cells increased the SOCE, which we have now demonstrated coincides with an increased HIF-1α expression.

Relevant changes in expression compared to LNCaP control are outlined in Table 5.1, indicating the increased $[Ca^{2+}]_i$ as a result of increased CaV1.3 is driving HIF signalling in PCa.

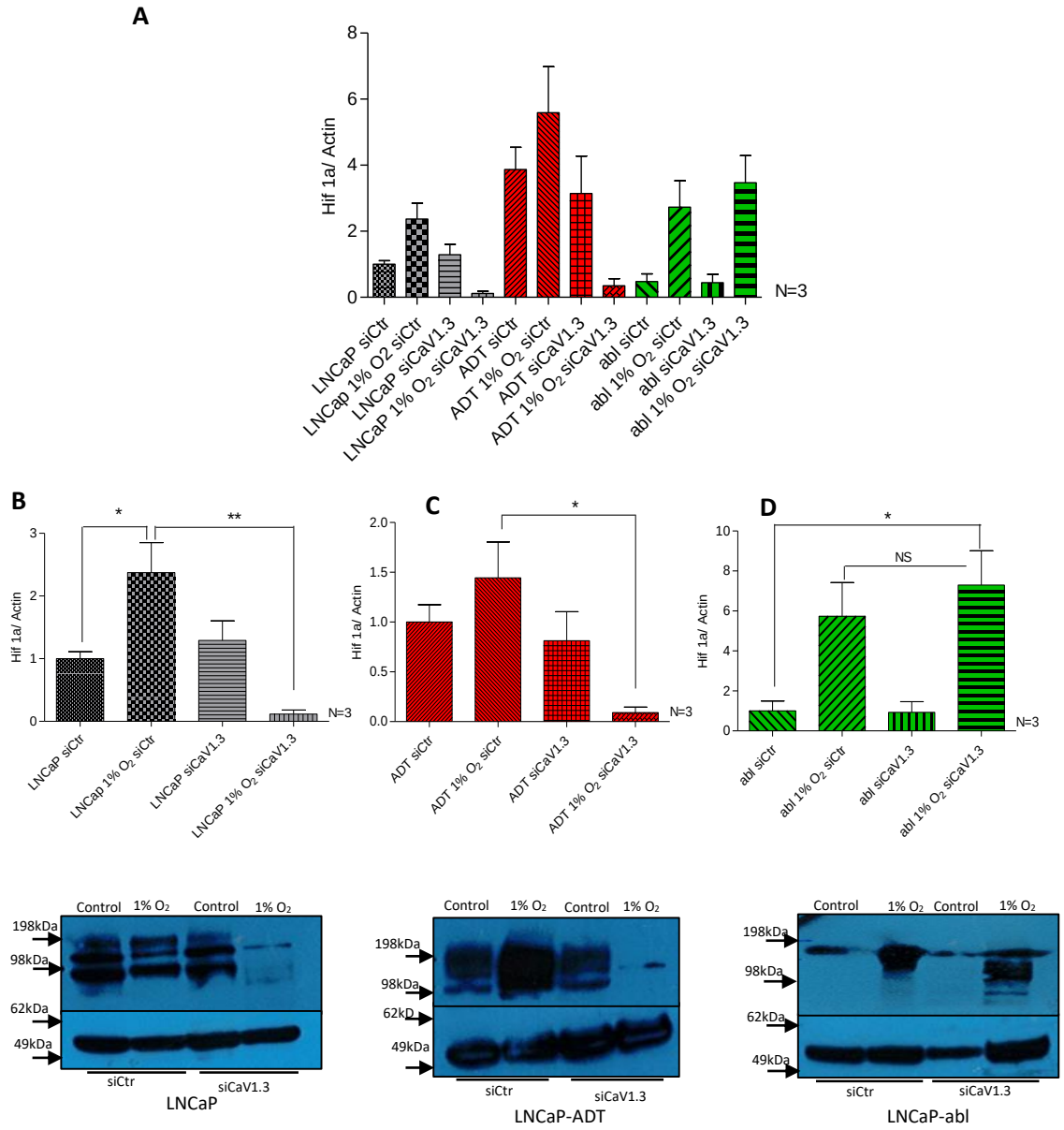

Figure 5.4: Protein expression of HIF-1α is significantly reduced in LNCaP and LNCaP-ADT when CaV1.3 expression is silenced but increased in LNCaP-abl: *Western blot analysis of protein expression of HIF-1α normalised by expression of the housekeeping gene Actin. Analysis of androgen sensitive LNCaP cells (black), LNCaP-ADT cells treated with 10 µM bicalutamide (7-10 days) (Red) and androgen insensitive long-term androgen deprived LNCaP-abl cells (Green) incubated in normal oxygen conditions or in hypoxic conditions (1% O_2) transfected with non-targeting control siRNA (siCtr) or siRNA targeting CaV1.3 (siCaV1.3). Protein expression of CaV1.3 in (A) all cell types normalised to LNCaP Ctr (B) LNCaP, (C) LNCaP-ADT and (D) LNCaP-abl normalised to control cell of type. Analysed using One-way analysis of variance and Tukey's multiple comparison post hoc test between cell types and treatments. * P<0.05, ** P<0.01, ***P<0.001, NS not significant.*

Table 5.1: Fold change expression of HIF-1α compared to LNCaP control: *Summarised changes detected in HIF-1α expression measured by relative densitometry between cell types in cells under normal oxygen conditions or hypoxic conditions (1% O_2) transfected with non-targeting siRNA (siCtr) or siRNA targeting CaV1.3 (siCaV1.3). Measured as fold change from LNCaP control (+/- standard error of the mean)*

	Control – 20% O_2	**1% O_2 Control**	**siCaV1.3 – 20% O_2**	**1% O_2 siCaV1.3**
LNCaP	1.000 (± 0.11)	2.373 (± 0.478)	1.292 (± 0.31)	0.116 (± 0.06)
LNCaP-ADT	3.871 (± 0.67)	5.593 (±1.39)	3.143 (± 1.13)	0.349 (± 0.21)
LNCaP-abl	0.476 (± 0.23)	2.732 (± 0.8)	0.442 (± 0.25)	3.473 (±0.818)

5.2.3 Silencing CaV1.3 reduces hypoxia enhanced proliferation in CRPC cells.

Hypoxia is reported to bear influence on malignant progression in PCa cells including enhancing proliferation and survival. We wanted to examine the effects silencing CaV1.3 would have on any hypoxic influence detected under ADT.

Our initial analysis shows that hypoxia has no effect on the proliferation of the LNCaP and the LNCaP-ADT cells (Figure 5.5 (A)(i)), with increased proliferation detected in the LNCaP-abl cells. Proliferation is significantly increased in LNCaP-abl cells cultured in normal oxygen conditions (63% increased +/- 15.11 sem) and further enhanced under hypoxic conditions (115% increased +/- 21.02 sem) compared to LNCaP control.

Analysis of the cell types individually by comparing the proliferation rates under hypoxia and CaV1.3 silencing back to control for each cell type, confirms that there is no significant effect on proliferation in the LNCaP cells under any of the conditions (Figure 5.5 (A)(ii)). Although under normal O_2 conditions silencing CaV1.3 reduces proliferation by 15% (+/- 0.5 sem) compared to control. The LNCaP-ADT cells have no change in the proliferation rate between control and CaV1.3 silenced cells under normal O_2 conditions (Figure 5.5 (A)(iii)). Under hypoxic conditions there is a 20.3% (+/- 12.7 sem) increased proliferation in the control cells which is significantly increased

when CaV1.3 is silenced under hypoxic conditions to 40.2% (+/- 1.09 sem) increased proliferation. Suggesting that hypoxia increases proliferation of the LNCaP-ADT cells, which is further increased when CaV1.3 is silenced.

The LNCaP-abl cells have a significantly reduced proliferation under normal O_2 conditions when CaV1.3 is silenced with a 34.59% (+/- 3.13 sem) reduced proliferation rate compared to control (Figure 5.5 (A)(iv)). When incubated in hypoxic conditions as stated already the proliferation rate is significantly increased, which when compared to LNCaP-abl control is increased by 32% (+/- 12.84 sem). When CaV1.3 is silenced under hypoxic conditions the proliferation of the LNCaP-abl cells is significantly reduced 21.53% (+/- 11.45 sem) less than the LNCaP-abl control. Indicating that the enhanced proliferative ability seen in the LNCaP-abl cells under both normal O_2, and hypoxia is reduced when CaV1.3 is silenced.

We then looked at the impact of hypoxia and CaV1.3 on cell survival through a CFA. It was noted that hypoxia reduces the CFA of the LNCaP and the LNCaP-ADT cells with no effect observed in the LNCaP-abl cells (Figure 5.5 (B)(i)). The LNCaP cells had a significant reduced ability under hypoxic conditions (86.21% reduced +/- 7.6 sem) compared to normal O_2 conditions. The LNCaP-ADT cells had a reduced CFA but no significant effect compared to control LNCaP under normal O_2 or hypoxic conditions with 23.45% (+/- 5.97 sem) and 46.21% (+/- 6.65 sem) reduced ability respectively. As observed in chapter 3 (Figure 3.5 (B)) these results confirm that the CFA of the LNCaP-abl cells is significantly increased, while hypoxic conditions do not alter the ability with a 3.46-fold (+/- 1.4 sem) and a 3.44-fold (+/- 2.94 sem) increased ability, respectively.

Direct analysis of each cell type individually comparing the cells under hypoxia with CaV1.3 silencing indicates that the LNCaP cells have a significant reduced viability under hypoxia which is further reduced when CaV1.3 is silenced (99.31% reduced +/- 0.06 sem) (Figure 5.5 (B)(ii)). The LNCaP-ADT cells showed a 29.73% (+/- 8.7 sem) reduction in viability compared to normal O_2 conditions, which was significantly reduces by 98% (+/- 1.8 sem) when CaV1.3 was knocked down (Figure 5.5 (B)(iii)). Whereas the LNCaP-abl cells, which have significantly increased colony forming ability compared to LNCaP cells, are unaffected under hypoxia. However, when CaV1.3 is silenced viability is reduced by 46.5% (+/- 12.72 sem) compared to the LNCaP-abl control (Figure 5.5 (B)(iv)).

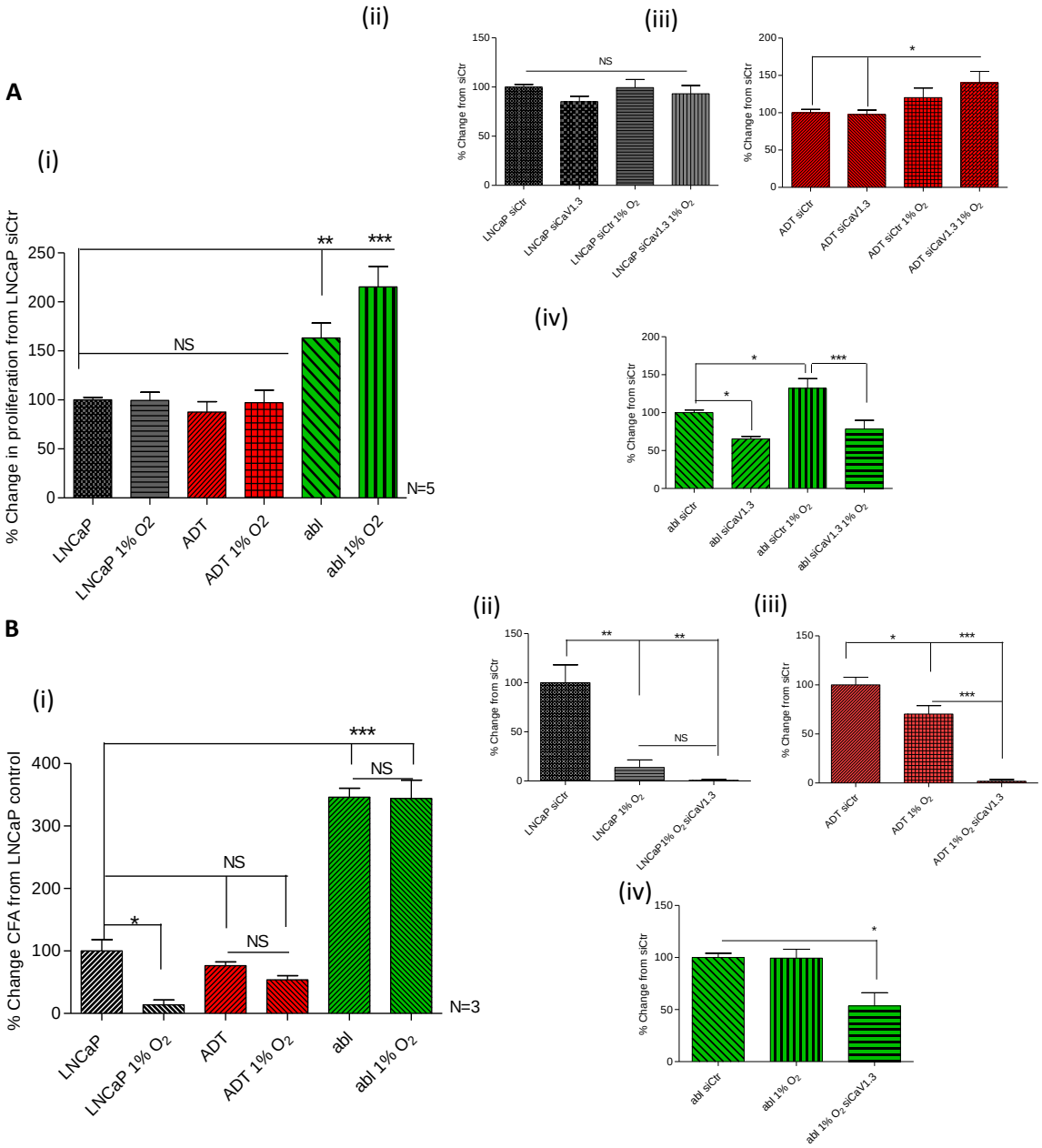

Figure 5.5: Proliferation and CFA is reduced in LNCaP-abl cells when CaV1.3 is silenced under hypoxic conditions: *(A) Proliferation assessed using WST-1 assay and (B) Colony forming assay, both normalised to control LNCaP. (i) compared to % change from LNCaP siCtr, (ii)(iii)(iv) compared to % change to siCtr of type. Comparing hypoxic conditioned (1% O2) and transfected with non-targeting control siRNA (siCtr) or siRNA targeting CaV1.3 (siCaV1.3). Analysis of androgen sensitive LNCaP cells (black), LNCaP-ADT cells treated with 10μM bicalutamide (7-10 days) (Red) and androgen insensitive long-term androgen deprived LNCaP-abl cells (Green). Analysed using One-way analysis of variance and Tukey's multiple comparison post hoc test between cell types and treatments. * P<0.05, ** P<0.01, ***P<0.001, NS not significant. * P<0.05, ** P<0.01, ***P<0.001, NS not significant.*

5.2.4 Effect of hypoxic conditions on PCa markers

There are some key processes which have been highlighted as potential mechanisms for PCa survival under ADT and progression to CRPC. Altered AR signalling (Coutinho et al., 2016), differentiation into a neuroendocrine phenotype (Patel et al., 2019) and the survival of the quiescent population of prostate cancer stem cells (Palapattu et al., 2009), which repopulate the tumour with a more resistant phenotype. All these processes have been linked to hypoxia (Danza et al., 2012; Lunardi et al., 2016; Marhold et al., 2015), so here we wanted to determine if under hypoxic conditions we could establish a link between these pathways of survival and expression of CaV1.3.

5.2.4.1 Calcium mobilisation through CaV1.3 enhances Androgen receptor expression under hypoxic conditions.

To determine if hypoxia had any influence on the AR expression, we analysed the expression changes seen in the cell model under normal and hypoxic conditions (Figure 5.6 (A)). Compared to the LNCaP cell line, the AR is upregulated in the LNCaP-ADT and the LNCaP-abl cells (1.768-fold +/- 0.47 sem, 1.751-fold +/- 0.37 sem respectively) under normal O_2 conditions, which replicates that observed previously (Figure 3.3). Under hypoxic conditions the expression is increased in the all the cell types which has significance in cells treated with ADT. The LNCaP-ADT cells incubated at 1% O_2 had 3.816-fold (+/- 0.25 sem) increased expression, while the expression observed in the LNCaP-abl cells was 4.225-fold (+/- 0.5 sem) increased under hypoxia.

We then looked to establish if CaV1.3 expression had any influence on the expression of AR in these cells. We observed an upregulated expression of AR in all cell lines under normal O_2 conditions when CaV1.3 was silenced. LNCaP cells have 1.6-fold (+/- 0.656 sem) (Figure 5.6 (B)), LNCaP-ADT cells have 1.776-fold (+/- 0.43 sem) (Figure 5.6 (C)), and the LNCaP-abl cells have 2.3-fold (+/- 0.6 sem) (Figure 5.6 (D)), although this did not reach significance in any cell type.

As already outlined all three cell lines indicated an increased expression of AR when cultured under hypoxic conditions. The LNCaP cells had a 2.5-fold (+/- 0.097 sem) increased expression under hypoxic conditions which was unchanged when CaV1.3 was silenced (2.5-fold +/- 0.2 sem) (Figure 5.6 (B)). LNCaP-ADT had a significant 1.99-fold (+/- 0.2 sem) increased expression of AR

under hypoxia compared to normal O_2 conditions (Figure 5.6 (C)). However, when CaV1.3 was silenced, the expression was 1.453-fold (+/- 0.3 sem), suggesting in these cells there is a reduced expression of AR when CaV1.3 is silenced. The LNCaP-abl cells again had a significant increased expression of AR under hypoxia (4.8-fold +/- 0.46 sem) compared to normal O_2 conditions. Interestingly these cells had a further significant increased expression under hypoxia when CaV1.3 was silenced which was 10.12-fold (+/- 1.7 sem) (Figure 5.6 (D)).

These results suggest that the expression of AR is associated with HIF-1α expression under hypoxic conditions in these cells. We have shown that HIF-1α expression under hypoxic conditions is reduced in LNCaP-ADT cells and increased in LNCaP-abl cells when CaV1.3 is silenced, which reflects the observations here with AR expression under hypoxia. More importantly the AR expression can also be associated with the SOCE observed in chapter 4, where silencing CaV1.3 reduced the SOCE in the LNCaP-ADT cells and increased the SOCE in the LNCaP-abl cells. Demonstrating that increased $[Ca^{2+}]_i$ is required for HIF-1α stabilisation under hypoxia and also enhances the expression of AR.

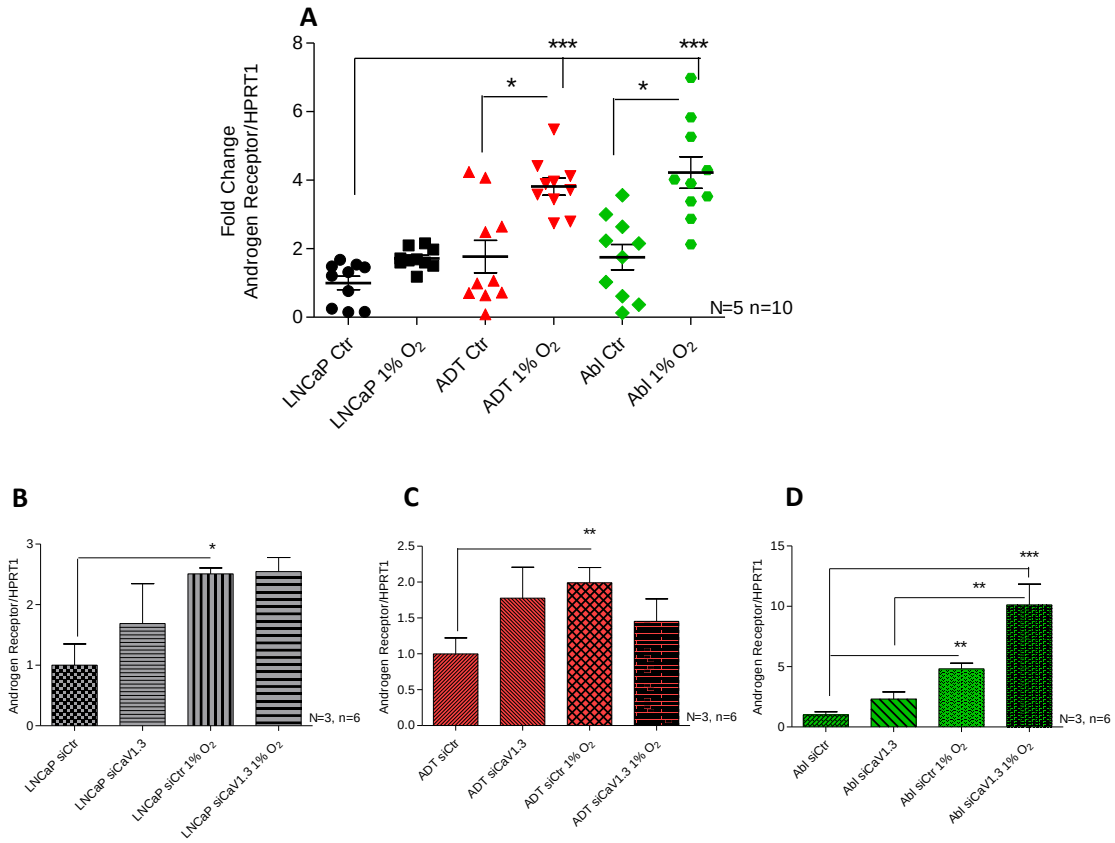

Figure 5.6: Expression of AR is increased under hypoxic conditions, driven by calcium mobilisation through CaV1.3: *Genetic expression of androgen receptor fold change was assessed using qPCR normalised to (A) control LNCaP or (B,C and D) siCtr cell of type. Analysis of androgen sensitive LNCaP cells (black), LNCaP-ADT cells treated with 10 µM bicalutamide (7-10 days) (red) and androgen insensitive long-term androgen deprived LNCaP-abl cells (green). (A) Tested under normal and hypoxic conditions (1% O_2) and (B,C,D) under similar conditions with non-targeting control siRNA (siCtr) or siRNA targeting CaV1.3 (siCaV1.3). Analysed using Kruskal-Wallis significance test and Dunn's multiple comparison post hoc test or a Mann-Whitney significance test between cell types and treatments * P<0.05, ** P<0.01, ***P<0.001, NS not significant.*

5.2.4.2 NED is increased under hypoxic conditions but is unaffected by CaV1.3 expression.

As previously discussed NSE represents a neuroendocrine phenotype, which is upregulated in the cell model under ADT (Figure 3.2) and is associated with treatment resistance and disease progression. Since this coincides with an increased expression of CaV1.3 and an enhanced HIF-1α response under hypoxia we wanted to look at the expression of NSE under hypoxic conditions to determine if CaV1.3 or HIF signalling was involved in the NED.

Similar to the results obtained for NSE expression in the cells after treatment with ADT under normoxia (Figure 3.2 (B)), these results have an increased expression of NSE in the LNCaP-ADT and the LNCaP-abl cells (2.178-fold +/- 0.3 sem and 1.825-fold +/- 0.16 sem respectively). Under hypoxic conditions a significant increase in the expression of NSE is observed (Figure 5.7 (A)), with the LNCaP having 6.5-fold (+/- 2.74 sem), LNCaP-ADT cells a 17-fold (+/- 4.78 sem) and LNCaP-abl cells a 9.5-fold (+/- 2.3 sem) increased expression compared to LNCaP control. Taken together this indicates that HIF signalling may have some influence on the NED of PCa cells.

Analysis of the expression of NSE in each individual cell line compared to control indicates that hypoxic conditions increase the expression of NSE in all cells with little effect observed when CaV1.3 is silenced. LNCaP cells have a 2.026-fold (+/- 0.08 sem) increased expression of NSE under hypoxic conditions which is unaltered when CaV1.3 is silenced (1.988-fold +/- 0.18 sem). LNCaP-ADT cells also have a 2.244-fold (+/- 0.2 sem) increase under hypoxic conditions which is slightly increased when CaV1.3 is silenced (2.687-fold +/- 0.4 sem), whereas the LNCaP-abl cells have 4.191-fold (+/- 0.6 sem) increased expression of NSE under hypoxic conditions which again has no difference when CaV1.3 is silenced (4.045-fold +/- 0.3 sem).

These results demonstrate that while ADT and hypoxia enhance the expression of NSE, the mechanism driving NED is not directly impacted through increased CaV1.3 expression and its associated increase in SOCE.

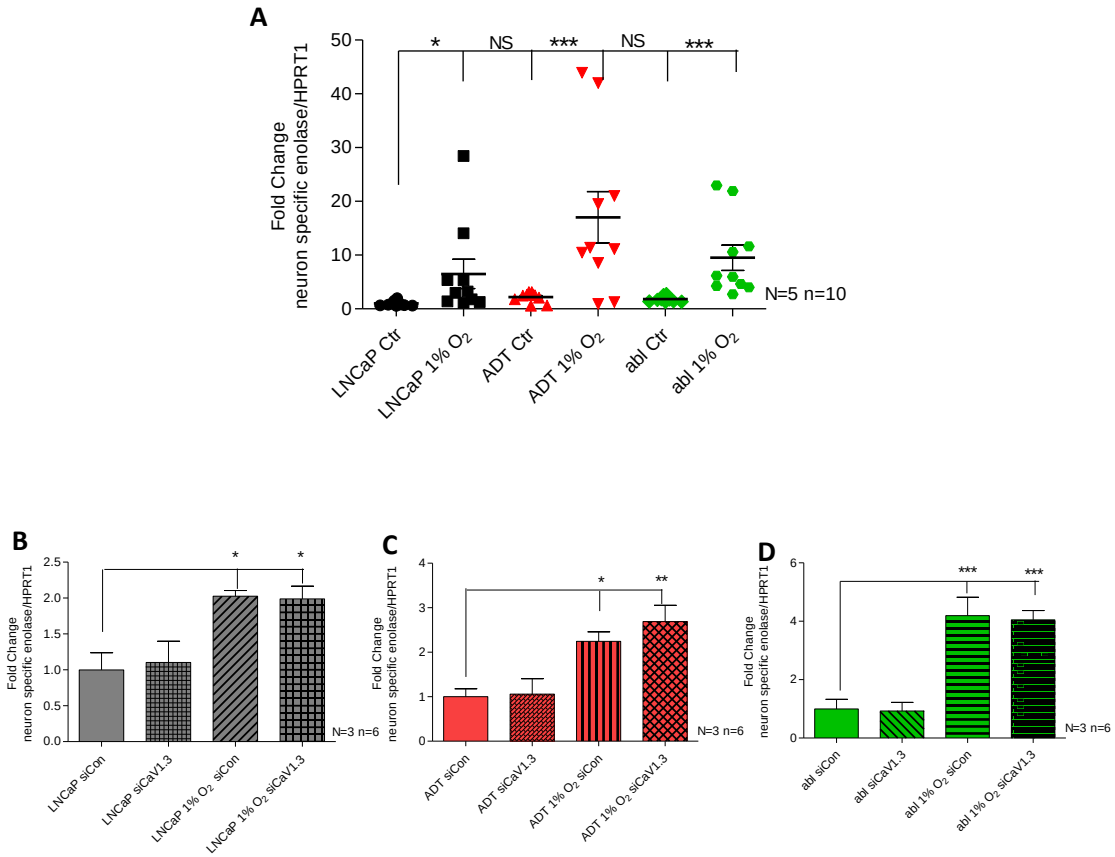

Figure 5.7: Cells under androgen deprivation therapy undergo neuroendocrine differentiation which is increased under hypoxic conditions but is not affected by CaV1.3 expression: *Genetic expression of neuron specific enolase was assessed using qPCR and normalised to LNCaP control. Analysis of androgen sensitive LNCaP cells (black), LNCaP-ADT cells treated with 10 µM bicalutamide (7-10 days) (red) and androgen insensitive long-term androgen deprived LNCaP-abl cells (green). (A) Tested under normal and hypoxic conditions (1% O_2) and (B,C,D) under similar conditions with non-targeting control siRNA (siCtr) or siRNA targeting CaV1.3 (siCaV1.3). Analysed using Kruskal-Wallis significance test and Dunn's multiple comparison post hoc test between cell types and treatments. * P<0.05, ** P<0.01, ***P<0.001, NS not significant.*

5.2.4.3 Hypoxic incubation does not enhance the stem cell population of PCa cells under ADT.

Hypoxia is a key signalling pathway in maintenance and proliferation of stem cells (Heddleston et al., 2010), including PCSC (Marhold et al., 2015). Since there is research pointing to PCSC in the evasion of ADT and subsequent progression to CRPC (Tang et al., 2009), we sought to investigate the potential association between increased CaV1.3 after ADT and the emergence of a stem cell population under hypoxic conditions. Since we had previously found the expression of stem cells in the cell model difficult to detect due to small numbers, we initially incubated the cells under hypoxic conditions to determine if there was a stem cell enrichment under hypoxia.

Here we found that the stem cell surface markers, CD44 and CD133 (Figure 5.8 (A)(B)), had no significant change detected between any of the cell lines and no enriched expression under hypoxic conditions. However, the overall trend suggests that there is a reduced expression of all the stem cell markers in the LNCaP-abl cells.

We also examined the expression of Nanog and OCT4 (Figure 5.8 (C)(D)), transcription factors which maintain pluripotency. There was no significant effect on the pluripotency markers between cell types or O_2 concentrations, although the LNCaP and the LNCaP-ADT cells had an increased trend under hypoxia. Expression of OCT4 had 1.3-fold increase in the LNCaP and the LNCaP-ADT cells under hypoxia, whereas the expression in LNCaP-abl cells had a reduced expression overall. Nanog had some increased expression under hypoxia conditions in the LNCaP and the LNCaP-ADT cells, the LNCaP had 1.406-fold (+/- 0.22 sem) increased expression under hypoxia, while the LNCaP-ADT cells had 1.512-fold (+/- 0.23 sem) increased expression under hypoxia. The LNCaP-abl cells had no altered expression of Nanog under normal O_2 or under hypoxia.

We then sought to determine if silencing CaV1.3 would have any influence on the expression of the stem cell surface markers, however, all cells transfected with non-targeting siRNA or siRNA against CaV1.3 had undetectable values (data not shown).

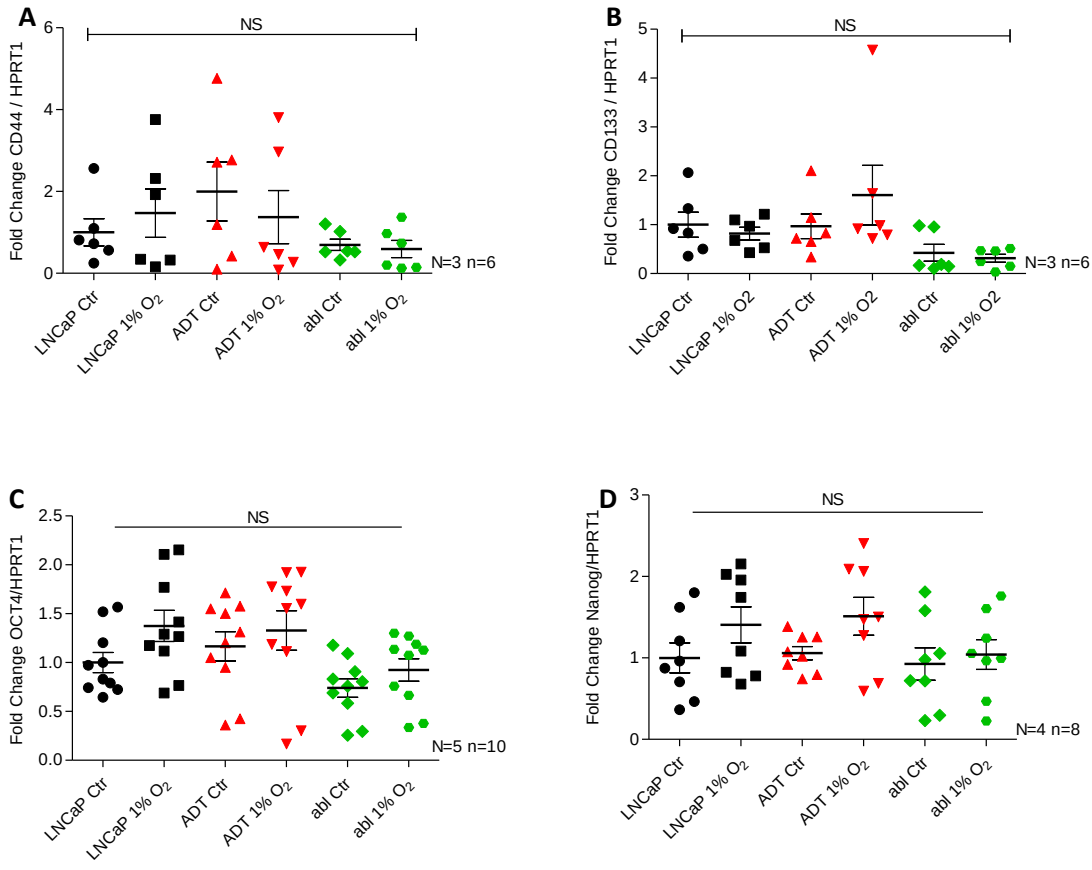

Figure 5.8: Hypoxic conditions have no significant increased expression of stem cell surface markers or pluripotency markers: *Fold change of the genetic expression of (A) CD44, (B) CD133, (C) Oct4 and (D) Nanog was assessed using qPCR normalised to control LNCaP. Analysis of androgen sensitive LNCaP cells (black), LNCaP-ADT cells treated with 10 µM bicalutamide (7-10 days) (red) and androgen insensitive long-term androgen deprived LNCaP-abl cells (green), under normal conditions (Ctr) and hypoxic conditions (1% O_2). Analysed using Kruskal-Wallis significance test and Dunn's multiple comparison post hoc test between cell types and treatments. * P<0.05, ** P<0.01, ***P<0.001, NS not significant.*

5.3 Chapter discussion

Hypoxia is associated with malignant progression in many cancers (Vaupel, 2004), with strong evidence linking it to treatment resistance and an aggressive phenotype in PCa (Alqawi et al., 2007; Fraga et al., 2015; Hompland et al., 2018). It has been highlighted that treatment with ADT has an immediate effect in reducing the O_2 levels in LNCaP PCa tumours (Byrne et al., 2016; Ming et al., 2013), while we have demonstrated that ADT is associated with increased expression of CaV1.3. Current research has also shown that Ca^{2+} is required to support HIF-1α signalling. Considering we have demonstrated enhanced SOCE promoted by CaV1.3 under ADT we aimed to investigate if this could be driving HIF signalling and thus promoting treatment resistance and disease progression. Here in we found that the expression of HIF-1α under hypoxic conditions reflected the trends seen in the SOCE, suggesting that the CaV1.3 regulated SOCE we have demonstrated is driving HIF-1α expression.

5.3.1 Associated expression of CaV1.3 and HIF-1α

5.3.1.1 HIF-1α expression under ADT and hypoxia

Research has demonstrated that hypoxia increases the expression of CaV1.2 and CaV1.3 in PC12 cells (R. Li et al., 2015), this increased expression was attenuated by addition of echinomycin a HIF-1α inhibitor. Therefore, we initially sought to examine the expression of CaV1.3 under hypoxic conditions. There was a similar expression profile detected as seen in previous chapters under normoxia, however, there was no significant difference seen in any of the cell lines after hypoxic incubation for 24 hours at 1% O_2. Suggesting that in LNCaP cells, hypoxia does not enhance the expression of CaV1.3 at any stage under ADT with bicalutamide. Although in the outlined study the PC12 cells were incubated at 3% O_2 so perhaps it may be beneficial in future experiments to alter the O_2 levels to see if this has any effect on CaV1.3 expression.

A number of Ca^{2+} channels are implicated in the regulation of HIF proteins (Azimi, 2018) and research has shown that Ca^{2+} influx is required to stabilise HIF-1α (Hui et al., 2006). Therefore, we hypothesised that the increased expression of CaV1.3 in PCa after ADT and the associated enhanced SOCE could potentially drive HIF signalling in these cells. Accordingly, we wanted to determine if this mechanism was involved in stabilising HIF-1α for the purpose of enhanced signalling under AR inhibition.

We initially looked at the expression of HIF-1α across our cell lines, to determine if there was any differential expression. Interestingly under normal O_2 conditions LNCaP-ADT displayed significantly enhanced HIF-1α expression. Previous research has also seen increased expression of HIF-1α with normal O_2 conditions in PCa under ADT (Thomas and Kim, 2008). While this has been attributed to reduced vasculature in tissue samples (Halin et al., 2007; Shabsigh et al., 2001, 1998), similar results seen in cell culture models demonstrate that other mechanisms are also influencing HIF-1α stabilisation (Sánchez et al., 2020; Thomas and Kim, 2008). There are many reasons we might observe an enhanced HIF-1α expression in these cells under normal O_2 conditions. Research has shown that the expression and stability of HIF-1α is influenced by a host of proteins, which may not require O_2 regulation, particularly in an oncogenic setting. Activation of pathways by various growth factors, such as the PI3K pathway, can enhance the translation of HIF-α. The PI3K pathway phosphorylates protein kinase B (AKT) resulting in the downstream activation of mammalian target of rapamysin m(TOR). mTOR in turn phosphorylates eukaryotic translation initiation factor 4E (elf4E) and its binding protein (4E-BP1). This prevents their inhibition of cap dependent mRNA translation and results in an enhanced translation of HIF-1α. A similar process occurs with the activation of the kinase cascade RAS/RAF/MEK/ERK whereby ERK phosphorylates 4E-BP1 enhancing transcription (Masoud and Li, 2015). However, the enhanced expression of CaV1.3 and the subsequent increased SOCE in the LNCaP-ADT cells may also be contributing to this phenomenon. While there are no studies which directly link ADT induced HIF-1α to enhanced Ca^{2+} entry, many studies have demonstrated a dependence on Ca^{2+} for translation, stabilisation and activation of the HIF1α protein (Azimi, 2018; Hui et al., 2006; Mottet Denis et al., 2006). In fact, a study by Yu *et al.* demonstrates an O_2 independent enhanced stabilisation of HIF-1α in LNCaP cells (Yu et al., 2014, p. 8) . Here they show that enhanced $[Ca^{2+}]_i$ results in inhibition of receptor for activated C-kinase 1 (RACK1) mediated HIF-1α ubiquination which prevents the O_2 dependant degradation of the protein. Nontheless, since we demonstrated silencing CaV1.3 had no significant reduced expression of HIF-1α in the LNCaP-ADT cells incubated under normal O_2 conditions, further work is required to clarify the mechanism of HIF-1α stabilisation under normal O_2 conditions post ADT.

When the cells were incubated under hypoxic conditions (1% O_2) the expression of HIF-1α was increased in all cell types. This would be the usual response to hypoxic conditions, with low O_2 levels preventing hydroxylation and subsequent proteolysis (Semenza, 2001). This increase was significant in the LNCaP and the LNCaP-abl cells. HIF-1α expression was also increased under hypoxia in the LNCaP-ADT cells, although this did not have significance when compared to LNCaP-ADT cells grown under normal O_2 conditions. This is most likely due to the elevated expression

seen in the LNCaP-ADT cells under normal O_2, as it is evident that overall the expression of HIF-1α was highest in the LNCaP-ADT cells both under hypoxia and normal O_2 levels.

5.3.1.2 HIF-1α expression under nifedipine incubation

As outlined previously, using nifedipine, Hui *et al*. reduced the expression of HIF-1α protein in PC12 cells (Hui et al., 2006). This demonstrates that HIF-1α stabilisation is dependent on the Ca^{2+} influx via VGCC in these cells. This association between Ca^{2+} signalling and HIF-1α is now well accecpted and has been demonstrated in many cancer studies (Azimi, 2018). We have shown that the upregulation of CaV1.3 in the LNCaP cells influences the SOCE rather than the canonical voltage dependent mechanism. We have also shown that incubation with nifedipine had no effect on SOCE in this cell model. However, we wanted to determine if nifedipine had an influence on the HIF-1α expression in these cells. As we did not observe any effect on the CaV1.3 regulated SOCE when we incubated the cells with nifedipine this would inform us if the increased $[Ca^{2+}]_i$ observed as a result of enhanced SOCE was influencing HIF-1α stabilisation or if it were under the influence of other VGCC. Contrary to the findings by Hui *et al*, we found that the expression of HIF-1α was unaffected after incubation with nifedipine. Hypoxic conditions still induced a significant increased expression of HIF-1α in all the cell lines despite the addition of nifedipine. This demonstrates that HIF-1α expression in PCa is not solely reliant on Ca^{2+} influx via VGCC, however we wanted to determine if the increased SOCE observed in LNCaP-ADT and LNCaP-abl cells had an effect on the hypoxic response.

5.3.1.3 HIF-1α expression associated with CaV1.3 expression

As we have previously shown silencing CaV1.3 significantly reduces the SOCE in the LNCaP-ADT cells and significantly increases the SOCE in the LNCaP-abl cells. Therefore, we silenced the expression of CaV1.3 and measured the expression of HIF-1α to determine if the altered SOCE had a role in stabilising HIF-1α. Here we found that the expression of HIF-1α was significantly reduced in the LNCaP-ADT cells under hypoxia when CaV1.3 was silenced, while expression of HIF-1α was significantly increased in the LNCaP-abl cells when CaV1.3 was silenced, reflecting the SOCE levels observed in these cells under the same conditions. This indicates that under hypoxic conditions

HIF-1α stabilisation is controlled by the SOCE in PCa cells which is regulated by the expression of CaV1.3. Previous studies have also shown that HIF-1α stability was reliant on intracellular Ca^{2+} (Hui et al., 2006), with one study implicating SOCE specifically (Y. Li et al., 2015). This research looking at liver cancer shows a regulatory circuit between STIM1 and HIF-1α under hypoxia. The hypoxic driven upregulation of HIF-1α enhances the transcription of STIM1 by binding to HRE upstream of the STIM1 promoter region. This increased the SOCE in the cells which in turn stabilised the expression of HIF-1α. They clearly illustrated that stable expression of HIF-1α required SOCE using the SOCE inhibitor 2-APB. Here we have demonstrated a similar SOCE reliant stabilisation of HIF-1α in PCa cells under hypoxic conditions.

Our research has also shown that inhibiting CaV1.3 had a significant effect on the expression of HIF-1α in the LNCaP cells. Since we have not detected any alteration on the SOCE in the LNCaP cells, this suggests that there may be another mechanism through which CaV1.3 is regulating the expression of HIF-1α. Interestingly the LNCaP and the LNCaP-ADT cell lines had the nuclear expression of the 70kDa band of CaV1.3 detected in the fractionation experiments (Figure 3.8). Indicating that there is a potential role for CaV1.3 c-terminus in the nucleus as a transcriptional enhancer of HIF-1α in the androgen sensitive LNCaP and LNCaP-ADT cells under hypoxia. However, since research has shown that HIF-1α mRNA levels are unchanged after ADT or androgen stimulation (Mabjeesh et al., 2003) , this suggests that the inhibition occurs at the stage of HIF-1α biosynthesis. Therefore, the potential effect on transcriptional regulation by the c-terminus of CaV1.3 could be through downregulating elements required for translation of HIF-1α under hypoxic conditions.

What was striking about these results was that despite LNCaP-ADT cells having the same increase in HIF-1α levels under normal O_2 conditions, as seen previously, silencing CaV1.3 had no effect on the expression of HIF-1α in normal O_2 conditions. In fact, silencing CaV1.3 had no effect on the base levels of HIF-1α expressed under normal O_2 levels in any of the cell lines (Appendix C, Figure C1). This suggests that CaV1.3 plays a role in the expression of HIF-1α under hypoxic conditions in the LNCaP-ADT cells but does not influence the enhanced expression under normal O_2 conditions. However in relation to this project, there is definitive clinical evidence supporting the idea that a hypoxic microenvironment is prevalent in a range of solid tumours (Vaupel and Mayer, 2007) including prostate (Stewart et al., 2010).

So here we have found a link between CaV1.3 associated SOCE and HIF-1α expression. The expression of HIF-1α under hypoxic conditions was reduced in the LNCaP-ADT cells when CaV1.3 was silenced but increased in the LNCaP-abl cells under the same conditions. This reflects the SOCE

observed in chapter 4 and since research has shown that HIF-1α requires Ca^{2+} mobilisation for stabilisation this demonstrates a link to CaV1.3 regulated SOCE and HIF-1α expression. Given that HIF signalling has been implicated in many functional aspects of cancer progression, we decided to investigate the impact that silencing CaV1.3 had on the functionality of the cells and the expression of PCa markers under hypoxia.

5.3.2 Functional effects under hypoxia

5.3.2.1 Proliferation under hypoxia

Research into the effects of hypoxia on cancer has identified some important functional aspects which contribute to malignant progression, such as angiogenesis, proliferation, differentiation, migration and metabolism (Wigerup et al., 2016). Hypoxia has been implicated in the proliferative enhancement of androgen independent cell lines (Tang et al., 2015), which was also associated with an increased survival, with recent research demonstrating that HIF-1α signalling is capable of restoring tumour growth under continued androgen deprivation (Tran et al., 2020). Here we looked at both proliferation and viability to determine if increased expression of CaV1.3 after ADT had an influence on the hypoxic driven cellular functions.

Under normal O_2 conditions the proliferation of the cells reflected our previous findings with a reduced proliferation in the LNCaP-ADT cells and a significant increased proliferation in the LNCaP-abl cells. Hypoxic conditions had no effect on the proliferation of the androgen sensitive cell lines, however the LNCaP-abl cells had significantly increased proliferation under hypoxia. However, we can assume that this is not due solely to HIF-1α expression since the level of HIF-1α was most prevalent in the LNCaP-ADT cells.

There was no effect observed on LNCaP proliferation under hypoxic conditions, silencing CaV1.3 had no effect on these cells either. This suggests that in these cells HIF-1α does not influence proliferation. Since we have shown that silencing CaV1.3 significantly reduces the expression of HIF-1α under hypoxic conditions. There is research which suggests that chronic hypoxia (1% O_2 for 6-months) is required to elicit increased proliferation and migration on LNCaP cells, as this was not observed in LNCaP cells treated with acute hypoxia (Yamasaki et al., 2013). As a consequence, this may explain our observation of no impact of hypoxia on proliferation.

LNCaP-ADT cells under hypoxic conditions show some increased proliferation although this does not achieve significance. However, when CaV1.3 is silenced in these cells under hypoxic conditions there is a significant increase in the proliferation. Suggesting that under hypoxic conditions these cells have some enhanced proliferative ability. What we have previously observed is that HIF-1α is significantly inhibited in these cells when CaV1.3 is silenced, which also reduces the Ca^{2+} influx. Suggesting that in the LNCaP-ADT cells neither Ca^{2+} signalling or HIF-1α expression enhance the proliferative ability of these cells since inhibiting expression of CaV1.3, which subsequently inhibits expression of HIF-1α under hypoxia results in an increased proliferation. However as highlighted by Thomas et al, the increased HIF-1α expression observed had a role in cell survival under serum deprivation stress, by increasing expression of growth factors such as IGF-2 rather than influencing proliferation (Thomas and Kim, 2008).

Examination of the LNCaP-abl cells demonstrated that hypoxic conditions increase the proliferation of these cells, which is consistent with research highlighting the role of HIF-1α in the proliferation of androgen independent cells indicating that targeting both HIF and AR may be a beneficial therapeutic strategy (Tang et al., 2015; Tran et al., 2020). However, we find that silencing CaV1.3 in these cells has a similar reduced proliferation in both the normal and hypoxic conditioned cells. As we have indicated silencing CaV1.3 in the LNCaP-abl cells does not inhibit the expression of HIF-1α under hypoxic conditions (Figure 5.4 (D)). Therefore, the reduced proliferation in the LNCaP-abl cells is not due to a loss of HIF-1α signalling. As previously discussed in chapter 4, the significant reduced proliferation with CaV1.3 inhibition could be due to Ca^{2+} induced apoptosis. High amplitude sustained cystolic Ca^{2+} levels induces apoptosis (N. Prevarskaya et al., 2007). We have shown that there is a large increased SOCE in LNCaP-abl cells when CaV1.3 was silenced (Figure 4.7), which would justify the findings here of a similar reduced proliferation detected in these cells under both normal and hypoxic conditions, indicating that this reduced proliferation was due to the inhibition of CaV1.3, increased sustained $[Ca^{2+}]_i$ and subsequent apoptosis. Highlighting the benefit of targeting Ca^{2+} signalling in these cells adding to the idea of combined therapeutic targets to achieve a beneficial inhibition of CRPC.

5.3.2.2 Viability under hypoxia

There are many studies highlighting the enhanced viability of PCa cells under hypoxic conditions (DAI et al., 2011; Khandrika et al., 2009). The CFA is significantly increased in the androgen

independent LNCaP-abl cells as was previously observed (Figure 3.5). However, there was no change observed in the LNCaP-abl under hypoxia, which remained significantly increased compared to LNCaP cells. Only the LNCaP cells have a significant reduced viability under hypoxic conditions.

Inhibiting CaV1.3 reduces cell viability at all stages in the progression to CRPC under hypoxic conditions. While the LNCaP cells were significantly reduced under hypoxic conditions inhibiting CaV1.3 further reduced the CFA. The LNCaP-ADT cells had a significant reduced CFA under hypoxia after silencing CaV1.3. It appears that the cells which have been treated with ADT (LNCAP-ADT) have a sustained ability to form colonies under hypoxic conditions which is inhibited when CaV1.3 is silenced. This supports the idea that HIF-1α expression in the LNCaP-ADT cells may be influencing the survival of these cells under ADT (Thomas and Kim, 2008). Since we have shown that CaV1.3 expression is required for the SOCE driven HIF-1α stabilisation in these cells under hypoxia, this highlights another mechanism through which CaV1.3 inhibition may be beneficial in preventing progression to CRPC.

5.3.3 CaV1.3 regulated PCa markers under hypoxia.

5.3.3.1 Androgen receptor expression under hypoxia

HIF-1α has been indicated as a key factor in assisting AR activity in the presence of low levels of androgens (Mitani et al., 2011) and there are many studies which highlight the crosstalk between the AR and HIF-1α (Mabjeesh et al., 2003; Mitani et al., 2011; Park et al., 2006). As we reported in chapter 3 (Figure 3.2) the AR is significantly upregulated in the LNCaP-ADT and the LNCaP-abl cells, which also had the increased expression of CaV1.3 (Figure 3.7). Here we wanted to determine if hypoxic conditions or inhibition of CaV1.3 altered the expression of the AR in the bicalutamide treated cells.

When we examined AR expression under normal O_2 conditions, we found that there was a significant increased expression in the LNCaP-ADT and the LNCaP-abl cells, which reflected our previous findings (Figure 3.2 (A)). Hypoxic conditions had a compounding effect with the level of AR increased in all cells, with a significant increase observed in the LNCaP-ADT and the LNCaP-abl cells. Suggesting that hypoxia and HIF signalling not only increases the AR activity as outlined in many studies (Mitani et al., 2011; Park et al., 2006), but it actually enhances the expression of AR in PCa cells treated with ADT. The study by Park *et al*., reported no change in the expression of AR

protein levels, however their analysis was carried out in LNCaP cells which had been incubated in 1% O_2 for up to 16 hours, followed by at least 2 hours reoxygenation in normal O_2 conditions (Park et al., 2006). Our data shows that hypoxia at least enhances the transcription of AR, further research would be required to determine if this translates to an enhanced protein expression.

Research has suggested that duel targeting of HIF-1α and AR may be an effective treatment strategy to prevent the progression to CRPC (Fernandez et al., 2015). However here we detect a correlation in the expression of AR and HIF-1α under hypoxia and the CaV1.3 controlled SOCE. When we silenced CaV1.3 under hypoxic conditions the expression of AR was unaffected in the LNCaP cells, reduced in the LNCaP-ADT cells and significantly increased in the LNCaP-abl cells. This directly correlates to the reduced SOCE detected in the LNCaP-ADT cells when CaV1.3 was knocked down and also the increased SOCE detected in the LNCaP-abl cells when CaV1.3 was knocked down. As we have discovered expression of HIF-1α under hypoxic conditions is significantly reduced in LNCaP and LNCaP-ADT cells and unaffected in LNCaP-abl cells when CaV1.3 is silenced. Indicating that increased $[Ca^{2+}]_i$ via the CaV1.3 regulated SOCE mechanism is stabilising HIF-1α and enhancing AR expression, potentially facilitating survival under androgen deprivation. Highlighting another molecular target which could be utilised in preventing disease progression under ADT.

5.3.3.2 NSE expression under hypoxia

As we previously demonstrated, NSE is significantly increased in the cell line after ADT (Figure 3.2 (B)) and NED is identified as a key characteristic in the progression of PCa under hypoxia (Danza et al., 2012; Lin et al., 2016; Sánchez et al., 2020). Therefore, we analysed the expression of NSE under hypoxic conditions in each cell line with and without CaV1.3 knockdown to determine if CaV1.3 was influencing NED under hypoxia. Expression of NSE was significantly increased under hypoxic conditions in all cell types, indicating a definite link with hypoxia. As we have highlighted previously NED has been associated with ADT in PCa (Patel et al., 2019; Yuan et al., 2006), however it has also been demonstrated in LNCaP cells under hypoxia (Ye et al., 2019). This process appears to be independent of upregulation of CaV1.3 as when we knockdown CaV1.3 there is no alteration to the expression of NSE (Figure 5.7 (B)(C)(D)). This suggests that the progression to neuroendocrine phenotype under ADT and under hypoxia conditions has no association with the increased expression of CaV1.3 or the associated SOCE. These results also demonstrate that the

enhanced expression of NSE under hypoxia is not reliant on HIF-1α expression, since we know that silencing CaV1.3 significantly reduces the HIF-1α expression under hypoxia in the LNCaP and the LNCaP-ADT cells.

5.3.3.3 Stem cell expression under hypoxia

Hypoxia and HIF signalling have been implicated in the emergence of a stem cell population in cancer through the dedifferentiation of mature cells back to stem like cells (Axelson et al., 2005; Bae et al., 2016; Kim et al., 2009). This was also demonstrated in PCa (Sánchez et al., 2020), where PCa cell lines had upregulated expression of Nanog, Oct4 and CD133 under ADT induced hypoxia. Therefore, we sought to look for expression of stem cell surface markers and pluripotency pathways which would indicate that hypoxia was influencing the expression of stem cell expansion to evade ADT. We hypothesised that since Ca^{2+} signalling is also indicated in the enrichment of stem cell populations, as we have reviewed previously (O'Reilly and Buchanan, 2019), there may be an association between ADT, increased CaV1.3 expression and stem cell enrichment. When we looked at the expression of the stem cell surface markers CD44 and CD133, we detected no significant increased expression under hypoxia (Figure 5.8 (A)(B)). These results are consistent with the results presented in chapter 3, where we were unable to detect differences between cell lines (Figure 3.4 (A)(i)(ii)). However, since there was an enriched population of stem cells present in the mouse model after treatment with bicalutamide (Figure 3.4 (B)(i)(ii)), we thought that this may be due to the hypoxic microenvironment in the mouse model. It appears that the population of stem cells present in the cell line grown in 2D cell culture is below the levels to detect significant expression, as reflected by the low Ct values (Appendix C, Figure C.3). Although when we look at the level of CD44 and CD133 expressed in the LNCaP-ADT cells, there does appear to be an increased trend, which would be consistent with what we found in the bicalutamide treated mice. We also looked at the expression of the pluripotency signalling molecules OCT4 and Nanog (Figure 5.8 (C)(D)). Again, we were unable to detect any significance, although, there appeared to be an increased trend in the androgen sensitive LNCaP and LNCaP-ADT cells under hypoxia, with a reduced expression in the LNCaP-abl cells. This would be consistent with research which highlights HIF-1α regulation of pluripotency (Forristal et al., 2010; Tong et al., 2018). Future studies may benefit from a longer exposure to hypoxic conditions to elicit a stronger expression. Our studies were performed after culturing the cells for 24 hours at 1% O_2, which reflects other studies looking for HIF-1α expression in LNCaP cells (Tsui et al., 2013). However, many studies looking at the

expression of stem cell markers under hypoxic conditions have various O_2 tensions and incubation times, implicating chronic hypoxia and the expression of HIF-2α in the emergence of a stem cell population (Bae et al., 2016). It may also be beneficial in future research to utilise 3D cell culture methods to further elucidate the role of stem cell treatment evasion in relation to PCa. There may be some association with CaV1.3 upregulation in this mechanism, which we are unable to establish in our 2D cell culture model. Since there is a clear increased expression detected after ADT in the mouse model which coincided with increased expression of CaV1.3 this is an area which warrants some further investigation in the future.

5.4 Concluding remarks.

Here we have shown that the expression of HIF-1α is significantly increased in LNCaP-ADT cells, which reflects research outlining an enhanced HIF-1α protein synthesis under conditions of serum deprivation under normal O_2 conditions (Thomas and Kim, 2008). Although we have not identified the mechanism through which HIF-1α is stabilised under normal O_2 conditions we have demonstrated that this mechanism is not Ca^{2+} reliant. We have shown that inhibiting Ca^{2+} influx with the VGCC blocker nifedipine or reducing the SOCE by silencing CaV1.3 had no effect on the expression of HIF-1α in the LNCaP-ADT cells under normal O_2 conditions.

However, under hypoxic conditions we have demonstrated that the expression of HIF-1α is regulated by the increased SOCE observed in the cells treated with ADT. We have shownthat silencing the expression of the VGCC CaV1.3 significantly decreased the expression of HIF-1α in the androgen sensitive cell lines but increased in the CRPC cell model. This follows the SOCE levels we have shown in this cell model, indicating that HIF-1α expression is stabilised under conditions of high Ca^{2+} which we have demonstrated to be regulated by CaV1.3. Hence, a combination therapy targeting CaV1.3 in conjunction with HIF-1α could enhance patient outcomes.

We have demonstrated a similar regulation in the expression of AR under hypoxic conditions. Silencing the expression of CaV1.3 had no effect on the level of AR detected in the LNCaP cells, reduced the expression in the LNCaP-ADT cells and increased the expression in the LNCaP-abl cells. This also replicates the SOCE levels outlined in chapter 4 and suggests a potential mechanism through which upregulation of CaV1.3 under ADT may be influencing the progression to CRPC by enhancing the expression of AR. Highlighting that CaV1.3 driven SOCE in PCa promotes expression of AR, which is associated with treatment resistance and disease progression. Therefore, developing treatments which target CaV1.3 and the associated SOCE could prolong progression free survival.

Overall, this chapter has highlighted a novel mechanism through which upregulated CaV1.3 expression under ADT is stabilising HIF-1α expression in the LNCaP-ADT cells and enhancing the expression of AR. Indicating a mechanism through which CaV1.3 may be assisting cell survival under ADT and the subsequent progression to CRPC.

Chapter 6 - Investigation of the non-canonical role of CaV1.3 in Calcium mobilisation throughout PCa disease progression.

6.1 Introduction

6.1.1 Background

Our research thus far has indicated that the increased expression of CaV1.3 is facilitating increased SOCE. However, it is not clear how this may be occurring as induced membrane depolarisation failed to activate the channel through its normal voltage gated mechanism (Figure 4.1). This suggests that the channel is working through a non-canonical mechanism either interacting with other channels and indirectly controlling Ca^{2+} entry or potentially regulating gene transcription of other channels through its c-terminus. As outlined here in, previously published research supports the notion that CaV1.3 has various non-canonical mechanisms in other tissues, working as a transcriptional regulator (Lu et al., 2015) or through interactions with other ion channels (Fourbon et al., 2017; Kim et al., 2007). Hence, we hypothesised that it may be assisting PCa progression through similar mechanisms by regulating transcription of Ca^{2+} associated proteins or through direct functional interactions with other Ca^{2+} transporting channels. We have also demonstrated that silencing the expression of CaV1.3 has opposing effects on the increased SOCE seen in the LNCaP-ADT and the LNCaP-abl cells. This suggests that there may be alternative mechanisms regulated by the increased expression of CaV1.3 as the disease progresses to CRPC.

We sought to establish the expression levels of some of the key genes associated with SOCE, such as STIM1, Orai1 and RyR. Research has shown that SOCE is dyregulated in PCa with the expression of STIM and Orai proteins differentially regulated depending on disease stage (Kappel et al., 2017; Perrouin Verbe et al., 2016). The upregulation of these channels have been implicated in cancer progression and the development of cancer hallmarks across many cancer types (Fiorio Pla et al., 2016; Jardin and Rosado, 2016). Research into the functional activity of CaV1.3 in the central nervous system highlighted a physical and functional role of CaV1.3 with the ER bound Ca^{2+} release channel RyR (Kim et al., 2007; Ouardouz et al., 2003). The research reported a colocalisation between the c-terminus of CaV1.3 and the c-terminus of RyR. This could indicate a protein interaction through which CaV1.3 could induce altered SOCE in PCa.

CaV1.3 has been identified as having functional interaction with NCX, a bidirectional ion channel which help control intracellular calcium concentration and cellular polarisation (Jeffs et al., 2007). In particular, research in colon cancer cells has identified CaV1.3 in the regulation of basal Ca^{2+} levels through the colocalization with NCX channels. Whereby CaV1.3 inhibits the action of NCX resulting in an elevated basal Ca^{2+} level in turn influencing migration (Fourbon et al., 2017), a similar mechanism may be influencing Ca^{2+} fluctuations in PCa.

In relation to controlling SOCE through transcription, CaV1.2 and CaV1.3 have been shown to have a c-terminal fraction found in the nucleus which can influence gene transcription in a range of cells (Gomez-Ospina et al., 2006) (Lu et al., 2015). One such study identified a direct regulation between the cleaved c-terminus of CaV1.3 and the transcriptional regulation of the potassium channel SK2 along with the membrane localisation of the channel (Lu et al., 2015). Our research has found the nuclear expression of the c-terminal fragment of CaV1.3 in the LNCaP and the LNCaP-ADT cells (Figure 3.8) indicating a potential for CaV1.3 to work as a transcriptional regulator in the androgen sensitive PCa cell lines.

Futhermore, changes in intracellular Ca^{2+}, such as that through SOCE, have been shown to influence the expression of genes required for malignant progression (Barbado et al., 2009). Thus we wanted to determine the downstream cascade effect as a result of the altered SOCE we have observed in PCa cells treated with ADT. Two key transcription factors activated via this mechanism include nuclear factor of activated T-cells (NFAT) and cAMP response element binding protein (CREB). CaN is a protein phosphatase which is triggered by increased intracellular Ca^{2+} and phosphorylates NFAT and research has shown that it is upregulated in PCa compared to normal prostate epithelia which enhances cell viability and migration (Kawahara et al., 2015; Manda et al., 2016). CREB has also been linked to PCa with research highlighting a role in NED and proliferation (Garcia et al., 2006; Xiao et al., 2010). Calmodulin, CAM, is another calcium activated protein, which can not only activate CREB downstream but also kinase cascades such as CaMK's (Hoeflich and Ikura, 2002). Specifically research has identified CAMKII with promoting cell survival in PCa through promoting androgen independence and increased levels of CAMKIIβ and CAMKIIγ (Rokhlin et al., 2007). Taken together with our previous results highlighting increased Ca^{2+} in LNCaP-ADT and LNCaP-abl cells, there is the potential that this could be driving activation of these downstream signalling pathways which in turn could help promote neoplastic transformation in PCa progression.

6.1.2 Aims of chapter 6

CaV1.3 is working through a non-canonical manner in influencing upregulated intracellular calcium as observed in chapter 4. To investigate the non-canonical mechanisms through which CaV1.3 upregulation under ADT was increasing the SOCE response, we sought to identify any associated enhanced expression in other calcium regulating ion channels that could be involved. In addition, we wished to explore if CaV1.3 could have a direct influence on the expression of these channels. Lastly, we sought to investigate the influence of CaV1.3 on associated downstream signalling pathways. Taken together this could provide insight into signalling pathways through which CaV1.3 could be controlling malignant progression.

Aim: Investigate the expression of other Ca^{2+} regulating proteins which may be involved in the CaV1.3 driven SOCE and the downstream signalling pathways, influencing PCa survival.

Hypothesis: CaV1.3 is regulating downstream signalling pathways through interaction with other SOCE channels, which is facilitating PCa progression.

1. Highlight any associated ion channels which may be assisting in the enhanced intracellular calcium promoted through CaV1.3 under ADT.
2. Determine if CaV1.3 influences the genetic expression of Ca^{2+} channels associated with SOCE.
3. Investigate expression of genes involved in the Ca^{2+} signalling pathways in association with CaV1.3 expression.

6.2 Results

6.2.1 Investigating the interaction between CaV1.3 and other calcium channels as a mechanism for regulating SOCE

6.2.1.1 SOCE channel, STIM1, is upregulated after ADT.

As we have seen in chapter 4, upregulated expression of CaV1.3 coincides with increased SOCE in LNCaP-ADT and the LNCaP-abl cells. It has been demonstrated in previous research that expression levels of the SOCE proteins STIM1 and Orai1 have altered expression at various stages of PCa progression (Kappel et al., 2017; Perrouin Verbe et al., 2016) with increased expression in the early stages which decreases as PCa progresses to the CRPC stage. Therefore, we wanted to investigate if there was a link between CaV1.3 and these proteins which could be driving the increased SOCE we observed previously.

Initial observations between cell types indicate that there was no significant change in the mRNA levels of Orai1, but a trend towards increased expression in the LNCaP-abl (Figure 6.1 (A)(i)). In addition, our results also show that CaV1.3 siRNA had no significant effect on Orai1 expression either. Investigation of STIM1 expression also found no significant change across all three cell types under normal culture conditions, although there is an increased trend observed in the LNCaP-ADT (Figure 6.1 (B)(i)). However, the expression of STIM1 in the cells treated with non-targeting siRNA (Figure 6.1 (B)(ii)) we see that there is a significant increased expression in the LNCaP-ADT cells which have 2.7-fold (+/- 0.23 sem) increased expression compared to the LNCaP siCon. However, CaV1.3 silencing had no significant effect on STIM1 expression in any of the cell lines.

Overall Orai1 and STIM 1 expression is not influenced by CaV1.3. There is an increased trend in STIM1 expression observed in the LNCaP-ADT cells which is significant in the transfection control. Indicating that STIM1 has an increased expression in the short term ADT cells, but not in the CRPC stage.

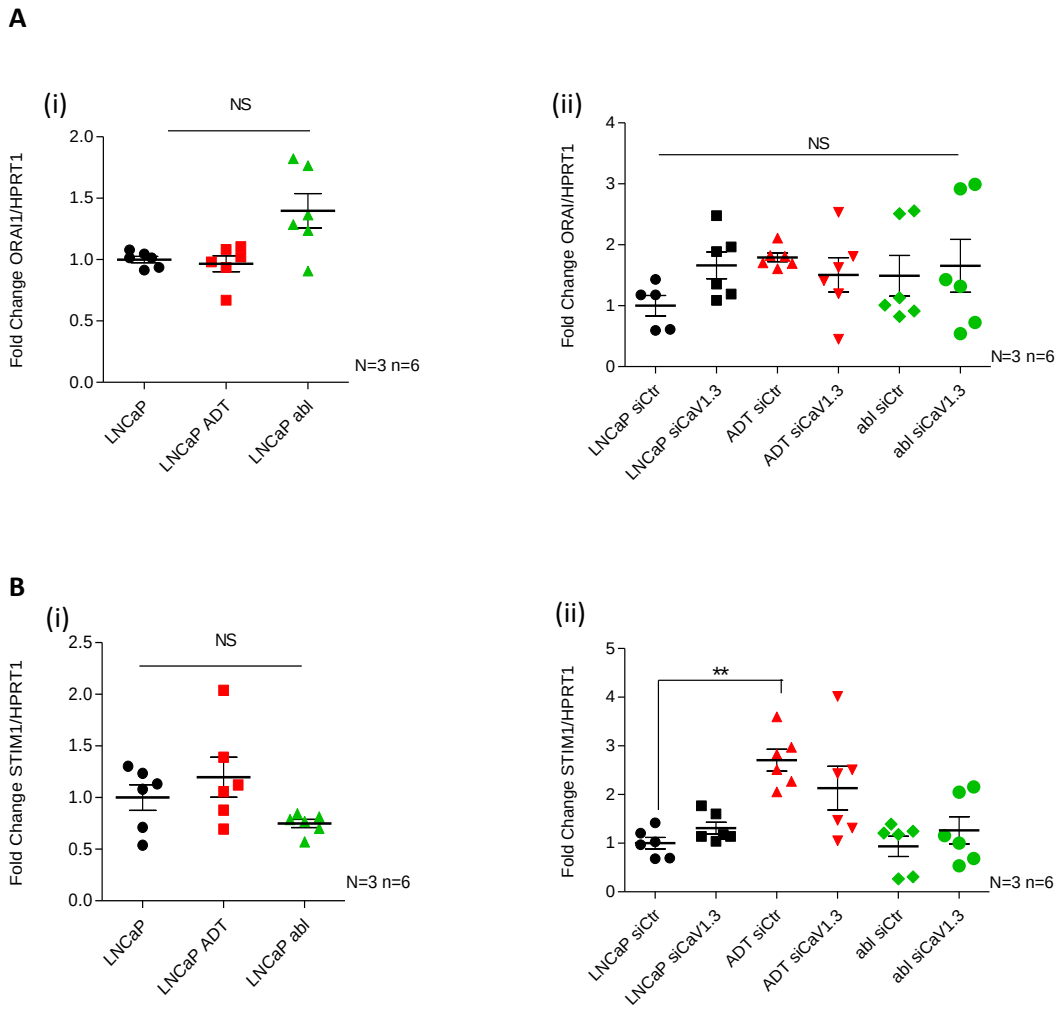

Figure 6.1: STIM1 is upregulated in LNCaP-ADT cells but is not influenced by the expression of CaV1.3: *Genetic expression of (A) ORAI1 and (B) STIM1 (i) under normal conditions & (ii) under siRNA transfection assessed using qPCR normalised to control. Analysis of androgen sensitive LNCaP cells (black), LNCaP-ADT cells treated with 10 µM bicalutamide (7-10 days) (red) and androgen insensitive long-term androgen deprived LNCaP-abl cells (green), transfected with non-targeting siRNA (siCtr) or siRNA targeting CaV1.3 (siCaV1.3). Analysed using Kruskal-Wallis significance test and Dunn's multiple comparison post hoc test between cell types and treatments. * P<0.05, ** P<0.01, ***P<0.001, NS not significant.*

6.2.1.2 Ryanodine receptors isotypes have altered expression over disease progression.

There is an association between RyR2 and CaV1.3 in the central nervous system (Kim et al., 2007; Ouardouz et al., 2003), with some evidence of CaV1.3 regulating Ca^{2+} release through stimulation of RyR in sinoatrial node pace making activity (Torrente et al., 2016). Since we observed an unexpected SOCE associated with CaV1.3 expression in PCa after ADT, we looked at the expression of RyR's in the cell lines and if silencing CaV1.3 had any effect on the expression of RyR.

Expression of RyR1 is significantly increased in LNCaP-ADT cells 3.09-fold (+/- 0.27 sem) compared to the LNCaP cells (Figure 6.2 (A)(i)). When these cells were transfected with non-targeting siRNA, they still had an increased in expression of RyR1 (1.838-fold +/- 0.1 sem) (Figure 6.2 (A)(ii)), which is significantly reduced when CaV1.3 is silenced (0.668-fold +/0 0.2 sem). In terms of our CRPC cell line, LNCaP-abl, the reverse was observed with significantly reduced expression in the transfected control having 0.35-fold (+/- 0.09 sem) and 0.29-fold (+/- 0.09 sem) following siRNA knockdown. Interestingly siRNA knockdown in LNCaP cells resulted in a 1.8-fold (+/- 0.1 sem) increase compared to matched control, although it was not significant. Interestingtly the observed increase of RyR1 in ADT correlates with increased CaV1.3 expression and SOCE suggesting a potential link.

With regards RyR2, it was the CRPC cell line, LNCaP-abl, that had a significant increase in expression (2.51-fold +/- 0.3 sem) (Figure 6.2 (B)(i)). This increased expression was also observed in the control transfected cells with expression of RyR2 significantly increased 5.3-fold (+/- 0.4 sem) in the LNCaP-abl cells (Figure 6.2 (B)(ii)) compared to LNCaP control, but no effect was seen when CaV1.3 is silenced (5.256-fold +/- 1.99 sem). While LNCaP-ADT did have an increase in expression in the siCtr samples, a similar trend of no impact on RyR2 expression following siRNA knockdown was observed. Contrary to this in LNCaP cells, silencing CaV1.3 did induce an increase in expression 3.88-fold (+/- 1.1 sem) compared to control, however again this was not significant. This suggests that RYR2 could potentially be contributing to the increases SOCE observed but it does not influence the increases following CaV1.3 siRNA.

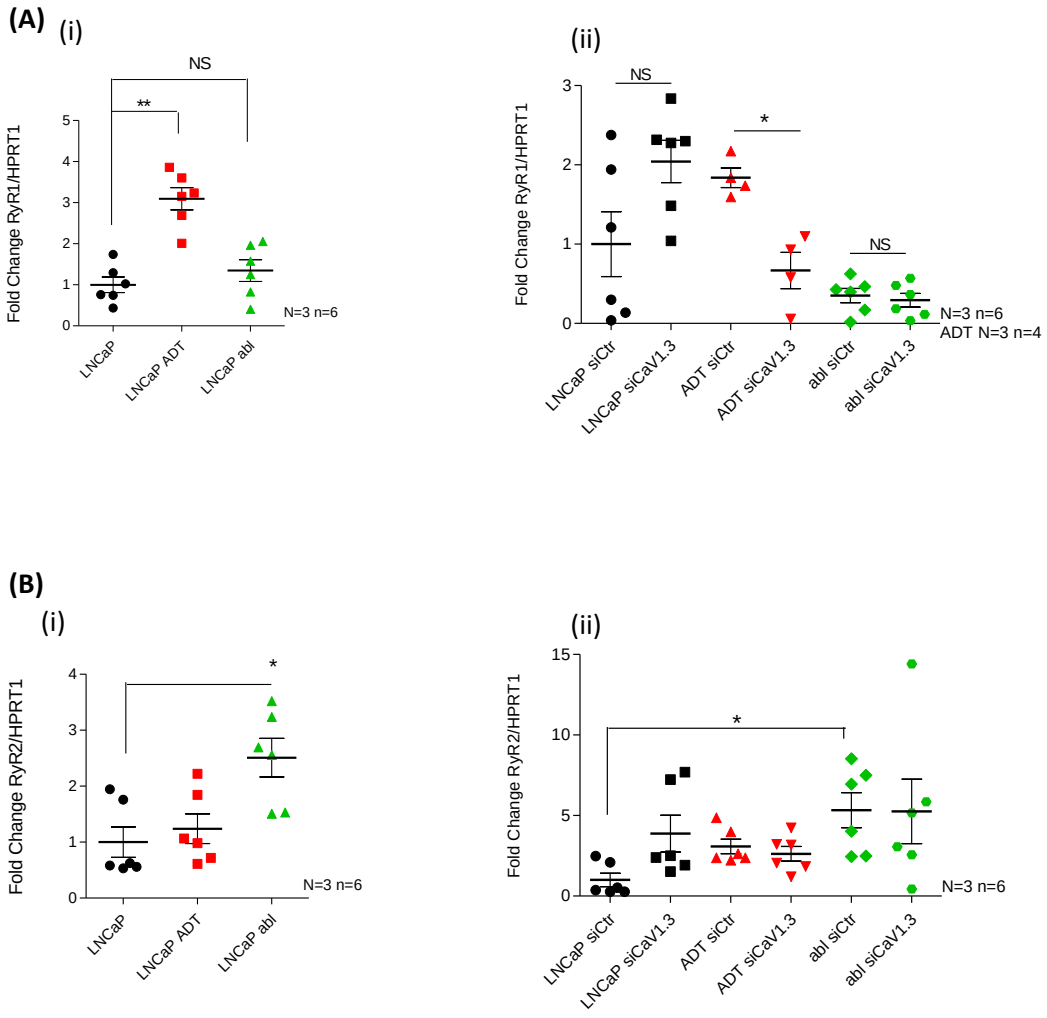

Figure 6.2: RyR1 is upregulated in androgen sensitive LNCaP-ADT and RyR2 is upregulated in the androgen insensitive LNCaP-abl cells: *Genetic expression of (A) RyR1 and (B) RyR2 (i) under normal conditions & (ii) under siRNA transfection assessed using qPCR normalised to control. Analysis of androgen sensitive LNCaP cells (black), LNCaP-ADT cells treated with 10 µM bicalutamide (7-10 days) (red) and androgen insensitive long-term androgen deprived LNCaP-abl cells (green), transfected with non-targeting siRNA (siCtr) or siRNA targeting CaV1.3 (siCaV1.3). (i) (ii) analysed using Kruskal-Wallis significance test and Dunn's multiple comparison post hoc test between cell types and treatments. (iii)(iv)(v) Mann-Whitney significance test between cell types and treatments. * P<0.05, ** P<0.01, ***P<0.001, NS not significant.*

6.2.1.3 Incubation with ryanodine prevents the enhanced SOCE seen in LNCaP-abl cells when CaV1.3 is silenced

Here we repeated the SOCE traces as per chapter 4 looking at the effect of silencing CaV1.3 on the SOCE, although here we also introduced the ryanodine receptor inhibitor, ryanodine, to investigate the effect RyR is having on the SOCE in the cells. While these experiments do not exhibit any significance, this is most likely due to the small number of repeats performed for these experiments. Further repeats would be required to achieve statistical significance as observed in chapter 4. However, if we look at the trends, we can gain some insight into any potential effect seen when RyR action is inhibited with and without CaV1.3.

The LNCaP cells have no altered Tg peak when cells are incubated with ryanodine in either siCtr or siCaV1.3 cells (Figure 6.3 (A)(ii)). The Ca^{2+} peak is unaltered with any treatment in the LNCaP cells (Figure 6.3 (A)(iii)).

The LNCaP-ADT cells have a reduced Tg peak in the siCaV1.3 cells both with and without ryanodine (0.654 +/- 0.2 sem and 0.673 +/- 0.7 sem respectively). There is no effect on the Tg peak in siCtr cells treated with ryanodine (Figure 6.3 (B)(ii)). The Ca^{2+} peak is unaffected by any treatment in these experiments (Figure 6.3 (B)(iii)). Demonstrating that in the LNCaP-ADT cells the SOCE increase observed is not dependant on the action of RyR.

The LNCaP-abl cells have an increased Tg peak in the siCaV1.3 cells which have not been incubated with ryanodine (1.187-fold +/- 0.1 sem). This increased Tg peak is not present in any of the cells treated with ryanodine either the siCtr or the siCaV1.3 cells (Figure 6.3 (C)(ii)). The Ca^{2+} peak in the LNCaP-abl cells is increased in the siCaV1.3 cells which have not been treated with ryanodine (1.115-fold +/- 0.3 sem), which reflects our previous findings. However, when the cells are treated with ryanodine there is no increased Ca^{2+} peak when CaV1.3 is silenced (Figure 6.3 (C)(iii)). This indicates that the increased SOCE seen in the LNCaP-abl cells when CaV1.3 is silenced may be reliant on the activation of RyR. Further repeats would be required to draw conclusive analysis of these results, however there is some indication of an association between RyR and CaV1.3.

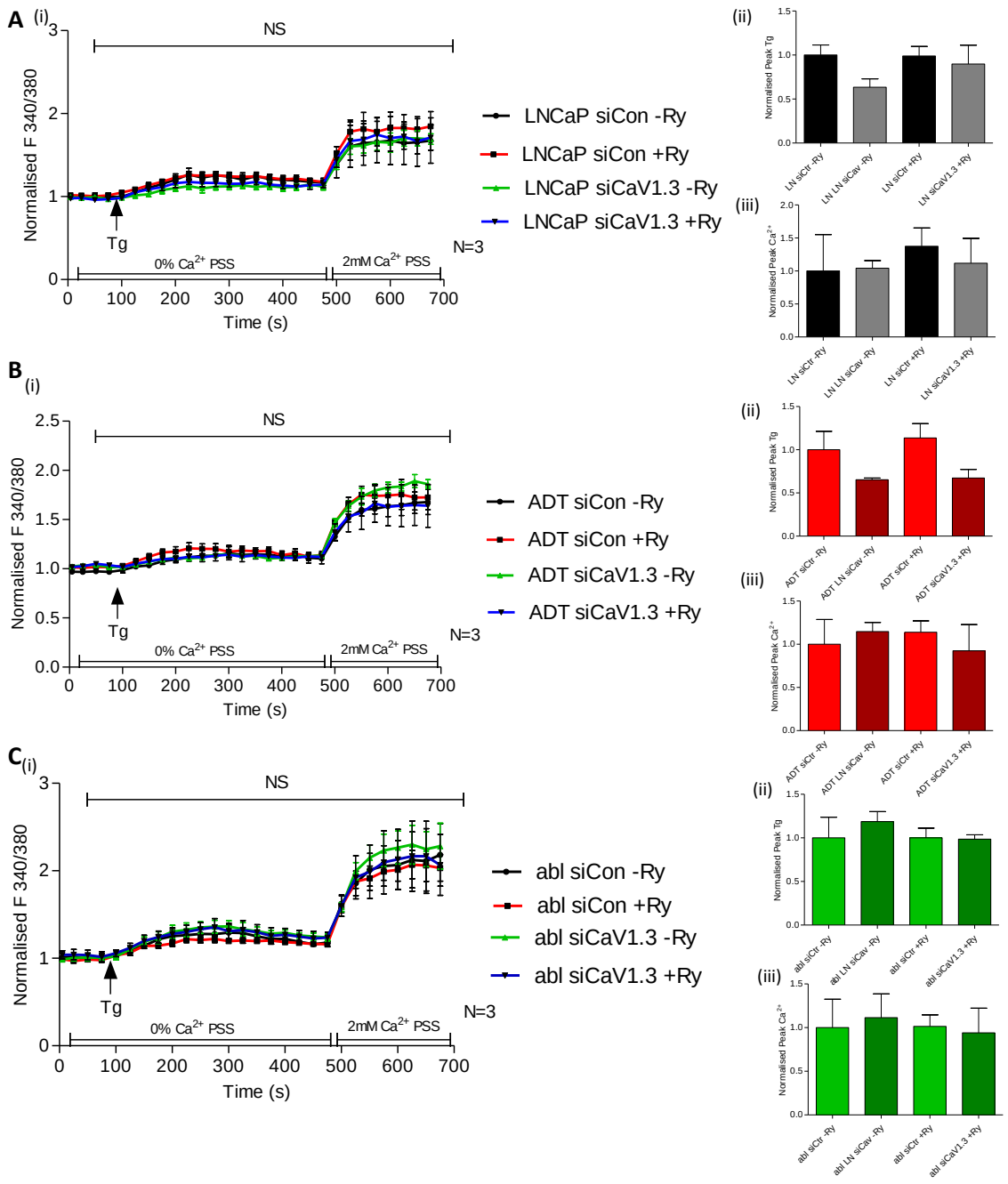

Figure 6.3: Incubating the cells with Ryanodine had no significant effect of Ca^{2+} mobilisation: *Store operated calcium entry (SOCE) indicated by Fura 2-AM ratiometric analysis of calcium concentration over time (s) in cells incubated with or without Ryanodine (Ry) (1 µM), transfected with siRNA non-targeting pool (ctr) or targeting Cav1.3 (siCaV1.3). Analysis of (A) androgen sensitive LNCaP cells, (B) LNCaP-ADT cells treated with 10 µM bicalutamide (7-10 days) and (C) androgen insensitive long-term androgen deprived LNCaP-abl cells. Analysed using 2-way ANOVA significance of fluorescence ratio 340:380 at time (s) between treatments and Kruskal-Wallis significance test and Dunn's multiple comparison post hoc test between cell types and treatments * P<0.05, ** P<0.01, ***P<0.001, NS not significant.*

6.2.1.4 NCX channels are upregulated after ADT and silencing CaV1.3 enhances expression of NCX2.

CaV1.3 has also been implicated in regulating intracellular Ca^{2+} oscillations through interaction with the sodium calcium exchanger NCX by preventing calcium efflux (Fourbon et al., 2017). We sought to determine if NCX was expressed at different levels across the cell lines and if silencing CaV1.3 influenced NCX expression.

Expression of NCX1 was significantly increased in the LNCaP-ADT (Appendix D, Figure D.1 (A)), with a 4.258-fold (+/- 0.97 sem) expression increase. There was also upregulation in the LNCaP-abl cells which had 2.67-fold (+/- 0.68 sem) increased expression of NCX1 compared to LNCaP cells. However, the ct values for the expression between cell lines was compared to the ct values recorded for NCX2 and NCX3 and found to be below 35 (Appendix D, Figure D.1 (B)). Therefore these results where not investigated further.

NCX2 had a significant increased expression in the LNCaP-abl cells (Figure 6.4 (A)(i)), which was 10.72-fold (+/- 1.8 sem) increased compared to LNCaP cells. The LNCaP-ADT cells also had an increased expression (4-fold +/- 0.73 sem). When we looked at the CaV1.3 silenced cells compared to the control transfected cells for each cell type, we found that there was a significant increased expression of NCX2 in the LNCaP-ADT cells when CaV1.3 was silenced which was 2.266-fold (+/- 0.28 sem) compared to LNCaP-ADT siCtr (Figure 6.4 (A)(ii)).

NCX3 had no significant change in expression between cell types (Figure 6.4 (B)(i)), although the LNCaP-ADT cells had a 3-fold (+/- 0.96 sem) increased expression there was a spread to the individual repeats which was skewing the results. When we look at the expression of NCX3 in the cell lines after they had been transfected (Figure 6.4 (B)(ii)) the cells which have had CaV1.3 silenced all had slight increased expression, LNCaP siCaV1.3 1.172-fold (+/- 0.3 sem), LNCaP-ADT siCaV1.3 1.3-fold (+/- 0.59 sem) and LNCaP-abl siCaV1.3 1.2-fold (+/- 0.6 sem), but none had significance.

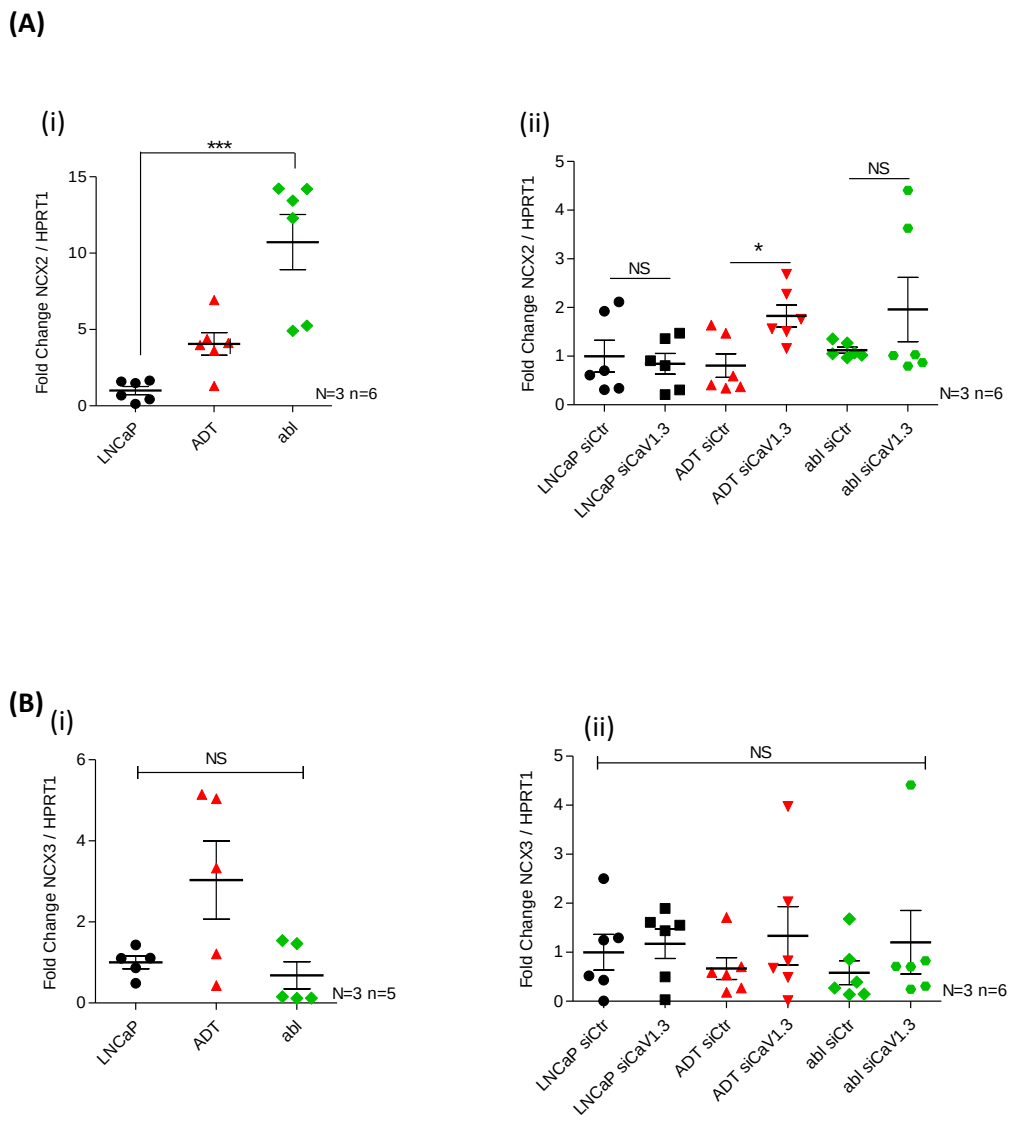

Figure 6.4: NCX2 is upregulated in cells treated with ADT but no difference observed in NCX3 expression: *Genetic expression of (A) NCX2 and (B) NCX3 was determined (i) under normal conditions & (ii) under siRNA transfection using qPCR normalised to control. Analysis of androgen sensitive LNCaP cells (black), LNCaP-ADT cells treated with 10 µM bicalutamide (7-10 days) (red) and androgen insensitive long-term androgen deprived LNCaP-abl cells (green), transfected with non-targeting siRNA (siCtr) or siRNA targeting CaV1.3 (siCaV1.3). Analysed using Kruskal-Wallis significance test and Dunn's multiple comparison post hoc test between cell types and treatments or Mann-Whitney significance test between cell types and treatments. * P<0.05, ** P<0.01, ***P<0.001, NS not significant.*

6.2.1.5 Potassium channels are significantly reduced in androgen independent cells but are not influenced by CaV1.3 expression.

It has been previously demonstrated that the c-terminus of CaV1.3 could influence the expression of the potassium channel SK2 (Lu et al., 2015), which in turn can control VGCC actiavation. Therefore, we wanted to establish the expression level of some Ca^{2+} regulated potassium channels to determine if CaV1.3 had a similar influence in PCa. Analysis of expression of the large conductance (BK) and the small conductance (SK) potassium channels, SK1, SK2 and SK3, found that there was an overall significant decreased expression in the androgen independent LNCaP-abl cells. There was no effect seen when CaV1.3 was silenced in any of the cells. Outlined below are BK_{Ca} and SK2 as they had the highest expression across all cells (Appendix D, Figure D.4).

The BK_{Ca} channel has reduced expression in the LNCaP-ADT cells and the LNCaP-abl cells (0.396-fold +/- 0.02 sem and 0.16-fold +/- 0.02 sem), with significance in the LNCaP-abl cells. When CaV1.3 was silenced, there was no significant change observed in the expression of BK_{Ca} channel. Although there was some additional reduced expression in the LNCaP-abl cells when CaV1.3 was silenced with expression after silencing having 0.859-fold (+/- 0.06 sem) reduced compared to the siCtr LNCaP-abl cells (Figure 6.5 (A)(ii)).

The SK2 channel also has reduced expression in the LNCaP-ADT (0.699-fold +/- 0.05 sem), with significant reduced expression in the LNCaP-abl 0.277-fold (+/- 0.06 sem) (Figure 6.5 (B)(i)). The transfected cells have no alteration in the expression of SK2. There was a similar lack of alteration when CaV1.3 was silenced in expression of the other small conductance K^+ channels (SK1 and SK3) (Appendix D, Figure D.3).

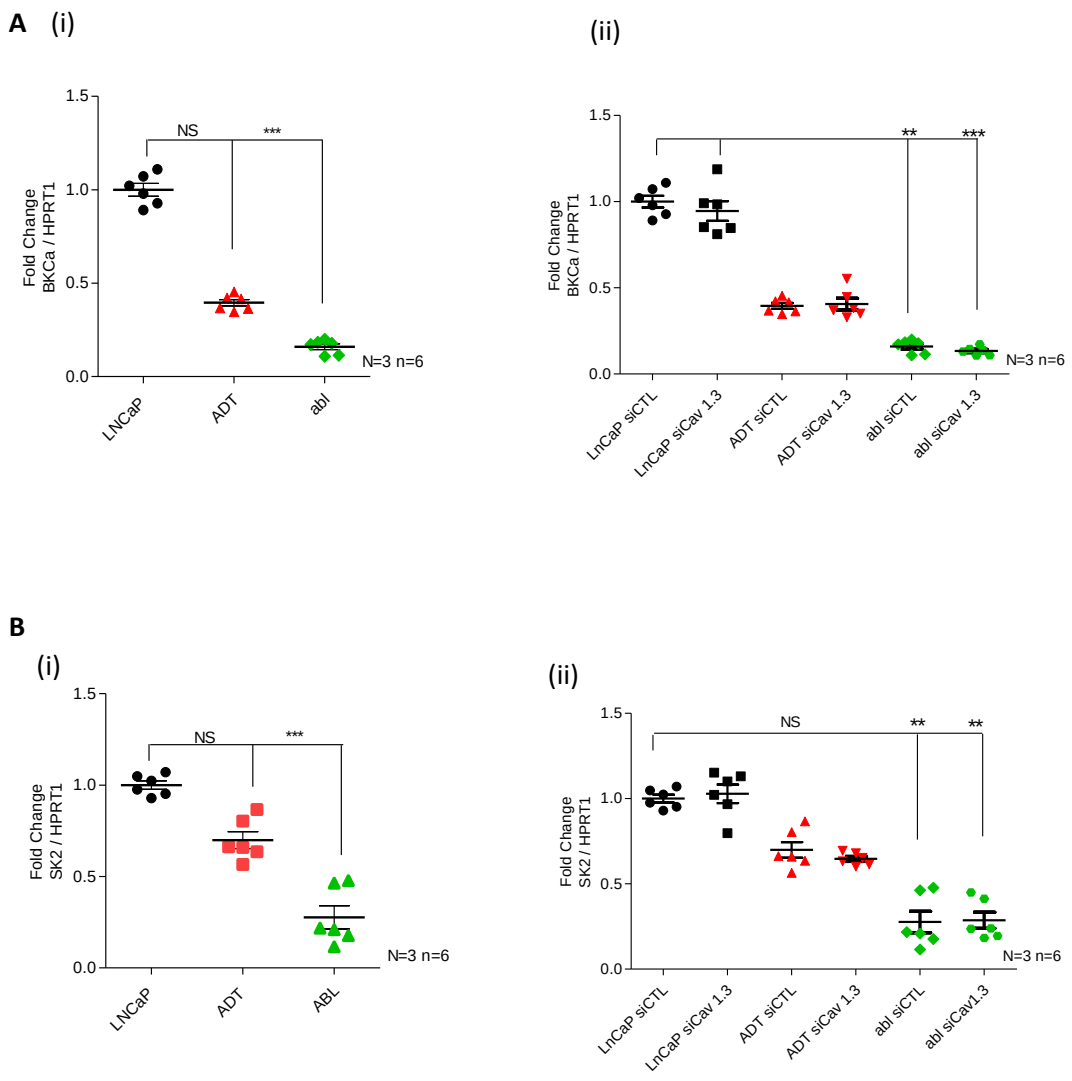

Figure 6.5: BK_{Ca} and SK2 are downregulated after ADT in PCa: *Genetic expression of (A) BK_{Ca} and (B) SK2 assessed (i) under normal conditions & (ii) under siRNA transfection using qPCR normalised to control. Analysis of androgen sensitive LNCaP cells (black), LNCaP-ADT cells treated with 10 µM bicalutamide (7-10 days) (red) and androgen insensitive long-term androgen deprived LNCaP-abl cells (green), transfected with non-targeting siRNA (siCtr) or siRNA targeting CaV1.3 (siCaV1.3). Analysed using Kruskal-Wallis significance test and Dunn's multiple comparison post hoc test between cell types and treatments. * P<0.05, ** P<0.01, ***P<0.001, NS not significant.*

6.2.2 Expression of calcium signalling molecules.

Fluctuations in $[Ca^{2+}]_i$ can activate a number of downstream signalling pathways, many of which are implicated in cancer development and progression. Here we look at the genetic expression of the most common Ca^{2+} regulated transcription factors NFAT and CREB to determine if they have altered expression across disease progression. We also investigate if CaV1.3 expression or the associated enhanced SOCE seen after ADT has any influence on their expression. Next we also looked at the genetic expression of CaM, a small Ca^{2+} binding protein, which undergoes a conformational change when bound to Ca^{2+} allowing it to bind to and activate a wide variety of enzymes (Swulius and Waxham, 2008). In this way CaM regulates many signalling pathways such as CAMKII which in turn activate Ca^{2+} regulated transcription factors such as NFAT and CREB. Taking this into consideration we investigated to see if these pathways where linked to the altered CaV1.3 expression and the enhanced SOCE we previously observed.

6.2.2.1 Transcription factors NFAT and CREB are upregulated in LNCaP-ADT cells

NFAT had no significant altered expression between cell lines (Figure 6.6 (A)(i)), although there was an increased trend observed in the LNCaP-ADT cells, which had 2-fold (+/- 0.3 sem) expression compared to LNCaP. When CaV1.3 was silenced there was no significance detected in the expression changes observed (Figure 6.6 (A)(ii)). We also looked at the expression in CREB (Figure 6.6 (B)(i)) which had a significant increased expression in the LNCaP-ADT cells (1.8-fold +/- 0.096 sem). However, there was no change in expression observed in any of the cell lines when CaV1.3 was silenced (Figure 6.6 (B)(ii)).

Both NFAT and CREB which are calcium regulated transcription factors, have increased expression in the LNCaP-ADT cells, although no direct association could be indicated due to increased expression of CaV1.3 since silencing CaV1.3 has no effect on the upregulation of these transcription factors.

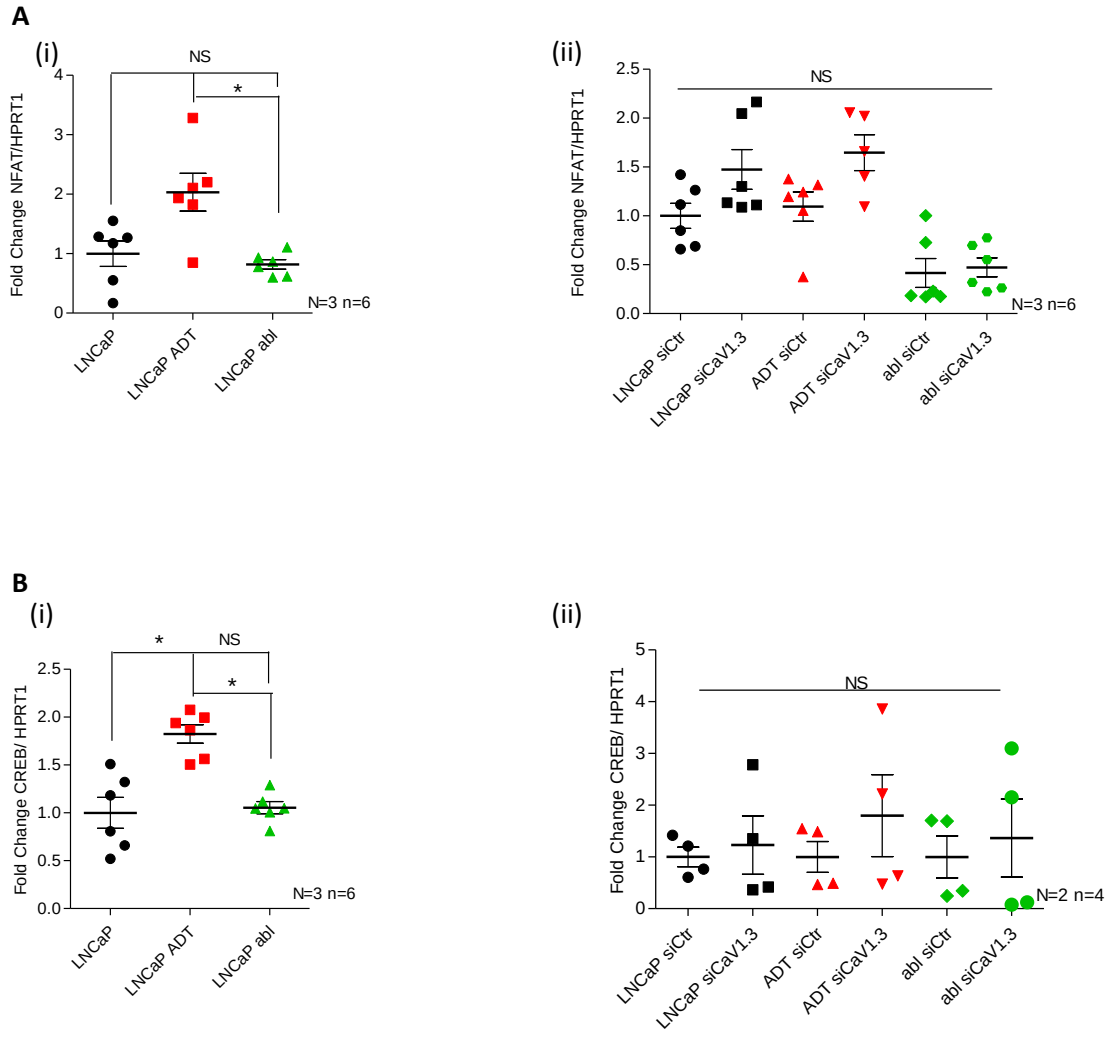

Figure 6.6: NFAT and CREB are upregulated in LNCaP-ADT cells while NFAT is downregulated in the androgen insensitive LNCaP-abl cells: *Genetic expression of (A) NFAT and (B) CREB assessed (i) under normal conditions & (ii) under siRNA transfection using qPCR normalised to control. Analysis of androgen sensitive LNCaP cells (black), LNCaP-ADT cells treated with 10 μM bicalutamide (7-10 days) (red) and androgen insensitive long-term androgen deprived LNCaP-abl cells (green), transfected with non-targeting siRNA (siCtr) or siRNA targeting CaV1.3 (siCaV1.3). Analysed using Kruskal-Wallis significance test and Dunn's multiple comparison post hoc test between cell types and treatments. * P<0.05, ** P<0.01, ***P<0.001, NS not significant.*

6.2.2.2 CaMKIIβ is significantly increased when CaV1.3 is silenced.

Expression of CALM1 is significantly upregulated in the androgen independent LNCaP-abl cells with a 1.5-fold (+/- 0.058 sem) increased expression compared to LNCaP (Figure 6.7 (A)(i)). When we silence CaV1.3 (Figure 6.7 (A)(ii)) there is no significant alteration in the expression of CALM1 in any of the cells.

CAMKIIβ had no significantly altered expression between cell lines (Figure 6.7 (B)(i)), with LNCaP-ADT and LNCaP-abl having 1.81-fold (+/- 0.6 sem) and 0.88-fold (+/- 0.2 sem) expression, respectively compared to LNCaP control. However, when CaV1.3 was silenced there was a significant upregulation of CAMKIIβ across all cells (Figure 6.7 (B)(ii)). The LNCaP, LNCaP-ADT and the LNCaP-abl cells had a 9.3-fold (+/- 2.7 sem), 6.2-fold (+/- 2.45 sem) and 3.355-fold (+/- 0.98 sem) increase respectively when CaV1.3 was silenced compared to control. Indicating that CaV1.3 expression has some inhibitory effect on the expression CAMKIIβ.

We also looked at the expression levels of CAMKIIγ, where there was no significance detected between cell types (Figure 6.7 (C)(i)). Although LNCaP-abl had an increased trend compared to LNCaP 2.37-fold (+/- 0.68 sem). Silencing CaV1.3 also had no significance detected on the expression of CAMKIIγ (Figure 6.7 (C)(ii)). However there also appears to be an increased trend detected when we compare the cells transfected with siRNA targeting CaV1.3 to the cells transfected with non-targeting control. The LNCaP cells had 2.269-fold (+/- 0.28 sem) increased expression compared to control, the LNCaP-ADT cells had 1.58-fold (+/- 0.4 sem) increased expression when CaV1.3 was silenced compared to control and the LNCaP-abl cells had 2.4-fold (+/- 0.78 sem) increased expression after CaV1.3 was silenced compared to LNCaP-abl siCtr.

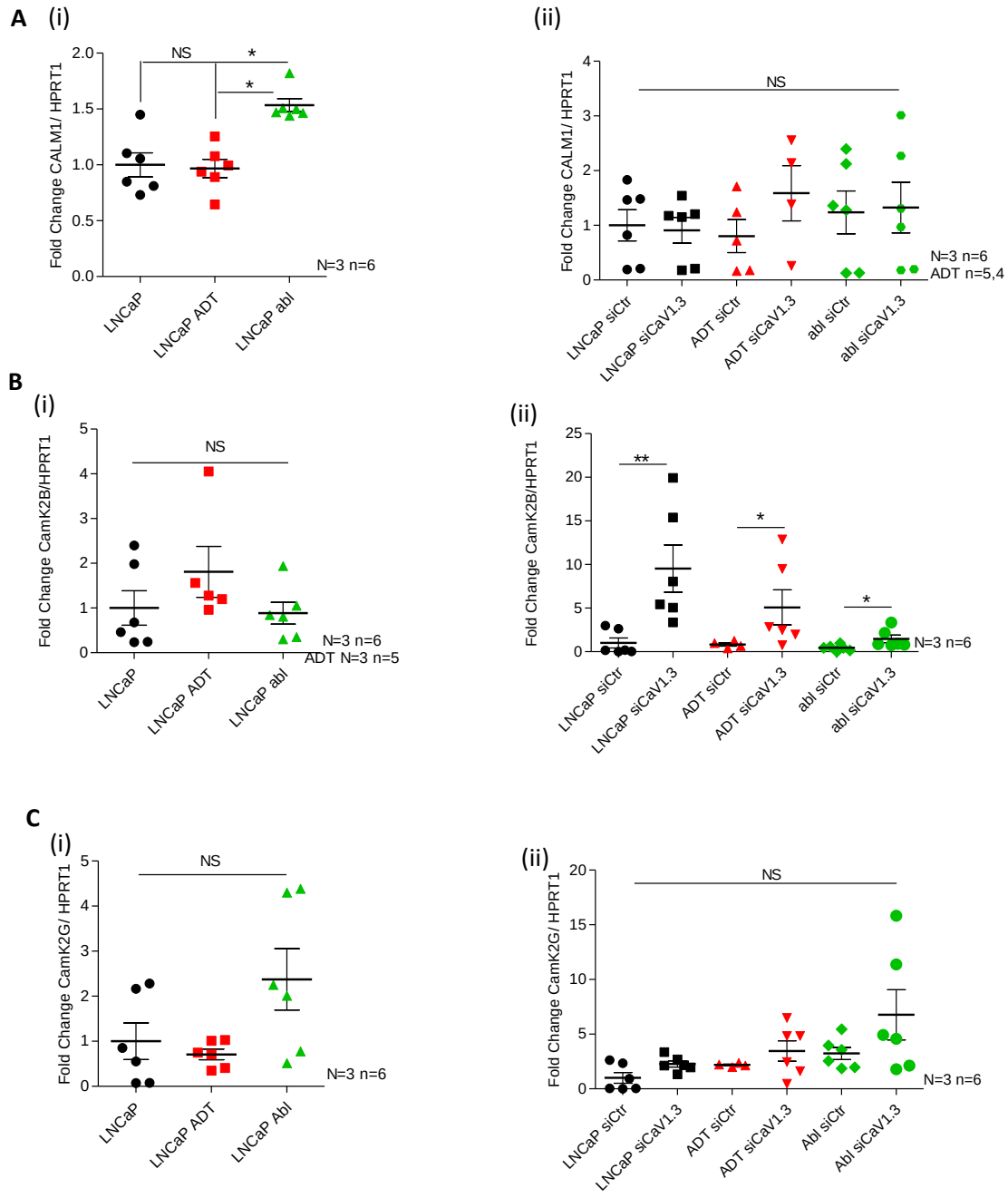

Figure 6.7: CALM1 is upregulated in androgen insensitive LNCaP-abl and CAMK2B is significantly upregulated when CaV1.3 is silenced: *Genetic expression of (A) CALM1 and (B) CAMK2B (C) CAMKG assessed (i) under normal conditions & (ii) under siRNA transfection using qPCR normalised to control. Analysis of androgen sensitive LNCaP cells (black), LNCaP-ADT cells treated with 10 µM bicalutamide (7-10 days) (red) and androgen insensitive long-term androgen deprived LNCaP-abl cells (green), transfected with non-targeting siRNA (siCtr) or siRNA targeting CaV1.3 (siCaV1.3). (i) (ii) Analysed using Kruskal-Wallis significance test and Dunn's multiple comparison post hoc test between cell types and treatments. (iii)(iv)(v) Mann-Whitney significance test between cell types and treatments. * P<0.05, ** P<0.01, ***P<0.001, NS not significant.*

6.3 Chapter discussion

CaV1.3 is upregulated in PCa, which we have demonstrated is associated with ADT. Our research has shown that the upregulation of CaV1.3 in these cells regulates SOCE rather than facilitating Ca^{2+} entry through its normal canonical mechanism under cellular depolarisation. This suggests that CaV1.3 is contributing to altered $[Ca^{2+}]_i$ through interactions with or the regulation of other Ca^{2+} channels which may influence downstream signalling pathways. CaV1.3 has been implicated in non-canonical activities in its predominant settings of the central nervous system (Kim et al., 2007) and the pace making cells of the heart (Lu et al., 2015) as well as in colon cancer (Fourbon et al., 2017). We have also demonstrated that there is nuclear expression of the CaV1.3 c-terminus in the androgen sensitive cell lines. Research has shown that the c-terminus of CaV1.3 can act as a transcriptional regulator (Lu et al., 2015). This chapter outlines the expression of other Ca^{2+} channels to identify potential alternative mechanisms through which CaV1.3 could be driving the altered SOCE observed and the effect on the associated downstream signalling genes.

6.3.1 Expression regulation of SOCE associated channels

The ubiquitous SOCE mechanism is mediated primarily through STIM and Orai proteins (Hogan and Rao, 2015), although other proteins have been implicated in the refilling of depleted stores such as TRPC channels and indeed VGCC (Power and Sah, 2005). Studies of patient tissue samples have shown an altered expression of STIM and Orai proteins over PCa stage (Kappel et al., 2017; Perrouin Verbe et al., 2016), with an initial increased expression in PCa tissues followed by a reduced expression in CRPC tissues. This coincided with the genetic expression of CaV1.3 in PCa progression under ADT (Figure 3.7 (A)) and may contribute to the increased SOCE we observed with this upregulation. We looked at the expression of both STIM1 and Orai1, to see if there was any correlation with CaV1.3 expression and also to determine the if it was linked to their expression. We found that the genetic expression of Orai1 was not significantly altered between cell types (Figure 6.1 (A)), nor was it affected by silencing CaV1.3. In agreement with the outlined research, expression of STIM1 was significantly increased in the LNCaP-ADT cells but reduced to pre-treatment levels in the LNCaP-abl cells (Figure 6.1 (B)). However, there was no change detected when CaV1.3 was silenced, indicating that CaV1.3 was not having an impact on gene expression at least. Although some research has outlined a correlated upregulation of both HIF-

1α and STIM-1 in hepatocarcinoma cells under hypoxic conditions (Y. Li et al., 2015). As we have demonstrated previously HIF-1α is significantly increased in LNCaP-ADT cells and silencing CaV1.3 significantly reduced the expression of HIF-1α and also reduced the SOCE in these cells.

In a study by Flourakis et al. gene expression of Orai1 and STIM1 were measured in LNCaP cells cultured for three days in steroid deprived media (Flourakis et al., 2010). Contra to our findings of unaltered Orai1 and increased STIM1 after ADT, this research indicated an unaltered expression of STIM1 and downregulation of Orai1 in LNCaP cells after ADT, which they attributed to increased apoptosis resistance. Others suggest that only Orai3 was upregulated in PCa tissue samples compared to normal prostate tissue, with other isoforms having no altered expression (Dubois et al., 2014). However, this research also identified that Orai3 did not contribute to the SOCE of the cells, finding only Orai1 and STIM1 controlled SOCE in LNCaP cells. Orai3 was found to contribute to a non-store depleted Ca^{2+} mechanism involving activation through binding of arachidonic acid. These differences in reported expression of SOCC could be due to the heterogeneous nature of PCa cells, with one review outlining the variety of research findings in relation to altered expression (Kappel et al., 2017). The findings of our research and the inverse findings of Flourakis et al's. could be down to the method of ADT used in the analysis. Our research inhibits AR signalling using bicalutamide antagonism, rather that androgen depleted media. Interestingly Flourakis et al. indicated an androgen regulation of Orai1 and identified androgen response elements in the promoter region of the gene that codes for Orai1. In keeping with these findings, another study highlighted a similar mechanism involving STIM1, which suggests that in prostate stromal cells there are androgen response elements in the promotor region of STIM1 also (Berry et al., 2011). This study went on to demonstrate effective gene transcription through AR binding the response element. Overall suggesting that activation of the AR through androgen binding and subsequent nuclear translocation is required for expression regulation of Orai1 and STIM1, in androgen sensitive cell lines.

The research pertaining to RyR's is predominantly focused on the function of this channel in relation to excitable cells. It is known that in excitable cells RyR's play a key role in excitation contraction (Numa et al., 1990), which also involves coupling with L-type VGCC (Franzini-Armstrong, 2004). There is also evidence of a role in the plasticity of neurons (Adasme et al., 2011; Bardo et al., 2006). However, the role that RyR's play in epithelial cells is less clearly defined. In relation to the association between CaV1.3 and RyR's there is extensive research indicating a coregulation and associated attachment in the sinoatrial node (Christel et al., 2012; Torrente et al., 2016) and the hippocampus (Kim et al., 2007). There is also research which highlights that

CaV1.3 forms a complex with potassium channels and RyR in neurons (Sahu et al., 2019; Vierra et al., 2019). This facilitates coupling and can result in activation of CaV1.3 at resting potential. Indicting a potential non-voltage dependent function associated with CaV1.3. Since we found no functional evidence of CaV1.3 activation under depolarised states, this could be a mechanism through which CaV1.3 is responsible for increased SOCE in the LNCaP-ADT and LNCaP-abl cells.

We examined the expression of RyR1 and RyR2 in our cell model, as these are the RyR isoforms previously identified in LNCaP cells (Kobylewski et al., 2012) (Mariot et al., 2000). However, our research found that RyR1 and RyR2 were differentially expressed between cell types, suggesting an alternating isoform prevalence with disease progression. RyR1 was significantly upregulated in the LNCaP-ADT cells (Figure 6.2 (A)(i)), whereas RyR2 was significantly upregulated in the LNCaP-abl cells (Figure 6.2 (B)(i)). The switch in isoform may also influence the altered effect on SOCE we detected upon silencing CaV1.3. Interestingly we found that RyR1 was significantly reduced in the LNCaP-ADT cells when CaV1.3 was silenced, which as shown previously also results in a reduced SOCE in this cell line. Indicating that expression of RyR1 and CaV1.3 may be required for the enhanced SOCE detected in the LNCaP-ADT cells. However, the expression of RyR2, the predominant isoform detected in the LNCaP-abl cells, was unaffected when CaV1.3 was silenced.

We also carried out some Ca^{2+} imaging experiments in cells incubated with ryanodine (Figure 6.3), a plant based RyR inhibitor (Jenden and Fairhurst, 1969). This was to determine if the RyR was responsible for the increased Ca^{2+} influx we had seen in the cells after ADT (Figure 4.2). However, these experiments did not produce significant results due to the low number of repeats. We could however draw some inference from these results. While the LNCaP and the LNCaP-ADT cells indicated little effect of interest, there may be an indication of a trend in the LNCaP-abl cells. The increased Ca^{2+} peak observed in the LNCaP-abl cells after CaV1.3 is silenced, which we have confirmed previously (Figure 4.7), is reduced when this silencing is combined with ryanodine incubation (Figure 6.3 (C)). There may be a mechanism in the LNCaP-abl cells through which CaV1.3 and RyR coregulate SOCE. This suggests that CaV1.3 may have an influence on the RyR induced ER Ca^{2+} release and the subsequent SOCE.

In future research it could be beneficial to look at the Ca^{2+} signalling in these cells under depolarised states, since the RyR has been shown to release Ca^{2+} from the ER in conjunction with depolarised activation of CaV1.3 (Ouardouz et al., 2003). Interestingly the LNCaP-abl cells were the cells which indicated a reduced expression of the Ca^{2+} regulated potassium channels. A reduced expression of these channels may affect the membrane potential and drive a depolarised state. This could explain the increased Ca^{2+} mobilisation observed in the LNCaP-abl cells.

Therefore, we hypothesise that in the LNCaP-abl cells the increased SOCE seen is regulated by an interaction between CaV1.3 and RyR2.

We also looked at the expression of NCX channels due to recent reports indicating the association between upregulated CaV1.3 in colon cancer and its bearing on the activity of NCX channels (Fourbon et al., 2017). NCX channels have been implicated in reverse mode activation in the progression of many cancers (Chovancova et al., 2020), including PCa (Long et al., 2016). Since the reverse mode of NCX channels result in an increase in $[Ca^{2+}]_i$, we hypothesised that CaV1.3 could also be influencing NCX here and triggering calcium increase by activating the channels in reverse mode. NCX channels have also been reported to have an increased expression in PCa (Long et al., 2016), contributing to the progression of the disease. When we looked at the expression of the three isoforms of NCX (1,2 & 3), we found NCX2 was upregulated in LNCaP-ADT and significantly upregulated in the LNCaP-abl cells (Figure 6.4 (A)(i)). This expression was increased further when CaV1.3 was silenced (Figure 6.4 (A)(ii)). This suggests that in CRPC at least, expression of NCX2 may be enhancing the $[Ca^{2+}]_i$, through the reverse mode activation. Also silencing the expression of CaV1.3 enhances the expression of NCX2, which also coincides with a significant increased SOCE in these CRPC cells. This may be a mechanism through which NCX2 is contributing to the enhanced Ca^{2+} in the LNCaP-abl.

We also demonstrated an increased expression of NCX1 in the LNCaP-ADT cells (Appendix D, Figure D1), however we were unable to determine the effect of silencing CaV1.3 on this isoform as we were unable to detect expression in the transfected experiments carried out, even in the non-targeting control samples. Since NCX1 is the most studied isoform, this leaves a gap in the research, although there is a 70% homology to the structure of the 3 isotypes (Chovancova et al., 2020), so there may be overlapping transcriptional regulation. Interestingly, among the transcription factors known to regulate expression of NCX are CREB and HIF-1α (Formisano et al., 2020), which we have shown are both upregulated in the LNCaP-ADT cells, therefore this may explain the increased expression of NCX channels in the LNCaP-ADT cells. However, this does not explain the increased expression seen when CaV1.3 is silenced, which we know had no influence on CREB expression and only inhibited HIF-1α expression under hypoxic conditions. Although we have shown that there is a significant increased expression of CAMKIIβ after CaV1.3 is silenced, which as described in the research by Ma et al., results in the activation of CREB (Ma et al., 2014). Indicating that there may be a mechanism through which silencing CaV1.3 enhances CAMKIIβ, which activates CREB and the transcription of NCX2. There is little evidence indicating the role NCX channels play in PCa progression, other than the study by Long et al. which demonstrates that

inhibiting the NCX action with the reverse mode inhibitor KB-R7943 promoted apoptosis and inhibited proliferation (Long et al., 2016). This could be indicative of a role for NCX in cell survival, which may benefit survival under ADT.

6.3.2 Expression regulation of other ion channels

Another area which we wanted to investigate was the potential for CaV1.3 expression to have a bearing on other plasma membrane ion channels. As highlighted throughout this project, emerging research demonstrates the contribution of many ion channels in cancer progression (Leanza et al., 2016; Litan and Langhans, 2015), including their subscription to most processes involved in PCa progression (Abdul and Hoosein, 2006; Du et al., 2016; Gackière et al., 2013b; Lallet-Daher et al., 2009). We have mainly focused on Ca^{2+} channels throughout this project due to the evidence of SOCE and the significant implications on Ca^{2+} fluctuations contribution to cancer progression. Nevertheless, we must not neglect the interdependency between Ca^{2+} and other ion channels in controlling cellular homeostasis. In particular, the contribution of K^+ channels, which have been shown to be transcriptionally regulated by CaV1.3 (Lu et al., 2015). We examined the expression of some Ca^{2+} activated K^+ channels, since these channels have been shown to have an associated function with CaV1.3 (Sahu et al., 2019; Vivas et al., 2017). Research has demonstrated a CaV1.3 reliant activation of both BK and SK channels in excitable cells (Marcantoni et al., 2010; Vandael et al., 2012), therefore we wanted to examine the expression of these channels in our cell model. We were also interested in the study which indicated that the c-terminus of CaV1.3 was implicated in the transcriptional regulation of SK channels (Lu et al., 2015).

Initially we looked at the expression of the large K^+ conductance channel BK_{Ca}, which drives the bulk of the voltage dependent K^+ current in LNCaP cells (Gackière et al., 2013b). We found that expression of BK_{Ca} was significantly reduced in LNCaP-abl cells (Figure 6.5 (A)(i)), which was further reduced when CaV1.3 was silenced (Figure 6.5 (A)(ii)). Indicating that the increased expression of CaV1.3 after treatment with ADT was not driving the reduced expression of the BK channel since silencing CaV1.3 reduced the expression even further in the LNCaP-abl and had no effect on the LNCaP or the LNCaP-ADT cells. This reduced expression may be a mechanism to attenuate the apoptosis associated with ADT. K^+ efflux from the cell controls cell volume and membrane potential, reducing the efflux can attenuate apoptosis by reducing cell shrinkage and altering the

membrane potential preventing VGCC activation reducing Ca^{2+} overload (N. Prevarskaya et al., 2007).

Significant decreased expression of BK channels after ADT may not eliminate activity and there could be an association with CaV1.3 on a protein level. The BK_{Ca} channel has been shown to be activated at resting potential in LNCaP cells (Gessner et al., 2005) where a functional coupling with CaV3.2 has been demonstrated (Gackière et al., 2013b). Interestingly the BK_{Ca} channel has also been associated with a functional coupling with CaV1.3 in transfected tsa-201 cells, where it results in the low voltage activation of the BK_{Ca} channel (Vivas et al., 2017). Vivas *et al*. demonstrated an associated proximity between these two channels which allowed them to be co-immunoprecipitated. This proximity resulted in these channels being electrically recorded as a single channel event. They further demonstrated that BK_{Ca} channels were not proportionately represented 1:1 with CaV1.3 channels but rather that clusters of BK channels were surrounded by clustered CaV1.3 channels. Indicating a potential role for CaV1.3 to control BK_{Ca}, potentially maintaining cell volume under stress of ADT.

We also examined some SK channels (SK1,2,3), these channels are not activated by voltage, but rather by relatively small levels of $[Ca^{2+}]_i$ through CaM binding the intracellular c-terminus (Girault et al., 2012). While there is not much research into the expression or function of SK channels in cancer they have been identified in breast (Potier et al., 2006), melanoma (Tajima et al., 2006) and glioma cells (Weaver et al., 2006). We examined the expression of all 3 isoforms and found that the most prominent expression was of the SK2 channel, which was highly expressed in all cell types compared to the other isoforms (Appendix D, Figure D.4). We found that expression, like the BK_{Ca} channel, was reduced when cells were treated with ADT and there was a significant reduced expression seen in the LNCaP-abl cells of all isoforms (Figure 6.5 (B)(i)) (Appendix D, Figure D.3). This suggests that inhibiting the action of the AR through ADT may be inhibiting the expression of K^+ channels in PCa. Sex hormones such as androgens have been shown to regulate both expression and activation of K^+ channels (Sakamoto and Kurokawa, 2019), although this has not been studied in PCa. However, we have shown that the reduced expression observed after ADT was not influenced by the expression of CaV1.3, as we did not observe any altered expression when CaV1.3 was silenced.

Overall, the reduced expression of K^+ channels seen after ADT must result in a reduced K^+ current in the cells. There are reports which suggest that NED occurs due to reduced potassium current (N. Prevarskaya et al., 2007). Since we have also observed an increased expression of NSE in the cells after ADT, there could be an association with the reduced expression of K^+ channels.

However, for this project it appears that there is no transcriptional regulation inferred from the nuclear localisation of CaV1.3 as there is no effect seen on K+ channel expression after CaV1.3 is silenced.

6.3.3 Calcium signalling

As indicated throughout this project, Ca^{2+} signalling is a complex system which has a diverse range of proteins involved in signal transduction. As previously outlined in chapter 1, there are Ca^{2+} regulated transcription factors CREB and NFAT which are activated when Ca^{2+} binds to the Ca^{2+} sensing signal transducer CaM. Interestingly both transcription factors had increased expression in the LNCaP-ADT cells with NFAT upregulated (Figure 6.6), while there was a significant increase detected in the expression of CREB (Figure 6.6 (B)). However, this increased expression was not due to transcriptional regulation by CaV1.3, as silencing CaV1.3 had no effect on the expression levels of either transcription factor. However further work looking at transcriptional activity and protein activation would also need to be investigated to confirm. Activation of CREB has been reported previously in LNCaP cells after ADT (Y. Zhang et al., 2018), in fact the progression to NED and androgen independence is widely associated with CREB activation (Deeble et al., 2007; Farini et al., 2003; Sang et al., 2016). This is consistent with our cell model indicating increased expression of CREB and increased NED in the LNCaP-ADT cells. Likewise there are many reports indicating NFAT signalling in PCa progression (Lehen'Kyi et al., 2007; Thebault et al., 2006), although usually associated with activation via calcium entry from TRPC channels, which we also found to be upregulated in LNCaP-ADT cells (Appendix D; Figure D2).

Calm1 is the gene that codes for CaM, a calcium binding protein involved in the proliferation of androgen sensitive prostate cancer cells (Cifuentes et al., 2004). This protein as outlined previously is responsible for the activation of NFAT, through calcineurin which dephosphorylates NFAT allowing nuclear translocation and transcriptional activation (Berridge et al., 2003). CaM also activates CAMKII, a protein kinase responsible for phosphorylating CREB and activating transcriptional regulation within the nucleus. Hence, CaM is an important part of the Ca^{2+} signal transduction pathway. This protein also regulates Ca^{2+} dependent inhibition (CDI) of CaV1.3, by binding to the c-terminal modulator domain (Kuzmenkina et al., 2019), so it has a direct role in regulating CaV1.3's open potential. We looked at the genetic expression of Calm1 and found that there was significantly increased expression in the LNCaP-abl cells (Figure 6.7 (A)(i)), again there

was no transcriptional regulation attributed to CaV1.3 expression as silencing CaV1.3 had no effect on expression of Calm1 (Figure 6.7 (A)(ii)). As outlined in research by Cifuentes et al. CaM has an affinity for AR in the presence of Ca^{2+} and they indicate that the expression level of CaM is increased with the expression of AR, as they have a significantly reduced expression in the AR negative PC3 cell line (Cifuentes et al., 2004). This could explain the increased expression of Calm1 in LNCaP-abl cells, which as we have demonstrated have an increased expression of AR (Figure 3.2).

Next, we examined the expression of the CAMKII genes, which are a family of CaM kinases with 4 isoforms (α, β, δ and γ). We focused our research on the expression of CAMKIIβ and CAMKIIγ, as research has shown that the kinase activity and expression of these two isoforms was increased when AR was silenced in PCa (Rokhlin et al., 2007). Our research indicated no significant change in expression between cell types, suggesting that ADT does not affect expression of CAMKII genes. Although there is an increased trend observed in CAMKIIβ expression in the LNCaP-ADT cells, which have 1.8-fold compared to LNCaP cells (Figure 6.7 (B)(i)). Research has demonstrated that CAMKII expression is inhibited by active AR, with expression of CAMKIIβ and CAMKIIγ increased after androgen withdrawal or when AR expression levels are reduced (Rokhlin et al., 2007). Since expression of AR is increased after treatment with bicalutamide in our cell model, it would suggest that the inhibited expression of CAMKII genes is regulated by AR activation rather than AR expression. Interestingly, we found that genetic expression of CAMKIIβ was significantly increased in all cells when CaV1.3 was silenced (Figure 6.7 (B)(ii)). We also detected an increased expression in CAMKIIγ in all cells when CaV1.3 was silenced, although this did not achieve significance (Figure 6.7 (C)(ii)). This suggests a mechanism in PCa cells involving CaV1.3 inhibiting expression of CAMKIIβ, potentially through AR activation. There is no research available in PCa specifically which identifies a link between CaV1.3 and CAMKIIβ, as with most research involving VGCC we find relevant research in the central nervous system. Although not directly relatable this could provide insights for future study. Research in neurons has indicated a clustering of CAMKII to the c-terminus of CaV1.3 (Jenkins et al., 2010; Malik et al., 2014; Wheeler et al., 2012). One such study outlines an interesting nuclear shuttle which involves accumulation of both CAMKIIβ and CAMKIIγ to the CaM bound region of CaV1.3 c-terminus. Subsequent increased $[Ca^{2+}]_i$, which they purported to be as a result of influx through CaV1.3, but equally may be as a result of the increased SOCE we have observed, results in activation of CAMKIIβ which phosphorylates CAMKIIγ. This then binds Ca^{2+}/CaM and translocate to the nucleus where it activates gene transcription via CREB (Ma et al., 2014). This correlates with our findings of an increased expression of CREB, which has been shown to increase NED and cell survival in ADT treated PCa (Y. Zhang et al., 2018). This increased

CREB and CaV1.3 after ADT highlights a potential mechanism through which CaV1.3 could be influencing survival and disease progression. It may be beneficial in future research to investigate the activity of CREB through analysis of the phosphorylation status in conjunction with CaV1.3 expression. This could identify an association between CaV1.3 expression and CREB activation.

6.4 Concluding remarks.

Here we have highlighted various associations between CaV1.3 and SOCE regulating genes which may indicate a mechanism through which CaV1.3 is influencing the altered SOCE driving PCa progression. We have observed a significant increased expression of RyR1 in the LNCaP-ADT cells which is reduced when CaV1.3 is silenced. This may indicate a mechanism through which the SOCE is enhanced in these cells and reduced when CaV1.3 is silenced. Although the Ca^{2+} imaging experiments were inconclusive and would require further investigation to elucidate an association. However, numerous studies have reported a functional interaction between RyR and CaV1.3 in excitable cells. Therefore, further research such as co-immunoprecipitation or immunofluorescence could identify similar functional interaction in relation to PCa progression.

We found that NCX channels were increased after ADT, with NCX2 having a significant increase in the LNCaP-abl cells which was further increased when CaV1.3 is silenced. NCX2 can increase the $[Ca^{2+}]_i$ when working in its reverse mode, which has been shown in PCa. Overall indicating a mechanism through which silencing CaV1.3 may be contributing to enhanced intracellular Ca^{2+} in the LNCaP-abl cells. Also, the increased expression of CAMKIIβ observed in these cells upon CaV1.3 silencing may increase the activity of CREB, a transcription factor for NCX.

There was also an increased expression of Ca^{2+} associated transcription factors in cells which have undergone ADT. Suggesting that upregulation of Ca^{2+} signalling is a process of PCa progression under ADT. Ca^{2+} signalling is associated with most cellular processes; therefore, this was not an unusual finding. Although, we did not detect transcriptional regulation which could be directly linked to CaV1.3, we did find that silencing CaV1.3 enhanced the expression of the kinase CAMKIIβ. This in turn is responsible for a Ca^{2+} signalling mechanism which results in transcription, indicating that CaV1.3 expression may be regulating this response.

Overall, this chapter identifies avenues for further research but there are some interesting indications. It appears that there may be a mechanism involving RyR1 and CaV1.3, which may be driving the SOCE increase seen in the LNCaP-ADT cells. Whereas the increased expression of RyR2 or NCX2 in the LNCaP-abl cells may contribute to the increased SOCE seen in these cells when CaV1.3 is silenced. Further analysis of with RyR or NCX inhibitors in conjunction with CaV1.3 silencing may be beneficial to explore these preliminary indications.

Chapter 7 - Final summary

7.1 Introduction

PCa is the most diagnosed cancer in Irish men, excluding non-cutaneous skin cancer, and the third most common cause of cancer related deaths in this cohort, highlighting the considerable burden of this disease. The most commonly utilised treatment for advanced PCa is ADT, which has a short term inhibitory effect on PCa progression, lasting approximately 2 years. After which the disease progresses to the incurable CRPC stage. There are limited treatments available for patients who develop CRPC, consisting predominantly of palliative cytotoxic chemotherapies, such as docetaxel.

Ca^{2+} signalling is involved in many regulatory pathways which are required for the emergence of cancer. Altered expression of Ca^{2+} channels have recently been identified as having a role in the emergence and progression of many cancers. In particular, the upregulation of the VGCC CaV1.3 has been identified in PCa, with a further enhanced expression identified in CRPC. However, there is no research into the mechanism through which this upregulation may be influencing the progression of PCa. Hence our research aimed to investigate CaV1.3 to identify new targets for alternative treatment strategies to prevent the disease progression to the CRPC stage, ultimately prolonging progression free survival.

7.2 Key findings

This research has identified mechanisms related to aberrant Ca^{2+} mobilisation under ADT in PCa. Highlighting throughout targets which could lead to the development of personalised treatment strategies that could prove beneficial in the fight against PCa and prevent the progression to CRPC. Outlined below are the key findings of our study and the overall conclusion to this work.

7.2.1 ADT drives the upregulation of CaV1.3 which correlates with Gleason score and biochemical relapse.

ADT is the main treatment used for PCa patients with advanced disease, however this treatment is associated with the development of an aggressive treatment resistant PCa phenotype. CRPC is unresponsive to ADT and results in patient mortality. In chapter 3 we confirmed that our cell model mimicked this progression under ADT, with an enhanced proliferation and viability demonstrated in the CRPC cell model (LNCaP-abl). We also detected an enhanced expression of AR and NSE associated with the emergence of a resistant phenotype. Along with that we have shown in the *in vivo* mouse model that ADT coincided with the emergence of a stem cell phenotype and EMT. All of which have been previously outlined in research to be associated with PCa progression and poor patient outcome.

Currently the underlying mechanisms driving PCa disease progression are unclear, however there is an increasing amount of emerging evidence implicating ion channels, particularly Ca^{2+} channels in neoplastic transformation. VGCC have been shown to have an altered expression across many cancer types. In particular, the VGCC CaV1.3 has been identified as having upregulated expression in PCa tissues, despite this there is no research to date indicating any associated functional influence on the disease. Our research sought to investigate CaV1.3, in particular in the progression to CRPC under ADT.

Initially our bioinformatic analysis of patient tissue samples established an increased expression of CaV1.3 in primary disease compared to adjacent normal tissue, which was further increased in metastatic disease – confirming previous results from other groups. However, this analysis also identified for the first time that CaV1.3 expression was significantly upregulated in patients treated with ADT. Suggesting that ADT is the driver for CaV1.3 expression. This increased expression also correlated with increased Gleeson score and reduced time to biochemical recurrence. These observations were replicated and validated in a range of other models. Our cell line model showed that genetic expression was significantly increased after treatment with ADT. The protein expression of CaV1.3 was also significantly increased after ADT in the CRPC cell model. These findings were confirmed in the *in vivo* mouse model with a significant increase in CaV1.3 expression in mice treated with ADT. Confirmation of this results across a range of models as we have outlined confirms the validity of this result demonstrating a true cause and effect between CaV1.3 expression and ADT.

The cellular location analysis of the CaV1.3 protein also indicated the expression of the c-terminus in the nucleus of the androgen sensitive cell lines, but absent from the CRPC cell line. The nuclear expression of the c-terminus of CaV1.3 has previously been observed in other tissues where it has been shown to have a role in transcriptional regulation. However, this is the first time that this has been identified in terms of cancer, let alone PCa. This area requires further research to determine if this expression is influencing transcriptional regulation in PCa. A chromatin immunoprecipitation and DNA sequencing (CHIP-seq) analysis could be beneficial in determining if the c-terminus fragment is binding to specific DNA sites of interest.

Overall, the research confirms that the expression of CaV1.3 is increased with the development of CRPC and is associated with ADT. Implicating CaV1.3 in PCa disease progression and identifying CaV1.3 as a potential treatment target. The correlation with Gleeson score suggests that CaV1.3 may also be indicated as a biomarker of disease progression and the development of treatment resistance.

7.2.2 CaV1.3 expression drives calcium mobilisation through the SOCE mechanism in PCa, which alters with disease progression.

Our initial findings identified upregulated CaV1.3 was associated with ADT and correlated to disease progression. However, we needed to determine if the channel was functional and contributing to PCa biology through the mobilisation of Ca^{2+}. In chapter 4 we discovered increased CaV1.3 resulted in increased Ca^{2+} in cells treated with ADT in the short term and the long term, up to CRPC. This novel finding led us to investigate how the increased expression of CaV1.3 influenced Ca^{2+} mobilisation in the cells, which we felt could be driving treatment resistance. However, we found that CaV1.3 was not functioning through the normal mechanism, whereby it would facilitate the passage of Ca^{2+} across the plasma membrane under cellular depolarisation. Instead we discovered an anamolous mechanism whereby CaV1.3 expression was facilitating an increased SOCE without having any influence on store release.

Interestingly, this enhanced SOCE seemed to alter with disease progression, with short term ADT increasing the Ca^{2+} entry significantly, with an even further increased SOCE in the CRPC cell line. We also found that the contribution CaV1.3 had on the SOCE mechanism altered with disease progression. Silencing the expression of CaV1.3 in the cells treated with ADT reduced the SOCE back to normal levels, however, the same process significantly increased the SOCE in the CRPC cell

line. This suggests that CaV1.3 may directly assist SOCE under ADT, but once the disease progresses to CRPC it acts as a Ca^{2+} regulator, since silencing the expression significantly enhances SOCE.

Despite the effective inhibition of SOCE observed in the cells under ADT when CaV1.3 was silenced, we did not observe any effect on the functional aspects that we tested. Therefore, an investigation looking at other hallmarks could identify how this altered Ca^{2+} is contributing to PCa survival in these cells treated with ADT. We did find silencing CaV1.3 significantly reduced the proliferation and the viability of the CRPC cell line. However, we hypothesise that this is most likely due to mitochondrial Ca^{2+} overload. These cells had a significant increased Ca^{2+} influx after CaV1.3 was knocked down and research has shown that a large influx in SOCE induces apoptosis. Therefore, CaV1.3 may be preventing Ca^{2+} overload thus inhibiting apoptosis in advanced PCa. Further investigation would be required to definitively assess the apoptosis status of these cells. It would also be beneficial to develop an *in vivo* model to further investigate our observations, along with analysing the effect of silencing CaV1.3 on the hallmarks we detected in the mouse models. CaV1.3 may be contributing to the markers we were unable to detect in the 2D model such as the expression of CSC surface markers or the EMT.

We have shown that CaV1.3 contributes to the aberrant intracellular Ca^{2+} in PCa which is altered as the disease develops castrate resistance. We have also shown that targeting this channel with siRNA can influence these cells depending on the stage of the disease, with CRPC potentially undergoing apoptosis. There are currently no drugs available to treat this incurable disease stage, so highlighting this mechanism identifies a target which, with some further investigation, may be used in treatment development. We investigated the idea of repurposing a dihydropyridine (nifedipine), which targets the dihydropyridine receptor on CaV1.3. However, we have been unable to elicit any significant effect from incubating the cells with this one CCB. There are many other CCB's available which target various channels with different affinities. We suggest going forward that a drug screening panel could be used to identify a drug with a better specificity to inhibiting CaV1.3. Also, given the fact that CaV1.3 does not appear to be functioning in its canonical way as a plasma membrane bound Ca^{2+} channel, it may be better to look at inhibiting the associated SOCE proteins. There are also many drugs which target SOCE pathways used currently to treat various other illnesses. Therefore, identifying an effective inhibitor could be beneficial in indicating a drug which could be repurposed to treat PCa.

7.2.3 HIF-1α expression is stabilised by the CaV1.3 regulated SOCE and enhances the expression of AR.

Our research demonstrates that ADT enhances the expression of CaV1.3 which leads to increased SOCE. We have shown that this coincides with an increased expression of NSE and AR, both which are associated with disease progression. Research has shown that not only is hypoxia a general feature of cancerous tumours which is associated with poor prognosis and disease progression, but that it is also enhanced after ADT in PCa. Hypoxia results in the stable expression of HIF-1α, a transcription factor which has been shown to promote tumour cell survival. Interestingly HIF signalling has also been shown to rely on the influx of Ca^{2+} to assist with the stable expression and nuclear translocation. Therefore, we decided to establish if there was any link between the increased CaV1.3 induced Ca^{2+} observed after ADT and the stable expression of HIF-1α. Which could indicate a mechanism through which PCa was evading treatment and progressing to CRPC.

Our research found that hypoxia had no bearing on the expression of CaV1.3, which was only influenced by ADT treatment. However, we have shown that the upregulation of CaV1.3 and the subsequent increased intracellular Ca^{2+} does influence the expression of HIF-1α under hypoxic conditions. We found that when we silenced the expression of CaV1.3 in the LNCaP-ADT cells, which corresponded with a reduction in SOCE, that the expression of HIF-1α was also reduced. However, in the LNCaP-abl cells, silencing CaV1.3 which increased the SOCE also increased the expression of HIF-1α. Suggesting that the alteration in intracellular Ca^{2+} was affecting the stability of HIF-1α under hypoxic conditions. Also highlighting the requirement of Ca^{2+} to induce and promote HIF signalling, which in turn we know promotes PCa progression. Interestingly the expression of the AR, which was upregulated under hypoxic conditions also followed this trend. There was an increased expression in the LNCaP-abl when CaV1.3 was silenced which coincided with the increased HIF-1α expression and the enhanced SOCE. This research highlight for the first time a link between the CaV1.3 driven Ca^{2+} regulation and the expression of HIF-1α as well as a link to AR in PCa, highlighting another mechanism which may be driving disease progression and treatment resistance. It is well known that AR and HIF both drive the emergence of NSE and EMT leading to treatment resistance. Thus, further illustrating the benefit in identifying a small molecule which could inhibit the enhanced SOCE observed in these cells.

However, we also observed that silencing CaV1.3 in the LNCaP cells had a similar effect on the expression of HIF-1α as that observed in the LNCaP-ADT cells. Although the LNCaP cells had no alteration observed in the SOCE when CaV1.3 was silenced. Significantly, both the LNCaP and the

LNCaP-ADT cells had the nuclear expression of the c-terminus, which may be having an influence on the expression of HIF-1α in these cells under hypoxia. As alluded to earlier a CHIP-seq analysis may be beneficial in determining if there is a link in the c-terminus nuclear expression of CaV1.3 and the transcriptional regulation of HIF-1α under hypoxic conditions. Since this association did not occur in these cells under normal O_2, with levels of HIF-1α unchanged when CaV1.3 was silenced, we can hypothesise that the regulation may be on the O_2 dependent HIF-1α regulating proteins such a von Hippel-Lindau (VHL).

Interestingly we also found that under normal O_2 conditions treatment with ADT significantly enhanced the expression of HIF-1α, which was not the case once the disease developed CRPC. There are many reasons why we might observe increased expression of HIF-1α under normal O_2, since research has shown that certain growth factors can enhanced the translation or the stability of HIF-1α independent of O_2 regulation pathways. This also coincides with an increased expression of CaV1.3 and AR in these cells. As we have shown, the expression of AR is enhanced by the expression of HIF-1a and the increased SOCE, this could be a mechanism through which the cells survive the initial ADT treatment.

Overall, this research has identified a novel CaV1.3/Ca^{2+}/AR/HIF-1α axis mechanism which may be driving treatment resistance and progression to CRPC. Again, this identifies a targetable mechanism which may be beneficial in treatment development that could lead to improved patient outcomes. There are also a panel of drugs available which target HIF signalling, which could be used to elicit a synergistic effect with ADT or SOCE targeting drugs.

7.2.4. Expression of SOCE associated channels and calcium regulated transcription factors are upregulated after ADT.

Our research has demonstrated for the first time that CaV1.3 does not function in PCa cells as a VGCC, but rather it regulates the SOCE. However, the exact mechanism underpinning the activation of CaV1.3 in SOCE is not fully clear, thus we sought to identify associated ion channels which may be influencing the SOCE in these cells. We also wanted to investigate the effect that this enhanced SOCE had on downstream Ca^{2+} signalling, potentially driving PCa progression.

We have formulated some hypothesis based on the expression of these associated Ca^{2+} proteins which could form the basis of future studies. We have shown that the regulatory influence CaV1.3

has on the SOCE mechanism alters over disease progression, here we show that there is also an altered expression of some channels involved in the SOCE process which may indicate the mechanism involved in CaV1.3 influence on SOCE and the progression to CRPC.

We have identified an association between RyR1 expression and CaV1.3 in the LNCaP-ADT cells which may be influencing the SOCE in these cells. RyR1 was significantly increased in these cells and was significantly reduced when CaV1.3 was silenced, reflecting the SOCE observed under these conditions. Since CaV1.3 has been shown previously to have an interactional role with RyR in other tissues, this suggests that an interaction between these channels may be influencing the SOCE in these cells.

We have also observed a significant increased expression of NCX2 in the CRPC cell line which is further enhanced when CaV1.3 is silenced. NCX has been associated with a reverse mode activation in PCa cells, with an inhibitory interaction between NCX and CaV1.3 also previously indicted in colon cancer. This suggests that CaV1.3 may be inhibiting the reverse mode activation of NCX in the CRPC cell line, since silencing CaV1.3 significantly increased both expression of NCX and the intracellular Ca^{2+} in these cells. Further work could develop this hypothesis, potentially using the reverse mode inhibitor KB-R7943 to identify if the increased SOCE seen after silencing the expression of CaV1.3 was due to NCX reverse mode Ca^{2+} influx.

Our research has also shown that the increased expression of CaV1.3 and the corresponding increased Ca^{2+} after ADT coincides with an enhanced expression of the Ca^{2+} regulated transcription factors CREB and NFAT. Both of which have been previously implicated in PCa progression. CREB activation has been shown in LNCaP cells under ADT, which was attributed to the enhanced NED. There is a significant increased expression of CREB in the LNCaP-ADT cells, which coincides with the emergence of NED marker NSE. This research suggests that the increased SOCE we observe in these cells may be contributing to enhanced activation of CREB which is driving the expression of NSE and the emergence of a treatment resistant cell type. The enhanced expression of NFAT has also been shown to assist in PCa progression, particularly associated with activation after Ca^{2+} influx via the TRPC channel. We have detected increased expression of TRPC1 in the cells treated with ADT in the short term. This may be enhancing the activation of NFAT which could drive PCa progression. Overall, these upregulated transcription factors may be indicative of a downstream mechanism through which enhanced Ca^{2+} entry after ADT is driving the progression to CRPC. Therefore, targeting this mechanism could reduce treatment resistance and disease progression.

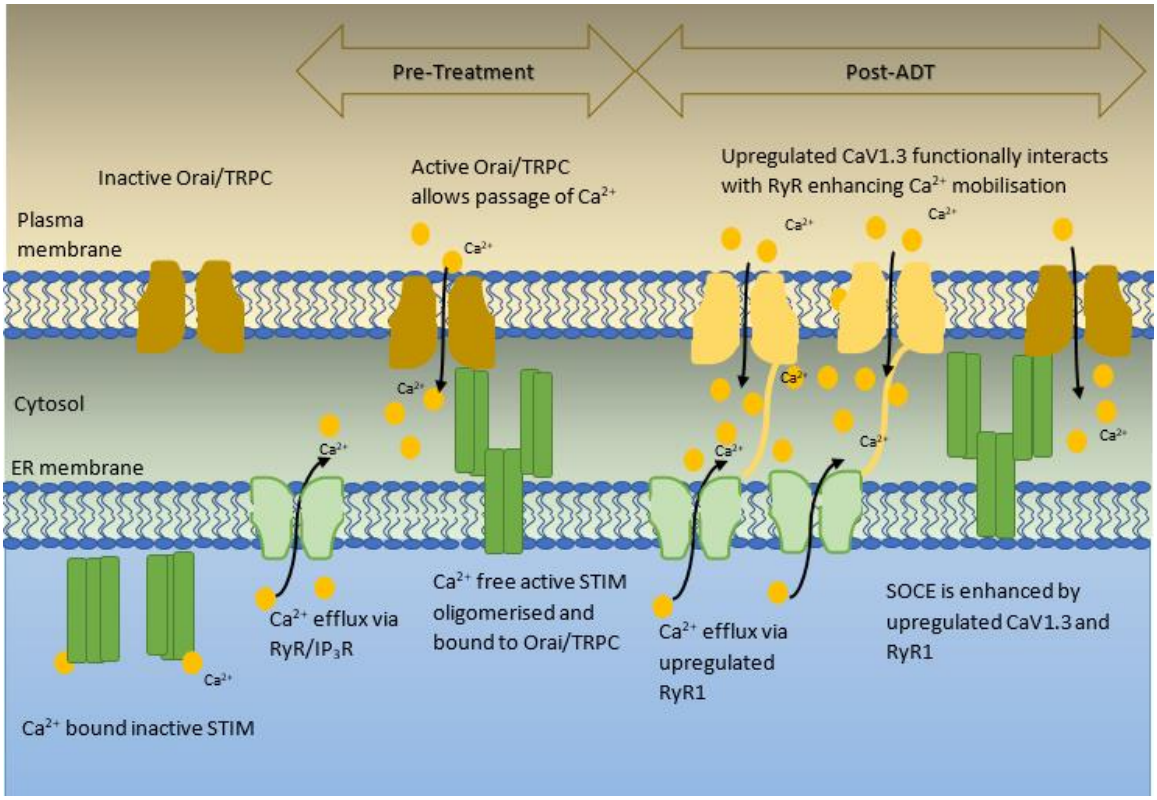

Figure 7.1: Proposed mechanism for the CaV1.3 enhanced SOCE in cells after initiation of ADT: The SOCE mechanism is usually facilitated by the release of Ca^{2+} from the ER through the ER channels IP3R and RyR. The loss of ER Ca^{2+} is detected by the ER bound protein STIM, which undergoes oligomerisation and translocation to the plasma membrane. Here it binds to and activates the plasma membrane bound Ca^{2+} permeable ion channels Orai or TRPC, facilitating the passage of Ca^{2+} into the cytosol where it replenishes the ER stores through the SERCA channel. When PCa cells are treated with ADT there is an enhanced expression of CaV1.3 and RyR1, which functionally interact. This functional interaction enhances the SOCE, increasing the intracellular Ca^{2+} concentration. Silencing the expression of CaV1.3 also reduces the expression of RyR1 and subsequently reduces the SOCE back to base level. The enhanced Ca^{2+} entry under ADT drives the activation of the Ca^{2+} regulated transcription factors (Figure 7.3) and the expression of genes such as NSE and AR which assist the cell survival and treatment resistance, which facilitates the disease progression to the incurable CRPC.

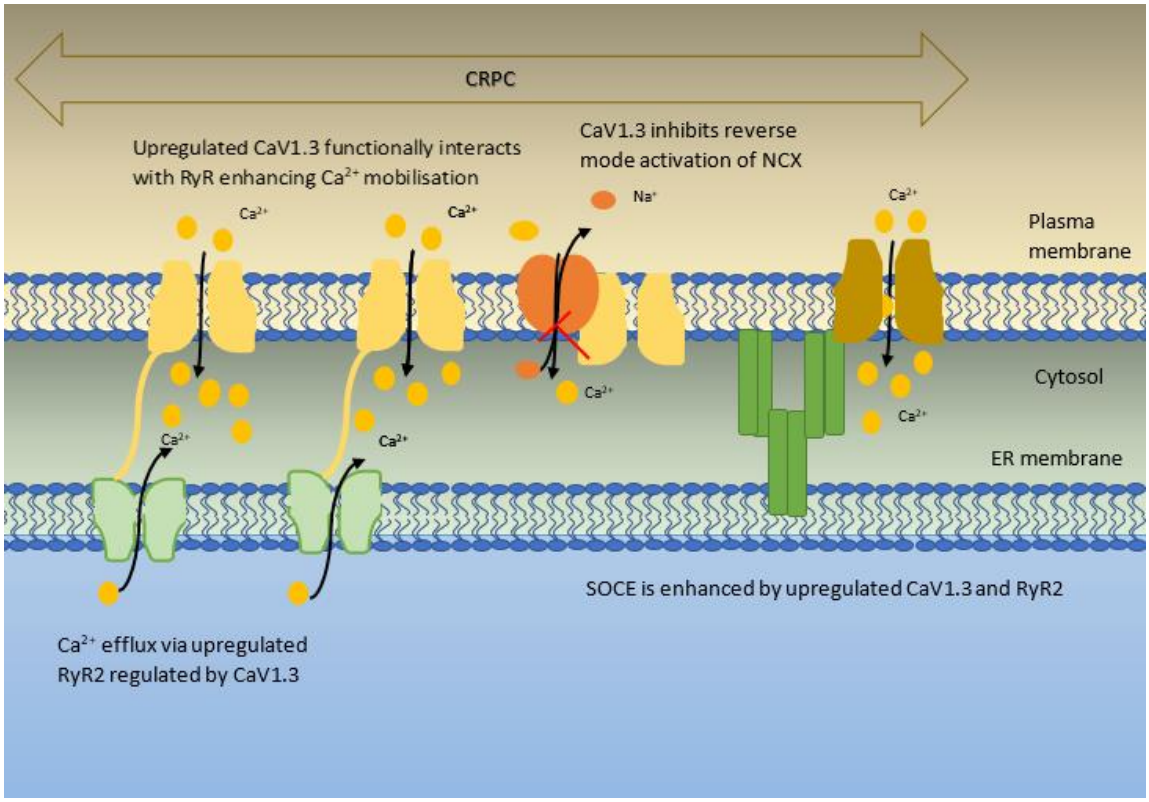

Figure 7.2: Proposed mechanism for the CaV1.3 regulated enhanced SOCE in the CRPC cells: As the disease progresses to the castrate resistant stage the contribution of CaV1.3 to the intracellular Ca^{2+} alters. There is an enhanced expression of CaV1.3 and RyR2, which functionally interact and enhances the SOCE, increasing the intracellular Ca^{2+} concentration. CaV1.3 also inhibits the reverse mode action of NCX2 in the plasma membrane, preventing Ca^{2+} overload. Silencing the expression of CaV1.3 in these cells has no effect on the expression of RyR2 but increases expression of NCX2. The loss of CaV1.3 allows NCX2 reverse mode activation which increases Ca^{2+} entry resulting in Ca^{2+} overload, resulting in reduced proliferation. Therefore, it appears that CaV1.3 enhanced the SOCE through interaction with RyR2 but inhibits calcium overload by inhibiting reverse mode activation of NCX.

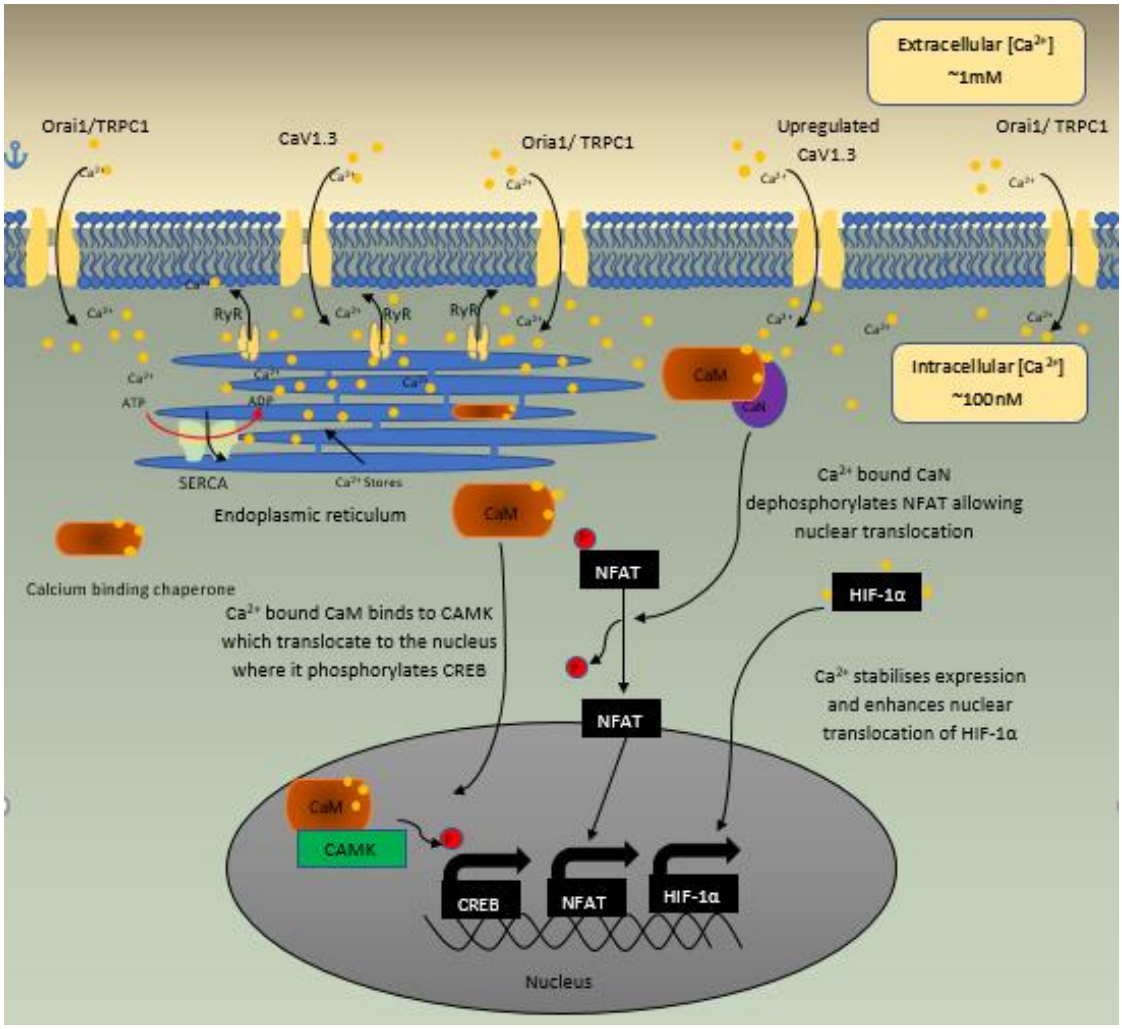

Figure 7.3: Proposed mechanism for the CaV1.3 driven enhanced Ca^{2+} signalling pathways: The Ca^{2+} signalling mechanism is enhanced in cells which have an increased intracellular Ca^{2+}, which enhances the activity of the Ca^{2+} regulated transcription factors. There is also a stabilising effect on the transcription factor HIF-1α. Overall enhancing the activity of these transcription factors under ADT may could drive the expression of genes which assist in treatment resistance and disease progression.

7.3 Overall conclusion

CaV1.3 is upregulated in PCa, particularly CRPC and is associated with Gleeson score and time to biochemical relapse, highlighting the need for new treatment targets in this disease. This project has investigated the role of CaV1.3 in driving the progression to CRPC. Herein we have identified for the first time that ADT enhances the expression of CaV1.3 in PCa, which drives disease progression as demonstrated by increased Gleason score. This expression is also associated with enhanced expression of PCa markers such as AR and we have shown that it directly drives PCa biology by enhancing viability under ADT and maintaining proliferation in CRPC. Taken together this confirms that CaV1.3 is associated in PCa progression and could be used as both a biomarker for treatment resistance and a drug target to prevent disease progression.

We have identified a novel association between CaV1.3 and the SOCE, this unprecedented work shows that CaV1.3 can differentially regulate this process over disease progression to CRPC. Most significantly we have identified that CaV1.3 is a key driving mechanism in the expression of HIF-1α, which has been shown to have a significant consequence in driving cancer progression. Inhibiting this CaV1.3 mediated HIF signalling could be a key target preventing treatment resistance in PCa with translational capacity to many cancers.

Overall, this project has highlighted a novel CaV1.3/SOCE/HIF-1α mechanism which validates the importance of Ca^{2+} signalling in PCa which could translate to many cancers. Highlighting a new area for drug development which could have a direct beneficial effect on preventing progression to CRPC. Ultimately prolonging progression free survival and patient life expectancy.

7.4 Future directions

Our research has identified many novel aspects in the progression of PCa under ADT to CRPC. We have identified a novel mechanism through which ADT drives the expression of CaV1.3 which enhances the SOCE in these cells, facilitating treatment resistance and cell survival.

Throughout this research we have highlighted some areas which could be further investigated to progress this important research and develop specific treatment strategies. Some indications for future work are outlined below.

1. The functional activity of the c-terminus

   We have shown for the first time that there is expression of the c-terminus fragment of CaV1.3 in the nucleus of the androgen sensitive PCa cells. However, it would be very beneficial to identify if this c-terminus was regulating transcription. A CHIP-seq analysis could be used to identify specific DNA regions associated with this nuclear expression of this protein fragment. This could be used to identify any genes of interest that may be regulated by CaV1.3 which could be driving the progression of PCa.

2. Develop an *in vivo* model to look at hallmarks of cancer to better elucidate the potential influence of CaV1.3.

   Our research has shown that increased Ca^{2+} mobilisation due to enhanced expression of CaV1.3 results in increased expression of CSC markers and EMT in the in vivo mouse model. It would be beneficial to develop this model further to determine if silencing the expression of CaV1.3 had any impact on this area.

3. Drug screen to identify a small molecule which may have the same effect as silencing CaV1.3, better suppress CaV1.3 action or synergistically target CaV1.3 and HIF.

   We have looked at the effect on Ca^{2+} mobilisation in the cells which had increased expression of CaV1.3. We have also looked at the effect on this Ca^{2+} mobilisation when the cells were treated with the dihydropyridine nifedipine. While we were unable to elicit an effect using this CCB, there are many other CCB on the market which have varying affinities for specific channels. Going forward it would be very beneficial to perform a drug screen analysis on these CCB's to identify a drug which could be used to target CaV1.3. As

stated, this could be extended to include drugs which target other channels involved in SOCE.

4. Investigate the mechanism through which CaV1.3 alters the SOCE through associated protein interactions.

   We have demonstrated that CaV1.3 is associated with enhanced SOCE in PCa cells which have undergone ADT. We have also shown that there is an associated expression profile between CaV1.3 and other ion channels responsible for Ca^{2+} mobilisation. Further work looking at protein interactions could further evaluate an association which could provide the mechanism through which SOCE is altered with disease progression. Co-immunoprecipitation could be utilised to establish if there are any protein-protein interactions involved and if these interactions are transitionary as the disease progresses to CRPC.

5. Establish if CaV1.3 has a similar function in other cancers

   The novel findings of this research could translate to other cancer types, specifically hormone regulated cancers. As we have outlined CaV1.3 has been shown to have upregulated expression in many cancers. Therefore, it would be advantageous to investigate CaV1.3 associated Ca^{2+} mobilisation in these diseases.

Bibliography

Abdul Kadir, L., Stacey, M., Barrett-Jolley, R., 2018. Emerging Roles of the Membrane Potential: Action Beyond the Action Potential. Front. Physiol. 9. https://doi.org/10.3389/fphys.2018.01661

Abdul, M., Hoosein, N., 2006. Reduced Kv1.3 Potassium Channel Expression in Human Prostate Cancer. J. Membr. Biol. 214, 99–102. https://doi.org/10.1007/s00232-006-0065-7

Abdul, M., Hoosein, N., 2002. Expression and activity of potassium ion channels in human prostate cancer. Cancer Lett. 186, 99–105. https://doi.org/10.1016/S0304-3835(02)00348-8

Adasme, T., Haeger, P., Paula-Lima, A.C., Espinoza, I., Casas-Alarcón, M.M., Carrasco, M.A., Hidalgo, C., 2011. Involvement of ryanodine receptors in neurotrophin-induced hippocampal synaptic plasticity and spatial memory formation. Proc. Natl. Acad. Sci. 108, 3029–3034. https://doi.org/10.1073/pnas.1013580108

Alberts, B., Johnson, A., Lewis, J., Raff, M., Roberts, K., Walter, P., 2002. Ion Channels and the Electrical Properties of Membranes. Mol. Biol. Cell 4th Ed.

Alex, A.B., Pal, S.K., Agarwal, N., 2016. CYP17 inhibitors in prostate cancer: latest evidence and clinical potential. Ther. Adv. Med. Oncol. 8, 267–275. https://doi.org/10.1177/1758834016642370

Alexander, S.P., Catterall, W.A., Kelly, E., Marrion, N., Peters, J.A., Benson, H.E., Faccenda, E., Pawson, A.J., Sharman, J.L., Southan, C., Davies, J.A., 2015. The Concise Guide to PHARMACOLOGY 2015/16: Voltage-gated ion channels. Br. J. Pharmacol. 172, 5904–5941. https://doi.org/10.1111/bph.13349

Al-Hajj, M., Clarke, M.F., 2004. Self-renewal and solid tumor stem cells. Oncogene 23, 7274–7282. https://doi.org/10.1038/sj.onc.1207947

Alinezhad, S., Väänänen, R.-M., Mattsson, J., Li, Y., Tallgrén, T., Ochoa, N.T., Bjartell, A., Åkerfelt, M., Taimen, P., Boström, P.J., Pettersson, K., Nees, M., 2016. Validation of Novel Biomarkers for Prostate Cancer Progression by the Combination of Bioinformatics, Clinical and Functional Studies. PLOS ONE 11, e0155901. https://doi.org/10.1371/journal.pone.0155901

Alqawi, O., Wang, H.P., Espiritu, M., Singh, G., 2007. Chronic hypoxia promotes an aggressive phenotype in rat prostate cancer cells. Free Radic. Res. 41, 788–797. https://doi.org/10.1080/10715760701361531

Amin, A.R.M.R., Karpowicz, P.A., Carey, T.E., Arbiser, J., Nahta, R., Chen, Z.G., Dong, J.-T., Kucuk, O., Khan, G.N., Huang, G.S., Mi, S., Lee, H.-Y., Reichrath, J., Honoki, K., Georgakilas, A.G., Amedei, A., Amin, A., Helferich, B., Boosani, C.S., Ciriolo, M.R., Chen, S., Mohammed, S.I., Azmi, A.S., Keith, W.N., Bhakta, D., Halicka, D., Niccolai, E., Fujii, H., Aquilano, K., Ashraf, S.S., Nowsheen, S., Yang, X., Bilsland, A., Shin, D.M., 2015. Evasion of anti-growth signaling: A key step in tumorigenesis and potential target for treatment and prophylaxis by natural compounds. Semin. Cancer Biol., A broad-spectrum integrative design for cancer prevention and therapy 35, S55–S77. https://doi.org/10.1016/j.semcancer.2015.02.005

Amini, S., Fathi, F., Mobalegi, J., Sofimajidpour, H., Ghadimi, T., 2014. The expressions of stem cell markers: Oct4, Nanog, Sox2, nucleostemin, Bmi, Zfx, Tcl1, Tbx3, Dppa4, and Esrrb in bladder, colon, and prostate cancer, and certain cancer cell lines. Anat. Cell Biol. 47, 1–11. https://doi.org/10.5115/acb.2014.47.1.1

Arcangeli, A., 2011. Ion channels and transporters in cancer. 3. Ion channels in the tumor cell-microenvironment cross talk. Am. J. Physiol. - Cell Physiol. 301, C762–C771. https://doi.org/10.1152/ajpcell.00113.2011

Ardura, J.A., Álvarez-Carrión, L., Gutiérrez-Rojas, I., Alonso, V., 2020. Role of Calcium Signaling in Prostate Cancer Progression: Effects on Cancer Hallmarks and Bone Metastatic Mechanisms. Cancers 12. https://doi.org/10.3390/cancers12051071

Armstrong, A.J., Garrett-Mayer, E.S., Yang, Y.-C.O., Wit, R. de, Tannock, I.F., Eisenberger, M., 2007. A Contemporary Prognostic Nomogram for Men with Hormone-Refractory Metastatic Prostate Cancer: A TAX327 Study Analysis. Clin. Cancer Res. 13, 6396–6403. https://doi.org/10.1158/1078-0432.CCR-07-1036

Armstrong, A.J., Lin, P., Tombal, B., Saad, F., Higano, C.S., Joshua, A.M., Parli, T., Rosbrook, B., van Os, S., Beer, T.M., 2020. Five-year Survival Prediction and Safety Outcomes with Enzalutamide in Men with Chemotherapy-naïve Metastatic Castration-resistant Prostate Cancer from the PREVAIL Trial. Eur. Urol. 78, 347–357. https://doi.org/10.1016/j.eururo.2020.04.061

Armstrong, A.J., Tannock, I.F., Wit, R. de, George, D.J., Eisenberger, M., Halabi, S., 2010. The development of risk groups in men with metastatic castration-resistant prostate cancer based on risk factors for PSA decline and survival. Eur. J. Cancer 46, 517–525. https://doi.org/10.1016/j.ejca.2009.11.007

Attard, G., Parker, C., Eeles, R.A., Schröder, F., Tomlins, S.A., Tannock, I., Drake, C.G., Bono, J.S. de, 2016. Prostate cancer. The Lancet 387, 70–82. https://doi.org/10.1016/S0140-6736(14)61947-4

Axelson, H., Fredlund, E., Ovenberger, M., Landberg, G., Påhlman, S., 2005. Hypoxia-induced dedifferentiation of tumor cells – A mechanism behind heterogeneity and aggressiveness of solid tumors. Semin. Cell Dev. Biol., Biology of Hypoxia and Myogenesis and Muscle Disease 16, 554–563. https://doi.org/10.1016/j.semcdb.2005.03.007

Azimi, I., 2018. The interplay between HIF-1 and calcium signalling in cancer. Int. J. Biochem. Cell Biol. 97, 73–77. https://doi.org/10.1016/j.biocel.2018.02.001

Bae, K.-M., Dai, Y., Vieweg, J., Siemann, D.W., 2016. Hypoxia regulates SOX2 expression to promote prostate cancer cell invasion and sphere formation. Am J Cancer Res 6, 1078–1088.

Baghban, R., Roshangar, L., Jahanban-Esfahlan, R., Seidi, K., Ebrahimi-Kalan, A., Jaymand, M., Kolahian, S., Javaheri, T., Zare, P., 2020. Tumor microenvironment complexity and therapeutic implications at a glance. Cell Commun. Signal. 18, 59. https://doi.org/10.1186/s12964-020-0530-4

Bagur, R., Hajnóczky, G., 2017. Intracellular Ca2+ sensing: role in calcium homeostasis and signaling. Mol. Cell 66, 780–788. https://doi.org/10.1016/j.molcel.2017.05.028

Baig, S.M., Koschak, A., Lieb, A., Gebhart, M., Dafinger, C., Nürnberg, G., Ali, A., Ahmad, I., Sinnegger-Brauns, M.J., Brandt, N., Engel, J., Mangoni, M.E., Farooq, M., Khan, H.U., Nürnberg, P., Striessnig, J., Bolz, H.J., 2011. Loss of Ca v 1.3 (CACNA1D) function in a human channelopathy with bradycardia and congenital deafness. Nat. Neurosci. 14, 77–84. https://doi.org/10.1038/nn.2694

Barbado, M., Fablet, K., Ronjat, M., De Waard, M., 2009. Gene regulation by voltage-dependent calcium channels. Biochim. Biophys. Acta BBA - Mol. Cell Res., 10th European Symposium on Calcium 1793, 1096–1104. https://doi.org/10.1016/j.bbamcr.2009.02.004

Bardo, S., Cavazzini, M.G., Emptage, N., 2006. The role of the endoplasmic reticulum Ca2+ store in the plasticity of central neurons. Trends Pharmacol. Sci. 27, 78–84. https://doi.org/10.1016/j.tips.2005.12.008

Barreto-Chang, O.L., Dolmetsch, R.E., 2009. Calcium Imaging of Cortical Neurons using Fura-2 AM. J. Vis. Exp. JoVE. https://doi.org/10.3791/1067

Bates, E., 2015. Ion Channels in Development and Cancer. Annu. Rev. Cell Dev. Biol. 31, 231–247. https://doi.org/10.1146/annurev-cellbio-100814-125338

Bell, D.C., Butcher, A.J., Berrow, N.S., Page, K.M., Brust, P.F., Nesterova, A., Stauderman, K.A., Seabrook, G.R., Nürnberg, B., Dolphin, A.C., 2001. Biophysical properties, pharmacology, and modulation of human, neuronal L-type (alpha(1D), Ca(V)1.3) voltage-dependent calcium currents. J. Neurophysiol. 85, 816–827. https://doi.org/10.1152/jn.2001.85.2.816

Beltran, H., Yelensky, R., Frampton, G.M., Park, K., Downing, S.R., MacDonald, T.Y., Jarosz, M., Lipson, D., Tagawa, S.T., Nanus, D.M., Stephens, P.J., Mosquera, J.M., Cronin, M.T., Rubin, M.A., 2013. Targeted next-generation sequencing of advanced prostate cancer identifies potential therapeutic targets and disease heterogeneity. Eur. Urol. 63, 920–926. https://doi.org/10.1016/j.eururo.2012.08.053

Bennett, E.S., Smith, B.A., Harper, J.M., 2004. Voltage-gated Na+ channels confer invasive properties on human prostate cancer cells. Pflugers Arch. 447, 908–914. https://doi.org/10.1007/s00424-003-1205-x

Bennett, H.L., Stockley, J., Fleming, J.T., Mandal, R., O'Prey, J., Ryan, K.M., Robson, C.N., Leung, H.Y., 2013. Does androgen-ablation therapy (AAT) associated autophagy have a pro-survival effect in LNCaP human prostate cancer cells? BJU Int. 111, 672–682. https://doi.org/10.1111/j.1464-410X.2012.11409.x

Berridge, M.J., Bootman, M.D., Roderick, H.L., 2003. Calcium signalling: dynamics, homeostasis and remodelling. Nat Rev Mol Cell Biol 4, 517–529. https://doi.org/10.1038/nrm1155

Berry, P.A., Birnie, R., Droop, A.P., Maitland, N.J., Collins, A.T., 2011. The calcium sensor STIM1 is regulated by androgens in prostate stromal cells. The Prostate 71, 1646–1655. https://doi.org/10.1002/pros.21384

Bery, F., Figiel, S., Kouba, S., Fontaine, D., Guéguinou, M., Potier-Cartereau, M., Vandier, C., Guibon, R., Bruyère, F., Fromont, G., Mahéo, K., 2020. Hypoxia Promotes Prostate Cancer Aggressiveness by Upregulating EMT-Activator Zeb1 and SK3 Channel Expression. Int. J. Mol. Sci. 21. https://doi.org/10.3390/ijms21134786

Bill-Axelson, A., Holmberg, L., Garmo, H., Rider, J.R., Taari, K., Busch, C., Nordling, S., Häggman, M., Andersson, S.-O., Spångberg, A., Andrén, O., Palmgren, J., Steineck, G., Adami, H.-O., Johansson, J.-E., 2014. Radical Prostatectomy or Watchful Waiting in Early Prostate Cancer. N. Engl. J. Med. 370, 932–942. https://doi.org/10.1056/NEJMoa1311593

Bong, A.H.L., Monteith, G.R., 2018. Calcium signaling and the therapeutic targeting of cancer cells. Biochim. Biophys. Acta BBA - Mol. Cell Res., Calcium signaling in health, disease and therapy 1865, 1786–1794. https://doi.org/10.1016/j.bbamcr.2018.05.015

Bonnet, D., Dick, J.E., 1997. Human acute myeloid leukemia is organized as a hierarchy that originates from a primitive hematopoietic cell. Nat. Med. 3, 730–737. https://doi.org/10.1038/nm0797-730

Bootman, M.D., Lipp, P., Berridge, M.J., 2001. The organisation and functions of local Ca2+ signals. J. Cell Sci. 114, 2213–2222.

Boutin, B., Tajeddine, N., Monaco, G., Molgo, J., Vertommen, D., Rider, M., Parys, J.B., Bultynck, G., Gailly, P., 2015. Endoplasmic reticulum Ca2+ content decrease by PKA-dependent hyperphosphorylation of type 1 IP3 receptor contributes to prostate cancer cell resistance to androgen deprivation. Cell Calcium 57, 312–320. https://doi.org/10.1016/j.ceca.2015.02.004

Bray, F., Ferlay, J., Soerjomataram, I., Siegel, R.L., Torre, L.A., Jemal, A., 2018. Global cancer statistics 2018: GLOBOCAN estimates of incidence and mortality worldwide for 36 cancers in 185 countries. CA. Cancer J. Clin. 68, 394–424. https://doi.org/10.3322/caac.21492

Bruce, J., James, A., 2020. Targeting the Calcium Signalling Machinery in Cancer. Cancers 12, 2351. https://doi.org/10.3390/cancers12092351

Bubendorf, L., Kononen, J., Koivisto, P., Schraml, P., Moch, H., Gasser, T.C., Willi, N., Mihatsch, M.J., Sauter, G., Kallioniemi, O.-P., 1999. Survey of Gene Amplifications during Prostate Cancer Progression by High-Throughput Fluorescence in Situ Hybridization on Tissue Microarrays. Cancer Res. 59, 803–806.

Buchanan, P.J., McCloskey, K.D., 2016. CaV channels and cancer: canonical functions indicate benefits of repurposed drugs as cancer therapeutics. Eur Biophys J 45, 621–633. https://doi.org/10.1007/s00249-016-1144-z

Buraei, Z., Yang, J., 2010. The β Subunit of Voltage-Gated Ca2+ Channels. Physiol. Rev. 90, 1461–1506. https://doi.org/10.1152/physrev.00057.2009

Butler, W., Huang, J., 2021. Neuroendocrine cells of the prostate: Histology, biological functions, and molecular mechanisms. Precis. Clin. Med. 4, 25–34. https://doi.org/10.1093/pcmedi/pbab003

Butterworth, M.B., 2010. Regulation of the epithelial sodium channel (ENaC) by membrane trafficking. Biochim. Biophys. Acta 1802, 1166–1177. https://doi.org/10.1016/j.bbadis.2010.03.010

Byrne, N.M., Nesbitt, H., Ming, L., McKeown, S.R., Worthington, J., McKenna, D.J., 2016. Androgen deprivation in LNCaP prostate tumour xenografts induces vascular changes and hypoxic stress, resulting in promotion of epithelial-to-mesenchymal transition. Br J Cancer 114, 659–668. https://doi.org/10.1038/bjc.2016.29

CACNA1D protein expression summary - The Human Protein Atlas [WWW Document], n.d. URL https://www.proteinatlas.org/ENSG00000157388-CACNA1D (accessed 12.3.20).

Carnero, A., Lleonart, M., 2016. The hypoxic microenvironment: A determinant of cancer stem cell evolution. Cell 1, 96–105. https://doi.org/10.1002/icl3.1039

Carsin, A.-E., Drummond, F.J., Black, A., Leeuwen, P.J. van, Sharp, L., Murray, L.J., Connolly, D., Egevad, L., Boniol, M., Autier, P., Comber, H., Gavin, A., 2010. Impact of PSA testing and prostatic biopsy on cancer incidence and mortality: comparative study between the Republic of Ireland and Northern Ireland. Cancer Causes Control 21, 1523–1531. https://doi.org/10.1007/s10552-010-9581-y

Catterall, W.A., 2011. Voltage-Gated Calcium Channels. Cold Spring Harb Perspect Biol 3. https://doi.org/10.1101/cshperspect.a003947

Catterall, W.A., 2000. Structure and Regulation of Voltage-Gated Ca2+ Channels. Annu. Rev. Cell Dev. Biol. 16, 521–555. https://doi.org/10.1146/annurev.cellbio.16.1.521

Catterall, W.A., Perez-Reyes, E., Snutch, T.P., Striessnig, J., 2005. International Union of Pharmacology. XLVIII. Nomenclature and Structure-Function Relationships of Voltage-Gated Calcium Channels. Pharmacol. Rev. 57, 411–425. https://doi.org/10.1124/pr.57.4.5

Chandrasekar, T., Yang, J.C., Gao, A.C., Evans, C.P., 2015. Mechanisms of resistance in castration-resistant prostate cancer (CRPC). Transl. Androl. Urol. 4, 365–380. https://doi.org/10.3978/j.issn.2223-4683.2015.05.02

Chemin, J., Nargeot, J., Lory, P., 2002. Neuronal T-type α1H Calcium Channels Induce Neuritogenesis and Expression of High-Voltage-Activated Calcium Channels in the NG108–15 Cell Line. J. Neurosci. 22, 6856–6862. https://doi.org/10.1523/JNEUROSCI.22-16-06856.2002

Chen, L., Cao, R., Wang, G., Yuan, L., Qian, G., Guo, Z., Wu, C.-L., Wang, X., Xiao, Y., 2017. Downregulation of TRPM7 suppressed migration and invasion by regulating epithelial-mesenchymal transition in prostate cancer cells. Med Oncol 34, 127. https://doi.org/10.1007/s12032-017-0987-1

Chen, R., Zeng, X., Zhang, R., Huang, J., Kuang, X., Yang, J., Liu, J., Tawfik, O., Brantley Thrasher, J., Li, B., 2014. Cav1.3 channel α1D protein is overexpressed and modulates androgen receptor transactivation in prostate cancers1. Urol. Oncol. Semin. Orig. Investig. 32, 524–536. https://doi.org/10.1016/j.urolonc.2013.05.011

Chen, Y., Clegg, N.J., Scher, H.I., 2009. Antiandrogens and androgen depleting therapies in prostate cancer: novel agents for an established target. Lancet Oncol. 10, 981. https://doi.org/10.1016/S1470-2045(09)70229-3

Chen, Y.-F., Lin, P.-C., Yeh, Y.-M., Chen, L.-H., Shen, M.-R., 2019. Store-Operated Ca2+ Entry in Tumor Progression: From Molecular Mechanisms to Clinical Implications. Cancers 11. https://doi.org/10.3390/cancers11070899

Chovancova, B., Liskova, V., Babula, P., Krizanova, O., 2020. Role of Sodium/Calcium Exchangers in Tumors. Biomolecules 10. https://doi.org/10.3390/biom10091257

Christel, C.J., Cardona, N., Mesirca, P., Herrmann, S., Hofmann, F., Striessnig, J., Ludwig, A., Mangoni, M.E., Lee, A., 2012. Distinct localization and modulation of Cav1.2 and Cav1.3 L-type Ca2+ channels in mouse sinoatrial node. J Physiol 590, 6327–6341. https://doi.org/10.1113/jphysiol.2012.239954

Chrysafides, S.M., Bordes, S., Sharma, S., 2020. Physiology, Resting Potential, in: StatPearls. StatPearls Publishing, Treasure Island (FL).

Chu, L.W., Ritchey, J., Devesa, S.S., Quraishi, S.M., Zhang, H., Hsing, A.W., 2011. Prostate Cancer Incidence Rates in Africa [WWW Document]. Prostate Cancer. https://doi.org/10.1155/2011/947870

Cifuentes, E., Mataraza, J.M., Yoshida, B.A., Menon, M., Sacks, D.B., Barrack, E.R., Reddy, G.P.-V., 2004. Physical and functional interaction of androgen receptor with calmodulin in prostate cancer cells. Proc. Natl. Acad. Sci. 101, 464–469. https://doi.org/10.1073/pnas.0307161101

Clapham, D.E., 2007. Calcium Signaling. Cell 131, 1047–1058. https://doi.org/10.1016/j.cell.2007.11.028

Clark, N.C., Nagano, N., Kuenzi, F.M., Jarolimek, W., Huber, I., Walter, D., Wietzorrek, G., Boyce, S., Kullmann, D.M., Striessnig, J., Seabrook, G.R., 2003. Neurological phenotype and synaptic function in mice lacking the CaV1.3 α subunit of neuronal L-type voltage-dependent Ca2+ channels. Neuroscience 120, 435–442. https://doi.org/10.1016/S0306-4522(03)00329-4

Clevers, H., 2011. The cancer stem cell: premises, promises and challenges. Nat. Med. 313–319. https://doi.org/10.1038/nm.2304

Cockman, M.E., Masson, N., Mole, D.R., Jaakkola, P., Chang, G.-W., Clifford, S.C., Maher, E.R., Pugh, C.W., Ratcliffe, P.J., Maxwell, P.H., 2000. Hypoxia Inducible Factor-α Binding and Ubiquitylation by the von Hippel-Lindau Tumor Suppressor Protein. J. Biol. Chem. 275, 25733–25741. https://doi.org/10.1074/jbc.M002740200

Collins, A.T., Berry, P.A., Hyde, C., Stower, M.J., Maitland, N.J., 2005. Prospective Identification of Tumorigenic Prostate Cancer Stem Cells. Cancer Res. 65, 10946–10951. https://doi.org/10.1158/0008-5472.CAN-05-2018

Collins, A.T., Maitland, N.J., 2006. Prostate cancer stem cells. Eur. J. Cancer, Cancer Stem Cells: Opportunities for Novel Diagnostics and Drug Discovery 42, 1213–1218. https://doi.org/10.1016/j.ejca.2006.01.037

Comes, N., Serrano-Albarrás, A., Capera, J., Serrano-Novillo, C., Condom, E., Ramón y Cajal, S., Ferreres, J.C., Felipe, A., 2015. Involvement of potassium channels in the progression of cancer to a more malignant phenotype. Biochim. Biophys. Acta BBA - Biomembr., Membrane Channels and Transporters in Cancers 1848, 2477–2492. https://doi.org/10.1016/j.bbamem.2014.12.008

Connor, J., Sawczuk, I.S., Benson, M.C., Tomashefsky, P., O'Toole, K.M., Olsson, C.A., Buttyan, R., n.d. Calcium channel antagonists delay regression of androgen-dependent tissues and suppress gene activity associated with cell death. The Prostate 13, 119–130. https://doi.org/10.1002/pros.2990130204

Coutinho, I., Day, T.K., Tilley, W.D., Selth, L.A., 2016. Androgen receptor signaling in castration-resistant prostate cancer: a lesson in persistence. Endocr. Relat. Cancer 23, T179–T197. https://doi.org/10.1530/ERC-16-0422

Cui, C., Merritt, R., Fu, L., Pan, Z., 2017. Targeting calcium signaling in cancer therapy. Acta Pharm. Sin. B 7, 3–17. https://doi.org/10.1016/j.apsb.2016.11.001

Culig, Z., Hobisch, A., Cronauer, M.V., Cato, A.C., Hittmair, A., Radmayr, C., Eberle, J., Bartsch, G., Klocker, H., 1993. Mutant androgen receptor detected in an advanced-stage prostatic carcinoma is activated by adrenal androgens and progesterone. Mol. Endocrinol. Baltim. Md 7, 1541–1550. https://doi.org/10.1210/mend.7.12.8145761

Culig, Z., Hoffmann, J., Erdel, M., Eder, I.E., Hobisch, A., Hittmair, A., Bartsch, G., Utermann, G., Schneider, M.R., Parczyk, K., Klocker, H., 1999. Switch from antagonist to agonist of the androgen receptor blocker bicalutamide is associated with prostate tumour progression in a new model system. Br. J. Cancer 81, 242–251. https://doi.org/10.1038/sj.bjc.6690684

DAI, Y., BAE, K., SIEMANN, D.W., 2011. IMPACT OF HYPOXIA ON THE METASTATIC POTENTIAL OF HUMAN PROSTATE CANCER CELLS. Int. J. Radiat. Oncol. Biol. Phys. 81, 521–528. https://doi.org/10.1016/j.ijrobp.2011.04.027

Damber, J.-E., Aus, G., 2008. Prostate cancer. The Lancet 371, 1710–1721. https://doi.org/10.1016/S0140-6736(08)60729-1

Danza, G., Di Serio, C., Rosati, F., Lonetto, G., Sturli, N., Kacer, D., Pennella, A., Ventimiglia, G., Barucci, R., Piscazzi, A., Prudovsky, I., Landriscina, M., Marchionni, N., Tarantini, F., 2012. NOTCH SIGNALLING MODULATES HYPOXIA-INDUCED NEUROENDOCRINE DIFFERENTIATION OF HUMAN PROSTATE CANCER CELLS. Mol Cancer Res 10, 230–238. https://doi.org/10.1158/1541-7786.MCR-11-0296

DaSilva, J.O., Amorino, G.P., Casarez, E.V., Pemberton, B., Parsons, S.J., 2013. Neuroendocrine-derived peptides promote prostate cancer cell survival through activation of IGF-1R signaling. Prostate 73, 801–812. https://doi.org/10.1002/pros.22624

Datta, D., Aftabuddin, M., Gupta, D.K., Raha, S., Sen, P., 2016. Human Prostate Cancer Hallmarks Map. Sci. Rep. 6, 30691. https://doi.org/10.1038/srep30691

Davenport, B., Li, Y., Heizer, J.W., Schmitz, C., Perraud, A.-L., 2015. Signature Channels of Excitability no More: L-Type Channels in Immune Cells. Front. Immunol. 6. https://doi.org/10.3389/fimmu.2015.00375

Davey, R.A., Grossmann, M., 2016. Androgen Receptor Structure, Function and Biology: From Bench to Bedside. Clin. Biochem. Rev. 37, 3.

Davis, F.M., Azimi, I., Faville, R.A., Peters, A.A., Jalink, K., Putney, J.W., Goodhill, G.J., Thompson, E.W., Roberts-Thomson, S.J., Monteith, G.R., 2014. Induction of epithelial-mesenchymal transition (EMT) in breast cancer cells is calcium signal dependent. Oncogene 33, 2307–2316. https://doi.org/10.1038/onc.2013.187

Debelec-Butuner, B., Alapinar, C., Ertunc, N., Gonen-Korkmaz, C., Yörükoğlu, K., Korkmaz, K.S., 2014. TNFα-Mediated Loss of β-Catenin/E-Cadherin Association and Subsequent Increase in Cell Migration Is Partially Restored by NKX3.1 Expression in Prostate Cells. PLoS ONE 9. https://doi.org/10.1371/journal.pone.0109868

Debes, J.D., Roberts, R.O., Jacobson, D.J., Girman, C.J., Lieber, M.M., Tindall, D.J., Jacobsen, S.J., 2004. Inverse Association between Prostate Cancer and the Use of Calcium Channel Blockers. Cancer Epidemiol. Prev. Biomark. 13, 255–259. https://doi.org/10.1158/1055-9965.EPI-03-0093

Debes, J.D., Tindall, D.J., 2002. The role of androgens and the androgen receptor in prostate cancer. Cancer Lett. 187, 1–7. https://doi.org/10.1016/S0304-3835(02)00413-5

Deeble, P.D., Cox, M.E., Frierson, H.F., Sikes, R.A., Palmer, J.B., Davidson, R.J., Casarez, E.V., Amorino, G.P., Parsons, S.J., 2007. Androgen-independent growth and tumorigenesis of prostate cancer cells are enhanced by the presence of PKA-differentiated neuroendocrine cells. Cancer Res. 67, 3663–3672. https://doi.org/10.1158/0008-5472.CAN-06-2616

Dehm, S.M., Tindall, D.J., 2006. Molecular regulation of androgen action in prostate cancer. J. Cell. Biochem. 99, 333–344. https://doi.org/10.1002/jcb.20794

Déliot, N., Constantin, B., 2015. Plasma membrane calcium channels in cancer: Alterations and consequences for cell proliferation and migration. Biochim. Biophys. Acta BBA - Biomembr., Membrane Channels and Transporters in Cancers 1848, 2512–2522. https://doi.org/10.1016/j.bbamem.2015.06.009

Deng, X., Liu, H., Huang, J., Cheng, L., Keller, E.T., Parsons, S.J., Hu, C.-D., 2008. Ionizing radiation induces prostate cancer neuroendocrine differentiation through interplay of CREB and

ATF2: implications for disease progression. Cancer Res. 68, 9663–9670. https://doi.org/10.1158/0008-5472.CAN-08-2229

Derler, I., Jardin, I., Romanin, C., 2016. Molecular mechanisms of STIM/Orai communication. Am. J. Physiol. - Cell Physiol. 310, C643–C662. https://doi.org/10.1152/ajpcell.00007.2016

Dondoo, T.-O., Fukumori, T., Daizumoto, K., Fukawa, T., Kohzuki, M., Kowada, M., Kusuhara, Y., Mori, H., Nakatsuji, H., Takahashi, M., Kanayama, H.-O., 2017. Galectin-3 Is Implicated in Tumor Progression and Resistance to Anti-androgen Drug Through Regulation of Androgen Receptor Signaling in Prostate Cancer. Anticancer Res. 37, 125–134.

Dong, L., Zieren, R.C., Xue, W., de Reijke, T.M., Pienta, K.J., 2019. Metastatic prostate cancer remains incurable, why? Asian J. Urol., In honor of Dr. Donald S. Coffey — Prostate cancer biology and therapy 6, 26–41. https://doi.org/10.1016/j.ajur.2018.11.005

Dozmorov, M.G., Hurst, R.E., Culkin, D.J., Kropp, B.P., Frank, M.B., Osban, J., Penning, T.M., Lin, H.-K., 2009. Unique Patterns of Molecular Profiling between Human Prostate Cancer LNCaP and PC-3 Cells. The Prostate 69, 1077–1090. https://doi.org/10.1002/pros.20960

Drummond, F.J., Barrett, E., Burns, R., O'Neill, C., Sharp, L., 2014. The number of tPSA tests continues to rise and variation in testing practices persists: a survey of laboratory services in Ireland 2008–2010. Ir. J. Med. Sci. 1971 - 183, 369–375. https://doi.org/10.1007/s11845-013-1022-y

Drummond, F.J., Kinnear, H., O'Leary, E., Donnelly, Gavin, A., Sharp, L., 2015. Long-term health-related quality of life of prostate cancer survivors varies by primary treatment. Results from the PiCTure (Prostate Cancer Treatment, your experience) study. J. Cancer Surviv. 9, 361–372. https://doi.org/10.1007/s11764-014-0419-6

Du, C., Zheng, Z., Li, D., Chen, L., Li, N., Yi, X., Yang, Y., Guo, F., Liu, W., Xie, X., Xie, M., 2016. BKCa promotes growth and metastasis of prostate cancer through facilitating the coupling between αvβ3 integrin and FAK. Oncotarget 7, 40174–40188. https://doi.org/10.18632/oncotarget.9559

Dubois, C., Vanden Abeele, F., Lehen'kyi, V., Gkika, D., Guarmit, B., Lepage, G., Slomianny, C., Borowiec, A.S., Bidaux, G., Benahmed, M., Shuba, Y., Prevarskaya, N., 2014. Remodeling of Channel-Forming ORAI Proteins Determines an Oncogenic Switch in Prostate Cancer. Cancer Cell 26, 19–32. https://doi.org/10.1016/j.ccr.2014.04.025

Edwards, J., Krishna, N.S., Grigor, K.M., Bartlett, J.M.S., 2003. Androgen receptor gene amplification and protein expression in hormone refractory prostate cancer. Br J Cancer 89, 552–556. https://doi.org/10.1038/sj.bjc.6601127

Endo, M., Tanaka, M., Ogawa, Y., 1970. Calcium Induced Release of Calcium from the Sarcoplasmic Reticulum of Skinned Skeletal Muscle Fibres. Nature 228, 34–36. https://doi.org/10.1038/228034a0

Ertel, E.A., Campbell, K.P., Harpold, M.M., Hofmann, F., Mori, Y., Perez-Reyes, E., Schwartz, A., Snutch, T.P., Tanabe, T., Birnbaumer, L., Tsien, R.W., Catterall, W.A., 2000. Nomenclature of Voltage-Gated Calcium Channels. Neuron 25, 533–535. https://doi.org/10.1016/S0896-6273(00)81057-0

Fahlke, C., 2001. Ion permeation and selectivity in ClC-type chloride channels. Am. J. Physiol.-Ren. Physiol. 280, F748–F757. https://doi.org/10.1152/ajprenal.2001.280.5.F748

Farini, D., Puglianiello, A., Mammi, C., Siracusa, G., Moretti, C., 2003. Dual effect of pituitary adenylate cyclase activating polypeptide on prostate tumor LNCaP cells: short- and long-term exposure affect proliferation and neuroendocrine differentiation. Endocrinology 144, 1631–1643. https://doi.org/10.1210/en.2002-221009

Ferlay, J., Colombet, M., Soerjomataram, I., Mathers, C., Parkin, D.M., Piñeros, M., Znaor, A., Bray, F., 2019. Estimating the global cancer incidence and mortality in 2018: GLOBOCAN sources and methods. Int. J. Cancer 144, 1941–1953. https://doi.org/10.1002/ijc.31937

Fernandez, E.V., Reece, K.M., Ley, A.M., Troutman, S.M., Sissung, T.M., Price, D.K., Chau, C.H., Figg, W.D., 2015. Dual Targeting of the Androgen Receptor and Hypoxia-Inducible Factor 1α

Pathways Synergistically Inhibits Castration-Resistant Prostate Cancer Cells. Mol. Pharmacol. 87, 1006–1012. https://doi.org/10.1124/mol.114.097477

Feske, S., Gwack, Y., Prakriya, M., Srikanth, S., Puppel, S.-H., Tanasa, B., Hogan, P.G., Lewis, R.S., Daly, M., Rao, A., 2006. A mutation in Orai1 causes immune deficiency by abrogating CRAC channel function. Nature 441, 179–185. https://doi.org/10.1038/nature04702

Fiorio Pla, A., Kondratska, K., Prevarskaya, N., 2016. STIM and ORAI proteins: crucial roles in hallmarks of cancer. Am. J. Physiol.-Cell Physiol. 310, C509–C519. https://doi.org/10.1152/ajpcell.00364.2015

Fitzpatrick, Annette L., Daling, J.R., Furberg, C.D., Kronmal, R.A., Weissfeld, J.L., 2001. Hypertension, Heart Rate, Use of Antihypertensives, and Incident Prostate Cancer. Ann. Epidemiol. 11, 534–542. https://doi.org/10.1016/S1047-2797(01)00246-0

Fitzpatrick, Annette L, Daling, J.R., Furberg, C.D., Kronmal, R.A., Weissfeld, J.L., 2001. Hypertension, Heart Rate, Use of Antihypertensives, and Incident Prostate Cancer. Ann. Epidemiol. 11, 534–542. https://doi.org/10.1016/S1047-2797(01)00246-0

Flourakis, M., Lehen'kyi, V., Beck, B., Raphaël, M., Vandenberghe, M., Vanden Abeele, F., Roudbaraki, M., Lepage, G., Mauroy, B., Romanin, C., Shuba, Y., Skryma, R., Prevarskaya, N., 2010. Orai1 contributes to the establishment of an apoptosis-resistant phenotype in prostate cancer cells. Cell Death Dis. 1, e75. https://doi.org/10.1038/cddis.2010.52

Flourakis, M., Prevarskaya, N., 2009. Insights into Ca2+ homeostasis of advanced prostate cancer cells. Biochim. Biophys. Acta BBA - Mol. Cell Res., 10th European Symposium on Calcium 1793, 1105–1109. https://doi.org/10.1016/j.bbamcr.2009.01.009

Foradori, C.D., Weiser, M.J., Handa, R.J., 2008. Non-genomic Actions of Androgens. Front. Neuroendocrinol. 29, 169–181. https://doi.org/10.1016/j.yfrne.2007.10.005

Foradori, C.D., Werner, S.B., Sandau, U.S., Clapp, T.R., Handa, R.J., 2007. Activation of the androgen receptor alters the intracellular calcium response to glutamate in primary hippocampal neurons and modulates sarco/endoplasmic reticulum calcium ATPase 2 transcription. Neuroscience 149, 155–164. https://doi.org/10.1016/j.neuroscience.2007.06.054

Formisano, L., Guida, N., Mascolo, L., Serani, A., Laudati, G., Pizzorusso, V., Annunziato, L., 2020. Transcriptional and epigenetic regulation of ncx1 and ncx3 in the brain. Cell Calcium 87, 102194. https://doi.org/10.1016/j.ceca.2020.102194

Forristal, C.E., Wright, K.L., Hanley, N.A., Oreffo, R.O.C., Houghton, F.D., 2010. Hypoxia inducible factors regulate pluripotency and proliferation in human embryonic stem cells cultured at reduced oxygen tensions. Reprod. Camb. Engl. 139, 85–97. https://doi.org/10.1530/REP-09-0300

Fourbon, Y., Guéguinou, M., Félix, R., Constantin, B., Uguen, A., Fromont, G., Lajoie, L., Magaud, C., Lecomte, T., Chamorey, E., Chatelier, A., Mignen, O., Potier-Cartereau, M., Chantôme, A., Bois, P., Vandier, C., 2017. Ca2+ protein alpha 1D of CaV1.3 regulates intracellular calcium concentration and migration of colon cancer cells through a non-canonical activity. Sci Rep 7. https://doi.org/10.1038/s41598-017-14230-1

Fraga, A., Ribeiro, R., Príncipe, P., Lopes, C., Medeiros, R., 2015. Hypoxia and Prostate Cancer Aggressiveness: A Tale With Many Endings. Clin. Genitourin. Cancer 13, 295–301. https://doi.org/10.1016/j.clgc.2015.03.006

Franzini-Armstrong, C., 2004. Functional implications of RyR-DHPR relationships in skeletal and cardiac muscles. Biol. Res. 37, 507–512. https://doi.org/10.4067/S0716-97602004000400003

Fraser, S.P., Diss, J.K.J., Chioni, A.-M., Mycielska, M.E., Pan, H., Yamaci, R.F., Pani, F., Siwy, Z., Krasowska, M., Grzywna, Z., Brackenbury, W.J., Theodorou, D., Koyutürk, M., Kaya, H., Battaloglu, E., De Bella, M.T., Slade, M.J., Tolhurst, R., Palmieri, C., Jiang, J., Latchman, D.S., Coombes, R.C., Djamgoz, M.B.A., 2005. Voltage-gated sodium channel expression and

potentiation of human breast cancer metastasis. Clin. Cancer Res. Off. J. Am. Assoc. Cancer Res. 11, 5381–5389. https://doi.org/10.1158/1078-0432.CCR-05-0327

Fraser, S.P., Pardo, L.A., 2008. Ion channels: functional expression and therapeutic potential in cancer: Colloquium on Ion Channels and Cancer. EMBO Rep. 9, 512–515. https://doi.org/10.1038/embor.2008.75

Frenzel, A., Grespi, F., Chmelewskij, W., Villunger, A., 2009. Bcl2 family proteins in carcinogenesis and the treatment of cancer. Apoptosis Int. J. Program. Cell Death 14, 584–596. https://doi.org/10.1007/s10495-008-0300-z

Gackière, F., Warnier, M., Katsogiannou, M., Derouiche, S., Delcourt, P., Dewailly, E., Slomianny, C., Humez, S., Prevarskaya, N., Roudbaraki, M., Mariot, P., 2013a. Functional coupling between large-conductance potassium channels and Cav3.2 voltage-dependent calcium channels participates in prostate cancer cell growth. Biol. Open 2, 941–951. https://doi.org/10.1242/bio.20135215

Gackière, F., Warnier, M., Katsogiannou, M., Derouiche, S., Delcourt, P., Dewailly, E., Slomianny, C., Humez, S., Prevarskaya, N., Roudbaraki, M., Mariot, P., 2013b. Functional coupling between large-conductance potassium channels and Cav3.2 voltage-dependent calcium channels participates in prostate cancer cell growth. Biol. Open 2, 941–951. https://doi.org/10.1242/bio.20135215

Gann, P.H., 2002. Risk Factors for Prostate Cancer. Rev. Urol. 4, S3–S10.

Gao, W., Wu, D., Wang, Y., Wang, Z., Zou, C., Dai, Y., Ng, C.-F., Teoh, J.Y.-C., Chan, F.L., 2018. Development of a novel and economical agar-based non-adherent three-dimensional culture method for enrichment of cancer stem-like cells. Stem Cell Res. Ther. 9. https://doi.org/10.1186/s13287-018-0987-x

Garcia, G.E., Nicole, A., Bhaskaran, S., Gupta, A., Kyprianou, N., Kumar, A.P., 2006. Akt- and CREB-Mediated Prostate Cancer Cell Proliferation Inhibition by Nexrutine, a Phellodendron amurense Extract. Neoplasia N. Y. N 8, 523–533.

Gessner, G., Schönherr, K., Soom, M., Hansel, A., Asim, M., Baniahmad, A., Derst, C., Hoshi, T., Heinemann, S.H., 2005. BKCa channels activating at resting potential without calcium in LNCaP prostate cancer cells. J. Membr. Biol. 208, 229–240. https://doi.org/10.1007/s00232-005-0830-z

Girault, A., Haelters, J.-P., Potier-Cartereau, M., Chantôme, A., Jaffrés, P.-A., Bougnoux, P., Joulin, V., Vandier, C., 2012. Targeting SKCa channels in cancer: potential new therapeutic approaches. Curr. Med. Chem. 19, 697–713. https://doi.org/10.2174/092986712798992039

Goldstein, A.S., Huang, J., Guo, C., Garraway, I.P., Witte, O.N., 2010. Identification of a cell-of-origin for human prostate cancer. Science 329, 568–571. https://doi.org/10.1126/science.1189992

Gomez-Ospina, N., Tsuruta, F., Barreto-Chang, O., Hu, L., Dolmetsch, R., 2006. The C Terminus of the L-Type Voltage-Gated Calcium Channel CaV1.2 Encodes a Transcription Factor. Cell 127, 591–606. https://doi.org/10.1016/j.cell.2006.10.017

Gorczynska, E., Handelsman, D.J., 1995. Androgens rapidly increase the cytosolic calcium concentration in Sertoli cells. Endocrinology 136, 2052–2059. https://doi.org/10.1210/endo.136.5.7720654

Gravdal, K., Halvorsen, O.J., Haukaas, S.A., Akslen, L.A., 2007. A Switch from E-Cadherin to N-Cadherin Expression Indicates Epithelial to Mesenchymal Transition and Is of Strong and Independent Importance for the Progress of Prostate Cancer. Clin Cancer Res 13, 7003–7011. https://doi.org/10.1158/1078-0432.CCR-07-1263

Gray, M.A., Winpenny, J.P., Verdon, B., McAlroy, H., Argent, B.E., 1995. Chloride channels and cystic fibrosis of the pancreas. Biosci. Rep. 15, 531–541. https://doi.org/10.1007/BF01204355

Gregory, C.W., Johnson, R.T., Mohler, J.L., French, F.S., Wilson, E.M., 2001. Androgen Receptor Stabilization in Recurrent Prostate Cancer Is Associated with Hypersensitivity to Low Androgen. Cancer Res. 61, 2892–2898.

Grossmann, M.E., Huang, H., Tindall, D.J., 2001. Androgen Receptor Signaling in Androgen-Refractory Prostate Cancer. J. Natl. Cancer Inst. 93, 1687–1697. https://doi.org/10.1093/jnci/93.22.1687

Guo, Z., Shi, F., Zhang, L., Zhang, H., Yang, J., Li, B., Jia, J., Wang, Xuan, Wang, Xiaomin, 2010. Critical role of L-type voltage-dependent Ca2+ channels in neural progenitor cell proliferation induced by hypoxia. Neurosci. Lett. 478, 156–160. https://doi.org/10.1016/j.neulet.2010.05.007

Halin, S., Hammarsten, P., Wikström, P., Bergh, A., 2007. Androgen-insensitive prostate cancer cells transiently respond to castration treatment when growing in an androgen-dependent prostate environment. The Prostate 67, 370–377. https://doi.org/10.1002/pros.20473

Hall, M., Todd, B., Allen, E.D., Nguyen, N., Kwon, Y.-J., Nguyen, V., Hearne, J.L., Martin-Caraballo, M., 2018. Androgen receptor signaling regulates T-type Ca2+ channel expression and neuroendocrine differentiation in prostate cancer cells. Am. J. Cancer Res. 8, 732–747.

Hamid, A.R.A.H., Kusuma Putra, H.W., Sari, N.P., Diana, P., Sesari, S.S., Novita, E., Gultom, F.L., Saraswati, M., Tanurahardja, B., Asmarinah, Umbas, R., Mochtar, C.A., 2020. Early upregulation of AR and steroidogenesis enzyme expression after 3 months of androgen-deprivation therapy. BMC Urol. 20, 71. https://doi.org/10.1186/s12894-020-00627-0

Hanahan, D., Weinberg, R.A., 2011. Hallmarks of Cancer: The Next Generation. Cell 144, 646–674. https://doi.org/10.1016/j.cell.2011.02.013

Hanahan, D., Weinberg, R.A., 2000. The Hallmarks of Cancer. Cell 100, 57–70. https://doi.org/10.1016/S0092-8674(00)81683-9

Hansen, P.B., Poulsen, C.B., Walter, S., Marcussen, N., Cribbs, L.L., Skøtt, O., Jensen, B.L., 2011. Functional importance of L- and P/Q-type voltage-gated calcium channels in human renal vasculature. Hypertens. Dallas Tex 1979 58, 464–470. https://doi.org/10.1161/HYPERTENSIONAHA.111.170845

Hao, J., Bao, X., Jin, B., Wang, X., Mao, Z., Li, X., Wei, L., Shen, D., Wang, J.-L., 2015. Ca2+ channel subunit α 1D promotes proliferation and migration of endometrial cancer cells mediated by 17β-estradiol via the G protein-coupled estrogen receptor. FASEB J. Off. Publ. Fed. Am. Soc. Exp. Biol. 29, 2883–2893. https://doi.org/10.1096/fj.14-265603

Harris, A.L., 2002. Hypoxia — a key regulatory factor in tumour growth. Nat. Rev. Cancer 2, 38–47. https://doi.org/10.1038/nrc704

Harris, W.P., Mostaghel, E.A., Nelson, P.S., Montgomery, B., 2009. Androgen deprivation therapy: progress in understanding mechanisms of resistance and optimizing androgen depletion. Nat. Clin. Pract. Urol. 6, 76–85. https://doi.org/10.1038/ncpuro1296

Hasan, R., Zhang, X., 2018. Ca2+ Regulation of TRP Ion Channels. Int. J. Mol. Sci. 19. https://doi.org/10.3390/ijms19041256

Hassanipour-Azgomi, S., Mohammadian-Hafshejani, A., Ghoncheh, M., Towhidi, F., Jamehshorani, S., Salehiniya, H., 2016. Incidence and mortality of prostate cancer and their relationship with the Human Development Index worldwide. Prostate Int 4, 118–124. https://doi.org/10.1016/j.prnil.2016.07.001

Hatano, N., Ohya, S., Muraki, K., Giles, W., Imaizumi, Y., 2003. Dihydropyridine Ca2+ channel antagonists and agonists block Kv4.2, Kv4.3 and Kv1.4 K+ channels expressed in HEK293 cells. Br. J. Pharmacol. 139, 533–544. https://doi.org/10.1038/sj.bjp.0705281

Hayes, J.H., Ollendorf, Mr.D.A., Pearson, S.D., Barry, M.J., Kantoff, P.W., Stewart, S.T., Bhatnagar, V., Sweeney, C.J., Stahl, J.E., McMahon, P.M., 2010. Active Surveillance Compared With Initial Treatment for Men With Low-Risk Prostate Cancer. JAMA J. Am. Med. Assoc. 304, 2373–2380. https://doi.org/10.1001/jama.2010.1720

Heddleston, J.M., Li, Z., Lathia, J.D., Bao, S., Hjelmeland, A.B., Rich, J.N., 2010. Hypoxia inducible factors in cancer stem cells. Br. J. Cancer 102, 789–795. https://doi.org/10.1038/sj.bjc.6605551

Heinlein, C.A., Chang, C., 2004. Androgen Receptor in Prostate Cancer. Endocr. Rev. 25, 276–308. https://doi.org/10.1210/er.2002-0032

Hemmerlein, B., Weseloh, R.M., Mello de Queiroz, F., Knötgen, H., Sánchez, A., Rubio, M.E., Martin, S., Schliephacke, T., Jenke, M., Heinz-Joachim-Radzun, Stühmer, W., Pardo, L.A., 2006. Overexpression of Eag1 potassium channels in clinical tumours. Mol. Cancer 5, 41. https://doi.org/10.1186/1476-4598-5-41

Hernandez-Plata, E., Ortiz, C.S., Marquina-Castillo, B., Medina-Martinez, I., Alfaro, A., Berumen, J., Rivera, M., Gomora, J.C., 2012. Overexpression of NaV 1.6 channels is associated with the invasion capacity of human cervical cancer. Int. J. Cancer 130, 2013–2023. https://doi.org/10.1002/ijc.26210

Hirano, D., Okada, Y., Minei, S., Takimoto, Y., Nemoto, N., 2004. Neuroendocrine differentiation in hormone refractory prostate cancer following androgen deprivation therapy. Eur. Urol. 45, 586–592; discussion 592. https://doi.org/10.1016/j.eururo.2003.11.032

Hoeflich, K.P., Ikura, M., 2002. Calmodulin in Action: Diversity in Target Recognition and Activation Mechanisms. Cell 108, 739–742. https://doi.org/10.1016/S0092-8674(02)00682-7

Hogan, P.G., Rao, A., 2015. Store-operated calcium entry: mechanisms and modulation. Biochem. Biophys. Res. Commun. 460, 40–49. https://doi.org/10.1016/j.bbrc.2015.02.110

Hollier, B.G., Evans, K., Mani, S.A., 2009. The Epithelial-to-Mesenchymal Transition and Cancer Stem Cells: A Coalition Against Cancer Therapies. J. Mammary Gland Biol. Neoplasia 14, 29–43. https://doi.org/10.1007/s10911-009-9110-3

Hompland, T., Hole, K.H., Ragnum, H.B., Aarnes, E.-K., Vlatkovic, L., Lie, A.K., Patzke, S., Brennhovd, B., Seierstad, T., Lyng, H., 2018. Combined MR Imaging of Oxygen Consumption and Supply Reveals Tumor Hypoxia and Aggressiveness in Prostate Cancer Patients. Cancer Res. 78, 4774–4785. https://doi.org/10.1158/0008-5472.CAN-17-3806

Hong, S., Bi, M., Wang, L., Kang, Z., Ling, L., Zhao, C., 2015. CLC-3 channels in cancer (Review). Oncol. Rep. 33, 507–514. https://doi.org/10.3892/or.2014.3615

Horoszewicz, J.S., Leong, S.S., Kawinski, E., Karr, J.P., Rosenthal, H., Chu, T.M., Mirand, E.A., Murphy, G.P., 1983. LNCaP Model of Human Prostatic Carcinoma. Cancer Res 43, 1809–1818.

House, C.D., Vaske, C.J., Schwartz, A.M., Obias, V., Frank, B., Luu, T., Sarvazyan, N., Irby, R., Strausberg, R.L., Hales, T.G., Stuart, J.M., Lee, N.H., 2010. Voltage-gated Na+ channel SCN5A is a key regulator of a gene transcriptional network that controls colon cancer invasion. Cancer Res. 70, 6957–6967. https://doi.org/10.1158/0008-5472.CAN-10-1169

Huang, F.-M., Li, X.-H., Liang, Y., 2018. [Risk factors for early castration-resistant prostate cancer after androgen deprivation therapy for bone-metastatic prostate cancer]. Zhonghua Nan Ke Xue Natl. J. Androl. 24, 690–694.

Huang, G.N., Zeng, W., Kim, J.Y., Yuan, J.P., Han, L., Muallem, S., Worley, P.F., 2006. STIM1 carboxyl-terminus activates native SOC, I crac and TRPC1 channels. Nat. Cell Biol. 8, 1003–1010. https://doi.org/10.1038/ncb1454

Huang, H., Yu, D., Soong, T.W., 2013. C-Terminal Alternative Splicing of CaV1.3 Channels Distinctively Modulates Their Dihydropyridine Sensitivity. Mol. Pharmacol. 84, 643–653. https://doi.org/10.1124/mol.113.087155

Huang, M., Du, H., Zhang, L., Che, H., Liang, C., 2018. The association of HIF-1α expression with clinicopathological significance in prostate cancer: a meta-analysis. Cancer Manag. Res. 10, 2809. https://doi.org/10.2147/CMAR.S161762

Huang, X., Jan, L.Y., 2014. Targeting potassium channels in cancer. J. Cell Biol. 206, 151–162. https://doi.org/10.1083/jcb.201404136

Huggins, C., Clark, P.J., 1940. Quantitative Studies of Prostatic Secretion. J. Exp. Med. 72, 747–762. https://doi.org/10.1084/jem.72.6.747

Huggins, C., Hodges, C.V., 1941. Studies on Prostatic Cancer. I. The Effect of Castration, of Estrogen and of Androgen Injection on Serum Phosphatases in Metastatic Carcinoma of the Prostate. Cancer Res. 1, 293–297.

Hui, A.S., Bauer, A.L., Striet, J.B., Schnell, P.O., Czyzyk-Krzeska, M.F., 2006. Calcium signaling stimulates translation of HIF-α during hypoxia. FASEB J. 20, 466–475. https://doi.org/10.1096/fj.05-5086com

Humez, S., Legrand, G., Vanden-Abeele, F., Monet, M., Marchetti, P., Lepage, G., Crepin, A., Dewailly, E., Wuytack, F., Prevarskaya, N., 2004. Role of endoplasmic reticulum calcium content in prostate cancer cell growth regulation by IGF and TNFalpha. J. Cell. Physiol. 201, 201–213. https://doi.org/10.1002/jcp.20049

Humphrey, P.A., 2004. Gleason grading and prognostic factors in carcinoma of the prostate. Mod. Pathol. 17, 292–306. https://doi.org/10.1038/modpathol.3800054

Irizarry, R.A., Bolstad, B.M., Collin, F., Cope, L.M., Hobbs, B., Speed, T.P., 2003. Summaries of Affymetrix GeneChip probe level data. Nucleic Acids Res. 31, e15–e15. https://doi.org/10.1093/nar/gng015

Islam, F., Gopalan, V., Smith, R.A., Lam, A.K.-Y., 2015. Translational potential of cancer stem cells: A review of the detection of cancer stem cells and their roles in cancer recurrence and cancer treatment. Exp. Cell Res. 335, 135–147. https://doi.org/10.1016/j.yexcr.2015.04.018

Ito, T., Yamamoto, S., Ohno, Y., Namiki, K., Aizawa, T., Akiyama, A., Tachibana, M., 2001. Up-regulation of neuroendocrine differentiation in prostate cancer after androgen deprivation therapy, degree and androgen independence. Oncol. Rep. 8, 1221–1224.

Iwasaki, K., Ninomiya, R., Shin, T., Nomura, T., Kajiwara, T., Hijiya, N., Moriyama, M., Mimata, H., Hamada, F., 2018. Chronic hypoxia-induced slug promotes invasive behavior of prostate cancer cells by activating expression of ephrin-B1. Cancer Sci. 109, 3159–3170. https://doi.org/10.1111/cas.13754

J, L., Ml, K., Wd, H., Jt, J., Jw, M., Jr, F.J., T, M., 2005. STIM is a Ca2+ sensor essential for Ca2+-store-depletion-triggered Ca2+ influx. Curr. Biol. CB 15, 1235–1241. https://doi.org/10.1016/j.cub.2005.05.055

Jardin, I., Rosado, J.A., 2016. STIM and calcium channel complexes in cancer. Biochim. Biophys. Acta BBA - Mol. Cell Res., Calcium and Cell Fate 1863, 1418–1426. https://doi.org/10.1016/j.bbamcr.2015.10.003

Jeffs, G.J., Meloni, B.P., Bakker, A.J., Knuckey, N.W., 2007. The role of the Na+/Ca2+ exchanger (NCX) in neurons following ischaemia. J. Clin. Neurosci. 14, 507–514. https://doi.org/10.1016/j.jocn.2006.07.013

Jenden, D.J., Fairhurst, A.S., 1969. The Pharmacology of Ryanodine. Pharmacol. Rev. 21, 1–25.

Jenkins, M.A., Christel, C.J., Jiao, Y., Abiria, S., Kim, K.Y., Usachev, Y.M., Obermair, G.J., Colbran, R.J., Lee, A., 2010. Ca2+-Dependent Facilitation of Cav1.3 Ca2+ Channels by Densin and Ca2+/Calmodulin-Dependent Protein Kinase II. J. Neurosci. 30, 5125–5135. https://doi.org/10.1523/JNEUROSCI.4367-09.2010

Jennbacken, K., Tešan, T., Wang, W., Gustavsson, H., Damber, J.-E., Welén, K., 2010. N-cadherin increases after androgen deprivation and is associated with metastasis in prostate cancer. Endocr Relat Cancer 17, 469–479. https://doi.org/10.1677/ERC-10-0015

Ji, Y., Han, Z., Shao, L., Zhao, Y., 2016. Ultrasound-targeted microbubble destruction of calcium channel subunit α 1D siRNA inhibits breast cancer via G protein-coupled receptor 30. Oncol. Rep. 36, 1886–1892. https://doi.org/10.3892/or.2016.5031

Jordan, C.T., Guzman, M.L., Noble, M., 2009. Cancer Stem Cells [WWW Document]. http://dx.doi.org/10.1056/NEJMra061808. https://doi.org/10.1056/NEJMra061808

K, R., Ej, C., X, L., Hp, C., B, L., Q, L., Ak, D., D, Z., X, C., J, M., Kn, D., Dg, T., 2016. Longitudinal tracking of subpopulation dynamics and molecular changes during LNCaP cell castration and identification of inhibitors that could target the PSA-/lo castration-resistant cells. Oncotarget 7, 14220–14240. https://doi.org/10.18632/oncotarget.7303

Kahn, B., Collazo, J., Kyprianou, N., 2014. Androgen Receptor as a Driver of Therapeutic Resistance in Advanced Prostate Cancer. Int. J. Biol. Sci. 10, 588–595. https://doi.org/10.7150/ijbs.8671

Kalluri, R., Weinberg, R.A., 2009. The basics of epithelial-mesenchymal transition. J. Clin. Invest. 119, 1420–1428. https://doi.org/10.1172/JCI39104

Kanatous, S.B., Mammen, P.P.A., Rosenberg, P.B., Martin, C.M., White, M.D., DiMaio, J.M., Huang, G., Muallem, S., Garry, D.J., 2009. Hypoxia reprograms calcium signaling and regulates myoglobin expression. Am. J. Physiol. - Cell Physiol. 296, C393–C402. https://doi.org/10.1152/ajpcell.00428.2008

Kang, H.-W., Park, J.-Y., Jeong, S.-W., Kim, J.-A., Moon, H.-J., Perez-Reyes, E., Lee, J.-H., 2006. A molecular determinant of nickel inhibition in Cav3.2 T-type calcium channels. J. Biol. Chem. 281, 4823–4830. https://doi.org/10.1074/jbc.M510197200

Kang, M.K., Kang, S.K., 2008. Pharmacologic blockade of chloride channel synergistically enhances apoptosis of chemotherapeutic drug-resistant cancer stem cells. Biochem Biophys Res Commun 373, 539–544. https://doi.org/10.1016/j.bbrc.2008.06.070

Kanwar, N., Carmine-Simmen, K., Nair, R., Wang, C., Moghadas-Jafari, S., Blaser, H., Tran-Thanh, D., Wang, D., Wang, P., Wang, J., Pasculescu, A., Datti, A., Mak, T., Lewis, J.D., Done, S.J., 2020. Amplification of a calcium channel subunit CACNG4 increases breast cancer metastasis. EBioMedicine 52. https://doi.org/10.1016/j.ebiom.2020.102646

Kappel, S., Marques, I.J., Zoni, E., Stokłosa, P., Peinelt, C., Mercader, N., Kruithof-de Julio, M., Borgström, A., 2017. Store-Operated Ca2+ Entry as a Prostate Cancer Biomarker — a Riddle with Perspectives. Curr. Mol. Biol. Rep. 3, 208–217. https://doi.org/10.1007/s40610-017-0072-8

Karantanos, T., Corn, P.G., Thompson, T.C., 2013. Prostate cancer progression after androgen deprivation therapy: mechanisms of castrate resistance and novel therapeutic approaches. Oncogene 32, 5501–5511. https://doi.org/10.1038/onc.2013.206

Kawahara, T., Kashiwagi, E., Ide, H., Li, Y., Zheng, Y., Ishiguro, H., Miyamoto, H., 2015. The role of NFATc1 in prostate cancer progression: cyclosporine A and tacrolimus inhibit cell proliferation, migration, and invasion. The Prostate 75, 573–584. https://doi.org/10.1002/pros.22937

Keith, B., Simon, M.C., 2007. Hypoxia Inducible Factors, stem cells and cancer. Cell 129, 465–472. https://doi.org/10.1016/j.cell.2007.04.019

Khandrika, L., Lieberman, R., Koul, S., Kumar, B., Maroni, P., Chandhoke, R., Meacham, R.B., Koul, H.K., 2009. Hypoxia-associated p38 mitogen-activated protein kinase-mediated androgen receptor activation and increased HIF-1α levels contribute to emergence of an aggressive phenotype in prostate cancer. Oncogene 28, 1248–1260. https://doi.org/10.1038/onc.2008.476

Kheirandish, P., Chinegwundoh, F., 2011. Ethnic differences in prostate cancer. Br. J. Cancer 105, 481–485. https://doi.org/10.1038/bjc.2011.273

Kim, J.-B., 2014. Channelopathies. Korean J. Pediatr. 57, 1–18. https://doi.org/10.3345/kjp.2014.57.1.1

Kim, S., Yun, H.-M., Baik, J.-H., Chung, K.C., Nah, S.-Y., Rhim, H., 2007. Functional interaction of neuronal Cav1.3 L-type calcium channel with ryanodine receptor type 2 in the rat hippocampus. J. Biol. Chem. 282, 32877–32889. https://doi.org/10.1074/jbc.M701418200

Kim, Y., Lin, Q., Glazer, P.M., Yun, Z., 2009. Hypoxic Tumor Microenvironment and Cancer Cell Differentiation. Curr. Mol. Med. 9, 425–434.

Kirby, M., Hirst, C., Crawford, E.D., 2011. Characterising the castration-resistant prostate cancer population: a systematic review. Int. J. Clin. Pract. 65, 1180–1192. https://doi.org/10.1111/j.1742-1241.2011.02799.x

Kizaka-Kondoh, S., Konse-Nagasawa, H., 2009. Significance of nitroimidazole compounds and hypoxia-inducible factor-1 for imaging tumor hypoxia. Cancer Sci. 100, 1366–1373. https://doi.org/10.1111/j.1349-7006.2009.01195.x

Klonisch, T., Wiechec, E., Hombach-Klonisch, S., Ande, S.R., Wesselborg, S., Schulze-Osthoff, K., Los, M., 2008. Cancer stem cell markers in common cancers – therapeutic implications. Trends Mol. Med. 14, 450–460. https://doi.org/10.1016/j.molmed.2008.08.003

Kobylewski, S.E., Henderson, K.A., Eckhert, C.D., 2012. Identification of ryanodine receptor isoforms in prostate DU-145, LNCaP, and PWR-1E cells. Biochem. Biophys. Res. Commun. 425, 431–435. https://doi.org/10.1016/j.bbrc.2012.07.119

Krizova, A., Maltan, L., Derler, I., 2019. Critical parameters maintaining authentic CRAC channel hallmarks. Eur. Biophys. J. 48, 425–445. https://doi.org/10.1007/s00249-019-01355-6

Kuhlmann, C.R.W., Trümper, J.R.F.C., Abdallah, Y., Lüdders, D.W., Schaefer, C.A., Most, A.K., Backenköhler, U., Neumann, T., Walther, S., Piper, H.M., Tillmanns, H., Erdogan, A., 2004. The K+-channel opener NS1619 increases endothelial NO-synthesis involving p42/p44 MAP-kinase. Thromb. Haemost. 92, 1099–1107. https://doi.org/10.1160/TH04-03-0196

Kunzelmann, K., 2005. Ion Channels and Cancer. J. Membr. Biol. 205, 159. https://doi.org/10.1007/s00232-005-0781-4

Kuriyama, M., Wang, M.C., Lee, C., Papsidero, L.D., Killian, C.S., Inaji, H., Slack, N.H., Nishiura, T., Murphy, G.P., Chu, T.M., 1981. Use of Human Prostate-specific Antigen in Monitoring Prostate Cancer. Cancer Res. 41, 3874–3876.

Kuriyama, M., Wang, M.C., Papsidero, L.D., Killian, C.S., Shimano, T., Valenzuela, L., Nishiura, T., Murphy, G.P., Chu, T.M., 1980. Quantitation of Prostate-specific Antigen in Serum by a Sensitive Enzyme Immunoassay. Cancer Res. 40, 4658–4662.

Kuzmenkina, E., Novikova, E., Jangsangthong, W., Matthes, J., Herzig, S., 2019. Single-Channel Resolution of the Interaction between C-Terminal CaV1.3 Isoforms and Calmodulin. Biophys. J. 116, 836–846. https://doi.org/10.1016/j.bpj.2019.01.025

Lallet-Daher, H., Roudbaraki, M., Bavencoffe, A., Mariot, P., Gackière, F., Bidaux, G., Urbain, R., Gosset, P., Delcourt, P., Fleurisse, L., Slomianny, C., Dewailly, E., Mauroy, B., Bonnal, J.L., Skryma, R., Prevarskaya, N., 2009. Intermediate-conductance Ca^{2+}-activated K^+ channels (IK$_\textrmCa1$) regulate human prostate cancer cell proliferation through a close control of calcium entry. Oncogene 28, 1792–1806. https://doi.org/10.1038/onc.2009.25

Lamouille, S., Xu, J., Derynck, R., 2014. Molecular mechanisms of epithelial–mesenchymal transition. Nat. Rev. Mol. Cell Biol. 15, 178–196. https://doi.org/10.1038/nrm3758

Langeler, E.G., Uffelen, C.J.C.V., Blankenstein, M.A., Steenbrugge, G.J.V., Mulder, E., 1993. Effect of culture conditions on androgen sensitivity of the human prostatic cancer cell line LNCaP. The Prostate 23, 213–223. https://doi.org/10.1002/pros.2990230304

Lastraioli, E., Iorio, J., Arcangeli, A., 2015. Ion channel expression as promising cancer biomarker. Biochim. Biophys. Acta BBA - Biomembr., Membrane Channels and Transporters in Cancers 1848, 2685–2702. https://doi.org/10.1016/j.bbamem.2014.12.016

Lawson, D.A., Zong, Y., Memarzadeh, S., Xin, L., Huang, J., Witte, O.N., 2010. Basal epithelial stem cells are efficient targets for prostate cancer initiation. Proc. Natl. Acad. Sci. U. S. A. 107, 2610–2615. https://doi.org/10.1073/pnas.0913873107

Leanza, L., Managò, A., Zoratti, M., Gulbins, E., Szabo, I., 2016. Pharmacological targeting of ion channels for cancer therapy: In vivo evidences. Biochim. Biophys. Acta BBA - Mol. Cell Res., Calcium and Cell Fate 1863, 1385–1397. https://doi.org/10.1016/j.bbamcr.2015.11.032

Legrand, G., Humez, S., Slomianny, C., Dewailly, E., Abeele, F.V., Mariot, P., Wuytack, F., Prevarskaya, N., 2001. Ca2+ Pools and Cell Growth EVIDENCE FOR SARCOENDOPLASMIC

Ca2+-ATPases 2B INVOLVEMENT IN HUMAN PROSTATE CANCER CELL GROWTH CONTROL. J. Biol. Chem. 276, 47608–47614. https://doi.org/10.1074/jbc.M107011200

Lehen'Kyi, V., Flourakis, M., Skryma, R., Prevarskaya, N., 2007. TRPV6 channel controls prostate cancer cell proliferation via Ca 2+ /NFAT-dependent pathways. Oncogene 26, 7380–7385. https://doi.org/10.1038/sj.onc.1210545

Lekås, E., Johansson, M., Widmark, A., Bergh, A., Damber, J.-E., 1997. Decrement of blood flow precedes the involution of the ventral prostate in the rat after castration. Urol. Res. 25, 309–314. https://doi.org/10.1007/BF01294656

Lesko, S.M., Rosenberg, L., Shapiro, S., 1996. Family history and prostate cancer risk. Am. J. Epidemiol. 144, 1041–1047.

Li, P., Yang, R., Gao, W.-Q., 2014. Contributions of epithelial-mesenchymal transition and cancer stem cells to the development of castration resistance of prostate cancer. Mol. Cancer 13, 55. https://doi.org/10.1186/1476-4598-13-55

Li, R., Wang, Y., Yang, Z., He, Y., Zhao, T., Fan, M., Wang, Xuan, Zhu, L., Wang, Xiaomin, 2015. Hypoxia-inducible factor-1α regulates the expression of L-type voltage-dependent Ca2+ channels in PC12 cells under hypoxia. Cell Stress Chaperones 20, 507–516. https://doi.org/10.1007/s12192-015-0575-2

Li, Y., Guo, B., Xie, Q., Ye, D., Zhang, D., Zhu, Y., Chen, H., Zhu, B., 2015. STIM1 Mediates Hypoxia-Driven Hepatocarcinogenesis via Interaction with HIF-1. Cell Rep. 12, 388–395. https://doi.org/10.1016/j.celrep.2015.06.033

Li, Z., Bao, S., Wu, Q., Wang, H., Eyler, C., Sathornsumetee, S., Shi, Q., Cao, Y., Lathia, J., McLendon, R.E., Hjelmeland, A.B., Rich, J.N., 2009. Hypoxia-Inducible Factors Regulate Tumorigenic Capacity of Glioma Stem Cells. Cancer Cell 15, 501–513. https://doi.org/10.1016/j.ccr.2009.03.018

Lieb, A., Scharinger, A., Sartori, S., Sinnegger-Brauns, M.J., Striessnig, J., 2012. Structural determinants of CaV1.3 L-type calcium channel gating. Channels 6, 197–205. https://doi.org/10.4161/chan.21002

Lin, T.-P., Chang, Y.-T., Lee, S.-Y., Campbell, M., Wang, T.-C., Shen, S.-H., Chung, H.-J., Chang, Y.-H., Chiu, A.W., Pan, C.-C., Lin, C.-H., Chu, C.-Y., Kung, H.-J., Cheng, C.-Y., Chang, P.-C., 2016. REST reduction is essential for hypoxia-induced neuroendocrine differentiation of prostate cancer cells by activating autophagy signaling. Oncotarget 7, 26137–26151. https://doi.org/10.18632/oncotarget.8433

Lipscombe, D., Helton, T.D., Xu, W., 2004. L-type calcium channels: the low down. J. Neurophysiol. 92, 2633–2641. https://doi.org/10.1152/jn.00486.2004

Litan, A., Langhans, S.A., 2015. Cancer as a channelopathy: ion channels and pumps in tumor development and progression. Front Cell Neurosci 9. https://doi.org/10.3389/fncel.2015.00086

Liu, M., Inoue, K., Leng, T., Guo, S., Xiong, Z., 2014. TRPM7 channels regulate glioma stem cell through STAT3 and Notch signaling pathways. Cell. Signal. 26, 2773–2781. https://doi.org/10.1016/j.cellsig.2014.08.020

Livak, K.J., Schmittgen, T.D., 2001. Analysis of Relative Gene Expression Data Using Real-Time Quantitative PCR and the 2−ΔΔCT Method. Methods 25, 402–408. https://doi.org/10.1006/meth.2001.1262

Llinás, R., Sugimori, M., Lin, J.W., Cherksey, B., 1989. Blocking and isolation of a calcium channel from neurons in mammals and cephalopods utilizing a toxin fraction (FTX) from funnel-web spider poison. Proc. Natl. Acad. Sci. U. S. A. 86, 1689–1693. https://doi.org/10.1073/pnas.86.5.1689

Long, Z., Chen, B., Liu, Q., Zhao, J., Yang, Z., Dong, X., Xia, L., Huang, S., Hu, X., Song, B., Li, L., 2016. The reverse-mode NCX1 activity inhibitor KB-R7943 promotes prostate cancer cell death by activating the JNK pathway and blocking autophagic flux. Oncotarget 7, 42059–42070. https://doi.org/10.18632/oncotarget.9806

Lu, H., Chen, I., Shimoda, L.A., Park, Y., Zhang, C., Tran, L., Zhang, H., Semenza, G.L., 2017. Chemotherapy-Induced Ca2+ Release Stimulates Breast Cancer Stem Cell Enrichment. Cell Rep. 18, 1946–1957. https://doi.org/10.1016/j.celrep.2017.02.001

Lu, L., Sirish, P., Zhang, Z., Woltz, R.L., Li, N., Timofeyev, V., Knowlton, A.A., Zhang, X.-D., Yamoah, E.N., Chiamvimonvat, N., 2015. Regulation of gene transcription by voltage-gated L-type calcium channel, Cav1.3. J. Biol. Chem. 290, 4663–4676. https://doi.org/10.1074/jbc.M114.586883

Lukashev, D., Ohta, A., Sitkovsky, M., 2007. Hypoxia-dependent anti-inflammatory pathways in protection of cancerous tissues. Cancer Metastasis Rev. 26, 273–279. https://doi.org/10.1007/s10555-007-9054-2

Lunardi, P., Beauval, J.-B., Roumiguié, M., Soulié, M., Cuvillier, O., Malavaud, B., 2016. [Mechanisms of castration resistance: Intratumoral hypoxia stimulates the androgen receptor expression]. Progres En Urol. J. Assoc. Francaise Urol. Soc. Francaise Urol. 26, 159–167. https://doi.org/10.1016/j.purol.2016.01.004

Lundgren, K., Nordenskjöld, B., Landberg, G., 2009. Hypoxia, Snail and incomplete epithelial–mesenchymal transition in breast cancer. Br. J. Cancer 101, 1769–1781. https://doi.org/10.1038/sj.bjc.6605369

Ma, H., Groth, R.D., Cohen, S.M., Emery, J.F., Li, B., Hoedt, E., Zhang, G., Neubert, T.A., Tsien, R.W., 2014. γCaMKII shuttles Ca^{2+}/CaM to the nucleus to trigger CREB phosphorylation and gene expression. Cell 159, 281–294. https://doi.org/10.1016/j.cell.2014.09.019

Mabjeesh, N.J., Willard, M.T., Frederickson, C.E., Zhong, H., Simons, J.W., 2003. Androgens Stimulate Hypoxia-inducible Factor 1 Activation via Autocrine Loop of Tyrosine Kinase Receptor/Phosphatidylinositol 3'-Kinase/Protein Kinase B in Prostate Cancer Cells. Clin Cancer Res 9, 2416–2425.

Malik, Z.A., Stein, I.S., Navedo, M.F., Hell, J.W., 2014. Mission CaMKIIγ: Shuttle Calmodulin from Membrane to Nucleus. Cell 159, 235–237. https://doi.org/10.1016/j.cell.2014.09.023

Maly, I.V., Hofmann, W.A., 2018. Calcium and Nuclear Signaling in Prostate Cancer. Int. J. Mol. Sci. 19. https://doi.org/10.3390/ijms19041237

Mancini, M., Toker, A., 2009. NFAT Proteins: Emerging Roles in Cancer Progression. Nat. Rev. Cancer 9, 810–820. https://doi.org/10.1038/nrc2735

Manda, K.R., Tripathi, P., Hsi, A.C., Ning, J., Ruzinova, M.B., Liapis, H., Bailey, M., Zhang, H., Maher, C.A., Humphrey, P.A., Andriole, G.L., Ding, L., You, Z., Chen, F., 2016. NFATc1 promotes prostate tumorigenesis and overcomes PTEN loss-induced senescence. Oncogene 35, 3282–3292. https://doi.org/10.1038/onc.2015.389

Mangoni, M.E., Couette, B., Bourinet, E., Platzer, J., Reimer, D., Striessnig, J., Nargeot, J., 2003. Functional role of L-type Cav1.3 Ca2+ channels in cardiac pacemaker activity. PNAS 100, 5543–5548. https://doi.org/10.1073/pnas.0935295100

Mani, S.A., Guo, W., Liao, M.-J., Eaton, E.Ng., Ayyanan, A., Zhou, A.Y., Brooks, M., Reinhard, F., Zhang, C.C., Shipitsin, M., Campbell, L.L., Polyak, K., Brisken, C., Yang, J., Weinberg, R.A., 2008. The epithelial-mesenchymal transition generates cells with properties of stem cells. Cell 133, 704–715. https://doi.org/10.1016/j.cell.2008.03.027

Marcantoni, A., Vandael, D.H.F., Mahapatra, S., Carabelli, V., Sinnegger-Brauns, M.J., Striessnig, J., Carbone, E., 2010. Loss of Cav1.3 Channels Reveals the Critical Role of L-Type and BK Channel Coupling in Pacemaking Mouse Adrenal Chromaffin Cells. J. Neurosci. 30, 491–504. https://doi.org/10.1523/JNEUROSCI.4961-09.2010

Marhold, M., Tomasich, E., El-Gazzar, A., Heller, G., Spittler, A., Horvat, R., Krainer, M., Horak, P., 2015. HIF1α Regulates mTOR Signaling and Viability of Prostate Cancer Stem Cells. Mol Cancer Res 13, 556–564. https://doi.org/10.1158/1541-7786.MCR-14-0153-T

Marín-Aguilera, M., Codony-Servat, J., Reig, Ò., Lozano, J.J., Fernández, P.L., Pereira, M.V., Jiménez, N., Donovan, M., Puig, P., Mengual, L., Bermudo, R., Font, A., Gallardo, E., Ribal, M.J., Alcaraz, A., Gascón, P., Mellado, B., 2014. Epithelial-to-mesenchymal transition

mediates docetaxel resistance and high risk of relapse in prostate cancer. Mol Cancer Ther 13, 1270–1284. https://doi.org/10.1158/1535-7163.MCT-13-0775

Mariot, P., Prevarskaya, N., Roudbaraki, M.M., Le Bourhis, X., Van Coppenolle, F., Vanoverberghe, K., Skryma, R., 2000. Evidence of functional ryanodine receptor involved in apoptosis of prostate cancer (LNCaP) cells. The Prostate 43, 205–214. https://doi.org/10.1002/(sici)1097-0045(20000515)43:3<205::aid-pros6>3.0.co;2-m

Mariot, P., Vanoverberghe, K., Lalevée, N., Rossier, M.F., Prevarskaya, N., 2002. Overexpression of an α1H (Cav3.2) T-type Calcium Channel during Neuroendocrine Differentiation of Human Prostate Cancer Cells. J. Biol. Chem. 277, 10824–10833. https://doi.org/10.1074/jbc.M108754200

Masoud, G.N., Li, W., 2015. HIF-1α pathway: role, regulation and intervention for cancer therapy. Acta Pharm. Sin. B 5, 378–389. https://doi.org/10.1016/j.apsb.2015.05.007

Mayr, B., Montminy, M., 2001. Transcriptional regulation by the phosphorylation-dependent factor CREB. Nat. Rev. Mol. Cell Biol. 2, 599–609. https://doi.org/10.1038/35085068

McKeown, S.R., 2014. Defining normoxia, physoxia and hypoxia in tumours—implications for treatment response. Br. J. Radiol. 87. https://doi.org/10.1259/bjr.20130676

McNeal, J.E., 1981. The zonal anatomy of the prostate. The Prostate 2, 35–49. https://doi.org/10.1002/pros.2990020105

Middelbeek, J., Visser, D., Henneman, L., Kamermans, A., Kuipers, A.J., Hoogerbrugge, P.M., Jalink, K., van Leeuwen, F.N., 2015. TRPM7 maintains progenitor-like features of neuroblastoma cells: implications for metastasis formation. Oncotarget 6, 8760–8776.

Ming, L., Byrne, N., Camac, S., Mitchell, C., Ward, C., Waugh, Dj, McKeown, S., Worthington, J., Waugh, David, 2013. Androgen deprivation results in time-dependent hypoxia in LNCaP prostate tumours; informed scheduling of the bioreductive drug AQ4N improves treatment response. Int. J. Cancer J. Int. Cancer 132, 1323–1332. https://doi.org/10.1002/ijc.27796

Minocherhomjee, A.E., Roufogalis, B.D., 1984. Antagonism of calmodulin and phosphodiesterase by nifedipine and related calcium entry blockers. Cell Calcium 5, 57–63. https://doi.org/10.1016/0143-4160(84)90154-4

Mitani, T., Yamaji, R., Higashimura, Y., Harada, N., Nakano, Y., Inui, H., 2011. Hypoxia enhances transcriptional activity of androgen receptor through hypoxia-inducible factor-1α in a low androgen environment. J. Steroid Biochem. Mol. Biol. 123, 58–64. https://doi.org/10.1016/j.jsbmb.2010.10.009

Mo, P., Yang, S., 2018. The Store-Operated Calcium Channels in Cancer Metastasis: from Cell Migration, Invasion to Metastatic Colonization. Front. Biosci. Landmark Ed. 23, 1241–1256.

Mochida, S., 2019. Presynaptic Calcium Channels. Int. J. Mol. Sci. 20. https://doi.org/10.3390/ijms20092217

Moltzahn, F., Thalmann, G.N., 2013. Cancer stem cells in prostate cancer. Transl. Androl. Urol. 2, 242–253. https://doi.org/10.3978/j.issn.2223-4683.2013.09.06

Monteith, G.R., McAndrew, D., Faddy, H.M., Roberts-Thomson, S.J., 2007. Calcium and cancer: targeting $Ca^{2+}$$ transport. Nat. Rev. Cancer 7, 519–530. https://doi.org/10.1038/nrc2171

Montell, C., Birnbaumer, L., Flockerzi, V., 2002. The TRP Channels, a Remarkably Functional Family. Cell 108, 595–598. https://doi.org/10.1016/S0092-8674(02)00670-0

Morel, A.-P., Lièvre, M., Thomas, C., Hinkal, G., Ansieau, S., Puisieux, A., 2008. Generation of Breast Cancer Stem Cells through Epithelial-Mesenchymal Transition. PLoS ONE 3. https://doi.org/10.1371/journal.pone.0002888

Motiani, R.K., Hyzinski-García, M.C., Zhang, X., Henkel, M.M., Abdullaev, I.F., Kuo, Y.-H., Matrougui, K., Mongin, A.A., Trebak, M., 2013. STIM1 and Orai1 mediate CRAC channel activity and are essential for human glioblastoma invasion. Pflüg. Arch. - Eur. J. Physiol. 465, 1249–1260. https://doi.org/10.1007/s00424-013-1254-8

Mottet Denis, Michel Gaetan, Renard Patricia, Ninane Noelle, Raes Martine, Michiels Carine, 2006. ERK and Calcium in Activation of HIF-1. Ann. N. Y. Acad. Sci. 973, 448–453. https://doi.org/10.1111/j.1749-6632.2002.tb04681.x

Movsas, B., Chapman, J.D., Greenberg, R.E., Hanlon, A.L., Horwitz, E.M., Pinover, W.H., Stobbe, C., Hanks, G.E., 2000. Increasing levels of hypoxia in prostate carcinoma correlate significantly with increasing clinical stage and patient age: an Eppendorf pO(2) study. Cancer 89, 2018–2024. https://doi.org/10.1002/1097-0142(20001101)89:9<2018::aid-cncr19>3.3.co;2-p

Movsas, B., Chapman, J.D., Hanlon, A.L., Horwitz, E.M., Pinover, W.H., Greenberg, R.E., Stobbe, C., Hanks, G.E., 2001. Hypoxia in human prostate carcinoma: an Eppendorf PO2 study. Am. J. Clin. Oncol. 24, 458–461. https://doi.org/10.1097/00000421-200110000-00009

Neely, A., Hidalgo, P., 2014. Structure-function of proteins interacting with the α1 pore-forming subunit of high-voltage-activated calcium channels. Front. Physiol. 5. https://doi.org/10.3389/fphys.2014.00209

Nevedomskaya, E., Baumgart, S.J., Haendler, B., 2018. Recent Advances in Prostate Cancer Treatment and Drug Discovery. Int. J. Mol. Sci. 19. https://doi.org/10.3390/ijms19051359

Nieto, M.A., 2013. Epithelial Plasticity: A Common Theme in Embryonic and Cancer Cells. Science 342, 1234850. https://doi.org/10.1126/science.1234850

Nilius, B., Owsianik, G., 2011. The transient receptor potential family of ion channels. Genome Biol. 12, 218. https://doi.org/10.1186/gb-2011-12-3-218

Nishida, N., Yano, H., Nishida, T., Kamura, T., Kojiro, M., 2006. Angiogenesis in Cancer. Vasc. Health Risk Manag. 2, 213–219.

Numa, S., Tanabe, T., Takeshima, H., Mikami, A., Niidome, T., Nishimura, S., Adams, B.A., Beam, K.G., 1990. Molecular insights into excitation-contraction coupling. Cold Spring Harb. Symp. Quant. Biol. 55, 1–7. https://doi.org/10.1101/sqb.1990.055.01.003

Odero-Marah, V., Hawsawi, O., Henderson, V., Sweeney, J., 2018. Epithelial-Mesenchymal Transition (EMT) and Prostate Cancer, in: Schatten, H. (Ed.), Cell & Molecular Biology of Prostate Cancer: Updates, Insights and New Frontiers, Advances in Experimental Medicine and Biology. Springer International Publishing, Cham, pp. 101–110. https://doi.org/10.1007/978-3-319-95693-0_6

Oh, W.K., Hurwitz, M., D'Amico, A.V., Richie, J.P., Kantoff, P.W., 2003. Biology of Prostate Cancer.

Ohl, F., Jung, M., Xu, C., Stephan, C., Rabien, A., Burkhardt, M., Nitsche, A., Kristiansen, G., Loening, S.A., Radonić, A., Jung, K., 2005. Gene expression studies in prostate cancer tissue: which reference gene should be selected for normalization? J. Mol. Med. 83, 1014–1024. https://doi.org/10.1007/s00109-005-0703-z

Ojo, D., Lin, X., Wong, N., Gu, Y., Tang, D., 2015. Prostate Cancer Stem-like Cells Contribute to the Development of Castration-Resistant Prostate Cancer. Cancers Basel 7, 2290–2308. https://doi.org/10.3390/cancers7040890

O'Reilly, D., Buchanan, P., 2019. Calcium channels and cancer stem cells. Cell Calcium 81, 21–28. https://doi.org/10.1016/j.ceca.2019.05.006

Ouardouz, M., Nikolaeva, M.A., Coderre, E., Zamponi, G.W., McRory, J.E., Trapp, B.D., Yin, X., Wang, W., Woulfe, J., Stys, P.K., 2003. Depolarization-Induced Ca2+ Release in Ischemic Spinal Cord White Matter Involves L-type Ca2+ Channel Activation of Ryanodine Receptors. Neuron 40, 53–63. https://doi.org/10.1016/j.neuron.2003.08.016

Ozaki, T., Nakagawara, A., 2011. Role of p53 in Cell Death and Human Cancers. Cancers 3, 994–1013. https://doi.org/10.3390/cancers3010994

Palapattu, G.S., Wu, C., Silvers, C.R., Martin, H.B., Williams, K., Salamone, L., Bushnell, T., Huang, L.-S., Yang, Q., Huang, J., 2009. Selective expression of CD44, a putative prostate cancer stem cell marker, in neuroendocrine tumor cells of human prostate cancer. Prostate 69, 787–798. https://doi.org/10.1002/pros.20928

Parekh, A.B., Putney, J.W., 2005. Store-Operated Calcium Channels. Physiol. Rev. 85, 757–810. https://doi.org/10.1152/physrev.00057.2003

Park, J.W., Lee, J.K., Phillips, J.W., Huang, P., Cheng, D., Huang, J., Witte, O.N., 2016. Prostate epithelial cell of origin determines cancer differentiation state in an organoid transformation assay. Proc. Natl. Acad. Sci. 113, 4482–4487. https://doi.org/10.1073/pnas.1603645113

Park, S.-Y., Kim, Y.-J., Gao, A.C., Mohler, J.L., Onate, S.A., Hidalgo, A.A., Ip, C., Park, E.-M., Yoon, S.Y., Park, Y.-M., 2006. Hypoxia Increases Androgen Receptor Activity in Prostate Cancer Cells. Cancer Res. 66, 5121–5129. https://doi.org/10.1158/0008-5472.CAN-05-1341

Parkash, J., Asotra, K., 2010. Calcium wave signaling in cancer cells. Life Sci. 87, 587–595. https://doi.org/10.1016/j.lfs.2010.09.013

Patel, G.K., Chugh, N., Tripathi, M., 2019. Neuroendocrine Differentiation of Prostate Cancer—An Intriguing Example of Tumor Evolution at Play. Cancers 11, 1405. https://doi.org/10.3390/cancers11101405

Peretti, M., Angelini, M., Savalli, N., Florio, T., Yuspa, S.H., Mazzanti, M., 2015. Chloride channels in cancer: Focus on chloride intracellular channel 1 and 4 (CLIC1 AND CLIC4) proteins in tumor development and as novel therapeutic targets. Biochim. Biophys. Acta BBA - Biomembr., Membrane Channels and Transporters in Cancers 1848, 2523–2531. https://doi.org/10.1016/j.bbamem.2014.12.012

Perez-Reyes, E., 2003. Molecular Physiology of Low-Voltage-Activated T-type Calcium Channels. Physiol. Rev. 83, 117–161. https://doi.org/10.1152/physrev.00018.2002

Perron, L., Bairati, I., Harel, F., Meyer, F., 2004. Antihypertensive drug use and the risk of prostate cancer (Canada). Cancer Causes Control CCC 15, 535–541. https://doi.org/10.1023/B:CACO.0000036152.58271.5e

Perrouin Verbe, M.-A., Bruyere, F., Rozet, F., Vandier, C., Fromont, G., 2016. Expression of store-operated channel components in prostate cancer: the prognostic paradox. Hum. Pathol. 49, 77–82. https://doi.org/10.1016/j.humpath.2015.09.042

Phan, N.N., Wang, C.-Y., Chen, C.-F., Sun, Z., Lai, M.-D., Lin, Y.-C., 2017. Voltage-gated calcium channels: Novel targets for cancer therapy. Oncol. Lett. 14, 2059–2074. https://doi.org/10.3892/ol.2017.6457

Pinto, M.C.X., Kihara, A.H., Goulart, V.A.M., Tonelli, F.M.P., Gomes, K.N., Ulrich, H., Resende, R.R., 2015. Calcium signaling and cell proliferation. Cell. Signal. 27, 2139–2149. https://doi.org/10.1016/j.cellsig.2015.08.006

Pitt, G.S., Matsui, M., Cao, C., 2021. Voltage-Gated Calcium Channels in Nonexcitable Tissues. Annu. Rev. Physiol. 83, null. https://doi.org/10.1146/annurev-physiol-031620-091043

Poch, M.A., Mehedint, D., Green, D.J., Payne-Ondracek, R., Fontham, E.T.H., Bensen, J.T., Attwood, K., Wilding, G.E., Guru, K.A., Underwood, W., Mohler, J.L., Heemers, H.V., 2013. The association between calcium channel blocker use and prostate cancer outcome. The Prostate 73, 865–872. https://doi.org/10.1002/pros.22632

Potier, M., Joulin, V., Roger, S., Besson, P., Jourdan, M.-L., Leguennec, J.-Y., Bougnoux, P., Vandier, C., 2006. Identification of SK3 channel as a new mediator of breast cancer cell migration. Mol. Cancer Ther. 5, 2946–2953. https://doi.org/10.1158/1535-7163.MCT-06-0194

Power, J.M., Sah, P., 2005. Intracellular calcium store filling by an L-type calcium current in the basolateral amygdala at subthreshold membrane potentials. J. Physiol. 562, 439–453. https://doi.org/10.1113/jphysiol.2004.076711

Prakriya, M., 2020. Calcium and cell function. J. Physiol. 598, 1647–1648. https://doi.org/10.1113/JP279541

Prevarskaya, N., Skryma, R., Bidaux, G., Flourakis, M., Shuba, Y., 2007. Ion channels in death and differentiation of prostate cancer cells. Cell Death Differ 14, 1295–1304. https://doi.org/10.1038/sj.cdd.4402162

Prevarskaya, Natalia, Zhang, L., Barritt, G., 2007. TRP channels in cancer. Biochim. Biophys. Acta BBA - Mol. Basis Dis., TRP Channels in Disease 1772, 937–946. https://doi.org/10.1016/j.bbadis.2007.05.006

Qu, Y., Karnabi, E., Ramadan, O., Yue, Y., Chahine, M., Boutjdir, M., 2011. Perinatal and Postnatal Expression of Cav1.3 α1D Ca2+ Channel in the Rat Heart. Pediatr. Res. 69, 479–484. https://doi.org/10.1203/PDR.0b013e318217a0df

Quang, C.T., Leboucher, S., Passaro, D., Fuhrmann, L., Nourieh, M., Vincent-Salomon, A., Ghysdael, J., 2015. The calcineurin/NFAT pathway is activated in diagnostic breast cancer cases and is essential to survival and metastasis of mammary cancer cells. Cell Death Dis. 6, e1658. https://doi.org/10.1038/cddis.2015.14

Radhakrishnan, V.M., Gilpatrick, M.M., Parsa, N.A., Kiela, P.R., Ghishan, F.K., 2016. Expression of Cav1.3 calcium channel in the human and mouse colon: posttranscriptional inhibition by IFNγ. Am. J. Physiol.-Gastrointest. Liver Physiol. 312, G77–G84. https://doi.org/10.1152/ajpgi.00394.2016

Raffo, A.J., Perlman, H., Chen, M.-W., Day, M.L., Streitman, J.S., Buttyan, R., 1995. Overexpression of bcl-2 Protects Prostate Cancer Cells from Apoptosis *in Vitro* and Confers Resistance to Androgen Depletion *in Vivo*. Cancer Res 55, 4438–4445.

Rajakulendran, S., Kaski, D., Hanna, M.G., 2012. Neuronal P/Q-type calcium channel dysfunction in inherited disorders of the CNS. Nat. Rev. Neurol. 8, 86–96. https://doi.org/10.1038/nrneurol.2011.228

Randall, A., Tsien, R.W., 1995. Pharmacological dissection of multiple types of Ca2+ channel currents in rat cerebellar granule neurons. J. Neurosci. 15, 2995–3012. https://doi.org/10.1523/JNEUROSCI.15-04-02995.1995

Rao, V.R., Perez-Neut, M., Kaja, S., Gentile, S., 2015. Voltage-Gated Ion Channels in Cancer Cell Proliferation. Cancers Basel 7, 849–875. https://doi.org/10.3390/cancers7020813

Rawla, P., 2019. Epidemiology of Prostate Cancer. World J. Oncol. 10, 63–89. https://doi.org/10.14740/wjon1191

Resende, R.R., Andrade, L.M., Oliveira, A.G., Guimarães, E.S., Guatimosim, S., Leite, M.F., 2013. Nucleoplasmic calcium signaling and cell proliferation: calcium signaling in the nucleus. Cell Commun. Signal. 11, 14. https://doi.org/10.1186/1478-811X-11-14

Rice, M.A., Malhotra, S.V., Stoyanova, T., 2019. Second-Generation Antiandrogens: From Discovery to Standard of Care in Castration Resistant Prostate Cancer. Front. Oncol. 9. https://doi.org/10.3389/fonc.2019.00801

Richardson, G.D., Robson, C.N., Lang, S.H., Neal, D.E., Maitland, N.J., Collins, A.T., 2004. CD133, a novel marker for human prostatic epithelial stem cells. J. Cell Sci. 117, 3539–3545. https://doi.org/10.1242/jcs.01222

Riganti, C., Doublier, S., Viarisio, D., Miraglia, E., Pescarmona, G., Ghigo, D., Bosia, A., 2009. Artemisinin induces doxorubicin resistance in human colon cancer cells via calcium-dependent activation of HIF-1α and P-glycoprotein overexpression. Br. J. Pharmacol. 156, 1054–1066. https://doi.org/10.1111/j.1476-5381.2009.00117.x

Rodda, D.J., Chew, J.-L., Lim, L.-H., Loh, Y.-H., Wang, B., Ng, H.-H., Robson, P., 2005. Transcriptional Regulation of Nanog by OCT4 and SOX2. J. Biol. Chem. 280, 24731–24737. https://doi.org/10.1074/jbc.M502573200

Rodriguez, C., Jacobs, E.J., Deka, A., Patel, A.V., Bain, E.B., Thun, M.J., Calle, E.E., 2009. Use of blood-pressure-lowering medication and risk of prostate cancer in the Cancer Prevention Study II Nutrition Cohort. Cancer Causes Control CCC 20, 671–679. https://doi.org/10.1007/s10552-008-9280-0

Rodriguez-Vida, A., Galazi, M., Rudman, S., Chowdhury, S., Sternberg, C.N., 2015. Enzalutamide for the treatment of metastatic castration-resistant prostate cancer [WWW Document]. Drug Des. Devel. Ther. https://doi.org/10.2147/DDDT.S69433

Rokhlin, O., Taghiyev, A.F., Bayer, K.U., Bumcrot, D., Kotelianski, V.E., Glover, R.A., Cohen, M.B., 2007. Calcium/calmodulin-dependent kinase II plays an important role in prostate cancer cell survival. Cancer Biol. Ther. 6, 732–742. https://doi.org/10.4161/cbt.6.5.3975

Ronquist, G., Rodríguez, L.A.G., Ruigómez, A., Johansson, S., Wallander, M.-A., Frithz, G., Svärdsudd, K., 2004. Association between captopril, other antihypertensive drugs and risk of prostate cancer. The Prostate 58, 50–56. https://doi.org/10.1002/pros.10294

Rosa, P., Sforna, L., Carlomagno, S., Mangino, G., Miscusi, M., Pessia, M., Franciolini, F., Calogero, A., Catacuzzeno, L., 2017. Overexpression of Large-Conductance Calcium-Activated Potassium Channels in Human Glioblastoma Stem-Like Cells and Their Role in Cell Migration. J. Cell. Physiol. 232, 2478–2488. https://doi.org/10.1002/jcp.25592

Rosenthal, E., Shapiro, E., Lepor, H., 1990. Characterization of 1,4, dihydropyridine calcium channel binding sites in the human prostate. J. Urol. 144, 1539–1542. https://doi.org/10.1016/s0022-5347(17)39794-x

Rothermund, C.A., Gopalakrishnan, V.K., Eudy, J.D., Vishwanatha, J.K., 2005. Casodex treatment induces hypoxia-related gene expression in the LNCaP prostate cancer progression model. BMC Urol. 5, 5. https://doi.org/10.1186/1471-2490-5-5

Ruggieri, P., Mangino, G., Fioretti, B., Catacuzzeno, L., Puca, R., Ponti, D., Miscusi, M., Franciolini, F., Ragona, G., Calogero, A., 2012. The Inhibition of KCa3.1 Channels Activity Reduces Cell Motility in Glioblastoma Derived Cancer Stem Cells. PLoS ONE 7. https://doi.org/10.1371/journal.pone.0047825

Rybak, A.P., Bristow, R.G., Kapoor, A., 2015. Prostate cancer stem cells: deciphering the origins and pathways involved in prostate tumorigenesis and aggression. Oncotarget 6, 1900–1919. https://doi.org/10.18632/oncotarget.2953

Sagredo, A.I., Sagredo, E.A., Cappelli, C., Báez, P., Andaur, R.E., Blanco, C., Tapia, J.C., Echeverría, C., Cerda, O., Stutzin, A., Simon, F., Marcelain, K., Armisén, R., 2018. TRPM4 regulates Akt/GSK3-β activity and enhances β-catenin signaling and cell proliferation in prostate cancer cells. Mol. Oncol. 12, 151–165. https://doi.org/10.1002/1878-0261.12100

Sahu, G., Wazen, R.-M., Colarusso, P., Chen, S.R.W., Zamponi, G.W., Turner, R.W., 2019. Junctophilin Proteins Tether a Cav1-RyR2-KCa3.1 Tripartite Complex to Regulate Neuronal Excitability. Cell Rep. 28, 2427-2442.e6. https://doi.org/10.1016/j.celrep.2019.07.075

Sakamoto, K., Kurokawa, J., 2019. Involvement of sex hormonal regulation of K+ channels in electrophysiological and contractile functions of muscle tissues. J. Pharmacol. Sci. 139, 259–265. https://doi.org/10.1016/j.jphs.2019.02.009

Salido, G.M., Sage, S.O., Rosado, J.A., 2009. TRPC channels and store-operated Ca2+ entry. Biochim. Biophys. Acta BBA - Mol. Cell Res. 1793, 223–230. https://doi.org/10.1016/j.bbamcr.2008.11.001

Salnikow, K., Kluz, T., Costa, M., Piquemal, D., Demidenko, Z.N., Xie, K., Blagosklonny, M.V., 2002. The Regulation of Hypoxic Genes by Calcium Involves c-Jun/AP-1, Which Cooperates with Hypoxia-Inducible Factor 1 in Response to Hypoxia. Mol. Cell. Biol. 22, 1734–1741. https://doi.org/10.1128/MCB.22.6.1734-1741.2002

Sánchez, B.G., Bort, A., Vara-Ciruelos, D., Díaz-Laviada, I., 2020. Androgen Deprivation Induces Reprogramming of Prostate Cancer Cells to Stem-Like Cells. Cells 9. https://doi.org/10.3390/cells9061441

Sang, M., Hulsurkar, M., Zhang, X., Song, H., Zheng, D., Zhang, Y., Li, M., Xu, J., Zhang, S., Ittmann, M., Li, W., 2016. GRK3 is a direct target of CREB activation and regulates neuroendocrine differentiation of prostate cancer cells. Oncotarget 7, 45171–45185. https://doi.org/10.18632/oncotarget.9359

Santoni, G., Santoni, M., Nabissi, M., 2012. Functional role of T-type calcium channels in tumour growth and progression: prospective in cancer therapy. Br. J. Pharmacol. 166, 1244–1246. https://doi.org/10.1111/j.1476-5381.2012.01908.x

Santos Ramos, F., Wons, L., João Cavalli, I., M.S.F. Ribeiro, E., 2017. Epithelial-mesenchymal transition in cancer: An overview. Integr. Cancer Sci. Ther. 4. https://doi.org/10.15761/ICST.1000243

Schally, A.V., Comaru-Schally, A.M., 2003. Mode of Action of LHRH Analogs. Holl.-Frei Cancer Med. 6th Ed.

Scholl, U.I., Goh, G., Stölting, G., de Oliveira, R.C., Choi, M., Overton, J.D., Fonseca, A.L., Korah, R., Starker, L.F., Kunstman, J.W., Prasad, M.L., Hartung, E.A., Mauras, N., Benson, M.R., Brady, T., Shapiro, J.R., Loring, E., Nelson-Williams, C., Libutti, S.K., Mane, S., Hellman, P., Westin, G., Åkerström, G., Björklund, P., Carling, T., Fahlke, C., Hidalgo, P., Lifton, R.P., 2013. Somatic and germline CACNA1D calcium channel mutations in aldosterone-producing adenomas and primary aldosteronism. Nat. Genet. 45, 1050–1054. https://doi.org/10.1038/ng.2695

Schröder, F., Crawford, E.D., Axcrona, K., Payne, H., Keane, T.E., 2012. Androgen deprivation therapy: past, present and future. BJU Int. 109, 1–12.

Seidel, S., Garvalov, B.K., Wirta, V., von Stechow, L., Schänzer, A., Meletis, K., Wolter, M., Sommerlad, D., Henze, A.-T., Nistér, M., Reifenberger, G., Lundeberg, J., Frisén, J., Acker, T., 2010. A hypoxic niche regulates glioblastoma stem cells through hypoxia inducible factor 2α. Brain 133, 983–995. https://doi.org/10.1093/brain/awq042

Semenza, G.L., 2012. Hypoxia-inducible factors: mediators of cancer progression and targets for cancer therapy. Trends Pharmacol. Sci. 33, 207–214. https://doi.org/10.1016/j.tips.2012.01.005

Semenza, G.L., 2001. HIF-1 and mechanisms of hypoxia sensing. Curr. Opin. Cell Biol. 13, 167–171. https://doi.org/10.1016/S0955-0674(00)00194-0

Seta, K.A., Yuan, Y., Spicer, Z., Lu, G., Bedard, J., Ferguson, T.K., Pathrose, P., Cole-Strauss, A., Kaufhold, A., Millhorn, D.E., 2004. The role of calcium in hypoxia-induced signal transduction and gene expression. Cell Calcium, Integrative aspects of calcium involvement in hypoxic response 36, 331–340. https://doi.org/10.1016/j.ceca.2004.02.006

Shabsigh, A., Chang, D.T., Heitjan, D.F., Kiss, A., Olsson, C.A., Puchner, P.J., Buttyan, R., 1998. Rapid reduction in blood flow to the rat ventral prostate gland after castration: Preliminary evidence that androgens influence prostate size by regulating blood flow to the prostate gland and prostatic endothelial cell survival. Prostate 36, 201–206. https://doi.org/10.1002/(SICI)1097-0045(19980801)36:3<201::AID-PROS9>3.0.CO;2-J

Shabsigh, A., Ghafar, M.A., de la Taille, A., Burchardt, M., Kaplan, S.A., Anastasiadis, A.G., Buttyan, R., 2001. Biomarker analysis demonstrates a hypoxic environment in the castrated rat ventral prostate gland. J Cell Biochem 81, 437–444. https://doi.org/10.1002/1097-4644(20010601)81:3<437::AID-JCB1057>3.0.CO;2-6

Shang, Z., Cai, Q., Zhang, M., Zhu, S., Ma, Y., Sun, L., Jiang, N., Tian, J., Niu, X., Chen, J., Sun, Y., Niu, Y., 2014. A switch from CD44+ cell to EMT cell drives the metastasis of prostate cancer. Oncotarget 6, 1202–1216.

Shapovalov, G., Skryma, R., Prevarskaya, N., 2012. Calcium Channels and Prostate Cancer. Recent Patents Anticancer Drug Discov. 8, 18–26. https://doi.org/10.2174/1574892811308010018

Shariat, S.F., Roehrborn, C.G., 2008. Using Biopsy to Detect Prostate Cancer. Rev. Urol. 10, 262–280.

Shcheglovitov, A., Zhelay, T., Vitko, Y., Osipenko, V., Perez-Reyes, E., Kostyuk, P., Shuba, Y., 2005. Contrasting the effects of nifedipine on subtypes of endogenous and recombinant T-type Ca2+ channels. Biochem. Pharmacol. 69, 841–854. https://doi.org/10.1016/j.bcp.2004.11.024

Shen, M.M., Abate-Shen, C., 2010. Molecular genetics of prostate cancer: new prospects for old challenges. Genes Dev. 24, 1967–2000. https://doi.org/10.1101/gad.1965810

Shiota, M., Itsumi, M., Takeuchi, A., Imada, K., Yokomizo, A., Kuruma, H., Inokuchi, J., Tatsugami, K., Uchiumi, T., Oda, Y., Naito, S., 2015. Crosstalk between epithelial-mesenchymal transition and castration resistance mediated by Twist1/AR signaling in prostate cancer. Endocr Relat Cancer 22, 889–900. https://doi.org/10.1530/ERC-15-0225

Shuba, Y.M., Prevarskaya, N., Lemonnier, L., Van Coppenolle, F., Kostyuk, P.G., Mauroy, B., Skryma, R., 2000. Volume-regulated chloride conductance in the LNCaP human prostate cancer cell line. Am. J. Physiol.-Cell Physiol. 279, C1144–C1154. https://doi.org/10.1152/ajpcell.2000.279.4.C1144

Silver, R.A., Bolsover, S.R., 1991. Expression of T-type calcium current precedes neurite extension in neuroblastoma cells. J. Physiol. (Paris) 85, 79–83.

Skryma, R., Mariot, P., Le Bourhis, X., Van Coppenolle, F., Shuba, Y., Abeele, F.V., Legrand, G., Humez, S., Boilly, B., Prevarskaya, N., 2000. Store depletion and store-operated Ca2+ current in human prostate cancer LNCaP cells: involvement in apoptosis. J. Physiol. 527, 71–83. https://doi.org/10.1111/j.1469-7793.2000.00071.x

Skvortsov, S., Skvortsova, I.-I., Tang, D.G., Dubrovska, A., 2018. Concise Review: Prostate Cancer Stem Cells: Current Understanding. STEM CELLS 36, 1457–1474. https://doi.org/10.1002/stem.2859

Smith, B.A., Sokolov, A., Uzunangelov, V., Baertsch, R., Newton, Y., Graim, K., Mathis, C., Cheng, D., Stuart, J.M., Witte, O.N., 2015. A basal stem cell signature identifies aggressive prostate cancer phenotypes. Proc. Natl. Acad. Sci. U. S. A. 112, E6544-6552. https://doi.org/10.1073/pnas.1518007112

Sørensen, B.S., Horsman, M.R., 2020. Tumor Hypoxia: Impact on Radiation Therapy and Molecular Pathways. Front. Oncol. 10. https://doi.org/10.3389/fonc.2020.00562

Sounni, N.E., Noel, A., 2013. Targeting the Tumor Microenvironment for Cancer Therapy. Clin. Chem. 59, 85–93. https://doi.org/10.1373/clinchem.2012.185363

Steinsapir, J., Socci, R., Reinach, P., 1991. Effects of androgen on intracellular calcium of LNCaP cells. Biochem. Biophys. Res. Commun. 179, 90–96. https://doi.org/10.1016/0006-291X(91)91338-D

Stenman, U.-H., Leinonen, J., Zhang, W.-M., Finne, P., 1999. Prostate-specific antigen. Semin. Cancer Biol. 9, 83–93. https://doi.org/10.1006/scbi.1998.0086

Stewart, G.D., Ross, J.A., McLaren, D.B., Parker, C.C., Habib, F.K., Riddick, A.C.P., 2010. The relevance of a hypoxic tumour microenvironment in prostate cancer. BJU Int. 105, 8–13. https://doi.org/10.1111/j.1464-410X.2009.08921.x

Stewart, T.A., Yapa, K.T.D.S., Monteith, G.R., 2015. Altered calcium signaling in cancer cells. Biochim. Biophys. Acta BBA - Biomembr., Membrane Channels and Transporters in Cancers 1848, 2502–2511. https://doi.org/10.1016/j.bbamem.2014.08.016

Streb, H., Irvine, R.F., Berridge, M.J., Schulz, I., 1983. Release of Ca2+ from a nonmitochondrial intracellular store in pancreatic acinar cells by inositol-1,4,5-trisphosphate. Nature 306, 67–69. https://doi.org/10.1038/306067a0

Sun, Y., Wang, B.-E., Leong, K.G., Yue, P., Li, L., Jhunjhunwala, S., Chen, D., Seo, K., Modrusan, Z., Gao, W.-Q., Settleman, J., Johnson, L., 2012. Androgen Deprivation Causes Epithelial–Mesenchymal Transition in the Prostate: Implications for Androgen-Deprivation Therapy. Cancer Res. 72, 527–536. https://doi.org/10.1158/0008-5472.CAN-11-3004

Sun, Y.-H., Gao, X., Tang, Y.-J., Xu, C.-L., Wang, L.-H., 2006. Androgens induce increases in intracellular calcium via a G protein-coupled receptor in LNCaP prostate cancer cells. J. Androl. 27, 671–678. https://doi.org/10.2164/jandrol.106.000554

Suo, A., Childers, A., D'Silva, A., Petersen, L.F., Otsuka, S., Dean, M., Li, H., Enwere, E.K., Pohorelic, B., Klimowicz, A., Souza, I.A., Hamid, J., Zamponi, G.W., Bebb, Dg., 2018. Cav3.1 overexpression is associated with negative characteristics and prognosis in non-small cell lung cancer. Oncotarget 9, 8573–8583. https://doi.org/10.18632/oncotarget.24194

Swulius, M.T., Waxham, M.N., 2008. Ca2+/Calmodulin-dependent Protein Kinases. Cell. Mol. Life Sci. CMLS 65, 2637–2657. https://doi.org/10.1007/s00018-008-8086-2

Tajada, S., Villalobos, C., 2020. Calcium Permeable Channels in Cancer Hallmarks. Front. Pharmacol. 11. https://doi.org/10.3389/fphar.2020.00968

Tajima, N., Schönherr, K., Niedling, S., Kaatz, M., Kanno, H., Schönherr, R., Heinemann, S.H., 2006. Ca2+-activated K+ channels in human melanoma cells are up-regulated by hypoxia involving hypoxia-inducible factor-1α and the von Hippel-Lindau protein. J. Physiol. 571, 349–359. https://doi.org/10.1113/jphysiol.2005.096818

Takahashi, M., Seagar, M.J., Jones, J.F., Reber, B.F., Catterall, W.A., 1987. Subunit structure of dihydropyridine-sensitive calcium channels from skeletal muscle. Proc. Natl. Acad. Sci. 84, 5478–5482. https://doi.org/10.1073/pnas.84.15.5478

Takemura, H., Putney, J.W., 1989. Capacitative calcium entry in parotid acinar cells. Biochem. J. 258, 409–412. https://doi.org/10.1042/bj2580409

Takubo, K., Goda, N., Yamada, W., Iriuchishima, H., Ikeda, E., Kubota, Y., Shima, H., Johnson, R.S., Hirao, A., Suematsu, M., Suda, T., 2010. Regulation of the HIF-1α Level Is Essential for Hematopoietic Stem Cells. Cell Stem Cell 7, 391–402. https://doi.org/10.1016/j.stem.2010.06.020

Tam, S.Y., Wu, V.W.C., Law, H.K.W., 2020. Hypoxia-Induced Epithelial-Mesenchymal Transition in Cancers: HIF-1α and Beyond. Front. Oncol. 10. https://doi.org/10.3389/fonc.2020.00486

Tan, J., Sharief, Y., Hamil, K.G., Gregory, C.W., Zang, D.Y., Sar, M., Gumerlock, P.H., deVere White, R.W., Pretlow, T.G., Harris, S.E., Wilson, E.M., Mohler, J.L., French, F.S., 1997. Dehydroepiandrosterone activates mutant androgen receptors expressed in the androgen-dependent human prostate cancer xenograft CWR22 and LNCaP cells. Mol. Endocrinol. Baltim. Md 11, 450–459. https://doi.org/10.1210/mend.11.4.9906

Tan, M.E., Li, J., Xu, H.E., Melcher, K., Yong, E., 2015. Androgen receptor: structure, role in prostate cancer and drug discovery. Acta Pharmacol. Sin. 36, 3–23. https://doi.org/10.1038/aps.2014.18

Tang, J., Chen, Y., Cui, R., Li, D., Xiao, L., Lin, P., Du, Y., Sun, H., Yu, X., Zheng, X., 2015. Upregulation of fractalkine contributes to the proliferative response of prostate cancer cells to hypoxia via promoting the G1/S phase transition. Mol. Med. Rep. 12, 7907–7914. https://doi.org/10.3892/mmr.2015.4438

Tang, Y., Hamburger, A.W., Wang, L., Khan, M.A., Hussain, A., 2009. Androgen deprivation and stem cell markers in prostate cancers. Int J Clin Exp Pathol 3, 128–138.

Tannock, I.F., de Wit, R., Berry, W.R., Horti, J., Pluzanska, A., Chi, K.N., Oudard, S., Théodore, C., James, N.D., Turesson, I., Rosenthal, M.A., Eisenberger, M.A., 2004. Docetaxel plus Prednisone or Mitoxantrone plus Prednisone for Advanced Prostate Cancer. N. Engl. J. Med. 351, 1502–1512. https://doi.org/10.1056/NEJMoa040720

Taplin, M.E., Bubley, G.J., Shuster, T.D., Frantz, M.E., Spooner, A.E., Ogata, G.K., Keer, H.N., Balk, S.P., 1995. Mutation of the androgen-receptor gene in metastatic androgen-independent prostate cancer. N. Engl. J. Med. 332, 1393–1398. https://doi.org/10.1056/NEJM199505253322101

Taylor, B.S., Schultz, N., Hieronymus, H., Gopalan, A., Xiao, Y., Carver, B.S., Arora, V.K., Kaushik, P., Cerami, E., Reva, B., Antipin, Y., Mitsiades, N., Landers, T., Dolgalev, I., Major, J.E., Wilson, M., Socci, N.D., Lash, A.E., Heguy, A., Eastham, J.A., Scher, H.I., Reuter, V.E., Scardino, P.T., Sander, C., Sawyers, C.L., Gerald, W.L., 2010. Integrative genomic profiling of human prostate cancer. Cancer Cell 18, 11–22. https://doi.org/10.1016/j.ccr.2010.05.026

Thebault, S., Flourakis, M., Vanoverberghe, K., Vandermoere, F., Roudbaraki, M., Lehen'kyi, V., Slomianny, C., Beck, B., Mariot, P., Bonnal, J.-L., Mauroy, B., Shuba, Y., Capiod, T., Skryma, R., Prevarskaya, N., 2006. Differential Role of Transient Receptor Potential Channels in Ca2+ Entry and Proliferation of Prostate Cancer Epithelial Cells. Cancer Res. 66, 2038–2047. https://doi.org/10.1158/0008-5472.CAN-05-0376

Thomas, R., Kim, M.H., 2008. HIF-1α: A key survival factor for serum-deprived prostate cancer cells. The Prostate 68, 1405–1415. https://doi.org/10.1002/pros.20808

Tong, W.-W., Tong, G.-H., Liu, Y., 2018. Cancer stem cells and hypoxia-inducible factors (Review). Int. J. Oncol. 53, 469–476. https://doi.org/10.3892/ijo.2018.4417

Torrente, A.G., Mesirca, P., Neco, P., Rizzetto, R., Dubel, S., Barrere, C., Sinegger-Brauns, M., Striessnig, J., Richard, S., Nargeot, J., Gomez, A.M., Mangoni, M.E., 2016. L-type Cav1.3 channels regulate ryanodine receptor-dependent Ca2+ release during sino-atrial node pacemaker activity. Cardiovasc. Res. 109, 451–461. https://doi.org/10.1093/cvr/cvw006

Tran, M.G.B., Bibby, B.A.S., Yang, L., Lo, F., Warren, A.Y., Shukla, D., Osborne, M., Hadfield, J., Carroll, T., Stark, R., Scott, H., Ramos-Montoya, A., Massie, C., Maxwell, P., West, C.M.L., Mills, I.G., Neal, D.E., 2020. Independence of HIF1a and androgen signaling pathways in prostate cancer. BMC Cancer 20, 469. https://doi.org/10.1186/s12885-020-06890-6

Tran, N.L., Nagle, R.B., Cress, A.E., Heimark, R.L., 1999. N-Cadherin Expression in Human Prostate Carcinoma Cell Lines. Am. J. Pathol. 155, 787–798.

Tsavaler, L., Shapero, M.H., Morkowski, S., Laus, R., 2001. Trp-p8, a Novel Prostate-specific Gene, Is Up-Regulated in Prostate Cancer and Other Malignancies and Shares High Homology with Transient Receptor Potential Calcium Channel Proteins. Cancer Res. 61, 3760–3769.

Tsui, K.-H., Chung, L.-C., Wang, S.-W., Feng, T.-H., Chang, P.-L., Juang, H.-H., 2013. Hypoxia upregulates the gene expression of mitochondrial aconitase in prostate carcinoma cells. J. Mol. Endocrinol. 51, 131–141. https://doi.org/10.1530/JME-13-0090

Vadde, R., Vemula, S., Jinka, R., Merchant, N., Bramhachari, P.V., Nagaraju, G.P., 2017. Role of hypoxia-inducible factors (HIF) in the maintenance of stemness and malignancy of colorectal cancer. Crit. Rev. Oncol. Hematol. 113, 22–27. https://doi.org/10.1016/j.critrevonc.2017.02.025

Vandael, D.H.F., Zuccotti, A., Striessnig, J., Carbone, E., 2012. CaV1.3-Driven SK Channel Activation Regulates Pacemaking and Spike Frequency Adaptation in Mouse Chromaffin Cells. J. Neurosci. 32, 16345–16359. https://doi.org/10.1523/JNEUROSCI.3715-12.2012

Vanoverberghe, K., Vanden Abeele, F., Mariot, P., Lepage, G., Roudbaraki, M., Bonnal, J.L., Mauroy, B., Shuba, Y., Skryma, R., Prevarskaya, N., 2004. Ca 2+ homeostasis and apoptotic resistance of neuroendocrine-differentiated prostate cancer cells. Cell Death Differ. 11, 321–330. https://doi.org/10.1038/sj.cdd.4401375

Varghese, E., Samuel, S.M., Sadiq, Z., Kubatka, P., Liskova, A., Benacka, J., Pazinka, P., Kruzliak, P., Büsselberg, D., 2019. Anti-Cancer Agents in Proliferation and Cell Death: The Calcium Connection. Int. J. Mol. Sci. 20, 3017. https://doi.org/10.3390/ijms20123017

Vaupel, P., 2004. The Role of Hypoxia-Induced Factors in Tumor Progression. The Oncologist 9, 10–17. https://doi.org/10.1634/theoncologist.9-90005-10

Vaupel, P., Mayer, A., 2007. Hypoxia in cancer: significance and impact on clinical outcome. Cancer Metastasis Rev. 26, 225–239. https://doi.org/10.1007/s10555-007-9055-1

Venkatachalam, K., Montell, C., 2007. TRP Channels. Annu. Rev. Biochem. 76, 387–417. https://doi.org/10.1146/annurev.biochem.75.103004.142819

Vergara, C., Latorre, R., Marrion, N.V., Adelman, J.P., 1998. Calcium-activated potassium channels. Curr. Opin. Neurobiol. 8, 321–329. https://doi.org/10.1016/S0959-4388(98)80056-1

Vierra, N.C., Kirmiz, M., List, D. van der, Santana, L.F., Trimmer, J.S., 2019. Kv2.1 mediates spatial and functional coupling of L-type calcium channels and ryanodine receptors in neurons. bioRxiv 702514. https://doi.org/10.1101/702514

Vinay, D.S., Ryan, E.P., Pawelec, G., Talib, W.H., Stagg, J., Elkord, E., Lichtor, T., Decker, W.K., Whelan, R.L., Kumara, H.M.C.S., Signori, E., Honoki, K., Georgakilas, A.G., Amin, A., Helferich, W.G., Boosani, C.S., Guha, G., Ciriolo, M.R., Chen, S., Mohammed, S.I., Azmi, A.S., Keith, W.N., Bilsland, A., Bhakta, D., Halicka, D., Fujii, H., Aquilano, K., Ashraf, S.S., Nowsheen, S., Yang, X., Choi, B.K., Kwon, B.S., 2015. Immune evasion in cancer: Mechanistic basis and therapeutic strategies. Semin. Cancer Biol., A broad-spectrum

integrative design for cancer prevention and therapy 35, S185–S198. https://doi.org/10.1016/j.semcancer.2015.03.004

Viola, J.P.B., Carvalho, L.D.S., Fonseca, B.P.F., Teixeira, L.K., 2005. NFAT transcription factors: from cell cycle to tumor development. Braz. J. Med. Biol. Res. 38, 335–344. https://doi.org/10.1590/S0100-879X2005000300003

Visakorpi, T., Hyytinen, E., Koivisto, P., Tanner, M., Keinänen, R., Palmberg, C., Palotie, A., Tammela, T., Isola, J., Kallioniemi, O.P., 1995. In vivo amplification of the androgen receptor gene and progression of human prostate cancer. Nat. Genet. 9, 401–406. https://doi.org/10.1038/ng0495-401

Vivas, O., Moreno, C.M., Santana, L.F., Hille, B., 2017. Proximal clustering between BK and CaV1.3 channels promotes functional coupling and BK channel activation at low voltage. eLife 6, e28029. https://doi.org/10.7554/eLife.28029

Wadosky, K.M., Koochekpour, S., Wadosky, K.M., Koochekpour, S., 2016. Molecular mechanisms underlying resistance to androgen deprivation therapy in prostate cancer. Oncotarget 7, 64447–64470. https://doi.org/10.18632/oncotarget.10901

Wang, C.-Y., Lai, M.-D., Phan, N.N., Sun, Z., Lin, Y.-C., 2015. Meta-Analysis of Public Microarray Datasets Reveals Voltage-Gated Calcium Gene Signatures in Clinical Cancer Patients. PLOS ONE 10, e0125766. https://doi.org/10.1371/journal.pone.0125766

Wang, P., Lan, C., Xiong, S., Zhao, X., Shan, Y., Hu, R., Wan, W., Yu, S., Liao, B., Li, G., Wang, J., Zou, D., Chen, B., Feng, H., Wu, N., Wang, P., Lan, C., Xiong, S., Zhao, X., Shan, Y., Hu, R., Wan, W., Yu, S., Liao, B., Li, G., Wang, J., Zou, D., Chen, B., Feng, H., Wu, N., 2017. HIF1α regulates single differentiated glioma cell dedifferentiation to stem-like cell phenotypes with high tumorigenic potential under hypoxia. Oncotarget 8, 28074–28092. https://doi.org/10.18632/oncotarget.15888

Wang, R., Brattain, M.G., 2007. The maximal size of protein to diffuse through the nuclear pore is larger than 60kDa. FEBS Lett. 581, 3164–3170. https://doi.org/10.1016/j.febslet.2007.05.082

Wang, T., Alavian, M.R., Goel, H.L., Languino, L.R., FitzGerald, T.J., 2008. Bicalutamide inhibits androgen-mediated adhesion of prostate cancer cells exposed to ionizing radiation. Prostate 68, 1734–1742. https://doi.org/10.1002/pros.20838

Wang, X., Julio, M.K., Economides, K.D., Walker, D., Yu, H., Halili, M.V., Hu, Y.-P., Price, S.M., Abate-Shen, C., Shen, M.M., 2009. A luminal epithelial stem cell that is a cell of origin for prostate cancer. Nature 461, 495–500. https://doi.org/10.1038/nature08361

Wang, Y., Hayward, S.W., Cao, M., Thayer, K.A., Cunha, G.R., 2001. Cell differentiation lineage in the prostate. Differentiation 68, 270–279. https://doi.org/10.1046/j.1432-0436.2001.680414.x

Wang, Z.A., Mitrofanova, A., Bergren, S.K., Abate-Shen, C., Cardiff, R.D., Califano, A., Shen, M.M., 2013. Lineage analysis of basal epithelial cells reveals their unexpected plasticity and supports a cell of origin model for prostate cancer heterogeneity. Nat. Cell Biol. 15, 274–283. https://doi.org/10.1038/ncb2697

Wang, Z.A., Toivanen, R., Bergren, S.K., Chambon, P., Shen, M.M., 2014. Luminal Cells Are Favored as the Cell of Origin for Prostate Cancer. Cell Rep. 8, 1339–1346. https://doi.org/10.1016/j.celrep.2014.08.002

Warburg, O., 1956. On the origin of cancer cells. Science 123, 309–314. https://doi.org/10.1126/science.123.3191.309

Warnier, M., Gackiere, F., Roudbaraki, M., Mariot, P., 2017. Expression and Role of T-type Calcium Channels during Neuroendocrine Differentiation. J. Cell Signal. 01. https://doi.org/10.4172/2576-1471.1000113

Warnier, M., Roudbaraki, M., Derouiche, S., Delcourt, P., Bokhobza, A., Prevarskaya, N., Mariot, P., 2015. CACNA2D2 promotes tumorigenesis by stimulating cell proliferation and angiogenesis. Oncogene 34, 5383–5394. https://doi.org/10.1038/onc.2014.467

Weaver, A.K., Bomben, V.C., Sontheimer, H., 2006. Expression and function of calcium-activated potassium channels in human glioma cells. Glia 54, 223–233. https://doi.org/10.1002/glia.20364

Wheeler, D.G., Groth, R.D., Ma, H., Barrett, C.F., Owen, S.F., Safa, P., Tsien, R.W., 2012. CaV1 and CaV2 Channels Engage Distinct Modes of Ca2+ Signaling to Control CREB-dependent Gene Expression. Cell 149, 1112–1124. https://doi.org/10.1016/j.cell.2012.03.041

Wigerup, C., Påhlman, S., Bexell, D., 2016. Therapeutic targeting of hypoxia and hypoxia-inducible factors in cancer. Pharmacol. Ther. 164, 152–169. https://doi.org/10.1016/j.pharmthera.2016.04.009

Williams, S.B., Lay, A.H., Lau, C.S., Josephson, D.Y., Wilson, T.G., Choueiri, T.K., Pal, S.K., 2011. New therapies for castrate-resistant prostate cancer. Expert Opin. Pharmacother. 12, 2069–2074. https://doi.org/10.1517/14656566.2011.590133

Witsch, E., Sela, M., Yarden, Y., 2010. Roles for Growth Factors in Cancer Progression. Physiol. Bethesda Md 25, 85–101. https://doi.org/10.1152/physiol.00045.2009

Worley, P.F., Zeng, W., Huang, G.N., Yuan, J.P., Kim, J.Y., Lee, M.G., Muallem, S., 2007. TRPC channels as STIM1-regulated store-operated channels. Cell Calcium 42, 205–211. https://doi.org/10.1016/j.ceca.2007.03.004

Wray, S., 2010. Chapter 127 - Calcium Signaling in Smooth Muscle, in: Bradshaw, R.A., Dennis, E.A. (Eds.), Handbook of Cell Signaling (Second Edition). Academic Press, San Diego, pp. 1009–1025. https://doi.org/10.1016/B978-0-12-374145-5.00127-3

Xiao, X., Li, B.X., Mitton, B., Ikeda, A., Sakamoto, K.M., 2010. Targeting CREB for Cancer Therapy: Friend or Foe. Curr. Cancer Drug Targets 10, 384–391.

Xing, N., Qian, J., Bostwick, D., Bergstralh, E., Young, C.Y.F., 2001. Neuroendocrine cells in human prostate over-express the anti-apoptosis protein survivin. Prostate 48, 7–15. https://doi.org/10.1002/pros.1076

Xu, W., Lipscombe, D., 2001. Neuronal CaV1.3α1 L-Type Channels Activate at Relatively Hyperpolarized Membrane Potentials and Are Incompletely Inhibited by Dihydropyridines. J. Neurosci. 21, 5944–5951. https://doi.org/10.1523/JNEUROSCI.21-16-05944.2001

Yamamura, H., Ohi, Y., Muraki, K., Watanabe, M., Imaizumi, Y., 2001. BK channel activation by NS-1619 is partially mediated by intracellular Ca2+ release in smooth muscle cells of porcine coronary artery. Br. J. Pharmacol. 132, 828–834. https://doi.org/10.1038/sj.bjp.0703885

Yamasaki, M., Nomura, T., Sato, F., Mimata, H., 2013. Chronic hypoxia induces androgen-independent and invasive behavior in LNCaP human prostate cancer cells. Urol. Oncol. Semin. Orig. Investig. 31, 1124–1131. https://doi.org/10.1016/j.urolonc.2011.12.007

Yang, M., Brackenbury, W.J., 2013. Membrane potential and cancer progression. Front Physiol 4. https://doi.org/10.3389/fphys.2013.00185

Yang, S., Zhang, J.J., Huang, X.-Y., 2009. Orai1 and STIM1 Are Critical for Breast Tumor Cell Migration and Metastasis. Cancer Cell 15, 124–134. https://doi.org/10.1016/j.ccr.2008.12.019

Yatani, R., Chigusa, I., Akazaki, K., Stemmermann, G.N., Welsh, R.A., Correa, P., 1982. Geographic pathology of latent prostatic carcinoma. Int. J. Cancer 29, 611–616.

Yates, S.L., Fluhler, E.N., Lippiello, P.M., 1992. Advances in the use of the fluorescent probe fura-2 for the estimation of intrasynaptosomal calcium. J. Neurosci. Res. 32, 255–260. https://doi.org/10.1002/jnr.490320215

Ye, C., Chen, G., Chen, X., Qin, S.-F., Shi, M., Zhou, T., 2019. Upregulation of erythropoietin and erythropoietin receptor in castration-resistant progression of prostate cancer. Asian J. Androl. https://doi.org/10.4103/aja.aja_80_19

Yeo, C.D., Kang, N., Choi, S.Y., Kim, B.N., Park, C.K., Kim, J.W., Kim, Y.K., Kim, S.J., 2017. The role of hypoxia on the acquisition of epithelial-mesenchymal transition and cancer stemness: a

possible link to epigenetic regulation. Korean J. Intern. Med. 32, 589–599. https://doi.org/10.3904/kjim.2016.302

Yu, S., Xu, Z., Zou, C., Wu, D., Wang, Y., Yao, X., Ng, C.-F., Chan, F.L., 2014. Ion channel TRPM8 promotes hypoxic growth of prostate cancer cells via an O2-independent and RACK1-mediated mechanism of HIF-1α stabilization. J. Pathol. 234, 514–525. https://doi.org/10.1002/path.4413

Yuan, T.-C., Veeramani, S., Lin, F.-F., Kondrikou, D., Zelivianski, S., Igawa, T., Karan, D., Batra, S.K., Lin, M.-F., 2006. Androgen deprivation induces human prostate epithelial neuroendocrine differentiation of androgen-sensitive LNCaP cells. Endocr. Relat. Cancer 13, 151–167. https://doi.org/10.1677/erc.1.01043

Yun, Z., Lin, Q., 2014. Hypoxia and Regulation of Cancer Cell Stemness. Adv Exp Med Biol 772, 41–53. https://doi.org/10.1007/978-1-4614-5915-6_2

Zarif, J.C., Miranti, C.K., 2016. The Importance of Non-Nuclear AR Signaling in Prostate Cancer Progression and Therapeutic Resistance. Cell. Signal. 28, 348–356. https://doi.org/10.1016/j.cellsig.2016.01.013

Zhang, D., Zhao, S., Li, X., Kirk, J.S., Tang, D.G., 2018. Prostate Luminal Progenitor Cells in Development and Cancer. Trends Cancer 4, 769–783. https://doi.org/10.1016/j.trecan.2018.09.003

Zhang, J., Tian, X.-J., Xing, J., 2016. Signal Transduction Pathways of EMT Induced by TGF-β, SHH, and WNT and Their Crosstalks. J. Clin. Med. 5, 41. https://doi.org/10.3390/jcm5040041

Zhang, L., Huang, G., Li, X., Zhang, Y., Jiang, Y., Shen, J., Liu, J., Wang, Q., Zhu, J., Feng, X., Dong, J., Qian, C., 2013. Hypoxia induces epithelial-mesenchymal transition via activation of SNAI1 by hypoxia-inducible factor -1α in hepatocellular carcinoma. BMC Cancer 13, 108. https://doi.org/10.1186/1471-2407-13-108

Zhang, Y., Yang, J.-M., 2013. Altered energy metabolism in cancer. Cancer Biol. Ther. 14, 81–89. https://doi.org/10.4161/cbt.22958

Zhang, Y., Zhang, J., Jiang, D., Zhang, D., Qian, Z., Liu, C., Tao, J., 2012. Inhibition of T-type Ca2+ channels by endostatin attenuates human glioblastoma cell proliferation and migration. Br. J. Pharmacol. 166, 1247–1260. https://doi.org/10.1111/j.1476-5381.2012.01852.x

Zhang, Y., Zheng, D., Zhou, T., Song, H., Hulsurkar, M., Su, N., Liu, Y., Wang, Z., Shao, L., Ittmann, M., Gleave, M., Han, H., Xu, F., Liao, W., Wang, H., Li, W., 2018. Androgen deprivation promotes neuroendocrine differentiation and angiogenesis through CREB-EZH2-TSP1 pathway in prostate cancers. Nat. Commun. 9, 4080. https://doi.org/10.1038/s41467-018-06177-2

Zhang Zhao, He Yuxia, Tuteja Dipika, Xu Danyan, Timofeyev Valeriy, Zhang Qian, Glatter Kathryn A., Xu Yanfang, Shin Hee-Sup, Low Reginald, Chiamvimonvat Nipavan, 2005. Functional Roles of Cav1.3(α1D) Calcium Channels in Atria. Circulation 112, 1936–1944. https://doi.org/10.1161/CIRCULATIONAHA.105.540070

Zhou, X., Wang, W., Zhang, S., Wang, X., Tang, Z., Gu, J., Li, J., Huang, J., 2017. CACNA1B (Cav2.2) Overexpression and Its Association with Clinicopathologic Characteristics and Unfavorable Prognosis in Non-Small Cell Lung Cancer [WWW Document]. Dis. Markers. https://doi.org/10.1155/2017/6136401

Zhu, G., Liu, Z., Epstein, J.I., Davis, C., Christudass, C.S., Carter, H.B., Landis, P., Zhang, H., Chung, J.-Y., Hewitt, S.M., Miller, M.C., Veltri, R.W., 2015. A Novel Quantitative Multiplex Tissue Immunoblotting for Biomarkers Predicts a Prostate Cancer Aggressive Phenotype. Cancer Epidemiol. Prev. Biomark. 24, 1864–1872. https://doi.org/10.1158/1055-9965.EPI-15-0496

Ziello, J.E., Jovin, I.S., Huang, Y., 2007. Hypoxia-Inducible Factor (HIF)-1 Regulatory Pathway and its Potential for Therapeutic Intervention in Malignancy and Ischemia. Yale J. Biol. Med. 80, 51–60.

Appendix A – Additional results for chapter 3

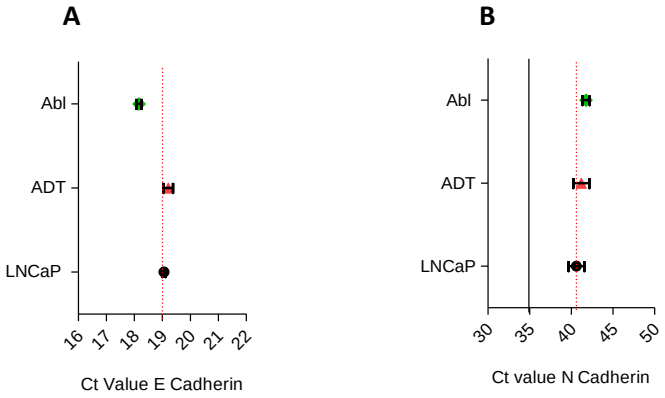

Figure A.1: Ct values of E-cadherin and N-cadherin show that N-cadherin is below the threshold of reliable qPCR analysis: *Ct values from qPCR analysis of E-cadherin* ***(A)*** *and N-cadherin* ***(B)****. Analysis of androgen sensitive LNCaP cells (black), LNCaP-ADT cells treated with 10µM bicalutamide (7-10 days) (red) and androgen insensitive long-term androgen deprived LNCaP-ablcells (green). Black line indicates threshold with dashed red line showing average Ct value for LNCaP control cell line.*

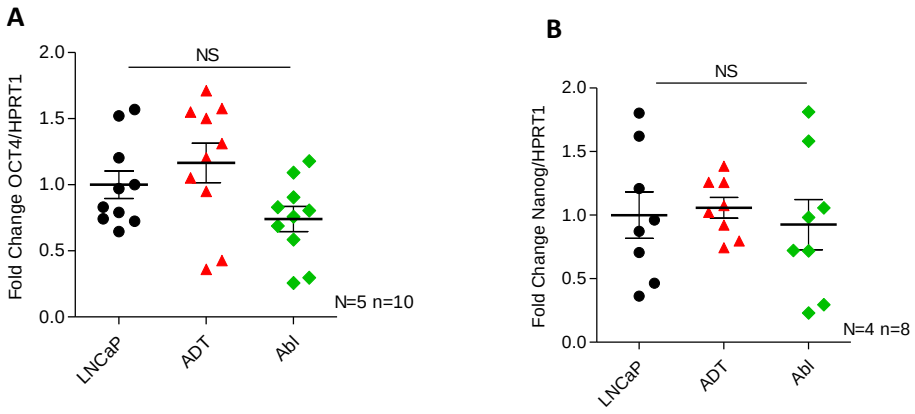

Figure A.2: Cells under androgen deprivation therapy have no significant altered expression of pluripotency markers: *Genetic expression of* ***(A)*** *Oct4 and* ***(B)*** *Nanog assessed using qPCR normalised to control LNCaP. Analysis of androgen sensitive LNCaP cells (black), LNCaP-ADT cells treated with 10µM bicalutamide (7-10 days) (red) and androgen insensitive long-term androgen*

*deprived LNCaP-abl cells (green). Analysed using Kruskal-Wallis significance test and Dunn's multiple comparison post hoc test between cell types and treatments. * P<0.05, ** P<0.01, ***P<0.001, NS not significant.*

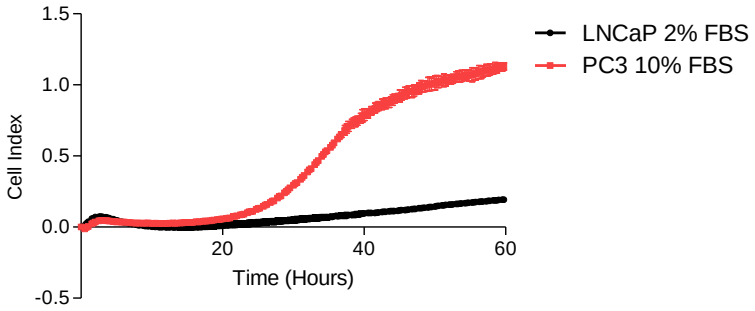

***Figure A.3: Migration is seen in PC3 cells as positive control**: Migration assessed using the Xcelligence™ system cell invasion and migration plates with chemoattractant 10% FBS or 2% control. Analysis of androgen sensitive LNCaP cells (black), PC3 cells (red) Assesses as cell index over 60 hours.*

Appendix B – Additional results for chapter 4

Table B.1: Fold change in Ca^{2+} measured in cells depolarised with high external K^{+} compared to basal Ca^{2+} level. *There is no significant change in cytosolic Ca^{2+} levels recorded in LNCaP cells which had increased expression of CaV1.3. Ca^{2+} peaks recorded at basal cytosolic levels and after cell membrane depolarisation fold change to LNCaP basal Ca^{2+}.*

Cell	Basal Ca2+ Peak	Ca^{2+} peak after KCl (60nM)	Basal Ca^{2+} Peak	Ca^{2+} Peak after KCl (80mM)
LNCaP	1.00 (+/- 0.005 sem)	0.9964 (+/- 0.001 sem)	1.00 (+/- 0.008 sem)	1.014 (+/- 0.002 sem)
LNCaP-ADT	1.026 (+/- 0.002 sem)	1.013 (+/- 0.002 sem)	1.034 (+/- 0.004 sem)	1.027 (+/- 0.017 sem)
LNCaP-abl	1.009 (+/- 0.009 sem)	0.9995 (+/- 0.002 sem)	1.004 (+/- 0.003 sem)	1.002 (+/- 0.005 sem)

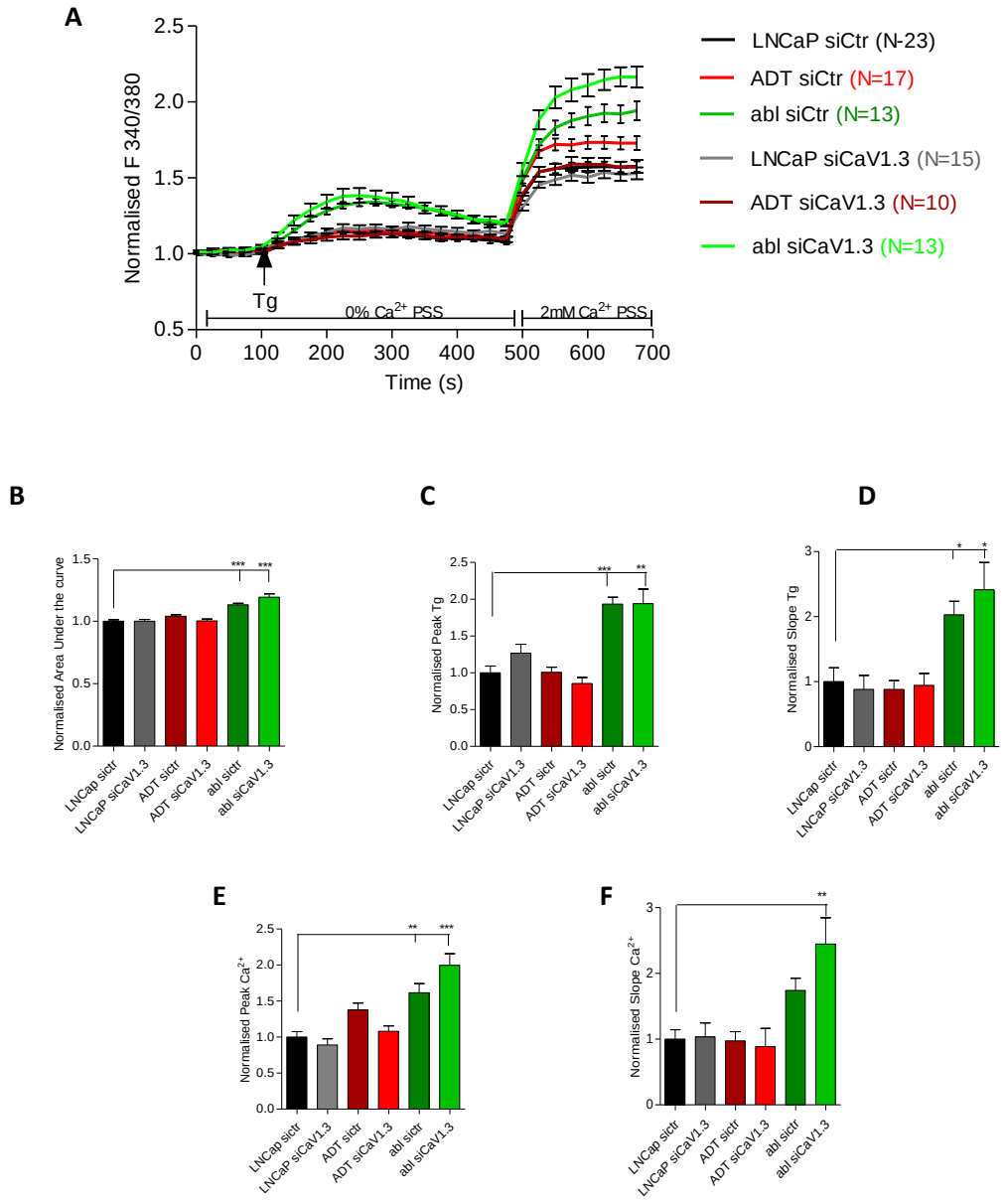

Figure B.1: SOCE is increased in LNCaP-ADT cells and further increased in LNCaP-ablcells, which is reduced to normal in LNCaP-ADT cells after siCaV1.3 but increased in LNCaP-ablcells after siCaV1.3: *Store operated calcium entry (SOCE) indicated by Fura 2-AM ratio metric analysis of calcium concentration over time (s). Analysis of androgen sensitive LNCaP cells (black), LNCaP-ADT cells treated with 10μM bicalutamide (7-10 days) (Red) and androgen insensitive long-term androgen deprived LNCaP-ablcells (Green). Transfected with non-targeting control siRNA or siRNA targeting CaV1.3.* **(A)** *Analysed using 2-way ANOVA significance of fluorescence ratio 340:380 at time (s) between transfections Normalised* ***(B)*** *Area under the curve,* ***(C)*** *Tg peak,* ***(D)*** *Tg slope,* ***(E)*** *normalised calcium peak and* ***(F)*** *calcium slope indicated for each cell type and treatment. Analysed*

*using Kruskal-Wallis significance test between cell types and treatments. * P<0.05, ** P<0.01, ***P<0.001, NS not significant.*

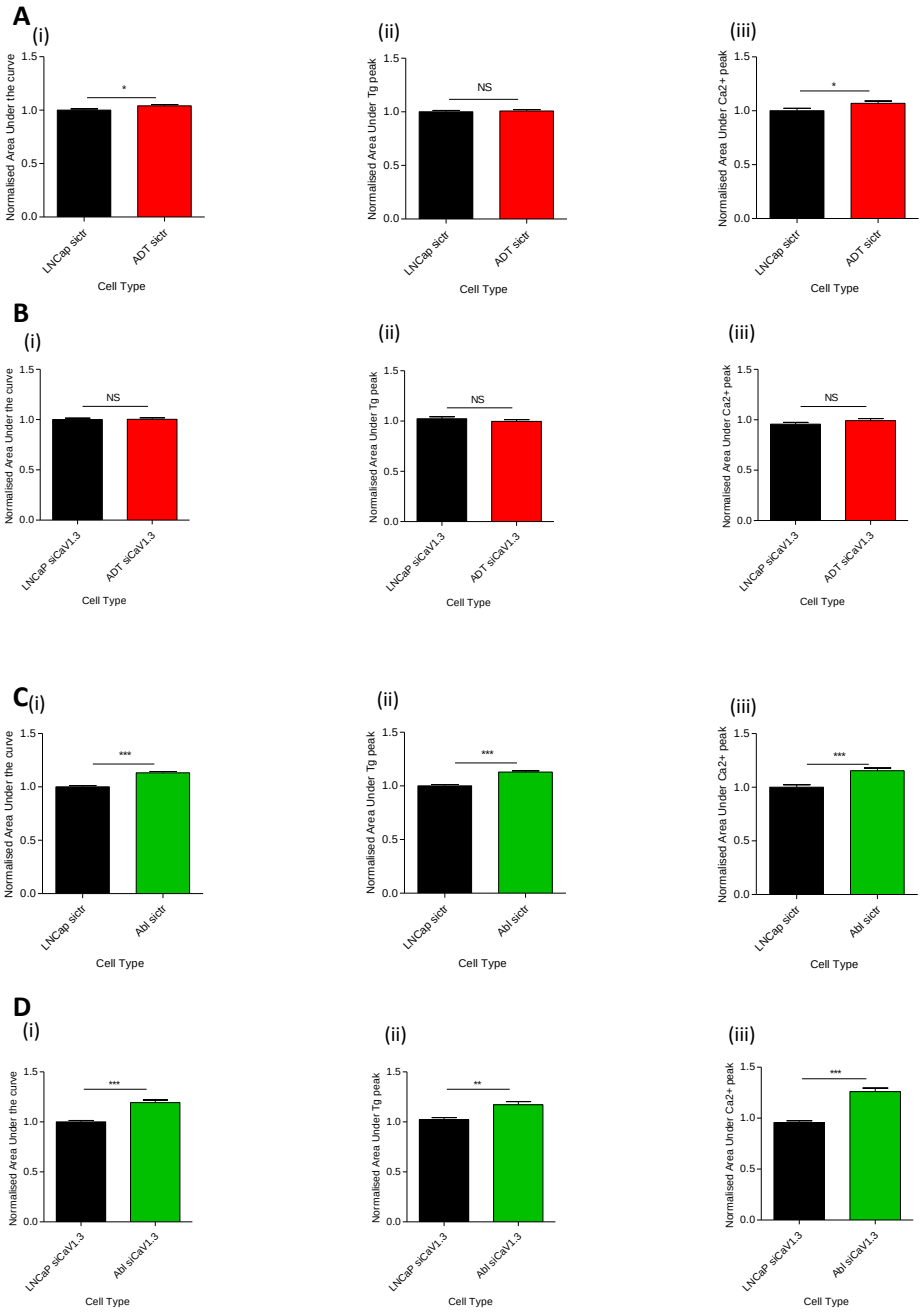

Figure B.2: The Ca^{2+} peak is the main contributary factor to the overall area under the curve representing $[Ca^{2+}]_i$ when compared to LNCaP control: *Store operated calcium entry (SOCE) indicated by Fura 2-AM ratio metric analysis of calcium concentration over time (s). Analysis of androgen sensitive LNCaP cells (black), LNCaP-ADT cells treated with 10µM bicalutamide (7-10 days) (red) and androgen insensitive long-term androgen deprived LNCaP-abl cells (green) transfected with siRNA targeting CaV1.3 (siCaV1.3) or non-targeting control (siCtr).* ***(i)*** *Normalised Area under the curve,* ***(ii)*** *area under Tg peak, and* ***(iii)*** *area under calcium slope indicated for each*

*cell type and treatment. Analysed using Kruskal-Wallis significance test between cell types and treatments. * P<0.05, ** P<0.01, ***P<0.001, NS not significant.*

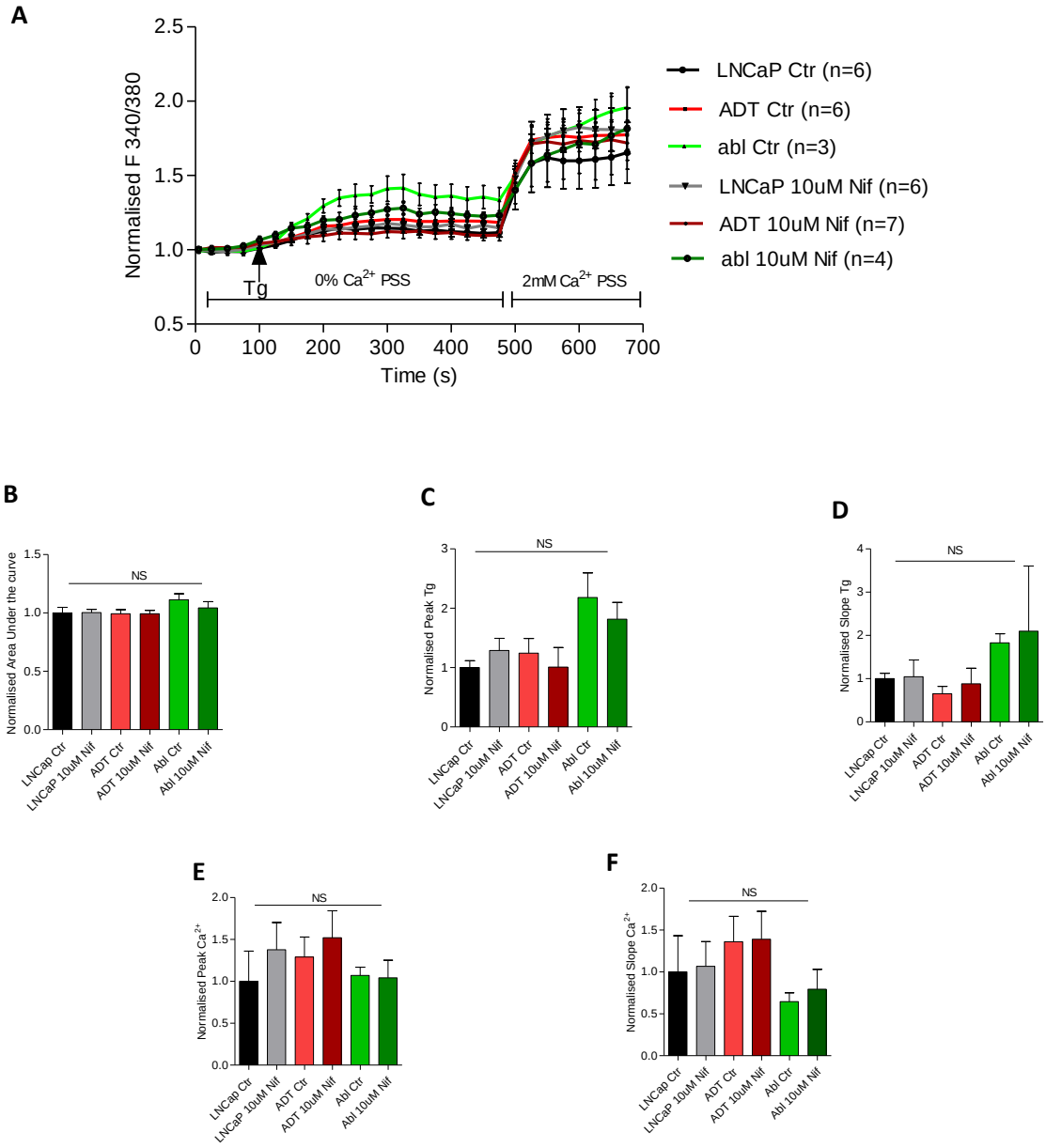

Figure B.3: Nifedipine has no significant effect on the Ca^{2+} mobilisation in LNCaP cells at any stage under ADT*: Store operated calcium entry (SOCE) indicated by Fura 2-AM ratio metric analysis of calcium concentration over time (s). Analysis of androgen sensitive LNCaP cells (black), LNCaP-ADT cells treated with 10µM bicalutamide (7-10 days) (Red) and androgen insensitive long-term androgen deprived LNCaP-ablcells (Green). Treated with 10µM Nifedipine or DMSO control.* **(A)** *Analysed using 2-way ANOVA significance of fluorescence ratio 340:380 at time (s) between transfections. Normalised* ***(B)*** *Area under the curve,* ***(C)*** *Tg peak,* ***(D)*** *Tg slope,* ***(E)*** *calcium peak and* ***(F)*** *calcium slope indicated for each cell type and treatment. Analysed using Kruskal-Wallis*

*significance test between cell types and treatments. * P<0.05, ** P<0.01, ***P<0.001, NS not significant.*

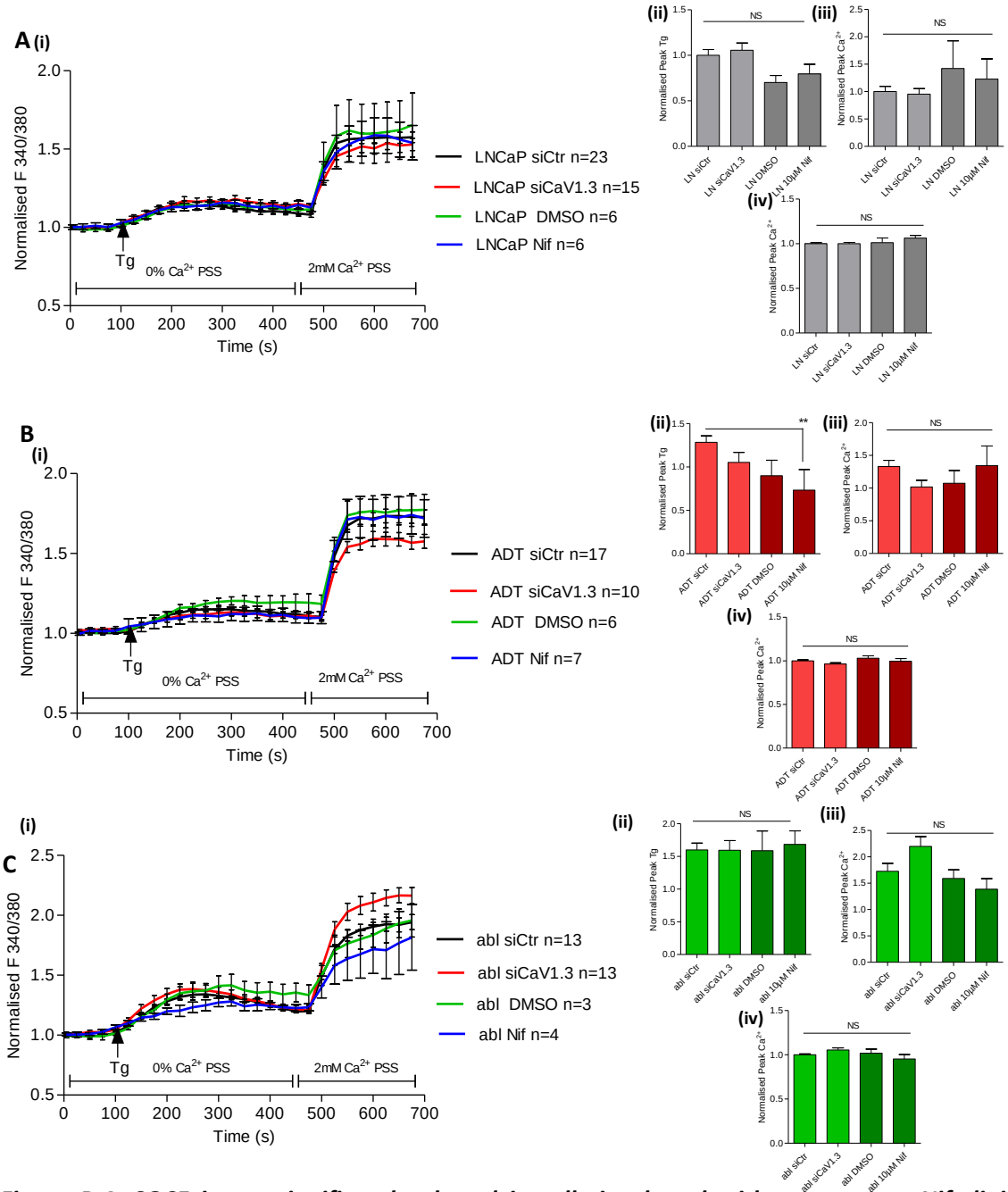

Figure B.4: SOCE is not significantly altered in cells incubated with Nifedipine compared to cells transfected with siCaV1.3*: Store operated calcium entry (SOCE) indicated by Fura 2-AM ratiometric analysis of calcium concentration over time (s). Analysis of (A) androgen sensitive LNCaP cells, (B) LNCaP-ADT cells treated with 10μM bicalutamide (7-10 days) and (C) androgen insensitive long-term androgen deprived LNCaP-abl cells. Treated with DMSO control **(Ctr)** or 10μM Nifedipine **(Nif)** or transfected with non-targeting control siRNA **(siCtr)** or siRNA targeting CaV1.3 **(siCaV1.3)**. **(i)** Analysed using 2-way ANOVA significance of fluorescence ratio*

340:380 at time (s) between cell types. ***(ii)*** *Normalised Tg peak,* ***(iii)*** *calcium peak* ***(iv)*** *AUC indicated for each cell type and treatment. Analysed using Kruskal-Wallis significance test between cell types and treatments. * P<0.05, ** P<0.01, ***P<0.001, NS not significant.*

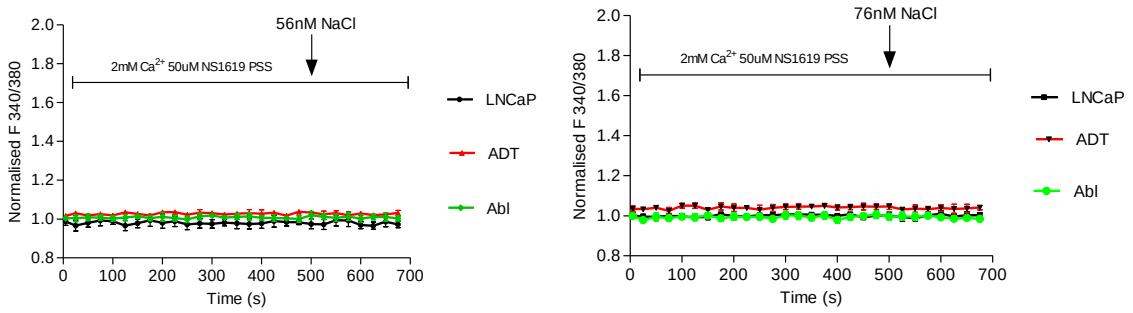

Figure B.5: NaCl control demonstrates how there was no osmotic effect influencing the KCl effect in PCa*: Cells incubated with NS1619 followed by Fura 2-AM underwent ratiometric analysis of calcium concentration over time. Androgen sensitive LNCaP cells (black), LNCaP-ADT cells treated with 10μM bicalutamide (7-10 days) (Red) and androgen insensitive long-term androgen deprived LNCaP-abl cells (Green) where depolarised with high external potassium concentrations of* ***(A)*** *60nM NaCl or* ***(B)*** *80nM NaCl. Analysed using 2-way ANOVA significance of fluorescence ratio 340:380 at time (s) between cell types. * P<0.05, ** P<0.01, ***P<0.001, NS not significant.*

Appendix C – Additional results for chapter 5

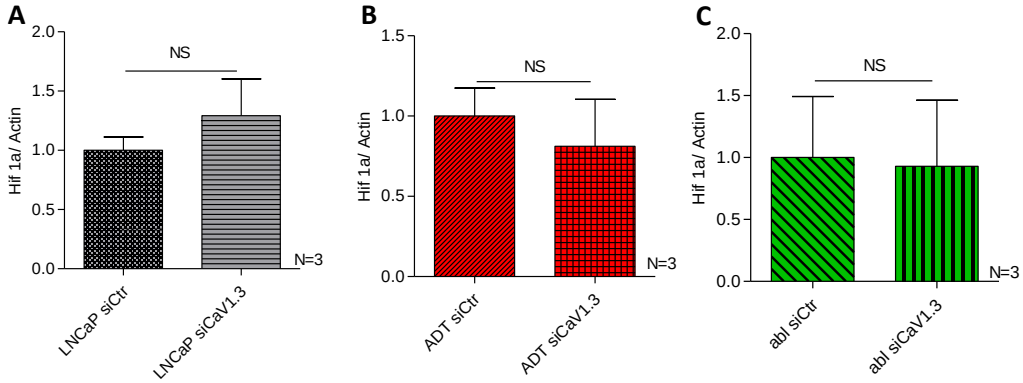

Figure C.1: Protein expression of HIF-1α unaltered when CaV1.3 expression is silenced in normal Oxygen conditions*: Western blot analysis of protein expression of HIF-1α normalised to control. Analysis of androgen sensitive LNCaP cells (black), LNCaP-ADT cells treated with 10μM bicalutamide (7-10 days) (Red) and androgen insensitive long-term androgen deprived LNCaP-abl cells (Green) incubated in normal oxygen conditions transfected with non-targeting control siRNA (siCtr) or siRNA targeting CaV1.3 (siCaV1.3). Protein expression of CaV1.3 in (A) LNCaP, (B) LNCaP-ADT and (C) LNCaP-abl. Analysed using One-way analysis of variance and Tukey's multiple comparison post hoc test between cell types and treatments. * P<0.05, ** P<0.01, ***P<0.001, NS not significant.*

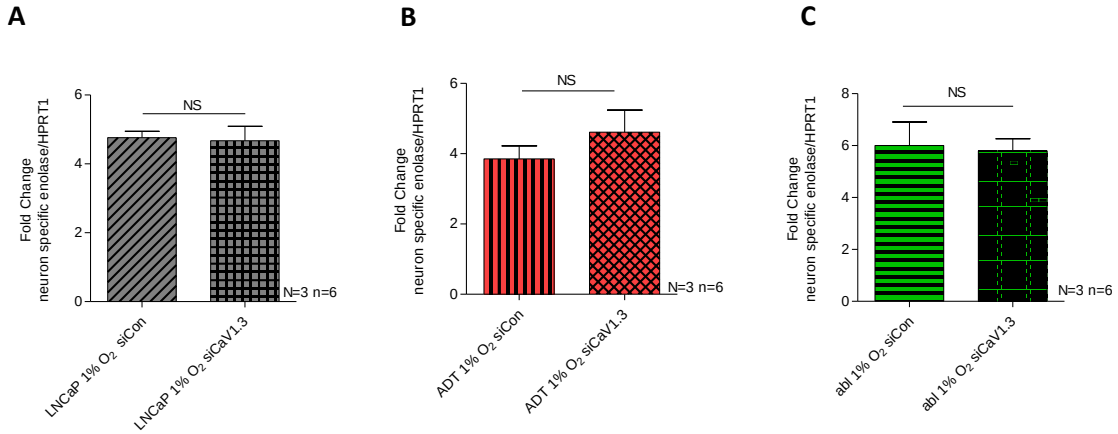

Figure C.2: Expression of NSE under hypoxic conditions is not affected by expression of CaV1.3: *Genetic expression of neuron specific enolase assessed using qPCR normalised to control. Analysis of androgen sensitive (A) LNCaP cells, (B) LNCaP-ADT cells treated with 10μM bicalutamide (7-10 days) and (C) androgen insensitive long-term androgen deprived LNCaP-abl cells. Tested under hypoxic conditions* ***(1% O_2)*** *transfected with non-targeting control siRNA* ***(siCtr)*** *or siRNA targeting*

CaV1.3 ***(siCaV1.3)*** *Analysed using Mann-Whitney significance test between treatments. * P<0.05, ** P<0.01, ***P<0.001, NS not significant.*

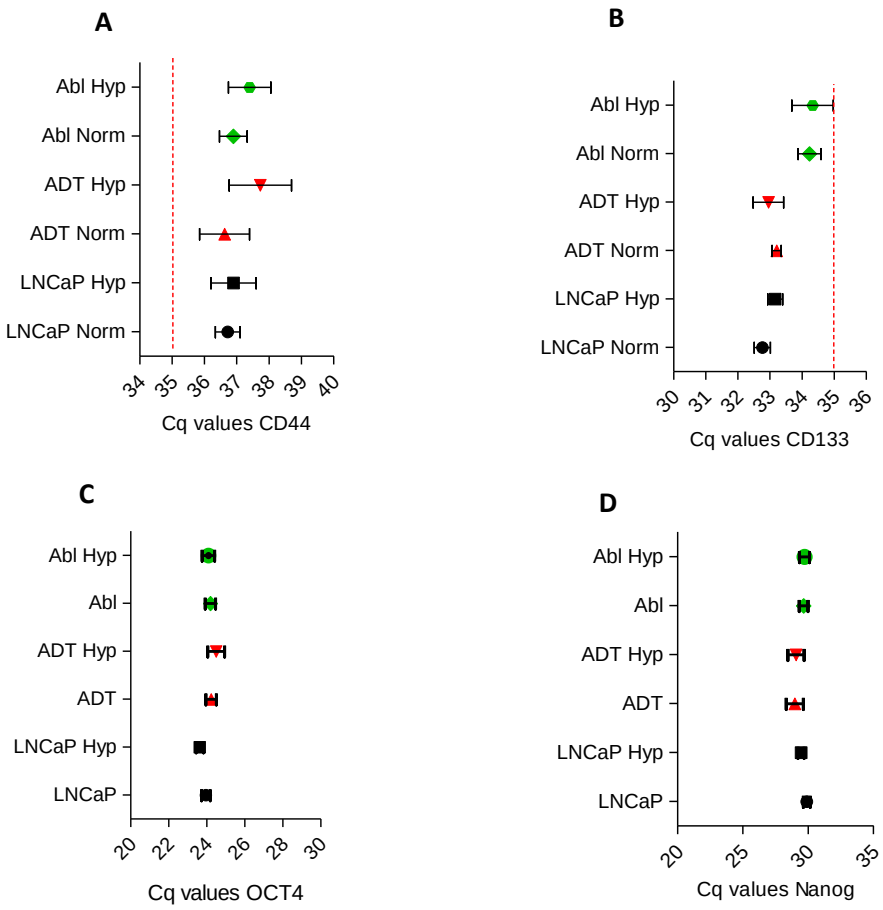

Figure C.3: Cq values obtained for stem cell surface markers or pluripotency markers: *Genetic expression of (A) CD44 (B) CD133 (C) Oct4 (D) Nanog assessed using qPCR. Analysis of androgen sensitive LNCaP cells (black), LNCaP-ADT cells treated with 10µM bicalutamide (7-10 days) (red) and androgen insensitive long-term androgen deprived LNCaP-abl cells (green), under normal conditions (Ctr) and hypoxic conditions (1% O2).*

Appendix D – Additional results for chapter 6

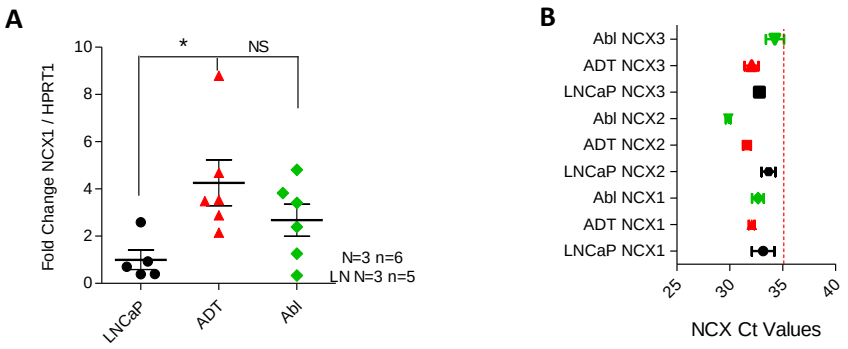

Figure D.1: NCX1 is upregulated in androgen sensitive LNCaP-ADT but was undetectable when transfection reagent was used: *Genetic expression of (A) NCX1 assessed using qPCR normalised to control. (B) Ct values obtained for NCX 1-3. Analysis of androgen sensitive LNCaP cells (black), LNCaP-ADT cells treated with 10µM bicalutamide (7-10 days) (red) and androgen insensitive long-term androgen deprived LNCaP-abl cells (green), transfected with non-targeting siRNA (siCtr) or siRNA targeting CaV1.3 (siCaV1.3). Analysed using Kruskal-Wallis significance test and Dunn's multiple comparison post hoc test between cell types and treatments. * P<0.05, ** P<0.01, ***P<0.001, NS not significant.*

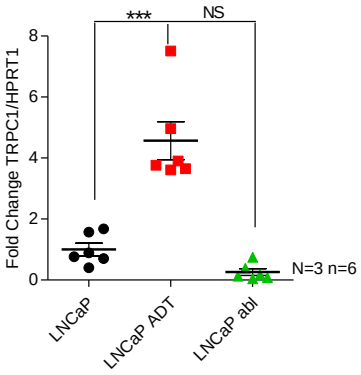

Figure D.2: TRPC1 is significantly upregulated in androgen sensitive LNCaP-ADT cells: *Genetic expression of TRPC1 assessed using qPCR normalised to control. Analysis of androgen sensitive LNCaP cells (black), LNCaP-ADT cells treated with 10µM bicalutamide (7-10 days) (red) and androgen insensitive long-term androgen deprived LNCaP-abl cells (green). Analysed using Kruskal-Wallis significance test and Dunn's multiple comparison post hoc test between cell types and treatments. * P<0.05, ** P<0.01, ***P<0.001, NS not significant.*

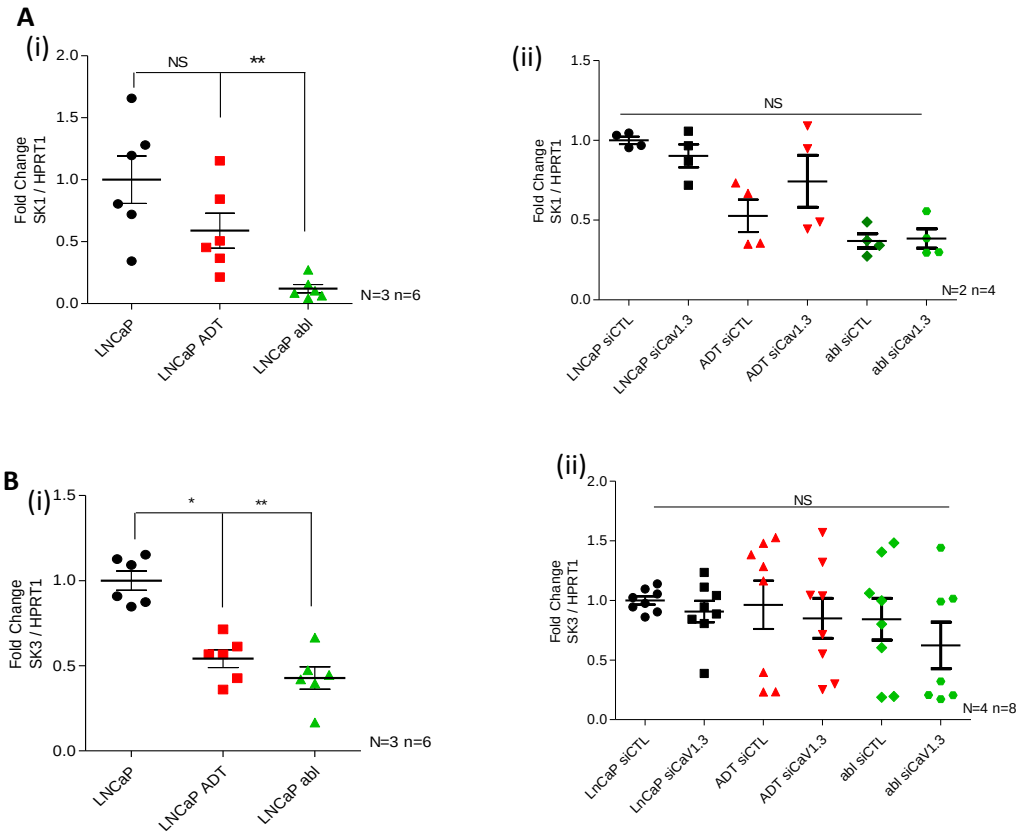

Figure D.3: SK1 and SK3 are downregulated after ADT with no significant change observed with CaV1.3 silencing: *Genetic expression of (A) SK1 and (B) SK3 assessed using qPCR normalised to control. Analysis of androgen sensitive LNCaP cells (black), LNCaP-ADT cells treated with 10μM bicalutamide (7-10 days) (red) and androgen insensitive long-term androgen deprived LNCaP-abl cells (green), transfected with non-targeting siRNA (siCtr) or siRNA targeting CaV1.3 (siCaV1.3). Analysed using Kruskal-Wallis significance test and Dunn's multiple comparison post hoc test between cell types and treatments. * P<0.05, ** P<0.01, ***P<0.001, NS not significant.*

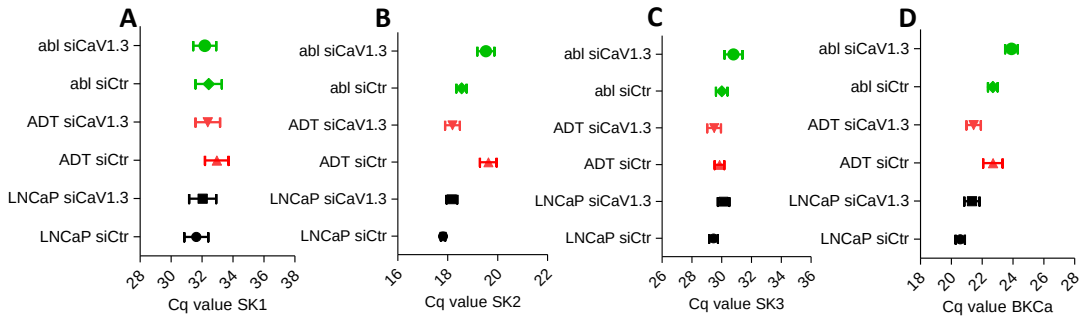

Figure D.4: SK2 and BK_{Ca} channels have the most expression in the cells: *Cq values obtained for (A) SK1, (B) SK2, (C) SK3 and (D) BK_{Ca}. Analysis of androgen sensitive LNCaP cells (black), LNCaP-ADT cells treated with 10µM bicalutamide (7-10 days) (red) and androgen insensitive long-term androgen deprived LNCaP-abl cells (green), transfected with non-targeting siRNA (siCtr) or siRNA targeting CaV1.3 (siCaV1.3).*